LEWIS ACIDIC PHOSPHORUS

GORDANA ILIC

2017

THESIS

NANYANG TECHNOLOGICAL UNIVERSITY

MOLECULES CONTAINING LEWIS ACIDIC PHOSPHORUS - SITES

GORDANA ILIĆ

SCHOOL OF PHYSICAL AND MATHEMATICAL SCIENCES

2017

LEWIS ACIDIC PHOSPHORUS

GORDANA ILIC

2017

MOLECULES CONTAINING LEWIS ACIDIC PHOSPHORUS - SITES

GORDANA ILIĆ

School of Physical and Mathematical Sciences

A thesis submitted to the Nanyang Technological University

in fulfilment of the requirement for the degree of

Doctor of Philosophy

2017

A young girl's dream becomes her reality.

To my parents and my grandma,
who provided me with the wings
to reach my dreams.

Acknowledgements

First and foremost, I would like to thank Assistant Professor Dragoslav Vidović for allowing me to pursue PhD studies as part of his group. Thank you for being understandive of my initial lack of knowledge and experience in this area of chemistry, I deeply appreciate your patience for my learning curve. Thank you for allowing me to experience the freedom of research, for being available for a piece of advice or guidance, and for shining clarity through piles of confusing NMR spectra. Most of all, thank you for being an example of positivity against all odds.

I would like to express graditude to my lab-mates, who have shared space, glassware, happiness and frustrations with me throughout these four years: Dr. Senthil Kumar, Dr Madelyn Tay, Dr Chitra Gurnani, Dr Balasubramanian Murugesapandian, Dr Zhu Di, Dr Zhi Zhou, Dr. Nemanja Djordjević, Monika Bjelčić, Militsa Yaneva, Ben Tombling, Jeremy Lim, and Do Dih Cao Huan. Dr. Alexey Kudlaev, I could never thank you enough – you were my mentor, my friend, my voice of sanity, and my guardian angel in this experience. You taught me how to think like an engineer when working with schlenk lines, but what I have learned stretches far beyond that skill. While I made your days stressful by yelling “Fire, fire!” or “I need help!”, your passion for chemistry transformed my regular days into the most interesting ones. I feel partially “responsible” for your prolonged lab stay – I always hoped that we would work together until my thesis completion, and somehow, that wish came true. I feel grateful to all the undergraduate students who trusted me as their mentor and a friend: Jeffery, Elizabeth, Hui Xing, Lok, Maitri and Nate. While teaching, I learned so much from each one of you. I grew with you professionally and personally, and the experience of being your mentor was invaluable.

I would also like to thank Dr. Rakesh Ganguly for help with X-ray crystallography; Dr. Milena Petković for assistance with DFT calculations; Ee Ling Goh and Derek Ong for NMR spectroscopy. Your experise was crucial to my research.

Thank you to my Balkan and Russian friends, this journey would not be the same without all the coffee/tea breaks filled with laughter. Ivan Šolić, thank you for being my tech-saviour at the end. Completing this dissertation would be much more inconvenient without your generosity. I am aslo grateful for my Singaporean and international friends who I met here, whose help and company were of great value.

Thank you, Minja, Vladimir, Višnja, Nataša, Vanessa, Prpa, Gabriel, and Marko for your friendships. Your encouragement, visits, mailbox gifts, long Skype calls, and touching messages on Facebook made distance seem closer.

Pratik Malia, I am grateful for you from the bottom of my heart. You have probably felt the stress of my PhD the most. Regardless of my mood swings, sleepless nights and keeping you alert and awake, you have always remained an embodiment of unconditional love, calmness and support. The page is not long enough for me to express my feelings, but life is.

I would like to thank my parents for instilling values and discipline that shaped me into who I am today; for supporting all my talents, science lessons and endeavours, for sleepless nights, trust, and freedom to pursue my dreams. I could never ask for better and more selfless parents.

Lastly, I would like to thank Assistant Professor Rei Kinjo for agreeing to step in as my supervisor at the end, and help me complete this journey; the Nanyang Technological University and the Singaporean government for providing me with the opportunity, facilities and a financial support to study in this wonderful country.

Abstract

Carbones (CL_2) are a group of ligands with a divalent carbon(0) center. Due to the two available electron-pairs, carbones are considered to be substantially basic, which allowed them to serve as stabilizing ligands for a variety of the highly labile species.

In this work, we report the synthesis of $[(Ph_3P)_2CPN^iPr_2]^{2+}$, its two additional analogues $[((RPh_2P)_2C)P(NR'_2)]^{2+}$ (R = Ph, R′ = Cy; R = 1/2 $(CH_2)_3$, R′ = ^{i}Pr;), and we explore its viability in the presence of various counterions. In addition, the oxophilic nature of $[(Ph_3P)_2CPN^iPr_2]^{2+}$ is further studied in reactions with pyridine *N*-oxide (PyO). Surprisingly the resulting oxophosphonium dication proved to be an intermediate for the subsequent Baeyer-Villiger (BV)-resembling oxidation reaction, which proceeds through a Criegee intermediate to finally yield a rare P-C bond activation under mild conditions. Apart from being the first example of a PyO-driven BV oxidation, it is a safer alternative to the formerly used highly reactive m-chlorobenzoic acid and hydrogen-peroxide. These results inspired us to also develop a route to the elusive parent-metaphosphonate species. This thesis also covers the synthetic pathway and the reactivity of the first carbone-stabilized parent-metaphosphonate $[(Ph_3P)_2CP(O)_2H]$.

Summary

Herein presented work expands on the recently reported synthesis and reactivity of the two-coordinate P(III)-containing dication $[((Ph_3P)_2C)P(N^iPr_2)]^{2+}$ (**3c**$^{2+}$), and its two analogues $[((RPh_2P)_2C)P(NR'_2)]^{2+}$ (**3d**$^{2+}$, R = Ph, R′ = Cy; **3e**$^{2+}$, R = 1/2 $(CH_2)_3$, R′ = ^{i}Pr;). Solution and solid-state ^{31}P NMR isotropic shifts for the dication class were observed at ~360 ppm. Except for [**3c**][SbF_6]$_2$, the ^{31}P CP/MAS NMR spectra reveal a high degree of structural disorder around the dicationic site in the solid state. Surprisingly, the synthesis of dication **3c**$^{2+}$ was only possible in the presence of $AlCl_4^-$, $GaCl_4^-$,and substituted tetraarylborates, while the use of ClO_4^-, OTf^-, BF_4^-, PF_6^-, and BPh_4^- resulted in complex product mixtures. Single-crystal X-ray analysis of a dication [**3c**][SbF_6]$_2$ indicated close interion contacts, which disrupt the previously reported 4π allyl-like system of the central CPN fragment in the solid state.

Reactivity studies of [**3c**][SbF_6]$_2$ towards water and methanol have confirmed its oxidative addition behavior, and the absence of the SbF_6^- counterion interference. High oxophilicity of [**3c**][SbF_6]$_2$ was also confirmed in reactions with Et_3PO and PyO.

With respect to the latter, the resulting oxophosphonium dication $[(Ph_3P)_2C(N^iPr_2)P(O)(O\text{-}py)]^{2+}$, **7**$^{2+}$, was surprisingly stabilized by a less nucleophilic O-py ligand instead of pyridine (py). This compound was then identified as an analogue of the elusive Criegee intermediate as it underwent oxygen insertion into the P-C bond through a mechanism usually observed for Baeyer–Villiger oxidations, to give $[(N^iPr_2)P(O)(OC(PPh_3)_2)(py)]^{2+}$, **8**$^{2+}$. This oxygen insertion appears to be the first example of a Baeyer–Villiger oxidation involving O-py. Conversion of **7**$^{2+}$ into **8**$^{2+}$ is counterion dependant, as we have shown that extent of counterion stabilization of **7**$^{2+}$

decreases in order SbF_6^- > $BAr^{Cl}{}_4^-$ > $BAr^F{}_4^-$ > $B(C_6F_5)_4^-$; where $BAr^F{}_4^-$ allows for the fastest conversion, and $B(C_6F_5)_4^-$ results in the absence of reaction. Initial stoichiometric oxygen transfer reactions between $\mathbf{7}^{2+}$ and substituted phosphines PR_3 (R = Me or Cy) were also successfully demonstrated.

Leveraging further on carbodiphosphoranes strong donor abilities and its ability to stabilize highly electron-deficient moieties, we have successfully synthesized and characterised a rare example of a parent-metaphosphonate system ($(Ph_3P)_2CP(O)_2H$) (**17**). In order to access a carbone-stabilized metaphosphonate, $[(Ph_3P)_2CP(O)_2]$, **17** was reacted with various proton-abstracting agents ($NaNH_2$, KHMDS, KO^tBu, ^{n}BuLi, ^{t}BuLi) and hydride-abstracting or substituting agents ($[Ph_3C][B(C_6F_5)_4]$ and $(COCl)_2$). Difficulties in removing a proton/hydride such as: inactivity towards the tested proton-abstracting agents, ligand protonation, trityl-cation preference for the oxygen, or reactivity of **17** towards chlorine-containing species; along with the a very short P-H bond of 1.357Å, IR values, and the high melting point for **17**, were conclusive of the strong P-H interaction as a reason behind the inability to access a metaphosphonate species $[(Ph_3P)_2CP(O)_2]$. On the other hand, a reaction with trityl-borate or trityl-triflate yielded $[(Ph_3P)_2CP(O)_2(OCPh_3)(H)]^+$, implying higher acidity of the terminal oxygen, with respect to the $P_{central}$-H hydrogen, which was confirmed in a methylation reaction, which yielded an analogues moiety $[(Ph_3P)_2CP(O)_2(OCH_3)(H)][OTf]$.

Reactivity of **17** has also been explored towards typical dioxophosphorane trapping agents, such as amines and alcohols. While **17** did not show reactivity towards primary and secondary amines ($MeNH_2$, $^tBuNH_2$, $CyNH_2$, $^iPr_2NH$), it reacted with a range of alcohols to yield compounds with the general formula $[(Ph_3P)_2CH][P(O)_2(OR)H]$. According to computations performed for the reaction of

17 with methanol, the reaction proceeds though a stepwise mechanism, *via* an intermediate [$^{[1]}$P(O)(OCH_3)(OH)H]. The final reaction products [$(Ph_3P)_2CH]^+$ and [$P(O)_2$(OR)H]$^-$ stay in close proximity, accounting for the ΔE_{el+ZPE} energy of 56.6 kcal/mol. Finally, we explored transition-metal catalyzed dehydrogenative coupling reactions of **17** with terminal alkynes (phenylacetylene and 4-bromo-phenylacetylene). While the catalyst coordination was evident from the NMR data, the P-H bond remained preserved, consistent with its exceptional strength.

Table of Contents

Table of Figures

Table of Schemes

Table of Tables

Table of Abbreviations

∇^2	Laplacian
°	Degree
°C	Degree Celsius
µL	Microliter
2,3-OPBO	2,3-oxaphosphabicyclo[2,2,2]octenes
2-PBO	2-phosphabicyclo[2,2,2]octenes
Å	Angstrom
ACN	Acetonitrile
AE	Addition - elimination
B3LYP	Becke's -3 parameter functional with Lee-Yang-Parr correlation
B3PW91	Becke's -3 parameter functional with Perdew and Wang 91 correlation
br	Broad
Bu	Butyl
BV	Baeyer-Villiger
CDP	Carbodiphosphorane
CP-MAS	Cross Polarization - Magic Angle Spinning
Cy	Cyclohexyl
d	Doublet
DCM	Dichloromethane
dd	Doublet of doublets
DFB	Difluorobenzene
DMAP	Dimethylaminopyridine
DMF	Dimethylformamide
DMSO	Dimethyl Sulfoxide
dq	Doublet of quartets
E	Energy
EA	Elimination - addition
EPC	Electrophilic Phosphorus Centre
EtO	Ethoxy
EtOAc	Ethyl Acetate
EWG	Electron - withdrawing
F.V.P.	Flash vacuum pyrolysis
FIA	Fluorine ion affinity
FLP	Frustrated Lewis pairs
FMO	Frontier Molecular Orbital
FTIR	Fourrier Transformation Infra-Red
g	Gram
HOMO	Highest Occupied Molecular Orbital
HPLC	High Performance Liquid Chromatography
HRMS	High Resolution Mass Spectrometry

HSAB	Hard Soft Acid Base
I	Intermediate
in situ	On site
^{i}Pr	Isopropyl
J	Coupling constant
K	Kelvin
kcal	Kilocalorie
KHMDS	Potassium bis(trimethylsilyl)amide
kJ	Kilojoule
KO^{t}Bu	Potassium *tert*-butoxide
L	Liter
LA	Lewis Acid
LB	Lewis Base
LUMO	Lowest Unoccupied Molecular Orbital
m/z	Mass to charge ratio
mCPBA	*meta*-chloroperoxybenzoic acid
Me	Methyl
MeO	Methoxy
MeOD	Deuterated methanol
MeOH	Methanol
MeOTf	Methyl triflate
mg	Milligram
mg	Miligram
mL	Millilitre
mL	Mililiter
mmol	Millimole
MO	Molecular orbital
NaBAr$^{cl}_{4}$	Sodium tetrakis[3,5-bis(chloro)phenyl]borate
NaBAr$^{f}_{4}$	Sodium tetrakis[3,5-bis(trifluoromethyl)phenyl]borate
NBO	Natural Bonding Orbital
n-BuLi	*N*-butyl lithium
NHC	*N*-heterocyclic carbene
NMR	Nuclear Magnetic Resonance
NRT	Natural Resonance Theory
o	Ortho
OTf	Triflate
p	Para
PA	Proton affinity
Ph	Phenyl
PNB	Phosphanobornenes
ppm	Parts per million
Py	Pyridine
PyO	Pyridine *N*-oxide

q	Quartet
r	Bond distance
s	Singlet
t	Triplet
^{t}BuLi	*Tert*-butyl lithium
TEA	Triethylamine
THF	Tetrahydrofuran
TM	Transition metal
TMS	Tetramethylsilane
TS	Transition state
WBI	Wiberg Bond Index
X	Halogen
δ	NMR chemical shift in ppm
η	Eta – ligand coordination through multiple atoms
π	Pi
σ	Sigma

CHAPTER I:

Introduction

Catalysis is the basis of many chemical and biological processes, and its importance in the modern world is indisputable. Appropriate catalysts increase reaction rates, time efficiencies, lower costs, and drive industrial processes. Whether it is the production of pharmaceuticals, polymers, materials, agrochemicals, electronics, fragrances and even food – they all rely on catalytic processes.

Most of the contemporary catalyst technologies are based on transition metals, particularly around precious metals. For example, Suzuki-Miyaura Coupling, Kumada and Heck reactions all use highly efficient and readily available catalysts based on platinum, palladium, rhodium, and other transition metals (TM). Arising issues related to their use are cost, toxicity, and questionable environmental practices of metal sourcing and disposal.

As a response to these issues, readily available "greener" and sustainable catalysts are emerging as alternatives. "Green" catalysts most commonly include earth abundant first row transition-metal catalysts[2] and metal-free organocatalysts.[3]

1.1 Organocatalysis and main group catalysis

Recent achievements in organocatalysis showed promising results, as the number of main-group species which mimic the catalytic behaviour of transition metals is increasingly being reported, and the subject has been thoroughly reviewed.[3-4] The field of organocatalysis is particularly interesting because it has developed into a third class of asymmetric catalysis, apart from the biocatalysis and the organometallic catalysis, in less than two decades.[5] The success is attributed mainly to its benefits over homogeneous metal catalysts. Some of the advantages include: lower-toxicity, availability, ease of preparation, lower cost, and increased stability towards oxygen and moisture.[4b]

Based on the mechanism of catalysis, organocatalysts can be classified into four groups: 1) Brønsted bases, 2) Brønsted acids, 3) Lewis bases, and 4) Lewis acids. The classification depends on whether a catalytic cycle is initiated by providing/abstracting protons (Brønsted acids and bases) or electrons (Lewis bases and acids) from a substrate or a transition state (Scheme 1).[6] Out of the four, Lewis base catalysts such as amines and carbenes largely predominate the area. Chiral organic Brønsted acids are emerging as a competent rival to the enzymes and superactive chiral transition metal catalysts. Examples of the use of chiral organic Brønsted acids include Noyori's hydrogenation reactions and several Suzuki reactions.[3] On the other hand, Lewis acid-organocatalysts are the least developed. Interestingly, metal-based catalysts are predominantly Lewis acidic.[4b]

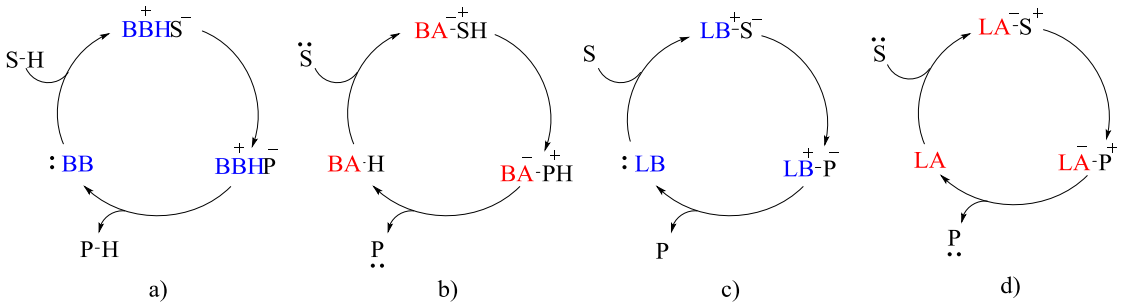

Scheme 1. Schematic examples of catalytic cycles catalysed by: Brønstead Base (a); Brønstead Acid (b); Lewis Base (c); Lewis acid (d).

Another issue is that only noble metals exhibit notable catalytic reactivity, while the majority of other metals are inert, conserning their Lewis acidity.[7] In general, stronger Lewis acidity correlates with enhanced reactivity. For instance, the catalytic activity of some metal halides (i.e., $AlCl_3$) had been improved by exchanging their anion for a more electron-withdrawing perfluorooctane sulfonic acid or trifluoromethyl sulfonate anion.[8] Some metal Lewis acids, such as $Ge(OTf)_3$, show remarkable stability towards air and moisture, allowing for their multi-cycle recycling.[9] On the other hand, increased acidity often increases catalyst's susceptibility to hydrolysis, resulting in the more challenging catalyst-recycling.[10]

Having in mind the scarcity of solutions, the need for efficient Lewis-acidic organocatalysts is ever-emerging.

With respect to recent developments, main group Lewis acids gained a prominent role as reagents in synthetic procedures, and as facilitators of many stoichiometric and catalytic reactions.[11]

1.2 Lewis acidity – the concept

In 1926, G. N. Lewis[12] classified chemical species into acids or bases, depending on their capability to accept or donate an electron pair, respectively. In a mutual interaction, a Lewis base (LB) donates its electron lone pair into the Lewis acid's (LA) vacant orbital, yielding an adduct in which two species are connected *via* a coordinate-covalent bond, also known as a formal dative bond (Figure 1). A dative bond is often represented *via* an arrow, which represents an origin of the lone pair of electrons that are being donated to an electron-deficient, Lewis acidic, species.[13]

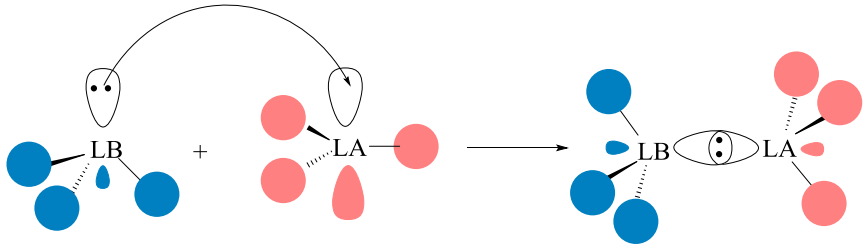

Figure 1. Lewis acid-base adduct formation

The corresponding acid-base adduct formation, as later been explained by Fukui's Frontier Molecular Orbital theory (FMO),[14] results from an interaction between the acid's lowest unoccupied molecular orbital (LUMO) and the base's highest occupied molecular orbital (HOMO) (Figure 2). The significance of this concept lies in its applicability to the compounds which do not contain protons.

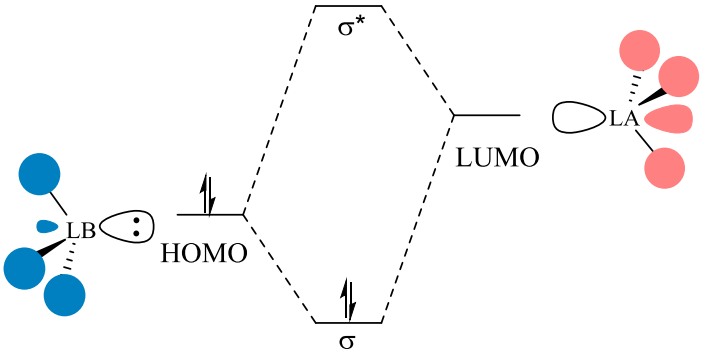

Figure 2. Molecular orbital diagram for the interaction between the Lewis base's highest occupied orbital (HOMO) and the Lewis acid's lowest unoccupied orbital (LUMO)

1.2.1 Lewis acidic group 13 and group 14 compounds

1.2.1.1 Boron species

Most of the known main group Lewis acids belong to the group 13. Their Lewis acidity derives from a vacant p orbital in their neutral, three-coordinate state, which accounts for their electron-deficiency and the ability to accept a lone pair of electrons (Figure 3a).

Boron-based Lewis acids are commonly used in the contemporary organic chemistry: borohydride reduction reactions,[15] C-C formation *via* Suzuki-Miyaura cross-couplings,[16] olefin hydroboration.[17] Lewis acidity of boranes was crucial for the design of sensors for detection of cyanide and fluoride anions,[18] carbohydrates, or medications;[18a, 19] structure deduction of supramolecular materials and B-B coordination polymers;[20] and the determination of the pharmacological action mechanisms of boron-containing pharmaceuticals.[21]

For instance, *tris*(pentafluorophenyl)borane (Figure 3b) results in over 20000 reaction records in SciFinder. This fact provides maybe the best overview of its widespread application; dominated by its use as Lewis acid catalyst,[22] and for activation of pre-catalysts for olefin polymerization.[23] In addition, $B(C_6F_5)_3$ produced notable results in the activation of small molecules, as part of

"Frustrated Lewis Pair" (FLPs) systems.[23f, 23i] FLPs comprise of the combinations of electron-aceeptor and electron-donor sites, in which the steric hindrance prevents them from forming a classical adduct. Most of the FLP systems in the past decade were based on boranes as Lewis acidic sites, and phosphorus- or nitrogen-based Lewis basic sites, to perform catalysis of a wide range of hydrogenation reactions and small molecule activations.[23f, 23h, 24]

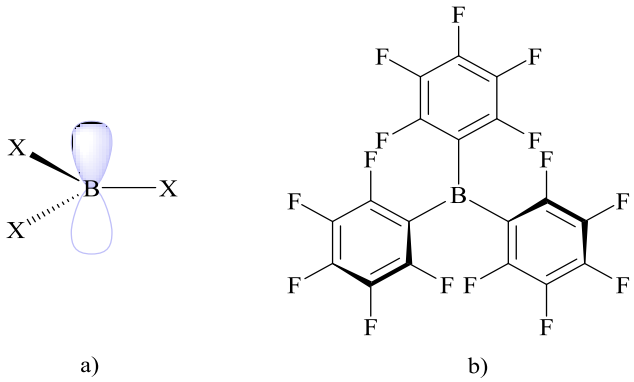

Figure 3. Borane derivatives: a) general BX_3, and b) tris(pentafluorophenyl)borane $B(C_6F_5)_3$

Other electrophilic boron-compounds, commonly used within FLP systems, include halogenated tri(aryl)boranes[25] and various borenium cations (usually NHC-stabilized).[26] A good overview of Lewis acidity of numerous borane catalysts can be found in a review by Sivaev and Bregadze.[27] A recent review by Eisenberger and Crudden summarizes catalytic applications of borenium species for E-H bond activations, where E = H, Si, B, C.[28]

1.2.1.2 Aluminium species

Among group 13 Lewis acids, aluminium is preferred mainlt for its abundance (about 8.3% of Earth's crust weight) and low cost.[29] For instance, $AlCl_3$ has been widely used as a catalyst, for degradation of perfluorinated compounds, alkyl-polymerizations, Beckmann transposition of oximes to amines, and, most frequently, Friedel-Crafts reactions (Scheme 2).[4a]

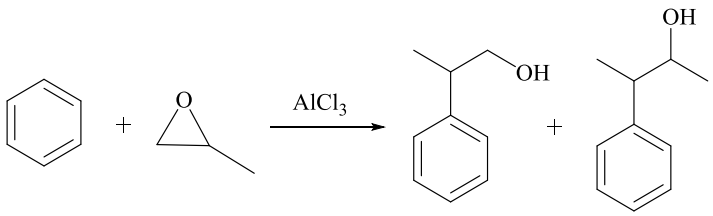

Scheme 2. An example of an $AlCl_3$-catalyzed Friedel-Crafts reaction.

A chiral aluminium complex (Figure 4a) synthesized by Shibasaki *et al.* proved to efficiently catalyze asymmetric Michael additions of various malonic esters and cyclic enones.[30] Our group has recently contributed to the field of Al-catalyzed Diels-Alder reactions, with several Al-based bis(imino)phenyl NCN pincer-supported complexes,[31] and a β-diketiminate-supported aluminiumbistriflate complex,[32] efficient for Diels-Alder transformations (Figure 4b-f).

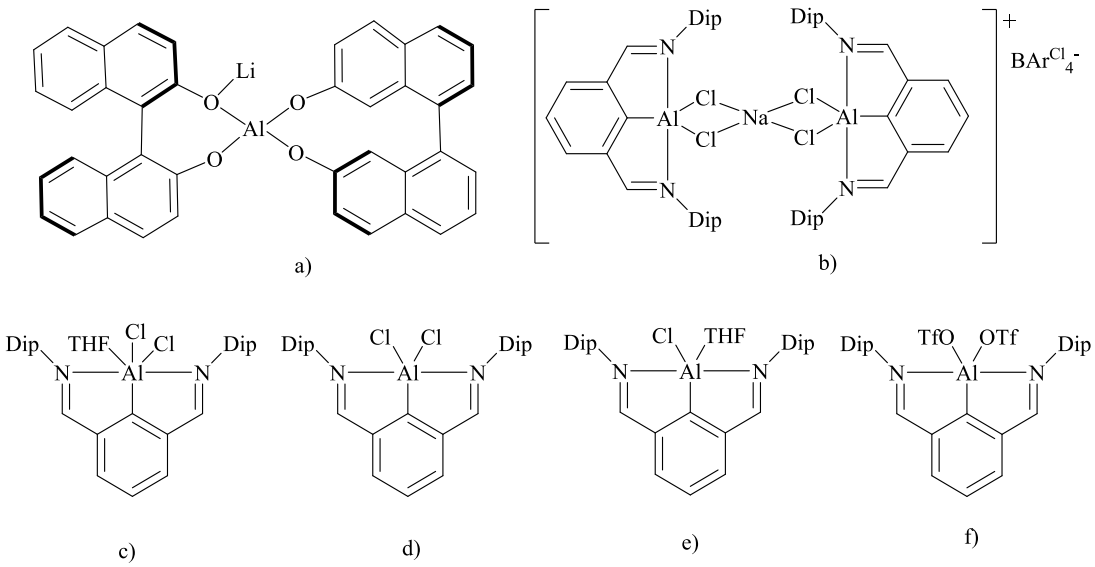

Figure 4. Some Al-based catalysts

1.2.1.3 Gallium species

Despite higher cost and lower nucleophilicity and Lewis acidity, gallium species are often good alternatives when other Group 13 species fail to mediate certain organic reactions.[33] $GaCl_3$ is undoubtedly the most used Ga-based Lewis acid, and its use has been reviewed by Amemiya *et al.*[34] Gallium(III) triflate, $Ga(OTf)_3$ is another

potent Lewis acid, with promising catalytic applications, due to the ease of reaction recovery without the loss of activity. For instance, $Ga(OTf)_3$ has been used to catalyze the synthesis of 2,3-dihydroquinazolin-4(1H)-ones which have broad pharmacological and biological applications.[35]

Chiral gallium complexes (Figure 5), analogous to the aluminium complexes in Figure 4a, have been applied in asymmetric epoxide ring opening reactions.

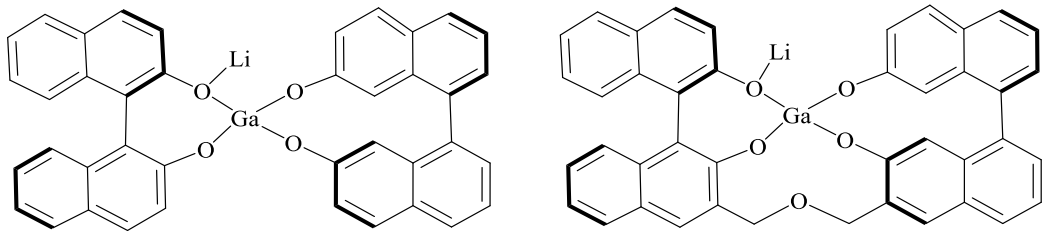

a) b)

Figure 5. Chiral gallium complexes

Another example of successful application of Gallium-based Lewis acids includes catalytic reduction of CO_2 to a methanol derivative using a β-diketiminato-supported gallium hydride complex, recently reported by Aldridge and co-workers.[36]

1.2.1.4 Silicon species

Tetravalent silicon species with Lewis acidic properties are commonly used in synthetic chemistry with the prominence of Me_3SiOTf (TMSOTf).[37] Their analogues, *in situ* prepared trialkylsilyl bistrifluoromethanesulfonamides (R_3SiNTf), proved to be more potent catalysts than TMSOTf, in Diels-Alder and Friedel-Crafts reactions.[38]

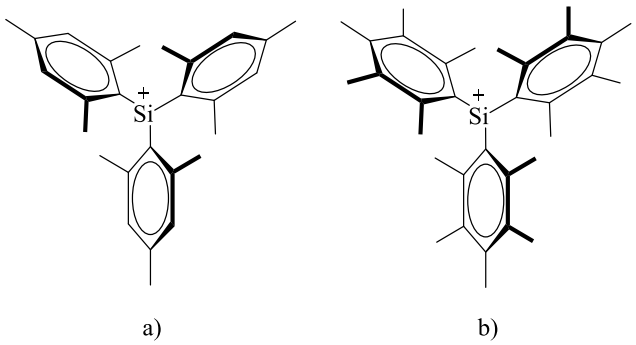

Figure 6. First examples of characterised silylium ions.

Even more acidic silicon species are silylium ions. Since the first structurally characterised example (Figure 6) in 1993,[39] several examples have been reported and increasingly studied for their catalytic activity. [40] Examples include defluorination reactions of fluoro- and perfluoroalkyl groups,[41] Diels-Alder and Mukaiyama aldol reaction catalysis,[42] and even C-C bond formation catalysis.[43]

1.2.1.5 Carbocations

Contrary to their history of more than 130 years, and evidence of Lewis acidic behaviour, carbocations are considered "neglected Lewis acids" in organocatalysis.[44] Trityl perchlorate was the first reported carbocationic catalyst 30 years ago with applications in numerous Michael and Mukaiyama aldol-type reactions (Scheme 3).[45]

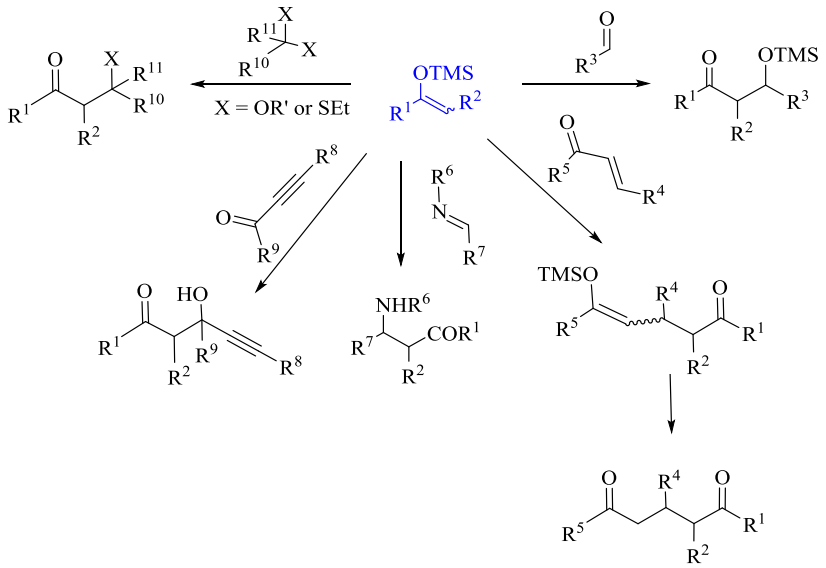

Scheme 3. Reactions catalyzed by Ph_3C^+, as discovered by Mukaiyama et al.

In addition, 1 mol% of $[Ph_3C][BF_4]$ was as efficient catalyst as HBF_4 or typical Lewis acids (BF_3•Et_2O, $AlCl_3$, $TiCl_4$) in Diels-Alder reaction of 1,3-cyclohexadiene and acrolein in less than an hour.[46] Some of the promising areas for their catalytic application include oxo-Metathesis, developing new chiral carbocations for applications in assymetric catalysis, and expanding the chemistry of the phenalenyl cation

(Figure 7).[46a]

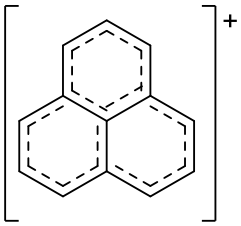

Figure 7. The structure of a phenalenyl cation

1.2.1.6 Group 13 and 14 polycations

Relying on the electron-rich properties of ligands such as NHCs, polyethers, pyridines, and diimines, many p-element centred polycations have been synthesized and structurally characterised. Usually, these species are coordinatively saturated, or their positive charge is distributed over ligands, which causes them to behave as classic Lewis bases or to be inactive as Lewis acids.

Lewis acidic polycationic boron species are rare, with only a handful of examples available in the literature. The first structurally characterised boron-centred dication was obtained using the stabilizing properties of the β-diketiminate ligand. The moiety was accessed by Cowley *et al.* in 2007, *via* the procedure shown in Scheme 4.

As it can be depicted from the scheme, the final step included a *bis*-triflate displacement by a bidentate 2,2'-bipyridine (bpy) ligand.[47] Other pioneering examples include a dicationic boron joined to a ferrocene moiety by Braunschweig *et*

al.,[48] and a dinuclear B^{II} dication obtained by Himmel *et al.* from a reaction between $B_2Cl_2(NMe_2)_2$ and a guanidine derivative hppH.[49]

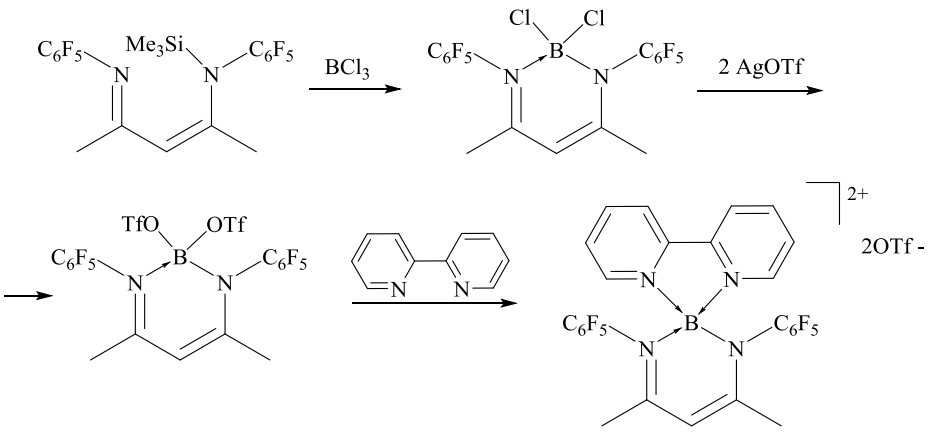

Scheme 4. Synthesis of first structurally characterised boron dicationic complex.

Concerning group 14 polycations, a Ge^{II}-centred dicationic complex $[Ge(^iPr_2IM)_3]^{2+}$ was synthesized by Ragogna *et al.* in a stepwise reaction represented in Scheme 5. The coordination complex between $GeCl_2$•dioxane and an NHC $^iPr_2IM$ ligand was subjected to the chlorine metathesis with TMS-I, followed by the iodine atoms displacement by the subsequent addition of excess $^iPr_2IM$.[50]

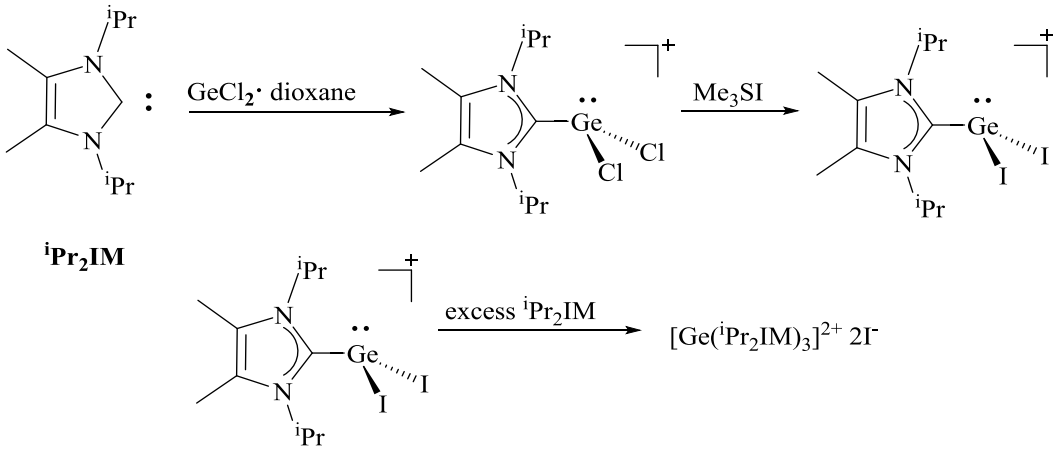

Scheme 5. Synthesis of the NHC $^iPr_2IM$-stabilized Ge(II)-dication, reported by Ragogna et al.

The study has shown that the formal charge of +2 was not localized on the germanium atom. In fact, positive charge accumulation on the central Ge amounted only up to +1.02. In another study, a residual positive charge on the "naked" germanium

encapsulated within the cryptand, was found to be astoundingly high (+1.38). However, the Ge^{II} coordination sphere in the latter was completed, rendering the species inactive as a Lewis acid.[51] Analogous behaviour was observed for other macrocyclic amine- and crown ether-sandwiched complexes of Ge^{II} and Sn^{II}.[52] Studies on polycationic silica species are rare, but an example of a dicationic, octahedral, silica complex $[(H)_2Si(Py)_4]^{2+}$, with hydride groups in the axial, and pyridine ligands in the equatorial positions, has been structurally characterised in 1998.[53]

1.2.2 Lewis acidic group 15 compounds

Examples of the polycationic Lewis acidic Group 15 elements are somewhat scarce.[54] In a recent review, Burford *et al.* summarised potential Lewis acidic pnictogen cations, as represented in Figure 8.

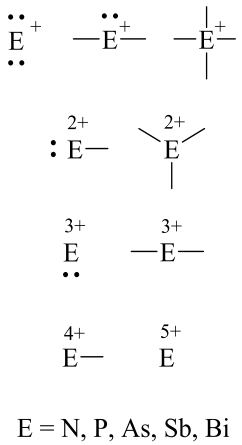

Figure 8. Predicted, potentially Lewis acidic, pnictogen cations.

Schmidpeter *et al.*[55] performed a methylation of a triphosphenium cation in the presence of $AlCl_3$ to generate a P^{III}-centred dicationic complex $[(Me)P(PPh_3)_2][AlCl_4]_2$.

$$2\ Ph_3P + MePCl_2 + 2\ AlCl_3 \longrightarrow [(Me)P(PPh_3)_2][AlCl_4]_2$$

Dillon *et al.* later accessed and structurally characterised a series of derivatives *via* protonation,[56] alkylation, and arylation reactions of cyclic triphosphenium ions (Figure 9).[54d, 57]

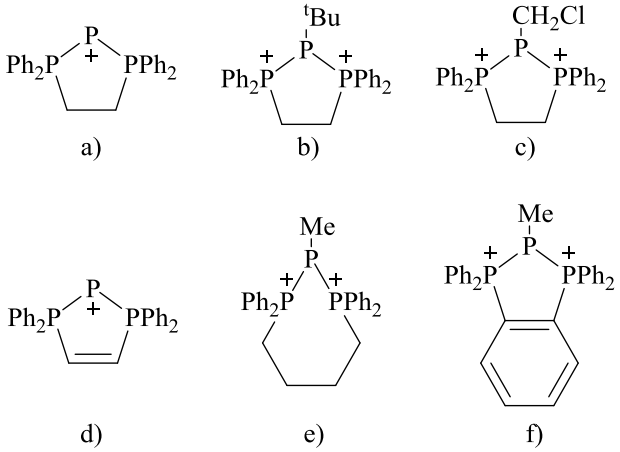

Figure 9. Examples of cyclic triphosphenium cations reported by Dillon et al.

A P^V-centred dication can be obtained from a reaction between a trimethylchlorophosphonium triflate and TMS-OTf in the presence of 4-dimethylaminopyridine (DMAP) ligand (Scheme 6). If DMAP is viewed as a stabilizing Lewis base, the resulting $[R_3P(DMAP)][OTf]_2$ complex can be regarded as a dicationic analogue of allane or a trialkyl borane, with substantial Lewis acidic properties.[58]

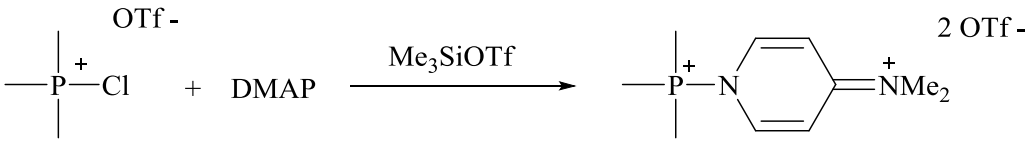

Scheme 6. DMAP-stabilized P(V)-centred dication

Lewis acidic and polycationic phosphorus species are reviewed in more details in the following section (Section 1.2). Furthermore, structurally characterised dicationic examples of other pnictogen species include ligand- ($OPPh_3$ or dmap) stabilized Ph_3Sb^{2+} and Ph_3Bi^{2+} complexes by Ferguson *et al.*[59].

1.2.3 Lewis acidic P(V) species

While FLP systems predominantly contain boron-based Lewis acids, recent discoveries in this field shed light on high Lewis acidic potency of phosphorus species,[60] and their usefulness in catalysis.

Wittig reagent ($R_3P{=}CHR'$) is an example of a P(V) neutral Lewis acid.[61] This phosphonium ylide is widely used in industry to form substituted alkenes from aldehydes or ketones.

Lewis acidity of group XIII species (BH_3, BF_3, $AlCl_3$, $AlMe_3$) derives from an empty p-orbital. On the contrary, phosphonium cations (PR_4^+) owe their Lewis acidity to the low-lying σ^* orbital facing the electron withdrawing (EWG) substituent.[62] This antibonding orbital (σ^* P^+-EWG) is capable of accepting a lone pair of electrons from a Lewis base (LB), which results in the formation of a bond trans to the EWG group. Consequently, the newly formed complex is more stable (Scheme 7).

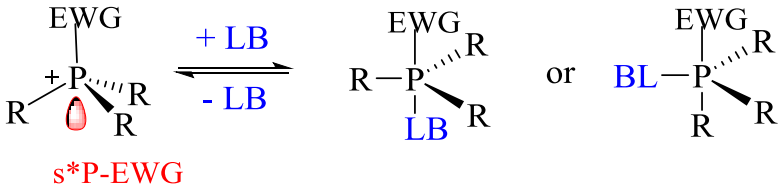

Scheme 7. An interaction between the σ^* P^+-EWG orbital of the phosphonium cation and a Lewis base.

The possibility to increase Lewis acidity of pentacoordinate phosphorus species with electron withdrawing substituents was recognised as far as in 1960s[63]. Electrophilic properties of P(V) species were limited to the scopes of coordination chemistry[64] until 1977 when a pentacoordinate amidophosphorane $CH_3(CF_3)_3P$-$N(CH_3)_2$ was used to capture CX_2 (X=O, S).[65] The resulting adduct was also a pioneering example of an FLP, as it contained a Lewis acidic (phosphonium) and a Lewis basic (amido) centre.

As far as in 1989, phosphonium salts were successfully used as catalysts in a Michael reaction between unsaturated ketones/acetals with nucleophiles. Similarly, phosphonium salts were found to catalyze aldol-type reactions between aldehydes/acetals and nucleophiles. Moreover, bisphosphonium salt $[PBu_3OPHBu_3][OTf]_2$ outperformed metal-based, Lewis acid catalysts ($TiCl_4$ and $SnCl_4$) in a reaction between *N*-benzylidene-aniline and ketene silyl acetal of methyl isobutylrate.[45g] Other catalytic applications of phosphonium salts include TMSCN addition to aldehydes/ketones,[66] cyanosilylation of aldehydes/ketones,[67] *N*,*N*-dimethylation of primary aromatic amines,[68] aldehyde cyclotrimerization,[69] protection/deprotection of alcohols in reactions as alkyl vinyl ethers.[70]

The importance of the low-lying σ^* orbital was experimentally confirmed in 2006, when Lewis acidic alkoxyphosphonium cations (Scheme 8) proved to be efficient catalysts for Diels-Alder reactions, using α,β -unsaturated amides as dienophiles.[71] As high as 91% yield in high endo-selectivity was achieved using the corresponding phosphonium salt for a reaction between a cyclopentadiene and an unsaturated amine. The authors remarked that the crucial requirement, for the catalytic success of the reaction, was hypervalent bonding between the phosphonium salt and a Lewis base, in the active species.

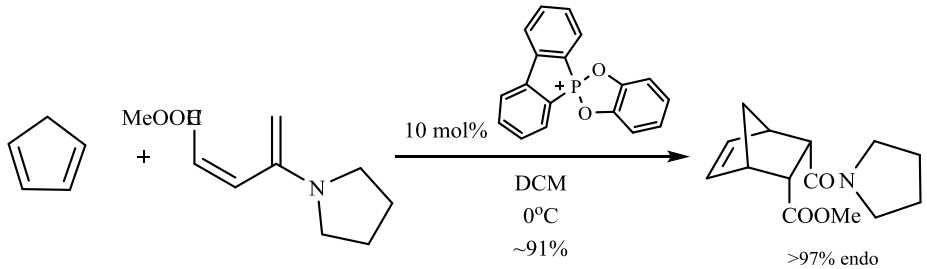

Scheme 8. Diels-Alder reaction catalyzed by a phosphonium salt.

Recent catalytic developments, which build upon this concept, are dominated by achievements in Stephan's group. [60] Relying on electron withdrawing substituents

to lower the energy of the antibonding orbital on the phosphonium cations, they have synthesized a range of electrophilic phosphonium cations (EPCs). General synthetic approach to the EPC species (Figure 10) included oxidation of a phosphine with XeF_2 and a subsequent fluoride abstraction with $B(C_6F_5)_3$.

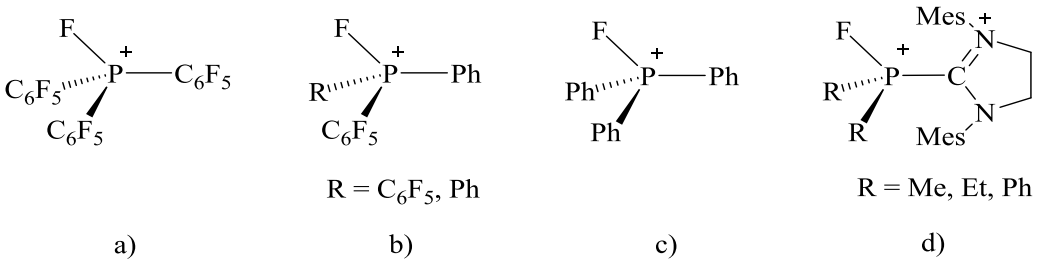

Figure 10. Selected EPCs synthesized by Stephan et al.

EPCs' Lewis acidic properties proved to be even higher than of $B(C_6F_5)_3$. Their remarkable catalytic properties were demonstrated for: hydrodefluorination reactions of fluoroalkanes,[72] olefin izomerisation to 2-hexane, Friedel-Crafts dimerizations, isobutylene polymerization,[73] hydrosilylations of olefins, alkynes, ketones and imines,[73-74] dehydrocoupling of acids, amines and thiols with silanes.[75]

1.2.4 Lewis acidic P(III) species

Contrary to the widely-acknowledged P(V) Lewis acids, the presence of a lone pair of electrons in P(III) compounds acclaimed P(III) species as Lewis bases. Interest for the Lewis acidic P(III) compounds was ignited with Dimroth and Hoffmann's discovery of phosphenium cations (R_2P^+) in 1964.[76]

Phosphenium cations are considered among the most stable phosphorus-based Lewis acids.[77] General features of a dicoordinate P(III) centre in phosphenium cations includes: sp^2-hybridized central phosphorus atom, a distinctively high accumulation of positive charge, a formally vacant 3p π-type orbital, and a lone pair of electrons in their σ-orbital.[78] These features make them isovalent to Group 14 species:

singlet state carbenes, silylenes, germylenes, stannylenes and plumbylenes (Figure 11); and isoelectronic to chloronium and silylenium ions.

While the localization of the positive charge on phosphorus allows for participation in a diversity of reactions,[79] their coordination-chemistry is substantially defined by the existence of the lone pair at phosphorus.[79]

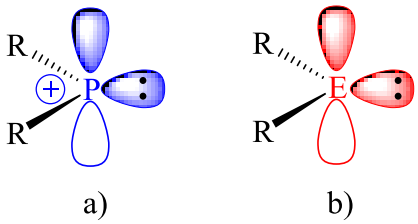

Figure 11. Isovalency of phosphenium cations (a) and analogues group 14 species (b): singlet carbenes (E=C), silylenes (E=Si), germylenes (E=Ge), stannylenes (E=Sn), and plumbylenes (E=Pb).

Their electronic structure qualifies them to act amphiphilic and amphoteric. Depending on the π-charge distribution, three types of R_2P^+ cations exist (Scheme 9).[80]

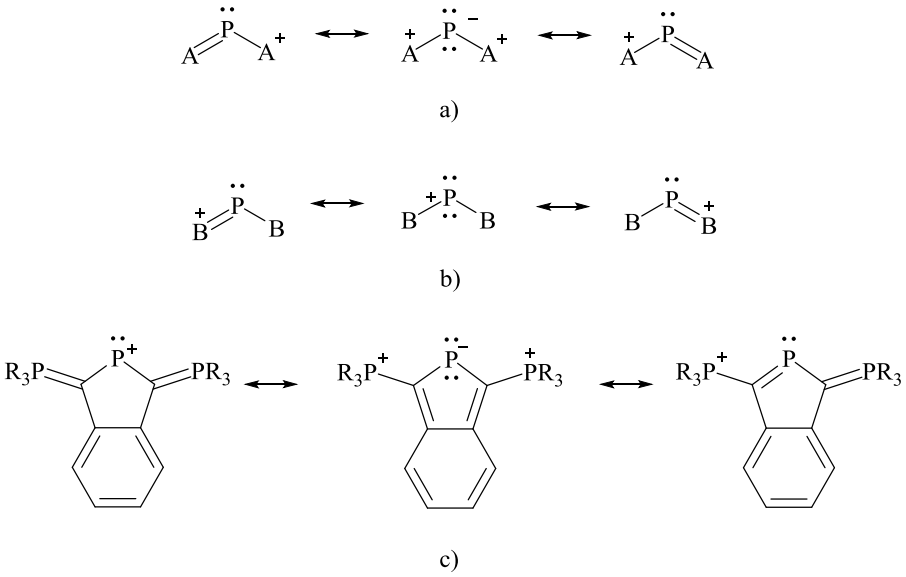

Scheme 9. Groups of phosphenium cations based on their π-charge distribution

In the first group, positive π-charge is localized solely on substituents, while the phosphorus atom bears overall neutral or negative π-charge. In these species, central phosphorus is nucleophilic, and a representative of the group is 2-

phosphaallylic cation.[80] Second group comprises of species with an ambiphilic (both electrophilic and nucleophilic) central phosphorus, with a localization of an overall positive π -charge. Aminophosphenium cations are examples of this charge distribution.[81] Species such as heterocyclic bis-phosphonio-isophosphindolide ions have an ambiphilic phosphorus centre with a reduced electrophilic character. As such, they represent a crossbreed of the former two groups and can be represented with a mesomeric formula as in Scheme 9.[82] ^{31}P NMR shift of 242 ppm which was within the range for phosphenium ions indicated that predominating structures are of a phosphenum ion stabilized by methylenephosphorane groups and of a phospholide anion.

Another characteristic feature that arises from the electrophilic nature and a low coordination number is the appearance of their chemical shift between δ_P +100 ppm and δ_P +500 ppm in the ^{31}P NMR spectrum. Rare exceptions occur in cases when substituents with conjugate effects, steric effects or ability to disperse positive charge are employed.[83]

1.2.4.1 Previous studies

Apart from the Dimroth and Hoffmann's report in 1964,[76] phosphenium cations have been observed as reactive intermediates[84] and species that result in the appearance of phosphine phosphinous halide peaks in mass spectra.[85] Fleming *et al.*'s synthesis of a "unique Dialkylaminophosphine cation" from 1972 was the first reported synthesis of a stabilized phosphenium cation.[86] The cyclic dimethylaminophosphine was obtained *via* fluoride abstraction from the cyclic 2-fluoro-1,3-dimethyl-1,3,2-diazaphospholidine precursor (Scheme 10), which caused a significant downfield shift of $\Delta\delta_P$ 126 ppm.

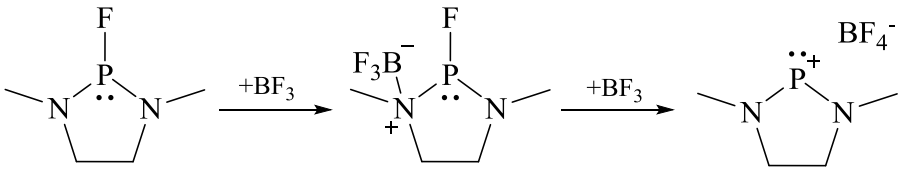

Scheme 10. Synthesis of the cyclic dimethylaminophosphine cation by Fleming et al.

The first acyclic diaminophosphenium cation was obtained by Schultz and Parry[87] from a reaction between $(Me_2N)_2PCl$ and $AlCl_3$ (Scheme 11). While the initial 1:1 ratio of reactants produced an adduct of the two species, subsequent addition of another equivalent of $(Me_2N)_2PCl$ yielded a unique phosphino-phosphenium cation $[(Me_2N)_2P{\leftarrow}P(NMe_2)_3]^+$.

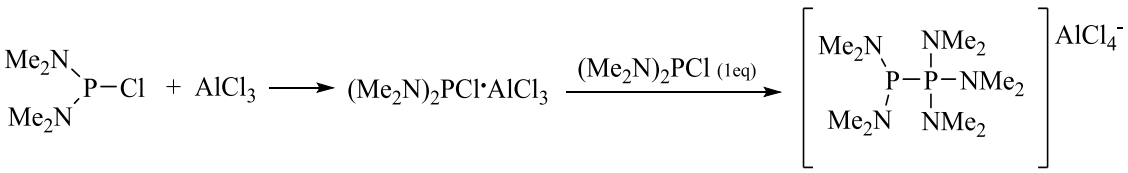

Scheme 11. Synthesis of the first phosphino-phosphenium cation

Alternatively, the same compound can be considered a phosphino-phosphonium cation when represented with a Lewis structure (Figure 12).

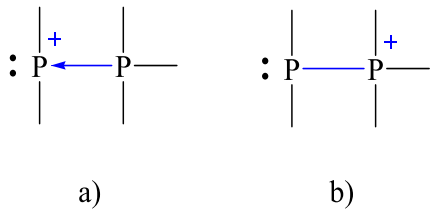

Figure 12. Phosphino-phosphenium cation, represented via a dative bonding model (a) and a phosphino-phosphonium cation, represented via Lewis model (b).

1.2.4.2 Synthesis

Various synthetic approaches to phosphenium cations have been established since their discovery, yielding an array of phosphenium species; many of which were reviewed in 1985.[83] The most commonly followed protocol to generate donor-stabilized dialkylphosphenium and diarylphosphenium salts is halide abstraction of a

halophosphine in the presence of a Lewis base.[83, 87-88] A range of similar adducts has also been generated *via* a subsequent Lewis base substitution with a stronger donor. A simple approach to stable phosphenium salts, such as diaminophosphenium salts, includes the addition of a Lewis base to the salt solution.[83]

Their versatility as reagents has been recognised and explored, and the role of an electrophilic, lone pair bearing, phosphorus centre acknowledged.[83] Despite this, almost thirty years after the discovery of phosphenium cations, Burford *et al.* noted: "The anticipated Lewis acidic behaviour of phosphenium cations has been demonstrated, but the diversity of such interactions is underestimated".[89] Contrary to the profoundly explored donor chemistry of phosphenium cations, their acceptor chemistry has remained relatively unexploited.

1.2.4.3 Reactivity

Theoretical and experimental studies conducted for different phosphenium cations show that stabilization of these species requires π-donation from the substituents (Lewis base) into the vacant P(3p) orbital.[78, 83] Most commonly, this stabilization is provided by one or two strongly π-donating and σ-withdrawing amido fragments. Delocalization of nitrogen lone pairs into the formally vacant P(3p) orbital results in a heteroallylic 3-centre-4-electron (3C-4e) system, which decreases the acceptor ability of the central phosphorus atom and favours the singlet ground state. Frontier molecular orbital studies of diaminophosphenium cations $(H_2N)_2P^+$ and $(Me_2N)_2P^+$ resulted in a general "olefinic" orbital sequence (Scheme 12).

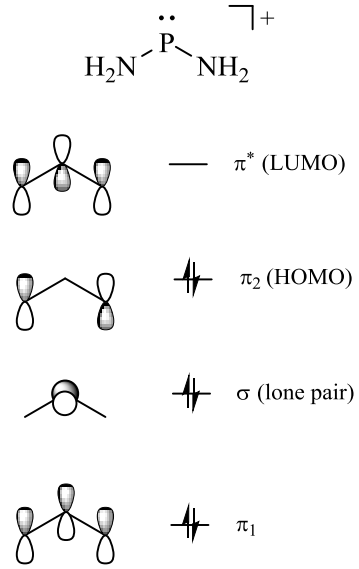

Scheme 12. Olefnic frontier molecular orbital diagram of the diaminophosphenium cation $(H_2N)_2P^+$

Phosphenium cation's Lewis acidic nature can be assigned to its LUMO, represented by a π^* orbital. Similarly, its weakly Lewis basicity derives from the lone pair of electrons occupying HOMO-1 (0.6eV below the HOMO), which point perpendicularly to the 2p AOs of the nitrogen atom. HOMO in a phosphenium cation corresponds to the π_2 orbital of the heteroallylic π-electron system.[90] Alkyl substituents in the amino group can inductively destabilize the lone pair on the nitrogen, resulting in a more "carbenic" frontier orbital sequence, which allows phosphenium cations to behave as electrophiles. Thus, HOMO becomes less relevant for describing R_2P^+ reactivity.[81, 83] Lowest energy level was found to be a $4B_1$ level, which corresponds to the above mentioned 3C-4e hetero-allylic system.[91]

1.2.4.4 R_2P^+ stabilization

According to experimental and theoretical data, thermodynamic stabilization of the phosphenium cations is best achieved through $L \rightarrow P^+$ π-bonding, with at least one amido substituent.

Another mean of stabilization is the delocalization of positive charge *via* cyclic π-electron destabilization, using substituents such as ferrocenyl,[92] Me_5C_5 (multihapto bonding)[93] or diazaphospholium cation (conjugated 6 π-electron system).

On the other hand, other substituents seemingly capable of participating in π-electron conjugation such as halogen, alkoxyl or phenyl groups, were not successful in achieving so. The negative outcome was assigned to insufficient π-donating abilities of halogen and alkoxyl groups to provide required thermodynamic stabilization. Successful stabilization with these groups requires additional support of a transition metal-based substituent.[94] In case of diphenylphosphenium cation Ph_2P^+, the reasons for this are: a) a lack of coplanarity between the phenyl π-orbitals and the P(3p) orbital, and b) a resulting loss of aromaticity within the phenyl groups in case of π-delocalization.[78] While these reasons make isolation of Ph_2P^+ challenging, they allow for the localized positive charge on P, which results in a lower LUMO and higher Lewis acidity compared to $(R_2N)_2P^+$.

1.2.4.5 Complexes with metals

Due to their ambiphilic nature, phosphenium cations are ideal candidates for coordination chemistry with low-valent transition metals. This property allows them to form very short bonds with metals, which is highly useful in allowing them to act as ancillary ligands to metals of groups 6-10. In principle, the interaction is constituted from a dative $P:\rightarrow TM$ σ-bond and a $TM\rightarrow P$ backbonding. In terms of orbital interactions, a dative bond arises from the mixing of metal-LUMO with the phosphenium-(HOMO-1) (P lone pair); and the backbonding is established from a combination of one of the metal's occupied d-orbitals with phosphenium-LUMO.[83]

Examples of phosphenium complexes with metals and their reactivity have been comprehensively reviewed in the past.[83, 95] Intramolecular ligand exchanges between L-type ligands ancillary to the phosphenium unit in phosphenium-metal complexes are typical and often accompanied by geometric izomerisation.[95b] Besides ligand exchanges, phosphenium-metal complexes readily undergo nucleophilic reactions with anionic nucleophiles, which frequently result in izomerisation as well.[83, 95b] Promising uses of phosphenium-metal complexes include catalysis and reactions with unsaturated organic molecules. However, examples of such applications are currently scarce.[96]

1.2.4.6 Complexes with Lewis bases

Phosphenium ions' ability to form donor-acceptor complexes with Lewis bases testifies to their pronounced Lewis acidity. The first such complex $[NHC{\rightarrow}PR_2]^+$ was obtained by Kuhn *et al.* from a reaction between NHC, Ph_2PCl and $AlCl_3$.[97] In their case, reaction favoured the formation of a $[LB{\rightarrow}PR_2][AlCl_4]$ complex (Scheme 13) due to the "base strength" of the NHC ligand. However, analogues reactions have been reported to result in the formation of R_2PCl and $LB{\rightarrow}AlCl_3$ instead (Scheme 13). As a result of the competition between the phosphenium cation and the counterion ($AlCl_4^-$), counterion can endure nucleophilic cleavage, resulting in $LB{\rightarrow}AlCl_3$ adduct formation.[81, 83, 98]

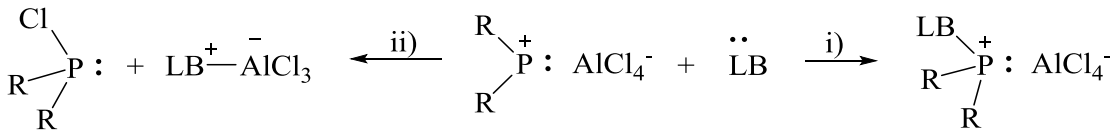

Scheme 13.Product formation, depending of the ligand (Lewis base, LB) strength. i) base strength is not high, so $LB{\rightarrow}PR_2^+$ product formation is favoured; ii) LB is a strong base ("hard" base), which causes a nucleophilic cleavage of the counterion ("hard" acid) and a $LB{\rightarrow}AlCl_3$ adduct formation.

The explanation for this can be inferred from the Pearson's extension of the HSAB principle.[99] Using DFT calculations, Pearson has studied the relationship between molecular properties and chemical bonding in Lewis acid-base complexes. Absolute electronegativity (χ) was used as a measure of base strength, and absolute hardness (η) as a measure of acid hardness. According to the HSAB principle, preferred combinations in a complex are hard acid-hard base, and soft acid-soft base. Thus, highly electronegative bases (hard bases) would prefer binding to $AlCl_3$ (hard acid), while bases of low χ prefer binding to the phosphenium cation (soft acid). Also, higher absolute electronegativity of the low coordinate P(III) cations ($(H_2N)_2P^+$<$(H)(H_2N)P^+$<$(NH)P^+$) was found to be directly proportional to their tendency to form complexes with bases.

Pearson's extension of the HSAB principle proves to be applicable also to the interion interactions between low coordinate P(III) species and their counterions. Some examples include $[(^iPr_2N)_2P][X]$ (X=$AlCl_4$, $GaCl_4$, BPh_4),[100] $[(^iPr_2N)(Mês)P][AlCl_4]$,[101] and [Mes*≡P][$AlCl_4$].[102]

With respect adduct formation with neutral donors, an array of donor-acceptor complexes have been synthesized with carbenes,[103] phosphines,[104] arenes,[105] amines,[106] nitriles,[107] imines,[106b, 108] urea,[106c] thiourea,[106c] selenourea[106c] and gallanes.[109] However, the first example of a dicoordinate P(III) phosphenium dication with has just recently been reported by our group, $[((Ph_3P)_2C)(^iPr_2N)P]^{2+}$, and will be discussed in detail further in the text.[110]

1.3 Carbones

Carbones comprise another group of carbon-based ligands, of a general formula CL_2 (where L stands for a ligand). Due to their unusual properties, they have

indisputably become an essential class of species in coordination chemistry; from assisting stabilization of the highly labile species and serving as ligands in general, to initiating scientific discussions over bonding principles.[111]

"Carbone" name derives from a divalent "naked" carbon(0) centre, which bears *two electron pairs*, to differentiate them from previously discussed carbenes - *one electron pair* donating carbon(II) ligands ($:CR_2$).[112]

Carbodiphosphoranes (CDPs) are carbone species in which both ligands are phosphines ($(R_3P)_2C$). Ramirez *et al.* have reported the first example of this kind in 1961.[113] Unfortunately, the new class of compounds did not further attract significant attention, since the formulas used (at that time) to describe carbodiphosphoranes (Figure 13, a-d) were not indicative of its nature as a carbon-complex.

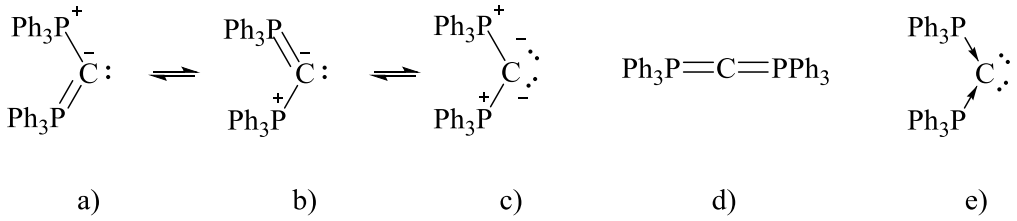

Figure 13. Different structural depictions of hexaphenylcarbodiphosphorane: in terms of resonance structures (a-c), a ylidic form (d), a dative structure (e).

Section 1.3.1. will cover some of the most important structural features of carbones that derived from the theoretical studies,[112, 114] as well as their comparison to the NHC ligands. These differences account for their different chemical properties and rationalize our reasons for using carbodiphosphorane over NHC as a donating ligand in our study.

1.3.1 Carbone versus carbene

1.3.1.1 Bonding analysis

The two highest lying occupied orbitals (HOMO and HOMO-1) of examined carbodiphosphoranes (L = PH_3, PMe_3, PPh_3) correspond to π and σ lone-pair orbitals, respectively, with contributions from σ^*(P-R) orbitals. In all three cases, the energy of $HOMO^{-1}$ is slightly lower than HOMO. As depicted in Figure 14, a prominent orbital interaction is the one where carbon attains its singlet (^{1}D) state of $2s^2\ 2p_{\pi\perp}^2\ 2p_{\sigma}^0\ 2p_{\pi\parallel}^0$ configuration (relative to the molecular plane), and ligand orbitals σ(+,+) and $\pi_{||}$(+,-) donate electrons into its vacant $2p_{\sigma}^0\ 2p_{\pi\parallel}^0$ atomic orbitals (L:→C←:L). As such, carbon atom in carbones formally attains an electron octet, in comparison to a sextet in carbenes.

The lone-pair character of orbitals at the central carbon was also suggested by NBO studies, with σ-MO electron occupation of 1.59 to 1.62 electrons, π-MO electron occupation 1.51 to 1.53 electrons, and partial atomic charge at the central carbon of -1.32 to -1.47 electrons. Since L-C bonds in carbones are not formed *via* direct participation of carbon valence electrons, carbon remains divalent. Thus, its σ and π available lone pairs account for carbone's high Lewis basicity, and ability to strongly bond to main-group Lewis acids or transitional-metal complexes.

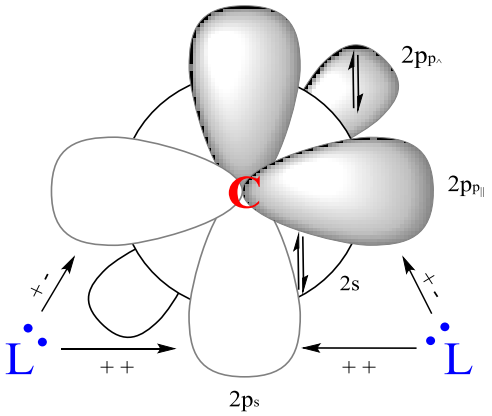

C: X^3P ⟶ ^1D 29.1 kcal/mol (calc. 43.5 kcal/mol)

L	CL_2	
	DE_{int} [kcal/mol]	D_e [kcal/mol]
PPh_3	189.3	158.5
CO	233.8	206.9
NHC	260.8	210.0

Figure 14. Left: Schematic representation of orbital interactions between ligands and the central carbon atom in CL_2. Right, top: Expected and calculated energies for C. Right, bottom: Interaction energies (ΔEnt) and dissociation energies (De) for fragments in frozen geometries and electronic reference states.[115]

In contrast, carbenes are neutral divalent carbon compounds of formula :CR_2, in which the central carbon atom possesses a lone pair of electrons, which can be associated with two nonbonding orbitals in various ways. The simplest representative is methylene, :CH_2.

The electronic geometry of carbenes can be nonlinear (bent) and linear (Scheme 15), and it is governed by their spin ground state and multiplicity. In the nonlinear structure, central carbon is sp^2 hybridized, while sp hybridization dominates the linear structure. A majority of carbenes are bent. Out of four possible ground states for sp^2 hybridized carbon, the most commons are: the $\sigma^1 p_\pi^1$ $^3B_1$ triplet ground state (Scheme 15a), where both electrons are of parallel spins; and the singlet state $\sigma^2 p_\pi^0$ $^1A_1$ (Scheme 15b), with both antiparallel oriented electrons in the σ orbital.

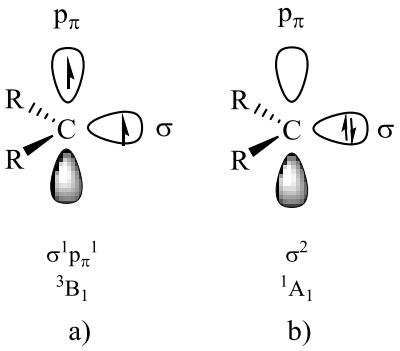

Scheme 14. Ground state spin multiplicity in the triplet carbene (a) and singlet carbene molecules (b).

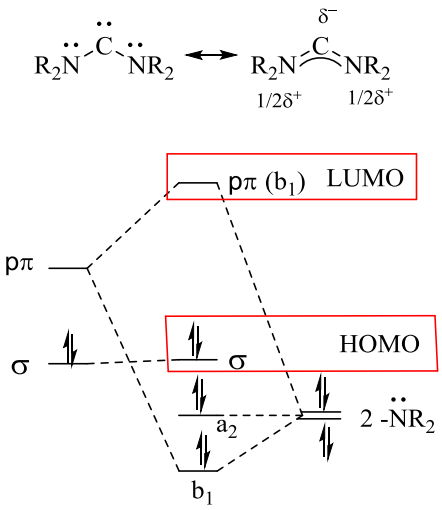

Figure 15. Mesomeric effects in the NHC substituents

An important representative of the singlet carbene class is N-heterocyclic carbene, which possess a heterocycle and a minimum of one nitrogen heteroatom. $HOMO^{-1}$ in an N-heterocyclic carbene (NHC^{H}) is a delocalized π orbital (p_π-p_π delocalization, Figure 15), which originates from the donation of the lone pair electrons on the nitrogen (in the ylidic form) to the vacant p-orbital on carbon. On the other hand, HOMO displays a σ-type lone pair orbital at the central carbene C(II) atom. Interestingly, overall charge distribution at the central carbon is +0.04e. Despite the slightly positive charge, the negative charge of its energetically high σ lone pair allows carbene carbon to exhibits nucleophilic behaviour.

1.3.1.2 Basicity studies

Prior to the discovery of the first stable carbene,[116],[117] amines and imines were considered the first choice for a highly basic neutral compound, due to the strongly attractive interaction of the nitrogen's lone pair of electrons with protons. In comparison to other second-row electron-pair bearing atoms, such as oxygen or fluorine atoms, lone-pair bearing nitrogen orbital is higher in energy. Proton affinity (PA) value is a gas-phase property of an atom or a molecule and as such, an important measure of basicity.[118] Energy of the higher lying lone-pair orbital is proportional to PA values. Consecutively, nitrogen bases have higher PA values than oxygen or fluorine bases. By this analogy, even higher basicity was expected from carbon-bearing lone pair compounds.[119]

Indeed, experimental and theoretical calculation displayed a PA of about 258 kcal/mol for parent NHC, and values above 220 kcal/mol for acyclic carbenes; which place carbenes among superbases. PA values can also be tuned by substituents, as calculated PAs for substituted NHCs go up to 275 kcal/mol.[114e, 120a, 120b] For instance, electron-withdrawing halogen substituents on NHC ligands decrease first proton affinity values, while σ-donating alkyl and aryl groups increase them. Whereas second PA values don't follow the same trend and make the second protonation challenging, they still remain relatively high, with the highest value (106.5 kcak/mol) reported for π-donating amino (-NMe_2) groups.[114e]

Since carbone compounds possess two lone pairs or electrons, PA values are key measures of their basicity. With respect to first PA strengths, halophosphine ligands in $C(PR_3)_2$ amount to 209-280 kcal/mol, slightly higher than PAs of carbenes, but enough to place them both among super bases. An overview of theoretical values

for selected normal N-heterocyclic carbenes and carbodiphosphoranes is displayed in Table 1, bellow.

Table 1. Reported calculated first (PA_1) and second (PA_2) proton affinities and NBO partial charges at the central carbon atom q(C) of selected N-heterocyclic and carbodiphosphorane compounds in kcal/mol[114e]

M	R	PA_1	PA_2	q(C) M	q(C) M-H^+	q(C) M-$(H^+)_2$
NHC	F	228.9	38.9	0.04	0.12	-0.17
	C	244.3	57.6	0.07	0.18	-0.13
	H	254.2	47.7	0.04	0.20	-0.14
	Me	262.3	71.8	0.04	0.21	-0.12
	Ph	264.7	100.1	0.08	0.21	-0.10
	NH_2	253.9	76.7	-0.01	0.23	-0.12
	NMe_2	259.8	106.5	0.02	0.22	-0.11
	^{t}Bu	270.6	92.3	0.05	0.20	-0.13
	Mes	270.4	105.3	0.08	0.22	-0.11
	Ad	274.9	105.7	0.05	0.20	-0.12
CDP	F	209.3	70.6	-1.69	-1.53	-1.30
	Cl	227.9	116.4	-1.35	-1.36	-1.13
	H	255.7	114.4	-1.32	-1.26	-1.01
	Me	278.4	156.2	-1.47	-1.36	-1.07
	Ph	280.0	185.6	-1.43	-1.33	-1.07
	NH_2	280.0	153.5	-1.51	-1.42	-1.17
	NMe_2	279.9	174.9	-1.64	-1.46	-1.18
	THP	287.6	188.9	-1.59	-1.44	-1.18
	Mes	280.7	201.1	-1.47	-1.33	-1.11
	Cy	280.5	184.0	-1.56	-1.39	-1.11

Whereas values in carbenes correlate to the electronegativity of the substituents, in carbodiphosphoranes this is not the case. However, a clear discrepancy between the two ligand species is reflected in astoundingly higher second PA values for carbodiphosphoranes of up to 201.1 kcal/mol (R=Mes). In comparsion, second PAs for NHC_{NMe2} and $C(P(NMe_2)_3)_2$ amount to 106.5 kcal/mol and 174.9 kcal/mol, respectively. High second PA values allow carbones to be isolated as deprotonated zerovalent carbon salt species in a condensed phase.

1.3.1.3 Reactivities

When a monoadduct $L{\rightarrow}BH_3$ (L = $(Ph_3P)_2C$ or NHC) was reacted with B_2H_6, Petz *et al.* obtained a unique bisadduct, $(Ph_3P)_2C{\rightrightarrows}(BH_3)_2$, a presumed precursor to the isolated and characterised $[(Ph_3P)_2C{\rightrightarrows}B_2H_4(\mu\text{-}H)][B_2H_7]$.[121] On the other hand, $NHC{\rightarrow}BH_3$ did not react with B_2H_6.

A reaction between $B(C_6F_5)_3$ and $L{\rightarrow}BH_3$ adducts, in case of $(Ph_3P)_2C$ ligand, yields a $[(Ph_3P)_2C{\rightrightarrows}BH_2]^+$ complex.[122] On the other hand, when L=NHC, a $[NHC\text{-}BH_2(\mu\text{-}H)BH_2\text{-}NHC]^+$ complex is formed, in which each NHC ligand donates a single lone pair of electrons.

These examples clearly portray the ability of a carbone ligand to employ its two available lone pairs and act as a two-fold base to Lewis acids, which is not the case for NHC ligands.

1.3.2 Carbodiphosphorane coordination modes to Lewis acids

Considering their high basicities, carbones can easily form adducts with Lewis acids in a monodentate coordination mode (Figure 16a). However, their main attribute derives from the π-lone pair located in HOMO, which can be used to enhance bonding in the form of an additional bond to a bidentate Lewis acid (Figure 16b), or to establish a bond with an additional monodentate Lewis acid (Figure 16c). Donor-acceptor model of depiction in this figure is chosen to emphasize CDPs donor-abilities, irrespective of the actual bonding nature in compounds, with awareness of the latest criticism over the use of dative bonds.[123]

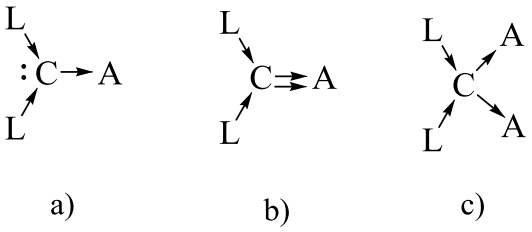

Figure 16. Carbone coordination modes to the Lewis acid A: a) via σ lone pair donation to a Lewis acid; b) via both, σ and π, lone pair donations to a single Lewis acid; c) via two lone pair donations, each to a separate Lewis acid.

In compounds where carbone is coordinated to a single monodentate, Lewis acid, lone pairs located in carbon's second HOMO can engage in negative hyperconjugation. As a result, some electron density will be back-donated to the ligand. In case of carbodiphosphoranes ($L=PR_3$), electron density will be back-donated into P-R σ^*orbital, which will slightly weaken the P-R bond, but strengthen the P→C bond.[13] Relatively many adducts of carbones and main-group species in this coordination mode are known, and they usually occupy a planar arrangement of atoms.[13] Carbones of choice can vary from carbodiphosphoranes, electron-rich allenes, carbodicarbenes, mixed and border-line carbones, to carbodiarsoranes and carbodiamines.

Electron-rich allenes $R(Me_2N)C=C=C(NMe_2)R$ ($R=NMe_2$, OEt) have been used in the past to successfully stabilize small molecules such as CO_2, CS_2 and SO_2.[124] However, the first example of $(Me_2N)_2C=C=C(NMe_2)_2$ (TAA)-assisted stabilization of a group 13 Lewis acid was reported just recently.[125] In particular, the TAA-$GaCl_3$ adduct was obtained as a mixture of two enantiomers, when $GaCl_3$ was added to a THF solution of the corresponding allene. Reaction of TAA with $[ClAu(PPh_3)]$ and a subsequent exchange of counterion Cl^- by SbF_6^-, resulted in the formation of $[(((Me_2N)_2C)_2C)Au(PPh_3)][SbF_6]$.[126]

In general, adducts of carbones and transition metals can be obtained by introducing a free double ylide to a transition metal species, containing a labile-bonded ligand or an available coordination position.[127] Bertrand's group recently introduced a carbodicarbene carbone. Its strong donor abilities were demonstrated in a reaction with $[Rh(\mu\text{-}Cl)(CO)_2]$ in benzene, which yielded an orange crystalline adduct $[RhCl(CO)_2\{C(PPh_3)_2]$.[128] With respect to main group chemistry, Chen *et al.* have reported group 13 adducts such as $[\{(PPh_3)_2C\}AlCl_3]$ and a dicationic hydridoborenium ion $[\{(NHC)_2C\}_2BH]^{2+}$, stabilized by two carbodicarbenes. Similarly, two carbodicarbenes were used by Vidovic *et al.* to achieve the unusual "bis(carbone) capture of a $P(III)^{3+}$ cation" $[\{(NHC)_2C\}_2P]^{3+}$.[129] Bond lengths of 1.733(4) Å (P1-C1) and 1.747(4) Å (P1-C4) and the increment in the resulting compound's average C1/C4-C bond distances were suggestive of the existing $(NHC)_2C\rightarrow P$ dative bonds.

Among carbodiphosphoranes, hexaphenylcarbodiphosphoranes predominate as Lewis bases in adducts with many group 13-15 compounds which serve as Lewis bases.

Some exceptions, such as cyclic carbone-stabilized species include its adducts with borane[130]and galliumtrichloride.[125]

While cyclic carbone adduct of borane BH_3 was firstly reported by Schmidbaur *et al.* in 1981, the first crystal structure of the carbone-borane adduct was published only recently by Petz *et al.*[121] who used a hexaphenylcarbodiphosphorane as a Lewis base. The crystals were obtained by introducing a toluene or a THF solution of $C(PPh_3)_2$ to the gaseous B_2H_6. The reaction product was replicable in the solvent-less conditions, in which the yielded crystals appeared colourless. In both cases, central

carbon atom displayed clear pyramidalization with the sum of the angles ~359°.[121] Similar synthetic method was applied to other Lewis acidic moieties of group 13, presented in Table 2.[13, 131] Average P-C bond values (Table 2) reflected short distances in all compounds, which indicated the involvement of the $HOMO^{-1}$ lone pair into the back-donation into the antibonding orbital of P-C_{Ph}.

Table 2. Summary of known triphenylcarbodiphosphorane adducts of Group 13 compounds, and their mean P-C bond values; L=C(PPh$_3$)$_2$

Adduct	Average P-C_{Ph} bond length [Å]
L-BH_3	1.685(3)
L-BPh_3	-
L-$AlBr_3$	1.718(3)
L-$GaCl_3$	1.714(1)
L-$InMe_3$	1.685(3)
L-$InCl_3$	1.706(7)
L-$InBr_3$	1.687(7)

Carbone-silica adducts (A = $SiMe_3$, $SiPh_2H$, $SiMe_2Et$, $SiCl_3$)[13, 132] have been known for a long time before Alcarazo *et al.*[125, 133] significant contributions to Group 14 with analogues of chlorinated Ge and Sn compounds, summarised in Scheme 16.

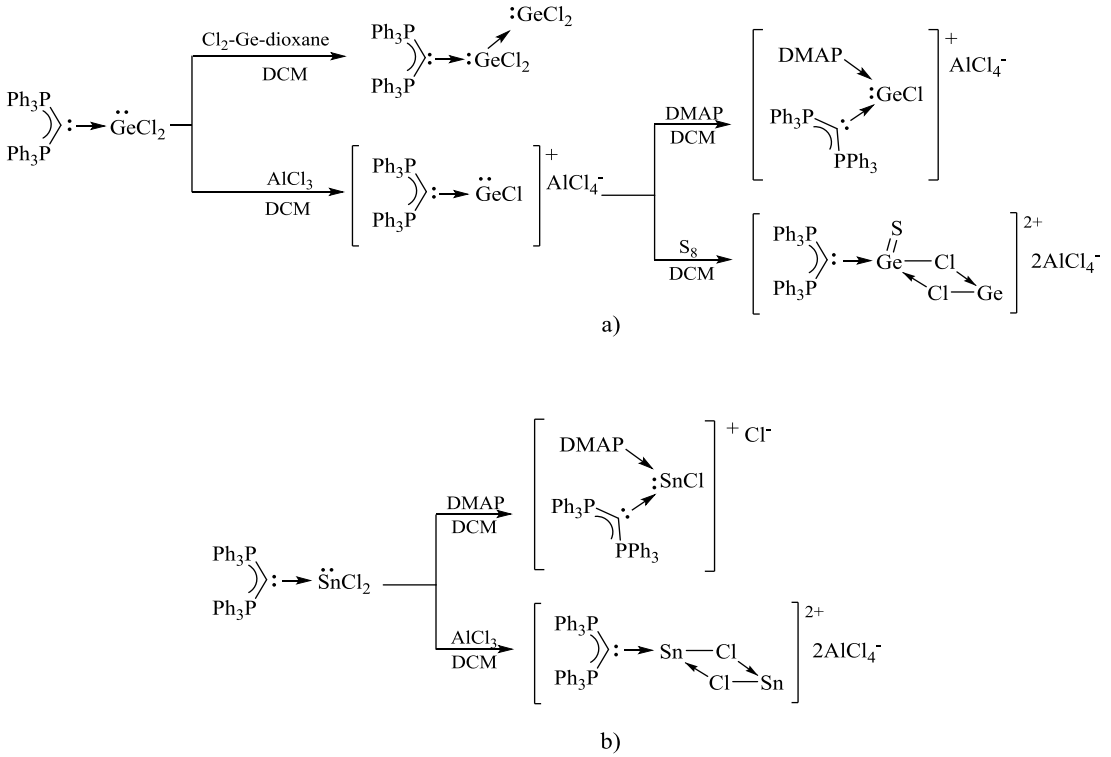

Scheme 15. Examples of a) carbone-germanium and b) carbone-stannanium complexes.

Surprisingly, not many species in which carbone simultaneously stabilizes two Lewis acids (Figure 17c) have been isolated and characterised so far. The simplest, and most abundant, isolated example is a diprotonated carbone $[H_2CL_2]^{2+}$, with different counteranion and ligand combinations, many of which have been reviewed recently by Petz.[13] A variation, concerning overall charge of such complexes, occurs when one of the ligands is replaced by an anionic species. Replacing one of the ligands with PPh_2OBF_3, PPh_2OBI_3 or PPh_2OAlBr_3, results in a monocationic adduct. A few neutral diprotonated carbone species have been accessed *via* a reaction between 1,1-Bis(diphenylphosphino)methane and a borane.[134]

Systems in which one or both hydrogen atoms are replaced with a halogen (X = F, Cl) have also been reported and structurally characterised (Figure 14a-c).[135] Since halogens bear higher electronegativity than carbon, the electron density of the donating lone pair will become more concentrated at the halogen, resulting in X^-,

suitable to donate the same electrons back to the carbon atom. Consequently, an arrow in the opposite direction has been suggested for these systems (Figure 17a).[13]

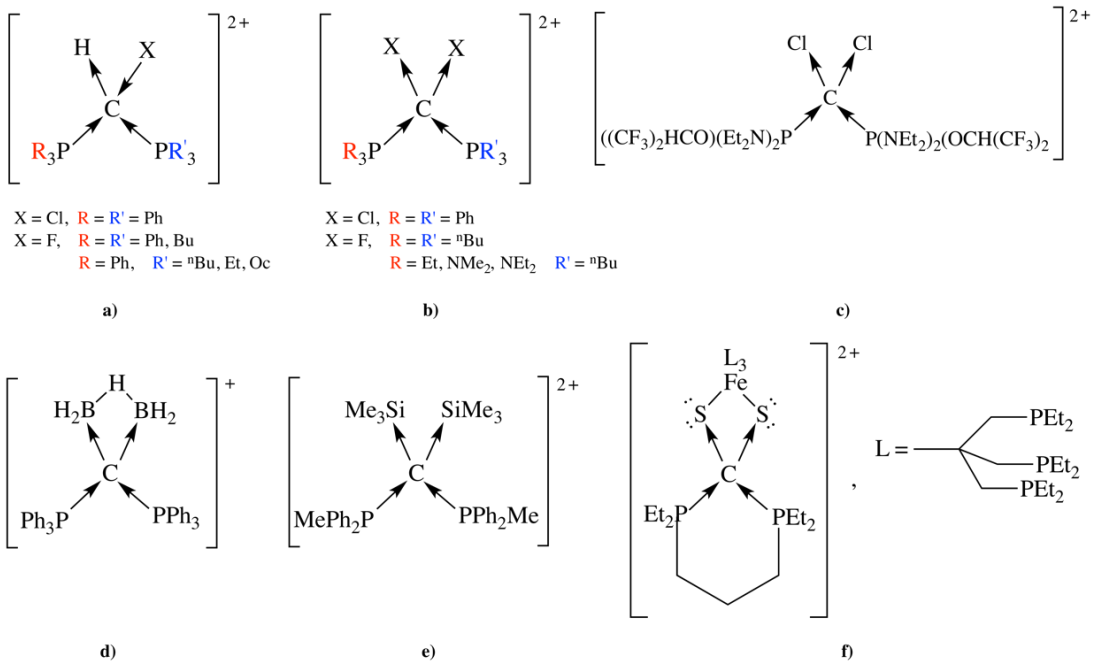

Figure 17. Selected known compounds in which carbone C is connected to two Lewis acid simultaneously

In 2009, Petz *et al.* synthesized [{(μ-H)H_4B_2}{$C(PPh_3)_2$}][B_2H_7] (Figure 17d) from a reaction between [H_3B{$C(PPh_3)_2$}] and dimethoxyethane. [121] The final complex is believed to form due to solvent-induced deprotonation of the originally formed bis-borane adduct. Resulting [{(μ-H)H_4B_2}{$C(PPh_3)_2$}][B_2H_7] is known as the first example of carbone as a twofold base to two main-group Lewis acids. However, back in 1976, Schmidtbaur *et al.* reported a species in which $(MePh_2P)_2C$ carbon was using both lone pairs to donate to two trimethylsilyl moieties, $[(Me_3Si)_2C(PMe_3)_2]^{2+}$ (Figure 17e).[136] The compound was obtained as a white precipitate resulting from a reaction between $(MePh_2P)_2C$ and Me_3SiCl in benzene but decomposed within minutes, rendering the full characterisation difficult to complete. While several examples of silylated carbodiphosphoranes are known,[132, 137] no other examples of similar bis-silyl carbones have been accessed since. Another complex, which

resembles a cyclic carbodiphosphorane donating its lone pairs to two Sulphur atoms (Figure 17f), was characterised by Bianchini *et al.* in 1980's.[138] Unfortunately, this five-coordinate iron(II) complex hasn't been acknowledged as a carbone-containing compound.

1.4 Carbone-stabilized phosphenium dication

Various electron-rich ligands have been recently employed to stabilize mono-nuclear polycations of main-group elements. Due to the coordinative saturation or Lewis base resemblance, novel species failed to exhibit Lewis acidic behaviour. Similar behaviour was also observed for NHC-stabilized polycationic P(III) compounds, which resembled Lewis basic neutral phosphines despite being successful in chloride substitution reactions and coordination chemistry. However, our group has reported the first example of a Lewis acidic, dicoordinate phosphenium dication, using the exceptional donor abilities of the carbone ligand.

The targeted phosphenium ion was obtained *via* the chloride abstraction from the monocationic precursor $[(Ph_3P)_2CP(N^iPr_2)(Cl)]^+$ according to the Scheme 17 below. ^{31}P NMR shift of 355.7 ppm for $P_{central}$ was characteristic of two-coordinate phosphenium cations (200-500 ppm). Electron-depletion at the $C_{carbone}$ was also evident from the ~40 ppm downfield shift in ^{13}C NMR compared to the monocationic precursor.

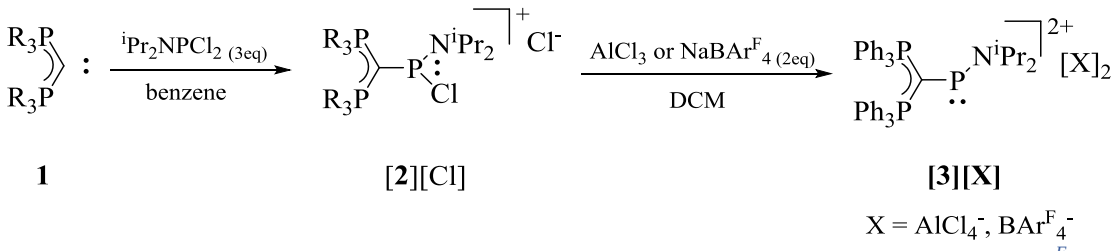

1 **[2][Cl]** **[3][X]**

X = $AlCl_4^-$, $BAr^F_4^-$

Scheme 16. The synthesis of a carbone-stabilized phosphenium dication, where X=$AlCl_4^-$ or $Bar^F_4^-$.

A crucial factor in providing thermodynamic stability to the dication was an allene-like nature of the C-P-N unit. Planarity of the P_2CPNC_2 fragment allowed for a "flow" of adjacent carbone and amino π-electron lone pairs into the vacant P($3p_\pi$) orbital. Conjugation of the C-P-N fragment was confirmed with the shortening of the bonds between $P_{central}$ and carbone and amino substituents, compared to the monocationic precursor.

1.4.1 Computational analysis

4π heteroallylic character of the C-P-N moiety was also confirmed by DFT calculations. Predicted $C_{carbone}$-P (1.745 Å) and P-N_{amino} (1.647 Å) bond lengths were in accordance with the experimental values 1.739(5) Å and 1.623(5) Å, respectively. HOMO was delocalized along the C-P-N fragment, while the molecular orbital corresponding to the lone pair on $P_{central}$ ($HOMO^{-12}$) indicated significant destabilization relative to $HOMO^{-12}$ of $[P(NMe_2)_2]^+$. These results indicated better σ-donating abilities of $\mathbf{3}^{2+}$. Calculations also showed better stabilization of $HOMO^{-14}$ and a low-lying LUMO (π^*) for $\mathbf{3}^{2+}$ compared to $[P(NMe_2)_2]^+$, indicating better π-interaction within the C-P-N fragment (versus N-P-N), and better electron-accepting properties of $\mathbf{3}^{2+}$.

Furthermore, Natural Bond Orbital (NBO) and Natural Resonance Theory (NRT) analysis for $\mathbf{3}^{2+}$ and an analogue $[(H_3P)_2CP(NH_2)]^{2+}$ further confirmed a 3-centre-4-electron (3C-4e) bond for the C-P-N moiety. Based on the analysis, the best description of the electronic structure is *via* two resonance forms, represented in Scheme 18. Consistent with the 3C-4e bond description, each resonance structure was characterised with a low lone pair electron occupancy (1.54-1.69 e) and a significant second order interaction energy (200-257 kJ/mol) for lone pair$\rightarrow \pi^*$. However, such

description suggested a formal neutral charge on $P_{central}$, which was not consistent with the reactivity that $\mathbf{3}^{2+}$ exhibited.

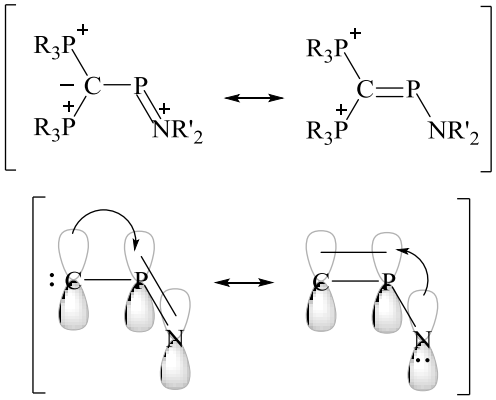

Scheme 17. Calculated resonance forms for $\mathbf{3}^{2+}$ and an analogue $[(H_3P)_2CP(NH_2)]^{2+}$

1.4.2 Lewis acidic reactivity of $[(Ph_3P)_2CP(N^iPr_2)]^{2+}$

The Lewis acidic behaviour of $\mathbf{3}^{2+}$ was confirmed in reactions with trimethylphosphine (PMe_3) and 4-Dimethylaminopyridine (DMAP)[110]. In the initially performed reaction of equivalent amounts $[\mathbf{3}^{2+}][AlCl_4]_2$ and PMe_3, a complex reaction system of two occurring equilibria was observed (Scheme 19).

Scheme 18. Proposed equilibria for the interaction of $[\mathbf{3}^{2+}][AlCl_4]_2$ and PMe_3 (1:1)

The observed equilibria could be manipulated by varying the reaction temperature and/or molar ratios. In general, low temperature favoured $\mathbf{3}^{2+}\cdot\mathbf{PMe_3}$ adduct formation, while molar increment of PMe_3 drove a reaction towards the $\mathbf{2}^{+}$ cation precursor and a $\mathbf{Me_3P{\cdot}AlCl_3}$ adduct. Formation of the $\mathbf{DMAP{\cdot}AlCl_3}$ was also favoured when DMAP was used as a choice of base. These results were consistent with the HSAB concept, as both (hard) bases preferred to react with $AlCl_4^-$ (hard acid) over $\mathbf{3}^{2+}$.

Counterion interference for this reaction was eliminated when $AlCl_4^-$ was changed to $BAr^F{}_4^-$. However, the equilibrium between the starting material and an adduct

formation was still present (Scheme 20). Van't Hoff plot by variable temperature showed that this was due to the establishment of a very weak P-P bond between the two species in the adduct.

$$[\mathbf{3}^{2+}\cdot PMe_3][BAr^F{}_4] \underset{}{\overset{+PMe_3}{\rightleftharpoons}} [\mathbf{3}^{2+}][BAr^F{}_4]_2$$

Scheme 19. Proposed equilibria between $\{3^{2+}\}\{Bar^F{}_4\}$ and $3^{2+}\cdot PMe_3$ complex

The oxophilic nature of the dication was confirmed in reactions with water and methanol. Equimolar addition of H_2O/MeOH resulted in oxidative addition, without the former breakage of the O-H bond.[139] NMR studies confirmed the formation of P-H and P-OR (R=H, OH) fragments, as well as the fluxionlity of the proton between P-O-R (R=H) and the N of the amino group, which was later abstracted with NEt_3• $\mathbf{3}^{2+}$ was the first non-metallic compound to perform such O-H bond activation, characteristic for transition metals[140], in the absence of any additives and at room temperature. Another proof of $\mathbf{3}^{2+}$ oxophilicity was its ability to polymerise THF.

While Lewis acidity and high oxophilicity of $\mathbf{3}^{2+}$ were undoubtedly confirmed in the previously discussed studies,[110, 139] counterion interference and purification difficulties with $BAr^F{}_4^-$ as a counterion rendered further reactivity studies challenging. Thus, overcoming those issues and performing subsequent reactivity studies formulated the outline of this thesis.

Chapter II primarily focuses on the synthetic viability and characterisation of $\mathbf{3}^{2+}$ in the presence of different counterions, followed by the reactivity studies which reveal its exceptional fluorophilic and oxophilic nature.

The highly oxophilic behaviour of $\mathbf{3}^{2+}$ is further elaborated in Chapter III, where a seemingly predictable reaction with pyridine *N*-oxide (PyO) leads to

unexpected oxygen insertion into a P-C bond *via* the Baeyer-Villiger reaction mechanism.

Finally, in Chapter IV, we continue to use exceptional electron-donating abilities of a carbone ligand to stabilize highly reactive dioxophosphorane moiety species. This is the first example of a parent-metaphosphonate in which the reactivity of the PO_2 unit is not quenched, and thus allows insight into the chemical nature of these elusive species.

CHAPTER II:

Preparation, structural analysis and Reactivity Studies of a Phosphenium Dication

2.1 Results and Discussion

The objective of this project was: 1) to synthesize analogues of $\mathbf{3}^{2+}$ by changing its carbone and amino substituents to investigate the dication's properties dependence on electronic and steric changes; 2) to find an appropriate counterion for $\mathbf{3}^{2+}$, that would allow for the simple purification and stability towards Lewis bases; 3) to explore the scope of $\mathbf{3}^{2+}$ reactivity.

The first objective was approached by introducing less steric hindrance or more stability *via* methyl and cyclic groups, respectively. For that purpose, carbone and its analogues ($C(PPh_2Me)_2$ and $C(PPh_2(CH_2)_{3/2})_2$), were used in combination with the following amino groups: $^{i}Pr_2N$, Cy_2N, Me_2N. The approach to the second objective consisted of exploring the synthetic viability of $\mathbf{3}^{2+}$ in the presence of eight counterions: $BAr^{Cl}{}_4^-$, SbF_6^-, $GaCl_4^-$, PF_6^-, OTf^-, BPh_4^-, BF_4^-, and ClO_4^-.

2.1.1 Ligand exchange

To address how phosphine substituents of the stabilizing carbone ligand affect the Lewis acidic behaviour of the targeted dication, monocationic precursor analogues of $\mathbf{2}^{+}$ were prepared according to the procedure shown in Scheme 20.

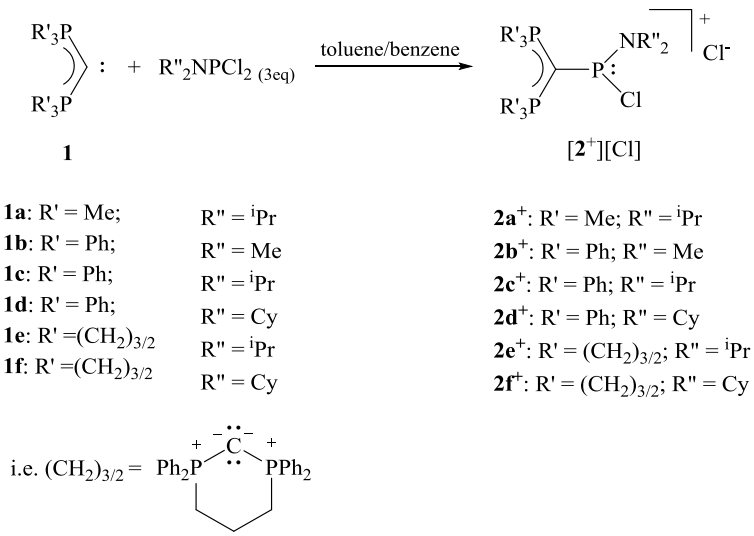

Scheme 20: Synthetic route for obtaining analogues of $\mathbf{2}^{+}$

This was achieved by adding a benzene solution of the carbone ligand into the corresponding aminodichlorophosphine (R''_2NPCl_2; R'' = ^{i}Pr, Cy, Me) in excess. Vigorous stirring of the reaction mixture resulted in the formation of the white precipitate within 30 min. The targeted carbone-for-chloride exchange was inferred from the ^{31}P NMR analysis of these reaction mixtures (Table 3).

Table 3. ^{31}P NMR shifts (δ_P in ppm) obtained for the isolated monocations of the formula $[R''_2NP(C(Ph_2R')_2Cl]^+$. Substituent combinations that were not synthetically attempted are denoted with a dash "-".

R' \ R''	Me	^{i}Pr	Cy
Me	-	138 (br), 21 (d)	-
Ph	162 (t), 23 (d)	133 (t), 25 (d)	139 (t), 25 (d)
$(CH_2)_{3/2}$	-	133 (t), 15 (d)	No reaction, starting material present

The successful synthesis was characterised by the appearance of two second-order signals in the ^{31}P NMR spectra of the resulting precipitate: a doublet around 20 ppm ($P_{carbone}$), and a triplet around 140 ppm ($P_{central}$). While triplet signals for $P_{central}$ are in a comparable range, δ_P of **2b**$^+$ is shifted more downfield (~162 ppm). The difference in the position of the δ_P shift can be assigned to the higher flexibility and the significantly reduced steric hindrance provided by Me groups, compared to ^{i}Pr and Cy in **2c**$^+$ and **2d**$^+$, respectively. ^{13}C NMR spectra of the obtained monocations were comparable, displaying a doublet of triplets that stems from the central carbon atom of the donating carbone ligand. The synthesis was successful for all attempted reactions, except for **2f**$^+$. A possible reason for such outcome is a high steric demand that the combination of two cyclic substituents would impose on the resulting **2f**$^+$, relative to other monocations.

2.1.2 Synthetic viability – counterions

A previously reported procedure for the synthesis of [**3c**][X]$_2$ (X=$AlCl_4^-$ or $BAr^F{}_4^-$) involved the addition of 2.1eq of either $AlCl_3$ or $NaBAr^F{}_4$ to the DCM solution containing the corresponding monocationic precursor **[2c]**[Cl].[141] The appearance of the ^{31}P NMR signal for the central P atom at around δ_P 356 ppm was the most indicative piece of evidence for the formation of the two-coordinate phosphorus species. The peak was within the reported range for the two-coordinate phosphenium cations, and more than 200 ppm downfield shifted, as compared to the analogous signal for the **2c**$^+$.[141] In addition, δ_P values for the central P were found to be independent of the nature of the counterion, indicative of the absence of close interion contacts in the solution state. Unfortunately, $AlCl_4^-$ and $BAr^F{}_4^-$ were not suitable counterion choices for **3**$^{2+}$; $AlCl_4^-$ interfered with dication's reactivity, while $BAr^F{}_4^-$ made dicaton's purification by recrystallization somewhat challenging. To overcome these issues, the initial step was to explore the suitability of another counterion. Considering the stability of **3c**$^{2+}$ with both coordinating ($AlCl_4^-$) and large, weakly-coordinating ($BAr^F{}_4^-$) counterions, it was assumed that virtually any other counterion could successfully be employed for the preparation of these species. For that reason, only the synthesis of **3c**$^{2+}$ was attempted in the presence of the following counterions: $BAr^{Cl}{}_4^-$ (Ar^{Cl} = 3,5-Cl_2-C_6H_3), SbF_6^-, PF_6^-, BF_4^-, $GaCl_4^-$, ClO_4^-, OTf^- (Tf = O_2SCF_3), BPh_4^- (Scheme 22).

Surprisingly, the successful isolation of **3**$^{2+}$ was only viable in the presence of $BAr^{Cl}{}_4^-$, $GaCl_4^-$ and SbF_6^-. Results of ^{31}P NMR spectroscopy indicated complete conversion of the starting material and excellent correlation with the previously reported[142] NMR data (δ_P for $P_{central}$ ~ 356 ppm).

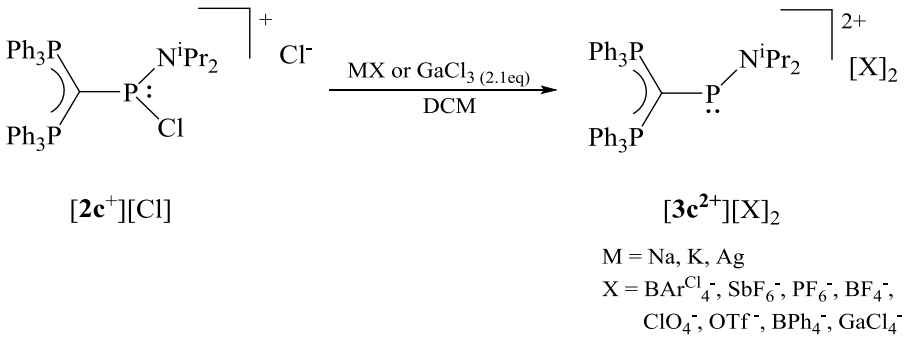

Scheme 21: The targeted reaction for the synthesis of 3^{2+}. Successful outcome was achieved when MX = $NaBAr^{Cl}{}_4$, $AgSbF_6$; and when $GaCl_3$ was used as adduct. In other cases, the targeted product was not acquired.

Reactions involving remaining anions resulted in complex mixtures of unknown products in almost all cases. It was suspected that such result was due to the highly oxophilic nature of **3**$^{2+}$, which causes it to react destructively towards oxygen-containing anions. To confirm this, [**3c**][X]$_2$ (X = $BAr^F{}_4$, SbF_6) was treated with an equivalent of NEt_4OCl_4 in dichloromethane, which resulted in the immediate formation of several unidentified products. Further proofs for the high oxophilicity of **3c**$^{2+}$ arose from the later conducted reactivity studies, presented in detail in Sections 2.1.5-2.1.7 and Chapter 3, below. [139]

Similarly, the behaviour of **3c**$^{2+}$ towards fluorine-containing substrates, which includes decomposition in the presence of BF_4^- and PF_6^-, versus the isolability of **[3][SbF$_6$]**, may be correlated with Fluorine Ion Affinity (FIA) of the dication. Introduced by Bartlett *et al.*,[143] FIA represents enthalpy that is being released when a Lewis acid (LA) binds a fluoride ion (F^-) (Eq. 1).

$$LA_{(g)} + F^-_{(g)} \xrightarrow{\Delta H = -FIA} [LA-F]^-_{(g)} \qquad \text{(Eq. 1)}$$

FIA value is proportional to the strength of the Lewis acid, and as such used as a reliable measure of Lewis acidity.[144] Higher FIA value implies stronger Lewis acidity. FIA literature values for the Lewis bases relevant to this work (Table 4), increase in the following order: BF_3<PF_5<$GaCl_3$<$AlCl_3$<$B(C_6H_3(CF_3)_2)_3$<SbF_5.[145]

Following the trend, our results reveal that $\mathbf{3}^{2+}$ exhibits higher fluorophilicity than BF_3 or PF_5, but lower than of $BAr^F{}_4$ and SbF_5^-; which is why dications with anions of the latter two can be isolated. Analogous observations have been previously reported for the synthesis of gallium cations.[125, 146]

Table 4. An overview of the Fluoride Ion Affinity (FIA) values (in KJmol^{-1}) reported in the literature for selected Lewis Acids.

Lewis Acid	BF_3	$AlCl_3$	$GaCl_3$	PF_5	SbF_5	$B(C_6H_3(CF_3)_2)_3$
FIA [KJ/mol]	342	498	434	398	493	482

In addition, it is worth mentioning that the choice of cation (Na^+, K^+, Ag^+) in the salt reactant had a considerate effect on the reaction outcome in some cases. For example, the starting material $\mathbf{2}^+$ exhibited absence of the reactivity towards $NaBF_4$ or KPF_6, while analogues Ag^+ salts yielded complete conversions into a mixture of products. Similarly, $AgSbF_6$ was preferred over $NaSbF_6$ based on the significantly increased reaction rate and a neat $\mathbf{3}^{2+}$ formation. Such results can be explained by the formation constants and lattice energies of the resulting salts (NaCl, KCl and AgCl), which can act as driving forces for the $\mathbf{3}^{2+}$ formation.[147]

2.1.3 X-ray Structure Analysis

The presence of **[3c][SbF$_6$]$_2$** and high compatibility with the hitherto reported **[3c][AlCl$_4$]$_2$**[110] were elucidated by single crystal X-ray diffraction (Figure 18). The $P_{central}$-$C_{carbone}$ bond length of 1.746(11) Å remained virtually the same as 1.745(7) Å, for **[3c][AlCl$_4$]$_2$**), consistent with a strong electron donation from the carbone ligand. Compared to the earlier value of 1.623(6) Å in **[3c][AlCl$_4$]$_2$**, $P_{central}$-N bond underwent additional shortening (1.608(10) Å in **[3c][SbF$_6$]$_2$**), which can be assigned to a higher degree of N→P←C π-interaction compared to the one reported for **[3c][AlCl$_4$]$_2$**. It has been previously suggested that the presence of π-symmetry lone pairs on both C1 and

N1 atoms, along with the practical planarity of the C_2NPCP_2 fragment, allow a "flow" of electron density from the adjacent $-N^iPr_2$ and $C(PPh_3)_2$ substituents into the empty $3p_z$ orbital on the $P_{central}$ in $\mathbf{3c^{2+}}$, establishing a 4π allyl-like C-P-N fragment. Results obtained for $\mathbf{[3c][SbF_6]_2}$ support this postulate, especially considering the average P1-C1 (~1.74 Å) and P1-N1 (~1.62 Å) bond distances, which are between the ones reported for single and double bonds.[148]

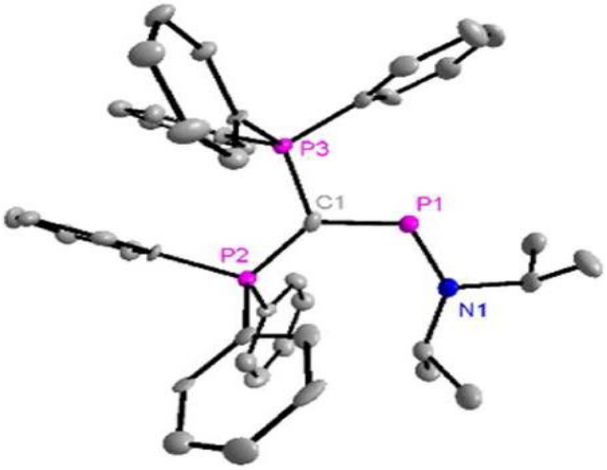

Figure 18. Crystal structure of 32+ (Thermal ellipsoids are shown at 50% probability). For clarity, hydrogen atoms have been omitted. Selected bonds (Å) and angles (°): P1-C1, 1.746(11); P1-N1, 1.608(10); N1-P1-C1,

X-ray analysis of $\mathbf{[3c][SbF_6]_2}$ also revealed the existing interion contacts (Figure 19). Fluorine atoms of two different SbF_6^- counterion units, are positioned atop and beneath the N-P-C plane, allowing them to easily interact with a vacant p_z orbital of the central phosphorus atom. Established $P_{central}\cdots F$ contact lengths in $\mathbf{[3c][SbF_6]_2}$ amount to 3.00 and 3.10 Å, which is substantially lower than the sum of $P\cdots F$ van der Waals radii of 3.36 Å,[149] implying a strong P-F interaction. While occurrence of interionic contacts in phosphenium salts is not surprising for cations such as $AlCl_4^-$, $GaCl_4^-$, and BPh_4^-,[150],[151] only a minimal interaction (3.54 Å) takes place in the previously reported $\mathbf{[3c][AlCl_4]_2}$, with only one $P\cdots Cl$(anion) interaction falling below

the sum of van der Waals radii of 3.72 Å for these two atoms. Furthermore, no interion contacts were observed in the crystal structure of **[3c][BAr$^{f}_{4}$]$_2$**.

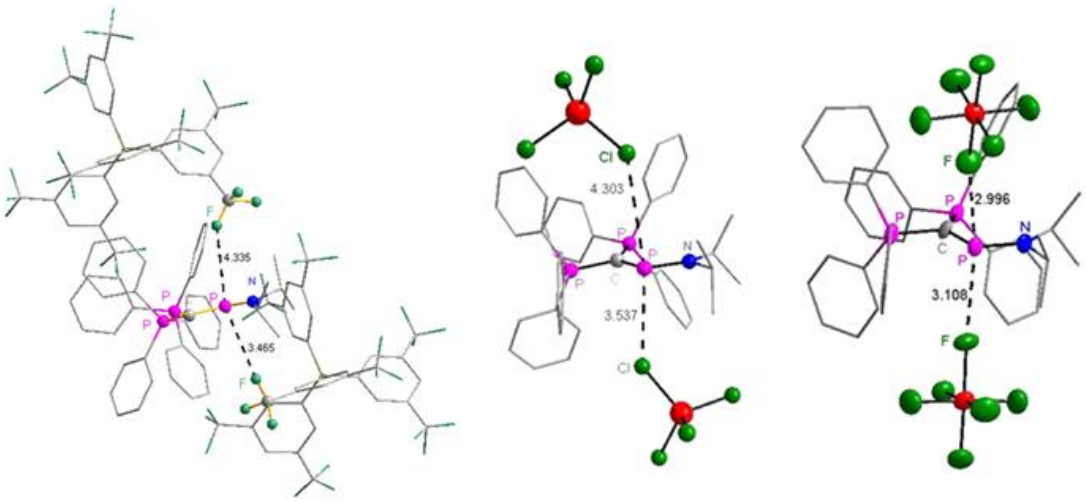

*Figure 19. Close interion contacts for [**3c**][BAr$^{f}_{4}$]$_2$ (left), [**3c**][AlCl$_4$]$_2$ (middle) and [**3c**][SbF$_6$]$_2$ (right).*

Figure 20. Color change as a result of interion contacts in [3c][SbF$_6$]$_2$ and [3c][BAr$^{F}_{4}$]

he occurrence of interion contacts also explains the physical differences in **[3c][SbF$_6$]$_2$**, as compared to **[3c][AlCl$_4$]$_2$** and **[3c][BAr$^{f}_{4}$]$_2$**. While the latter two are yellow in their solid state, **[3c][SbF$_6$]$_2$** is colourless (Figure 20). We believe that the notable P···F proximity, and resulting interaction, quench the 4 π allyl-like system of the C-P-N fragment, resulting in the quenched yellow colour of **[3c][SbF$_6$]$_2$** in its solid state. Further evidence for this claim is derived from the appearance of the typical yellow colour once **[3c][SbF$_6$]$_2$** is dissolved in DCM, clearly indicating a lesser prominence of contacts in the solution.

The interion contacts seem to be minimal or absent in solutions, provided that the $^{31}P_{cetral}$ shifts of the dication (δ_P ~356 ppm) were consistent among all viable counterions: $AlCl_4^-$, $BAr^f{}_4^-$, $BAr^{Cl}{}_{4,}$ SbF_6^-, $GaCl_4^-$.

2.1.4 ^{31}P Solid State NMR Spectroscopy

^{31}P cross-polarization (CP)/magic angle spinning (MAS) NMR spectra obtained for [**3c**][SbF_6]$_2$ were compared to the analogous dications (Figure 21). Spectra in Figure 21a is displayed over the full observed chemical shift range, and enlargements of the relevant peaks are presented in Figure 21b. The spectra of [**3c**][SbF_6]$_2$ was acquired at 6 kHz MAS spinning frequency, while the remaining ones were taken at 9 kHz. Comparisons between the spectra measured at different spinning frequencies for each sample (not shown) allow the distinction between spinning sidebands and centre bands (see Tables 5 and 6). All spectra show intense features between −5 and 35 ppm and resonances farther downfield (see Figures 21 and 22) with varying line widths. In solid-state NMR, the line widths reveal the extent of structural disorder around the observed phosphorus nucleus, such as bond angle and bond length distributions. Therefore, it is interesting to note that the 31P CP/MAS NMR spectra of the monocations (Figure 21) are sharper than those of the dication series (Figure 22) and within the dication series the spectra of [**3c**][SbF_6]$_2$ are strikingly sharper than the others. Signals from the compounds with cyclic carbones, i.e. $C(PPh_2)_2C_3H_6$ (**2e**$^+$ and **3e**$^{2+}$), are broader than those containing acyclic carbones (**2c**$^+$**, 2d**$^+$**, 3c**$^{2+}$**,** and **3d**$^{2+}$), i.e. materials with $C(PPh_3)_2$ ligands.

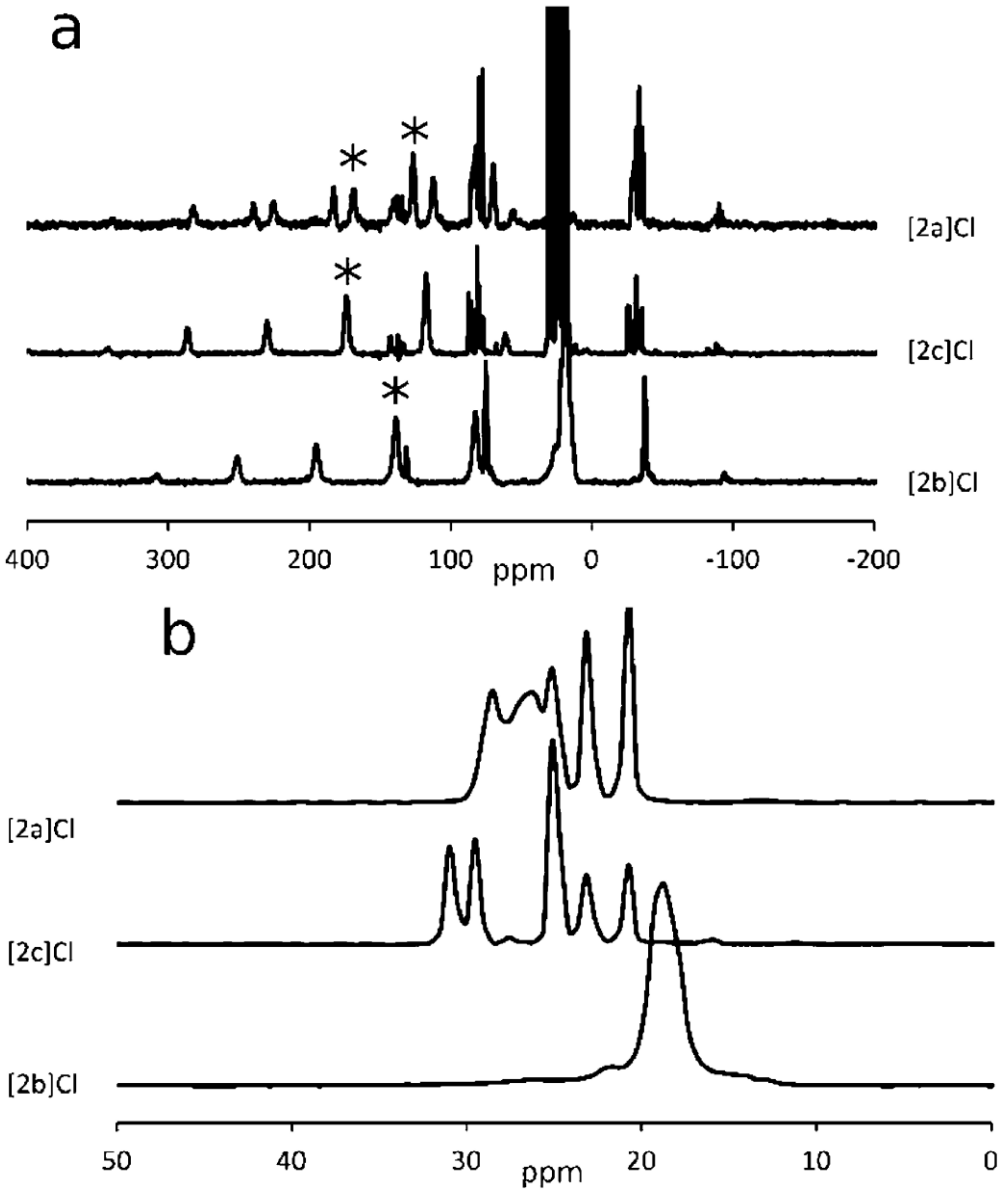

Figure 20. (a) 31P CP/MAS NMR spectra of the monocationic precursors, specifically of [2c] (top), [2d] (centre), and [2e] (bottom) with Cl– counterions taken at 9 kHz spinning speed. Isotropic peaks are indicated with asterisks in (a). (b) Enlargements of the spectral region between 0 and 50 ppm showing only isotropic shift resonances

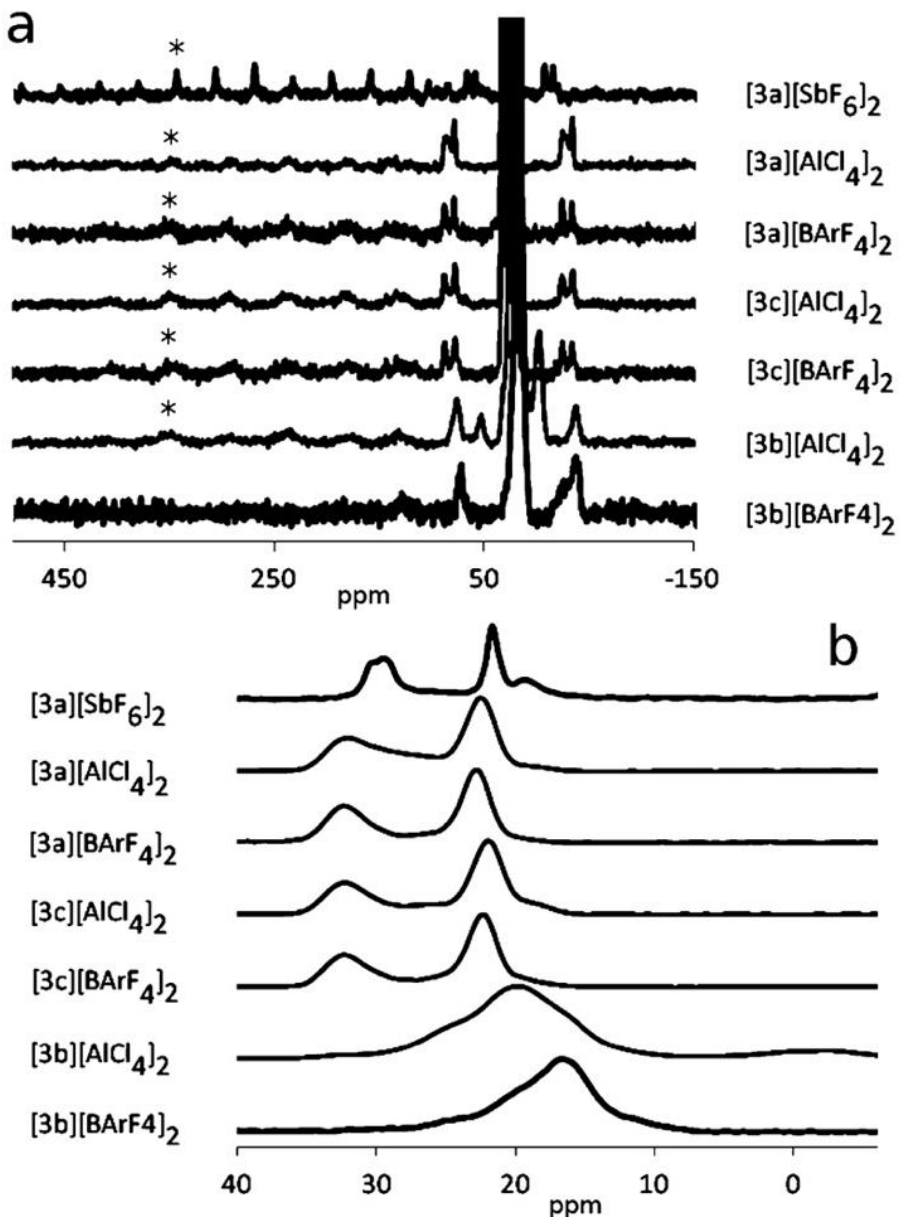

*Figure 21. (a) 31P CP/MAS NMR spectra of the dicationic products as indicated by the labels. Isotropic peaks are indicated with asterisks in (a). (b) Highlights of the spectral region of the carbodiphosphorane resonances showing only isotropic shift resonances. The spectra were acquired at 9 kHz MAS spinning rate, except for the top spectra of [**3c**][SbF_6]$_2$, which were taken at 6 kHz.*

Table 5. ^{31}P Solid-State NMR Isotropic Chemical Shift Positions (ppm) of All Dicationic Compounds

Compound	[3a][SbF_6]$_2$	[3a][$AlCl_4$]$_2$	[3a][BAr^F_4]$_2$	[3b][$AlCl_4$]$_2$	[3c][$AlCl_4$]$_2$	[3c][BAr^F_4]$_2$
Solid-State δ_P (ppm)	19.3			-2.3		
	21.7	22.7	22.7	19.8	22.2	22.2
	29.5	32	32.5	32.5	32.5	32.5
	344±2	349±10	354±10	351±10	354±10	349±10

Table 6. Solid state 31P CP/MAS NMR isotropic chemical shift positions of monocationic precursors

[**2c**]Cl	[**2e**]Cl	[**2d**]Cl
20.7	18.8	20.7
23.2		23.2
25.1		25.1
26.1		29.5
28.5		31.0
126.8		
168.8	139	174.2

On assignment of the resonances, the peak clusters between −5 and 35 ppm (Figures 21b and 22b) stem from the phosphorus nuclei in the carbodiphosphorane groups, given their similarity with the solid-state 31P CP/MAS NMR spectra of $[HC(PPh_3)_2]^+Br^-$ (23.2 and 21.2 ppm; spectra not shown, possibly present as an impurity in **[2c]Cl** and **[2d]Cl**. For compounds **[2c]Cl** and **[2d]Cl**, some peak intensities come in pairs, likely from two magnetically nonequivalent PPh_3 groups within each carbodiphosphorane in the solid state. In contrast to the acyclic compounds, the peaks of the series containing cyclic carbones, **[2e]** and **[3e],** are disorder broadened and shifted further upfield. Interestingly, within the dications, the signals in the spectra of **$[3c][SbF_6]_2$** are strikingly sharper than the others. Its phosphorane isotropic shifts at 19.3 and 21.7 ppm resonate at frequencies where the spectra of the other compounds, **$[3c][X]_2$** and **$[3d][X]_2$** (X = $AlCl_4$, $BAr^F{}_4$), only show shoulders. It seems that the phosphorane groups in **$[3c][SbF_6]_2$** crystallize predominantly in configurations only occupied to a minor extent by the other materials.

The ^{31}P CP/MAS NMR signals from the central phosphorus nuclei resonate further downfield: for the monocation series **[2]Cl**, the chlorine-bound phosphorus nuclei show sharp isotropic chemical shift peaks between 126 and 174 ppm (Table 6). The differences between the shifts in the solid state and those observed in the solution (~134 ppm) stem from crystal

packing. The intensity differences of the two isotropic shift peaks in the spectra of compound **[2c]Cl** are likely due to a mixture of crystal structures, possibly caused by the chiral properties of the central phosphorus; two independent molecules in the asymmetric unit cell, as found by X-ray, should give equally intense lines.

Unlike the spectra of the monocation precursors, the central phosphorus nuclei of the dicationic products **3c–e**$^{2+}$ show broad isotropic peaks shifted even farther downfield around 350 ppm. The widths of these peaks in the solid state reveal a significant amount of structural disorder, such as variations in bond angles and bond distances. Interestingly, the phosphorane substitutions, amino group ligands, and counterions do not affect the peak positions and widths of the centre phosphorus, except for the compound **[3a][SbF$_6$]$_2$**. For the latter, the comparatively sharp peak of the centre phosphorus at 344 ppm resonates at the lower shift range sampled by the other dicationic compounds. It seems that the **SbF$_6^-$** counterion in the dication series causes the material to crystallize with less disorder in a structure only present to a minor amount in the other compounds. Overall, the isotropic chemical shifts of these phosphorus centres agree with the values observed in solution (356 ppm), and the sizable downfield shift is consistent with electron depletion at the central phosphorus nucleus. The spread of the total intensities over a wide range of spinning sidebands reveal large chemical shift anisotropies, consistent with the highly asymmetric electron distribution around the doubly bonded phosphorus nuclei and its empty p_z orbital.

2.1.5 Lewis acidity tests of 3^{2+}

Quantification of Lewis acidity has been a useful tool to design and tune new Lewis acids, to foresee the catalytic reaction rates, and select apt reactants.[24b, 152] In general, higher strength of a Lewis acid is associated with stronger interaction with hard bases and higher reaction rates.[24b, 153] Whereas acidity of Brønsted acids can

successfully be estimated *via* pKa scale; a single universal approach is not developed for Lewis acids. Different approaches include calorimetric approach,[154] benzylation reactions with methyl-benzyl chlorides as a reference of Lewis acidity,[155] and most successfully employed-spectroscopic methods:[156] *Lappert's* method,[156e] *Gutman-Beckett's method,*[157],[152b] and *Childs*' method:[158]

- *Lappert's* approach is based on a reaction between a Lewis acid and *ethyl-acetate (EtOAc)*, where the acyl-oxygen serves as the donor site, and Lewis acidity is measured by the scope of C-O bond polarization apparent from the difference in carbonyl stretching frequency shifts ν(CO) due to the adduct formation.
- *Gutman-Beckett* developed another experimental method which evaluates Lewis acidity of a compound compared to *triethylphosphine oxide (Et_3PO)* as a reference molecule (δ_P = 50.4 in CD_2Cl_2) and ^{31}P NMR spectroscopy as a mean of evaluation. The method is based on mutual competition between Et_3PO and the heteroatoms attached to the Lewis acidic centre, for an empty orbital of that centre, to preferably form an Et_3PO-LA adduct. A greater ^{31}P downfield shift correlates to a higher Lewis acidity.
- *Childs'* method determines Lewis acidity based upon the induced ^1H NMR shift (Δδ) deriving from the H3 resonance upon the formation of the final LA adduct with crotonaldehyde as a reference.

Hypothetical adducts between an oxygen donor molecule and dication **3c**$^{2+}$ (Lewis acid in our case) for three of the three conventional methods are depicted in Figure 23 below.

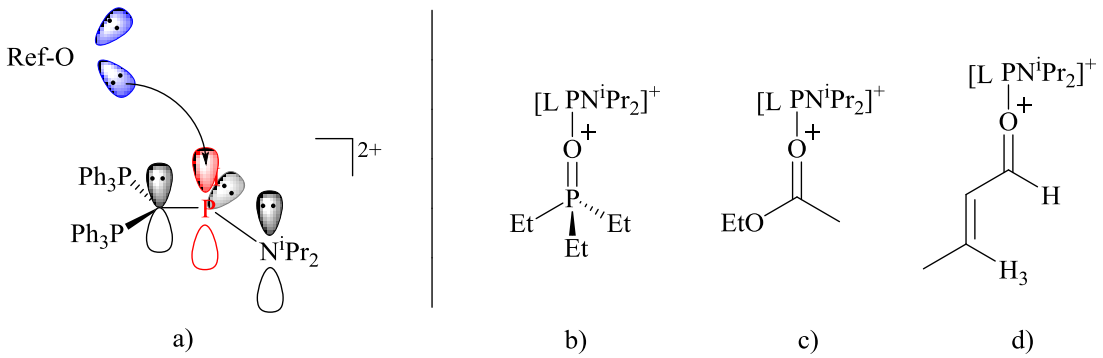

Figure 22. Hypothetical adduct formation between Lewis acidic dication 3^{2+} and a) an oxygen donor-molecule (ORef) which serves as a reference in the acidity tests, b) ethyl-acetate used in Lappert's method (RefO =EtOAc); c) triphenylphosphine oxide used in Gutman-Beckett's acidity test (RefO = $OPEt_3$), and d) crotonaldehyde in Childs' method (ORef = C_4H_6O).

Lewis acidity of **3c**$^{2+}$ has been confirmed theoretically *via* DFT calculations, which implied the existence of a low lying LUMO,[110] and experimentally, in reactions towards PMe_3,[110] DMAP,[110] water,[139] methanol,[139] THF. However, quantification of its Lewis acidity would be valuable for its efficient utilization in reactions.

2.1.6 Results

Considering the air sensitive nature of dication **3c**$^{2+}$, its decomposition during earlier attempts of FTIR characterisation, and the requirement for adduct (Figure 23b) isolation and successive IR measurements, we immediately abandoned Lappert's methodology. On the other hand, Gutmann-Beckett's method proved successful in resolving Lewis acidity of similarly sensitive Lewis acidic compounds.[24b, 152a, 153, 159] In addition, the convenience of performing ^{31}P NMR for our system in Gutmann-Beckett's method played a role in it being preferred over Childs' method.

Addition of equivalent amounts of Et_3PO to a DCM solution of **[3c][X]**$_2$ (X=SbF_6^-, $BAr^{Cl}{}_4^-$) resulted in the incomplete conversion of the starting material and a formation of a complex mixture of products. Some of the products were identified based on the analogy of their ^{31}P NMR shifts with the previously obtained products;

they included protonated ligands $[(Ph_3P)_2CH_2]^{2+}$, $[(Ph_3P)_2CH]^{2+}$ and a cation $[\{(Ph_3P)_2C\}P(N^iPr_2)(O)(H)]^+$. Layering the reaction mixture ([**3c**][SbF_6]$_2$ + $OPEt_3$) with hexane resulted in the formation of crystals suitable for single crystal X-Ray crystallography. Despite the bad quality, preliminary data indicated the presence of the compound shown in Figure 24.

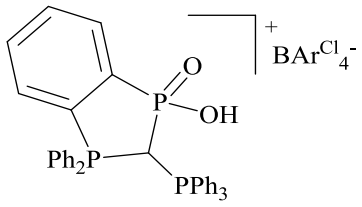

4$^+$

Figure 23. One of the mixture products obtained from the Gutmann-Beckett acidity test.

Based on these results, it can be concluded that the dominant oxophilic nature of **3c**$^{2+}$ prevents Et_3PO from coordinating to the central P. Instead, **3c**$^{2+}$ abstracts the oxygen from the donor and oxidizes phosphorus. Similar behaviour was also observed for a dicationic fluoro-phosphonium salt by Stephan *et al.*,[160] where both Gutmann-Beckett's and Childs' acidity tests resulted in an oxygen-fluoride exchange, resulting in a formation of $[(SIMes)POPh_2][B(C_6F_5)_4]$, among other products. Despite the inability to quantify acidity of **3c**$^{2+}$ by the Gutmann-Beckett's method, it was evident that the compound was highly electrophilic.

An alternative way to estimate Lewis acidity *via ab inito* and DFT calculation based on the Christe's[144a][142a][141a][141a]249 theoretical fluoride ion affinity (FIA) methodology.[144a, 161] This approach provides a direct correlation between a Lewis acidity and an enthalpy from the reaction between a fluoride ion and a Lewis acid, and it has been successfully developed for Lewis acidic phosphenium salts.[161] Due to time-constraints, FIA calculations were not performed for our system. However, separately performed reaction between **[3c][X]$_2$** (X = SbF_6 or BAr^F_4) and XeF_2 could

provide an insight into the reactivity of **3c**$^{2+}$ towards fluorine-containing species. $^{31}P\{^{1}H\}$ NMR spectra of the reaction mixture showed a major product formation characterized by a doublet (~ δ_P 22 ppm) and a doublet of triplets (δ_P ~53 ppm), indicative of the preserved $P_{(central)}$-$C_{(carbone)}$ unit integrity. Relatively low δ_P values fall within the range of four-coordinate phosphorus species. In addition, a direct P-H bond was revealed from the ^{31}P NMR spectroscopy results (52.1 ppm, $^{1}J_{P\text{-}H}$ = 692 Hz). A set of doublet signals at about δ_F -75 ppm and matching splitting constants of 1032 Hz, confirmed the existence of a direct P-F bond. In fact, similar $^{1}J_{P\text{-}F}$ value of 1040Hz was previously reported for the four-coordinate $[(SIMes)PFPh_2][B(C_6F_5)_4]_2$.[162] In comparison, a similar, five-coordinate $[(SIMes)PF_2Ph_2][B(C_6F_5)_4]$ displayed a triplet for the P central peak at δ_P -62.9 ppm ($^{1}J_{P\text{-}F}$ = 733 Hz). Based on the obtained data, it is evident that our product possessed a proton, a fluorine atom, and a carbone ligand directly bonded to a four-coordinate phosphorus-centre. A hypothesized product is one of the two species shown in Figure 22.

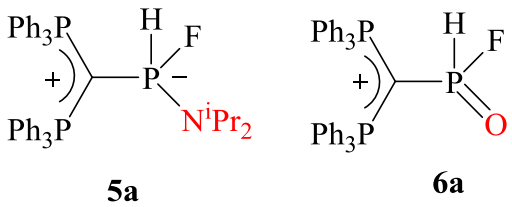

Figure 24. Hypothetical products from the reaction between ***[3c][SbF$_6$]$_2$*** *and XeF_2*

Unfortunately, all attempts to isolate the product in a solid form failed, as the second dominant species in the mixture was a product of hydrolysis, which would rise with any purification attempt. Every effort to grow a crystal from the reaction mixture yielded a protonated carbone salt. While this data does not quantify Lewis acidity, it allows us to draw a comparison with other phosphenium cations and provides more insight into the compounds reactive oxophilic and fluorophilic nature.

2.1.7 Counterion stability studies

As previously discussed, initial reactivity studies of $\mathbf{3c}^{2+}$, which included: 1) a unique O-H bond activation of water and methanol at a single site; 2) preliminary THF polymerization results; 3) reactivity towards oxygen-containing anions and/or substrates; drew attention to its highly oxophilic nature. However, the interference of the $AlCl_4^-$ cation, and the difficulties in purifying $\mathbf{3c}^{2+}$ with a bulky borate as its counterion ($BAr^F{}_4$, $BAr^{Cl}{}_4$) *via* crystallization, posed a challenge for further investigations. This issue was overcome by our ability to crystallize **[3c][SbF$_6$]$_2$**. To test its stability towards Lewis bases and possible counterion interference with oxidative additions, **[3c][SbF$_6$]$_2$** was reacted with MeOH and water according to the protocol in Scheme 23.

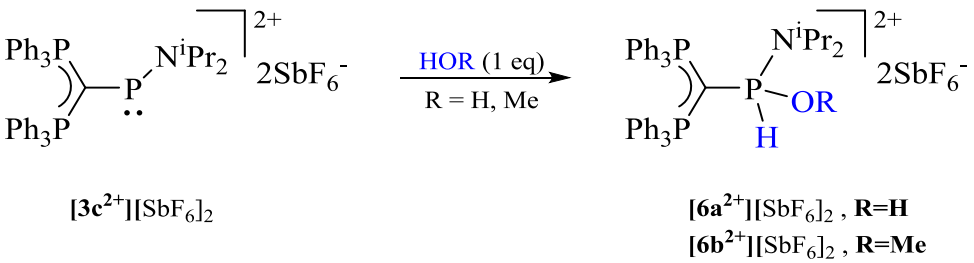

[3c^{2+}][SbF$_6$]$_2$

[6a^{2+}][SbF$_6$]$_2$, R=H
[6b^{2+}][SbF$_6$]$_2$, R=Me

Scheme 22: Methanol/water activation reaction protocols

Immediate conversion of the solution colour from yellow to colourless was consistent with the previously described reaction observations. $^{31}P\{^1H\}$ NMR of the solution revealed a complete conversion of the starting material and the positions of the $P_{central}$ peak compatible with the values formerly reported for $\mathbf{6a}^{2+}$ (triplet at δ_P 42.3 ppm) and $\mathbf{6b}^{2+}$ (a broad signal at δ_P 31.0 ppm).[139] To our delight, SbF_6^- displayed no interference in any of the two oxidative additions, which made it a suitable counterion for $\mathbf{3}^{2+}$ in forthcoming reactivity studies towards oxygen-containing substrates.

2.2 Summary

In summary, we have isolated several analogues to $\mathbf{2}^{+}$ which is a precursor to the Lewis acidic P(III)-centred dication $\mathbf{3}^{2+}$, these are: $[Cy_2NP(C(PPh_3)_2Cl)^{+}$, $[Me_2NP(C(PPh_3)_2Cl)^{+}$, $[^{i}Pr_2NP(C(PPh_2Me)_2Cl)^{+}$, $[^{i}Pr_2NP(C(PPh_2(CH_2)_{3/2})_2Cl)^{+}$. All monocations showed similar ^{31}P NMR shift, except $[Me_2NP(C(PPh_3)_2Cl]^{+}$, whose $P_{(central)}$ was shifted more downfield in comparison to the other species. Such result could be due to the higher degree of flexibility of methyl groups and their decreased steric ability to shield $P_{(central)}$.

Furthermore, out of eight counterions ($BAr^{Cl}{}_4^-$, SbF_6^-, $GaCl_4^-$, PF_6^-, OTf^-, BPh_4^-, BF_4^-, and ClO_4^-) tested for the synthetic viability of $\mathbf{3}^{2+}$, only $BAr^{Cl}{}_4^-$, SbF_6^- and $GaCl_4^-$ proved successful. The best stability of $\mathbf{3}^{2+}$ was achieved in the presence of SbF_6^- as a counterion. Due to the strong interaction between the central phosphorus and fluorine atoms in SbF_6^-, $\mathbf{[3^{2+}][SbF_6]_2}$ exhibited interesting properties in terms of its colour in the solution and the solid state.

Finally, SbF_6^- as a cation for $\mathbf{3}^{2+}$ displayed stability, as confirmed by the reactions with water and methanol. Oxophilic nature of the compound was also indicated by the high reactivity towards Et_3PO, while its fluorophilicity was suggested according to the results of the reaction with XeF_2.

CHAPTER III:

P-C Bond Activation under Mild Conditions

3.1 Introduction

Overall, organic oxidation reactions are substantially less developed than the analogous reduction reactions.[23i, 163] Most of the oxygen insertion reactions, acknowledged as oxidation reactions are known for C-C and C-H bonds.[163e-g] However, examples of oxygen insertions into C-B (Brown oxidations)[164] and C-Si (Fleming-Tameo-Kumada oxidations)[165] also exist. On the other hand, examples of oxygen insertion into C-P bonds are limited to phosphorus heterocycles, which contain ring-strained P-C bonds.[166]

3.1.1 Metal-mediated oxy-insertions

Most of the examples of metal-mediated oxy-insertions include mechanistic studies based on transitional metal chemistry.[167] Two possible mechanisms arise from the calculations: 1) an organometallic Bayer-Villiger (OMBV) route (Scheme 24); 2) a two-step, Oxygen Atom Transfer/Methyl Migration (OAT/MM) redox route (Scheme 25).

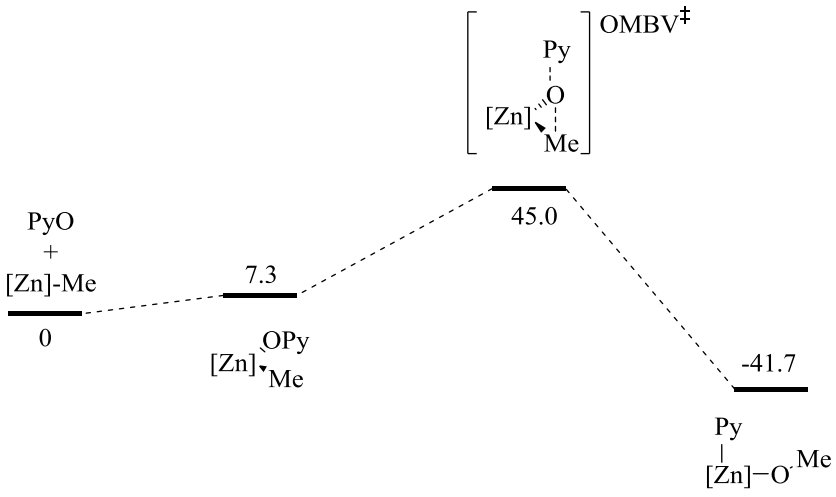

Scheme 23. An example of the computed reaction coordinate (OMBV) for a zinc-methyl complex, where numbers represent energies in kJ/mol.

OMBV route is a single-step, non-redox oxygen insertion into M-C bond, where the precursor to oxy-insertions is formed *via* coordination of the oxidant to the

TM-methyl reactant complex. The intermediate formed in the OMBV insetion is also known as a metallo-Criege intermediate (MCI), analoguos to the Criege intermediate in the organic Baeyer-Villiger reactions (see Section 2.1.2). Oxygen atom transfer in OAT/MM insertions is followed by the oxo-intermediate, and then the final alkyl to the oxo-ligand migration. The OAT/MM route is dominant among the d^2, d^4, d^6, d^8 metals. Due to the occurring redox process, the metals also need to have stable formal oxidations states separated by two units, not often found among transition metals. In general, OMBV route is easier to control, thus preferred over the OAT/MM route.

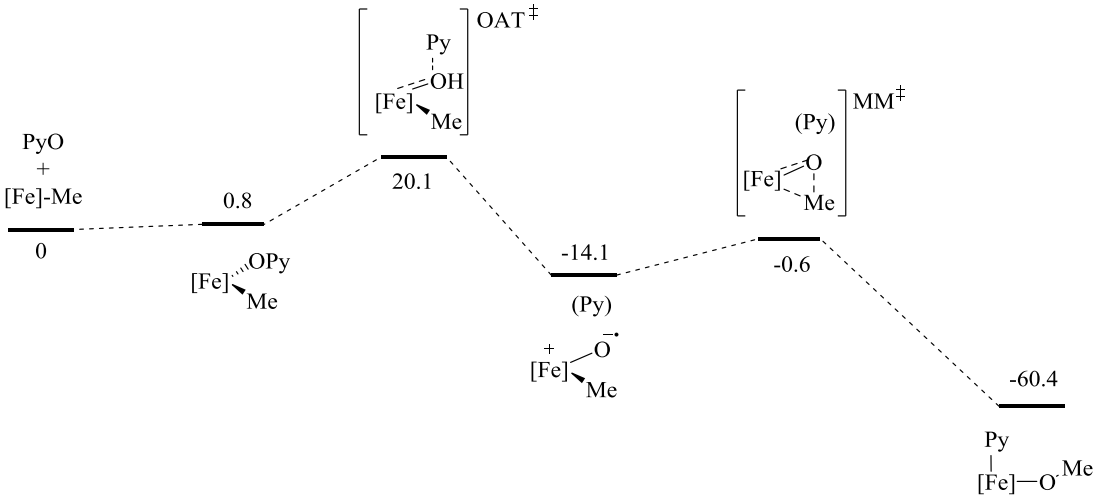

Scheme 24. An example of the computed reaction coordinate (OMBV) for a iron-methyl complex, where numbers represent energies in kJ/mol.

To the best of our knowledge, very few examples including experimental results are known, mostly resembling the BV route.[168] However, no examples including oxy-insertion with main-group elements as centres are found in the literature. With respect to the main group elements, theoretical studies performed for Ca and Ge preferred an organometallic Bayer-Villiger route.[167f]

3.1.2 Oxy-insertion into P-C bonds

The first example of an oxygen insertion into the C-P bond was reported in 1975 by Kashman and Awerbouch, as a result of the reaction between 8-phosphabicyclo[3.2.1]oct-6-ene 8-oxide and *meta*-chloroperbenzoic acid

(mCPBA).[166a] The reaction mechanism was related to the Bayer-Villiger reaction of ketones and lactones. Initially, it was believed that the presence of the allylic carbon as a "migrating group" was crucial for the reaction proceedings, apart from the ring strain. The C-P-C bond angle in the precursor was between 79° and 84°.[169] Later studies have shown that the reaction can proceed even in saturated compounds with strained C-P-C bonds.[166g]

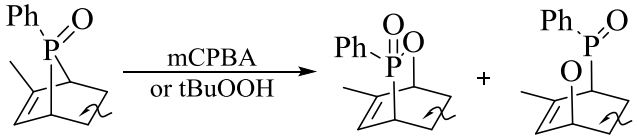

Scheme 25. Simplified depiction of strained P-heterocycles undergoing oxygen insertion

More than 40 years later, progress in the C-P bond oxidations did not evolve much further. Groups of Quin and Jankowski have subsequently used different 2,3-oxaphosphabicyclo[2.2.2]octenes (2,3-OPBO) and 2-phosphabicyclo[2.2.2]octenes (2-OPBO) systems as phosphorylation, phosphinylation and phosphonylation agents, since their fragmentation leads to the transient dioxophosphorane (metaphosphonate) species.[166g] In all cases, highly reactive mCPBA was used as an oxygen-donor to the precursor, 7-phosphanorbornenes (7-PNB) (Scheme 26).[166c] Upon the oxygen insertion, a remaining mixture containing the excess of mCPBA and meta-chlorobenzoic acid would be treated with KF and removed *via* the resulting complex.[166g]

Similar oxidative cleavage of the P-C bond was observed by Mathey *et al.*[166h, 170] Oxidation with excess H_2O_2 in xylene, resulted in an oxygen insertion into the P-CH_2 bond of the bridge in the starting phosphabornadienes, as a result of the bridge strain (Scheme 27).

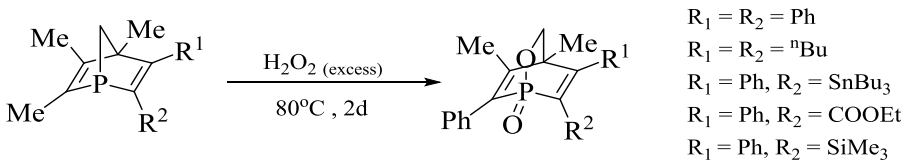

Scheme 26. Oxidation of phosphabornadienes reported by Mathey et al

As previously mentioned, the dicationic phosphenium species developed in our lab $[(Ph_3P)_2CPN^iPr_2]^{2+}$ exhibited highly oxophilic behaviour by being able to insert into

O-H bonds.[142, 171] Thus, we were interested in examining its reactivity to other oxidants.

With respect to oxidizing and oxygen-transfer abilities of *N*-oxides,[172] our first substrate of choice was pyridine *N*-oxide (O-Py). In contrast to simple pyridines, which display higher basic properties in a solution state, pyridine *N*-oxide is peculiar to the rule due to its slightly higher basicity relative to pyridine,[173] making it more prone to react with our Lewis acidic system.

In all mentioned C-P oxidation reactions, harsh oxidants and reaction conditions are required: a highly reactive mCPBA at 0°C, or hydrogen peroxide under elevated reaction temperatures. In contrast, we reported a P-C bond oxidation under mild conditions, using a "greener", O-Py oxidant. Similarly to the previously reported systems, ours also resembled a Baeyer-Villiger (BV) oxidation mechanism.[174] In addition, calculations have shown that a key intermediate in this transformation closely resembles an elusive Criegee intermediate.[175]

Baeyer-Villiger oxidation is a reaction between a ketone (cyclic ketone) and a peroxide derivative, which yields an ester (lactone). An example of a general Baeyer-Villiger reaction mechanism is represented in Scheme 27.[176]

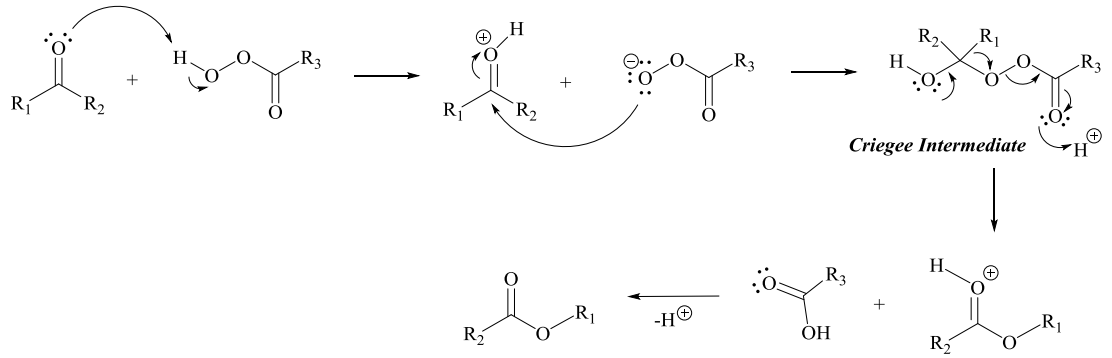

Scheme 27. Reaction mechanism for the general Baeyer-Villiger reaction.

Dioxirane and 1,2,4,5-tetraoxocyclohexane were initially speculated as the reaction intermediates for BV reactions; however, the true mechanism which involved a nucleohlic attack of the oxidant on the carbon of the carbonyl group was suggested by Rudolf Criegee.

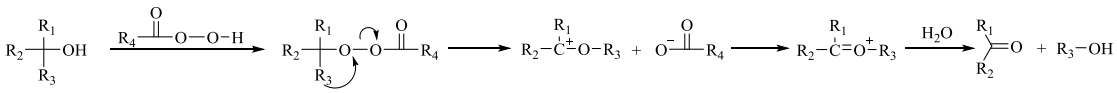

Scheme 28. An example of general reaction which proceeds via the Criegee rearrangement

Criegee intermediate in the Baeyer-Villiger oxidation reactions is not to be confused with the Criegee rearrangement (Scheme 28). Although Baeyer-Villiger oxidations and Criegee rearrangements share resemblence, the intermediates for the two are not the same. Apart from the intermediates, Criegee rearrangement differs from BV oxidations by the ability for consecutive rearrangements and the requirement for acidic reaction conditions.[176]

3.2. Results and Discussion

Identical to previous reactions with oxygen donors (e.g. H_2O, MeOH),[171b] addition of pyridine *N*-oxide to a DCM solution containing **[3c][SbF$_6$]$_2$** (Scheme 28) instantly discoloured the initially yellow solution.

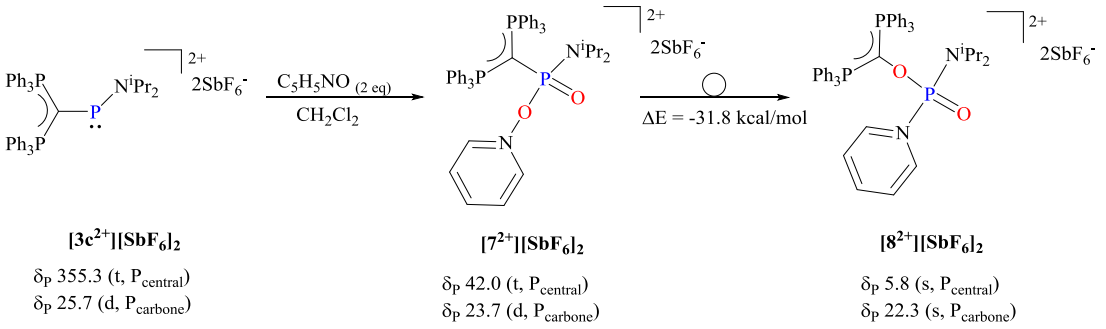

Scheme 29: Reaction of $[\mathbf{3c}^{2+}][SbF_6]_2$ with 2eq Py-O. Initially formed product $\mathbf{7}^{2+}$ undergoes spontaneous transformation into $\mathbf{8}^{2+}$.

Regardless of the numbers of oxidant equivalents added, ^{31}P NMR spectroscopy of the crude reaction mixture indicated the presence of at least three different species, with ~50% of the dominance of the major product at about δ_P 42 and 24 ppm. The use of two equivalents of PyO proved to be optimal for the reaction completion. Upon layering the reaction mixture with hexane, the major product was successfully isolated in a crystal form. As expected, single-crystal X-ray analysis of $\mathbf{7}^{2+}$ disclosed an oxophosphonium dication (Scheme 28). The assymetric unit for $\mathbf{7}^{2+}$ contained two independent molecules. However, instead of being stabilized by pyridine (Py) which was generated upon the oxidation of the central phosphorus atom, the oxophosphonium dication was stabilized by an O-Py molecule. Regardless of the stoichiometry used (1:1; 1:2; 2:1) the presence of $\mathbf{7}^{2+}$ was always identified.

This outcome was unexpected considering that: 1) Masuda *et al.* reported a pyridine-stabilized oxophosphenium cation obtained *via* a similar reaction of pyridine *N*-oxide with a cyclic phosphenium cation $[(CH_2)_2(N\text{-}Dip)_2P]^+$ (Dip = 2,6-^{i}Pr$_2$-C$_6$H$_4$) (Scheme 29);[177] and 2) O-Py is substantially less basic (pKa= 0.79) than Py (pKa = 5.2). Oxophilic nature of the supposedly "naked" dication $[(PPh_3)_2C(N^iPr_2)P{=}O]^{2+}$ $\mathbf{7c}^{2+}$ and steric factors are possible causes for the favoured coordination of a less sterically-imposing, and oxygen-containing, O-Py ligand over Py. Nevertheless, the formation of $\mathbf{7}^{2+}$ is an additional example of distinctive reactivity that dication $\mathbf{3}^{2+}$

demonstrates towards oxygen-donors, with respect to comparable monocationic, phosphenium species.

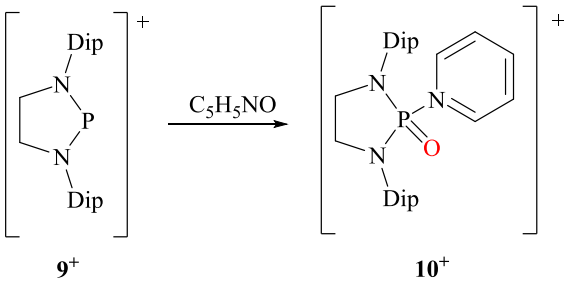

*Scheme 30. Reported reaction of a monocation **9**$^{+}$ with pyridinr N-oxide*

Whereas crystallographically elucidated examples of the simple coordination of O-Py to transitional metals are conventional, this is not the case with non-metals. Apart from the carbon or hydrogen species, examples of O-Py coordination to non-metals in the Cambridge Structural Database[178] are limited to boron[179] and silica[180] compounds. With that in mind, **7**$^{2+}$ (Figure 26) appears to be the first example of O-Py coordination to a phosphorus centre.

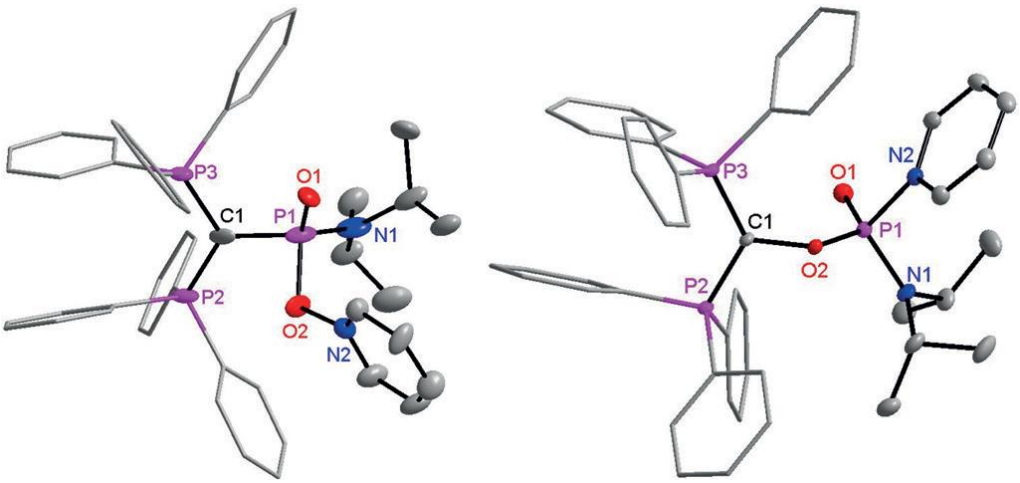

*Figure 25. Molecular structures of **7**$^{2+}$ (left) and **8**$^{2+}$ (right) (thermal ellipsoids shown at 50% probability, except the phenyl rings on the carbone substituent). Hydrogen atoms, SbF_6^- counterions, solvent molecules, and the second molecule in the asymmetric unit for **7**$^{2+}$ have been omitted for clarity. Selected bond lengths (Å) and angles (°); **7**$^{2+}$: P1-C1 1.879 (14); P1-O1 1.456 (10); P1-O2 1.711 (11); O1-P1-N1 112.6 (7); **8**$^{2+}$: O2-C1 1.457 (3); P1-O1 1.451 (2); P1-O2 1.581 (2); O1-P1-N1 118.6 (1).*

Compared to the starting dication **3c**$^{2+}$, $P_{central}$-$C_{carbone}$ bond in **7**$^{2+}$ (1.746 Å) is significantly longer than Å in **3c**$^{2+}$, with no significant changes to the P1-N1 bond.

With respect to O-Py coordination, P1-O2 bond length of 1.711(11) Å along with the calculated Wiberg bond index (WBI) of 0.46[176] is indicative of the donor-acceptor character of the P1-O2 interaction.

DFT calculations were also carried out for the hypothetical $[(PPh_3)_2C(N^iPr_2)P{=}O]^{2+}$ $\mathbf{7c^{2+}}$. As expected, excluding the O-py ligand caused the shortening of all the bond distances between the central P and its neighbouring atoms. The same observation was also reported for $\mathbf{10^{2+}}$ and its base-free analogue.[177, 181] Greater formal charge of $\mathbf{7^{2+}}$ than of $\mathbf{10^{2+}}$ seemed to cause no difference in NBO partial charges for the central P=O fragment of the two species. In fact, $\mathbf{7^{2+}}$ carried a slightly less positive partial charge (+ 1.257) than $\mathbf{10^{2+}}$ (+ 1.332) for the same P=O fragment. This could be due to electronegativity difference among the atoms surrounding the central phosphorus in both species, and/or the carbone ligand in $\mathbf{7^{2+}}$ over-compensating the electron density.

Initially unapparent, $\mathbf{7^{2+}}$ was a crucial intermediate for the formation of $\mathbf{8^{2+}}$, which could be identified in the original reaction mixture by the appearance of new upfield ^{31}P NMR signals at δ_p 22.3 ppm and 5.8 ppm. The convenience of isolating $\mathbf{6^{2+}}$ in a crystal form allowed us to follow the kinetics of this conversion by ^{31}P NMR spectroscopy. Intermediate $\mathbf{6^{2+}}$ was stable in the dichloromethane solution for about 10 hours before undertaking spontaneous conversion into $\mathbf{7^{2+}}$. The full conversion takes about eight days to complete, but it can be accomplished in only 4 hours when the reaction mixture is heated to 50^{O}C (Figure 27). The reaction is irreversible, and the final product $\mathbf{8^{2+}}$ is stable in the solution for more than 30 days. In addition, the increment of the starting reactant Py-O did not alternate the reaction pathway.

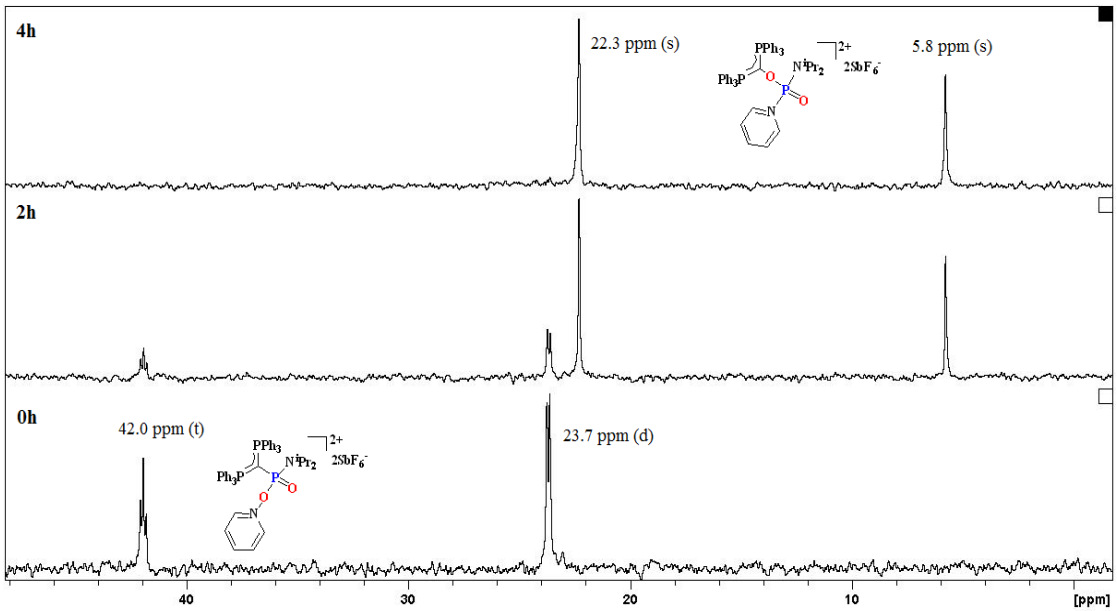

Figure 26. Full conversion of $\mathbf{7}^{2+}$ *into* $\mathbf{8}^{2+}$*, achieved in approx. 4h by heating* $\mathbf{7}^{2+}$ *crystals in DCM at 50˚C*

In contrast to the previously reported species with a P-$C_{(carbone)}$ bonding interaction, the new compound did not show the usual P-P coupling. Such result suggested the absence of the formerly present P-$C_{(carbone)}$ bond, possibly triggered by an insertion of some moiety into the bond. Indeed, results of the solid-state analysis (Figure 26) for $\mathbf{8}^{2+}$ revealed that an oxygen insertion into the P1-C1 bond of $\mathbf{7}^{2+}$ to form $\mathbf{8}^{2+}$ indeed occurred (Scheme 28). However, $\mathbf{8}^{2+}$ included a Py ligand coordinated to the phosphorus centre, as opposed to a O-Py ligand in $\mathbf{7}^{2+}$.

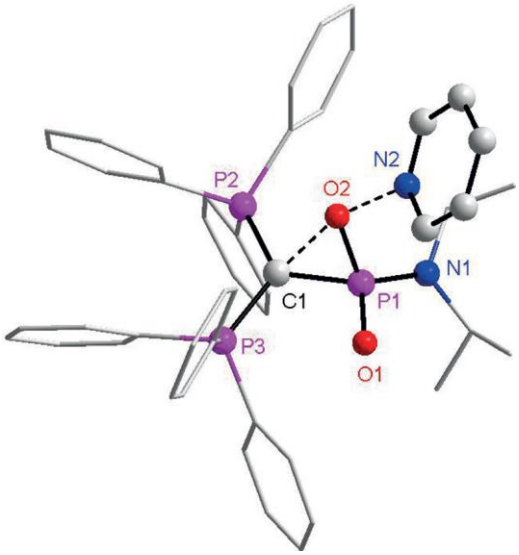

Figure 27. Computationally determined transition state for the transformation of $\boldsymbol{7}^{2+}$ *into* $\boldsymbol{8}^{2+}$.

In order to establish the most plausible mechanism for this transformation, computational studies were carried out (see Supporting Information). Identification of the transition state (Ea = 24 kcal mol^{-1}) presented in Figure 28 revealed an apparent resemblance to the Metallo-Criegee intermediate calculated for the OMBV oxy-insertion reactions (Scheme 30). Additional computational studies further suggested: 1) a concerted mechanism; 2) an analogy between the overall process and the Baeyer–Villiger (BV) oxidations.

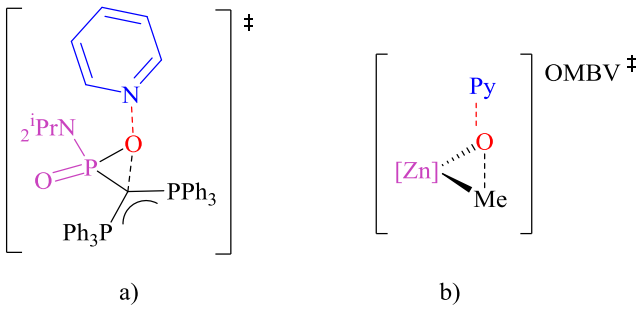

Scheme 31. Analogy between a) a transition state in the the transformation of $\boldsymbol{7}^{2+}$ *into* $\boldsymbol{8}^{2+}$, *and b) a mettalo-Criegee intermediate calculated for the OMBV reactions.*

As mentioned earlier, the accurate mechanism for the BV oxidations was proposed by Criegee, but later confirmed by von E. Doering in the reaction of O_{18}-labeled benzophenone and perbenzoic acid (Scheme 22a).[1, 182] The initial step of the

mechanism includes a peroxy acid attack on the carbonyl group, followed by an intramolecular proton shift and a subsequent formation of the carbonyl oxide, also called Criegee intermediate. In a following quasiconcerted step, the initial carbonyl group undergoes a reorganization, "one substituent migrates from the carbonyl carbon atom to the partially positively charged oxygen atom" which results in a heterolytic cleavage of the peroxy acid's O-O bond.[174a, 174b, 174d, 182] Primary and secondary stereoelectronic requirements for a Baeyer-Villiger oxidation to occur are: 1) O-O bond in the peroxide group need to be in an antiperiplanar position to the migratory group; 2) lone pairs at the oxygen of the hydroxyl- group have to be antiperiplanary positioned to the migratory group.

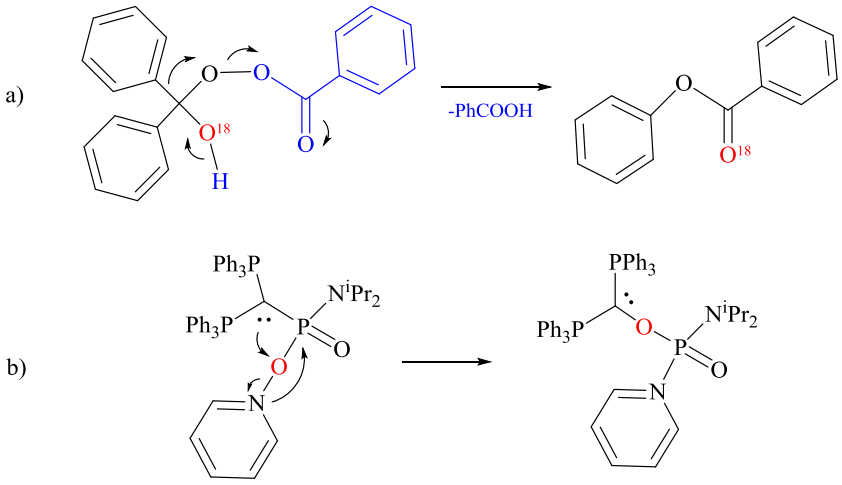

Scheme 32. a) A typical Bayer-Villiger oxidation reaction mechanism between an O_{18}-labeled benzophenone and a perbenzoic acid; b) calculated mechanism for the 6^{2+} to 7^{2+} transformation.

In accordance with computational studies, the formation of $\mathbf{8}^{2+}$ occurs *via* an analogous mechanism (Scheme 32b). Main differences between the $\mathbf{7}^{2+}$ intermediate and the Criegee intermediate are: 1) the presence of a phosphine oxide instead of a carbonyl group, 2) the protonation of the carbonyl group, and 3) the nature of the migratory group. Considering the nonprotic nature of the O-Py oxidant, the absence of phosphine oxideprotonation was expected. Moreover, P-C bond oxidation seems to be governed by the migratory group's electronic (ylide) and steric nature. Electron

population of 1.74e at C1 would imply a high likelihood of its lone pair to be delocalized over the neighbouring atoms/bonds. However, NBO analysis results suggest the presence of a lone pair, restricted to a p orbital, on the C1 atom. The same lone pair is later absent in the transition state, which denoted its participation in the formation of the initial C1-O2 bond. This is concurred by NBO analysis, which suggests a p–p atomic orbital overlap for the formation of the initial interaction. Specifically, the C1-O2 bond formation is initiated by the C1 lone pair attack on O2 and a subsequent heterolytic cleavage of the O2-N1 bond (Scheme 32b). The initial attack (C1→O2) appears viable due to the higher electophilicity of O2 when coordinated to the electron poor P atom in $\mathbf{7}^{2+}$, compared to the free O-Py molecule. Thus, the lone pair on C1 in $\mathbf{7}^{2+}$, which becomes "re-established" in the final product, appears to be one of the vital reasons behind the observed facile oxygen insertion into the P1-C1 bond. The antiperiplanar position of the carbone/ylide substituent (migratory group) with respect to the O-N bond in the transition state[174b] fulfils another prerequisite for the BV mechanism. Furthermore, the mechanism of the formerly mentioned P-C bond oxidation of strained P heterocyclic compounds (Scheme 26) is of extreme resemblance with the Bayer-Villiger oxidations of lactones and ketones.[166c, 166e, 183] Considering all the experimental and theoretical evidence, an undisputable correlation exists between our P-C bond activation and the typical BV oxidations, despite the fact that a P=O group in our system is replacing a typical C=O group and an ylide serving as the migratory group.

Mechanistically speaking, the less apparent is the analogy between the Criegee intermediate and $\mathbf{7}^{2+}$. However, in both systems, a migratory group "attack" and a heterolytic cleavage of the O-X (X = N in our system; X = O for BV) bond occur simultaneously. Besides the absence of the protonation at the carbonyl group, the only

difference arises from the initiation of the attack by the lone pair on C1, which is non-occurring in the Criegee intermediate. However, as previously discussed, the presence of the lone pair most likely helps lower the E_a of the oxygen insertion step. Hence, compound $\mathbf{7}^{2+}$ could be regarded as a Criegee intermediate analogue,[175a, 184] and the process overall as the first example of a BV oxidation reaction in which pyridine *N*-oxide served as the oxidant.[166c, 166e, 183]

As hitherto mentioned, stabilization of the oxophosphonium dication by a less basic O-Py ligand in $\mathbf{7}^{2+}$ was surprising considering the presence of the more basic Py in the solution. The observation was attributed to oxophilic nature of $\mathbf{7c}^{2+}$ and/or steric factors since O-Py contained oxygen as a donor atom and seemed to be less sterically demanding than Py. This result intrigued us to explore the role of the steric strain of $\mathbf{7}^{2+}$ in the overall transformation of $\mathbf{7}^{2+}$ to form $\mathbf{8}^{2+}$. In fact, according to the single crystal X-Ray analysis of both dications, the O1-P1-N1 angle widened from 112.6(7) for $\mathbf{7}^{2+}$ to 118.6(1) for $\mathbf{8}^{2+}$, suggesting an increase in the steric strain upon the oxygen insertion.

Absence of significant difference in the P1-O1 and P1-N1 bond values and their orbital makeup (NBO analysis), along with the consistency in electronic population of the C1 lone pair (1.70 and 1.71 e for $\mathbf{7}^{2+}$ and $\mathbf{8}^{2+}$, respectively) upon the oxidation, further subsided the possibility of electronic effects of the ligands surrounding the P1 atom to be responsible for the widening of the O1-P1-N1 angle. Thus, it can be interpreted that partial alleviation of the steric strain resulted from the oxygen insertion into the P1-C1 bond of $\mathbf{7}^{2+}$, which "pushed" the bulky carbone ligand away from the central phosphorus. To quantify the energy which is being released by reducing the steric crowding, carbone coordinates have been extracted from the optimized structures for $\mathbf{7}^{2+}$ and $\mathbf{8}^{2+}$ and their corresponding energy computed with no

further optimizations, yielding an energy difference of. With the assumption that the carbone ligand in $\mathbf{7}^{2+}$ has been sterically strained by the obtained 7.0 kcal mol^{-1}, three conclusions arise. 1) The steric strain does not affect the overall oxidation reaction outcome, as it is exergonic by 31.8 kcal mol^{-1}. 2) Steric strain seems to substantially increase the reaction rate, since increasing the Ea by 7.0 $kcalmol^{-1}$ would cause the activation temperature to increase by ~ 25%. Specifically, reaction conditions would require temperature of about 90°C (or 366 K) and the reaction would not have occurred at room temperature (20°C or 293 K). Despite the general limitations in means of steric strain quantification on reaction rates, an abundance of examples exists of the numerous steric factors being the cause behind the improvement of the respective reaction rates.[185] 3) Lastly, occurring steric strain in our system may be partially responsible for averting the coordination of a more sterically demanding, although more nucleophilic, Py ligand to $\mathbf{7c}^{2+}$, with the preference of O-py to form $\mathbf{7}^{2+}$. Nonetheless, the well-known oxophilicity of these cationic compounds may have played a role the coordinative preference for the oxygen-containing ligand.

3.2.1 Counterion dependence

As shown in Scheme 33, the synthesis of $\mathbf{7}^{2+}$ was repeated for weakly coordinating borate counterions, namely: BAr^{Cl}_4, Bar^{F}_4, and $B(C_6F_5)_4$.

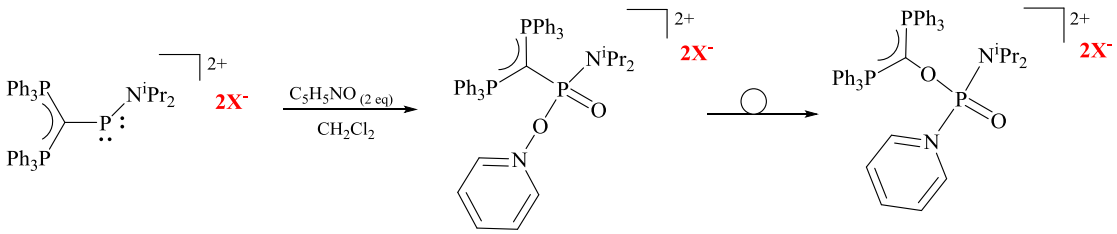

$[\mathbf{3c}^{2+}][\mathbf{X}]_2$ $[\mathbf{7}^{2+}][\mathbf{X}]_2$ $[\mathbf{8}^{2+}][\mathbf{X}]_2$

$\mathbf{X^- = SbF_6^-, BAr^F{}_4^-, BAr^{Cl}{}_4^-, B(C_6F_5)_4^-}$

Scheme 33. Synthesis of $\mathbf{7}^{2+}$ and $\mathbf{8}^{2+}$ in presence of different counterions.

While dication $\mathbf{7^{2+}}$ can be successfully synthesized in all cases, important differences arose with the use of different substituents. Firstly, reaction between $\mathbf{3c^{2+}}$ and PyO proceeded significantly neater in cases of $\mathbf{[7][X]_2}$ (X = BAr^{Cl}_4, Bar^{F}_4). Secondly, in contrast to $\mathbf{[7][SbF_6]_2}$, products $\mathbf{[7][X]}_2$ (X = BAr^{Cl}_4, Bar^{F}_4, $B(C_6F_5)_4$) could not be isolated in the form of a crystal. While precipitation with pentane was the means of obtaining the $\mathbf{7^{2+}}$ borates, application of the same method to $\mathbf{[7][SbF_6]_2}$ resulted in hydrolysis of the product. Thirdly, $\mathbf{[7][X]_2}$ where X^- = $Bar^{F}_4{}^-$ underwent a spontaneous conversion into $\mathbf{8^{2+}}$ in its *solid* form, at room temperature (~50% conversion in 24h). In comparison, crystals of $\mathbf{[7][SbF_6]_2}$ are indefinitely stable under the same storage conditions, and no conversion was observed within 3 days for solid $\mathbf{[7][BAr^{Cl}_4]}$. Lastly, the conversion of $\mathbf{7^{2+}}$ into $\mathbf{8^{2+}}$ by heating its dichloromethane solution at 50°C proceeded significantly *faster* for X = Bar^{F}_4, BAr^{Cl}_4. Reaction times increase in the following order: $\mathbf{[7][BAr^{F}_4]}$ < $\mathbf{[7][BAr^{Cl}_4]}$ < $\mathbf{[7][SbF_6]_2}$ with reaction times of 1.5h, 2.5h, and 4h, respectively. The reaction time order was independent of the amount of $\mathbf{7^{2+}}$ used, solution concentration, or temperature. Results imply that: 1) SbF_6^- stabilizes dication $\mathbf{7^{2+}}$ the most; 2) $BAr^{Cl}_4{}^-$ stabilizes dication to an extent; and 3) $BAr^{F}_4{}^-$ acts as a non-coordinating counterion to $\mathbf{7^{2+}}$, allowing for the fastest conversion into $\mathbf{8^{2+}}$. Unfortunately, no indications of $\mathbf{8^{2+}}$ formation were observed when $\mathbf{[7][B(C_6F_5)_4]}$ was subjected to heating. ^{31}P NMR spectrometry indicated the existence of multiple species in the solution, resulting either from the starting material's decomposition or participation in side-reactions.

Table 7. Counterion dependence comparison for the synthesis of $\mathbf{7^{2+}}$ *and* $\mathbf{8^{2+}}$

	SbF_6^-	$BAr^{F}_4{}^-$	$BAr^{Cl}_4{}^-$	$B(C_6F_5)_4^-$
3^{2+} to 7^{2+} reaction neatness	complex mixture	neat	neat	neat
Insertion (7^{2+} into 8^{2+}) reaction time when the reaction is performed at 50°C	4h	2.5h	1.5h	N/A

7^{2+} purification means	crystallization	precipitation with pentane		
Stability of 7^{2+} in the solid state	stable	50% conversion in 1 day	2 days	On-set decomposition

3.2.2 Oxygen transfer reactions

According to the previously discussed reaction mechanism for the $\mathbf{7^{2+}}$ to $\mathbf{8^{2+}}$ transformation, the oxygen for the insertion clearly originated from added O-Py. Based on this, we believed that it was possible to use $\mathbf{7^{2+}}$ as a starting material for oxygen-transfer reactions, if the insertion and the formation of $\mathbf{8^{2+}}$ were to be disfavoured. To the best of our knowledge, two possible approaches included trapping the oxygen *via* a substrate, or a redox agent, represented in Scheme 34. In case of the former one (a), catalytic activation also seemed viable, as Py could potentially coordinate back to the phosphorus centre upon the oxygen transfer.

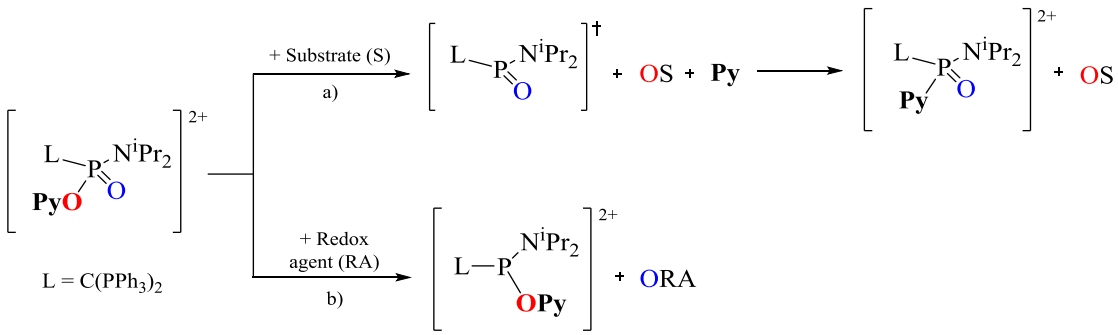

Scheme 34. Predicted pathways of oxygen transfer via a substrate (a), or a redox agent (b).

Addition of PR_3 (R = Me or Cy) to **[7][BAr$^{Cl}_4$]$_2$** instantly resulted in the formation of δ_p signals at approximately 22 (doublet) and 26 ppm (triplet), indicative of the preserved carbone→$P_{central}$ bond. Other present reaction peaks were identified as the various $BAr^{Cl}_4^-$ salts: protonated ligand, PPh_4^+, $PPhMe_3^+$, $[LP(N^iPr_2)(O)(H)]^+$. In addition, a peak corresponding to the OPR_3 moiety could also be observed in $^{31}P\{1H\}$ NMR at δ_p 41.5 ppm (for $OPMe_3$), or at δ_p 52.2 ppm (for $OPCy_3$). Two possible scenarios could be envisioned from this data: 1) oxygen abstraction by the phosphine

followed by the pyridine coordination; or 2) a OPR_3 coordination to the $P_{central}$ (Figure 29).

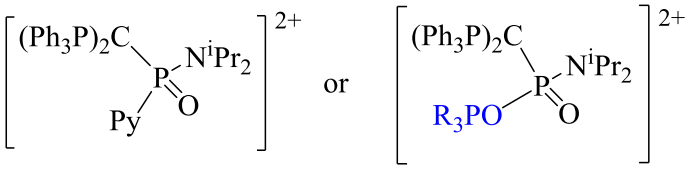

Figure 28. Suggested reaction products

Kinetic studies with different substrate amounts were subsequently conducted (0.5 eq, 1 eq, 1.1 eq and 10 eq). In all cases, the reaction was stoichiometric. Irrespective of the amount of the added substrate, product decomposition would occur upon about 30h from the start of the reaction, resulting in the phosphine oxide peak shift to δ_p 39.2 ppm ($OPMe_3$) or δ_p 49.8 ppm ($OPCy_3$). A similar observation was reported by Burford *et al.*,[186] where free $OPMe_3$ was detected at δ_p 36.3 ppm, as a result of reversible association from the $OPMe_3$-stabilized antimony cation $[Ph_4Sb(OPMe_3)][OTf]$, which displayed a $OPMe_3$ peak at δ_p 42.6 ppm. The correlation with the behaviour of our system made us believe that our reaction product was indeed $OPMe_3$-stabilized, followed by the release of $OPMe_3$ resulting from the subsequent decomposition. In reactions with 10 eq of phosphine, the amount of free OPR_3 was about three times higher than in reactions with 1.1eq. A possible explanation is that excess PR_3 reacts with $[LP(N^iPr_2)(O)(H)]^+$, which is present as a side-product, and abstracts one of the oxygens from it. In addition, oxygen transfer reaction was attempted catalytically, with the addition of 10eq of PR_3 and OPy. Unfortunately, the reaction outcome did not differ from the one when only 10eq of phosphine are added. In addition to the NMR characterisation, small quantities of $OPCy_3$ were detected *via* mass spectroscopy m/z 297.2349, confirming the successful oxygen transfer.

3.3 Conclusion

In conclusion, we have demonstrated an oxygen insertion into a P-C bond under mild conditions, rendering $\mathbf{7}^{2+}$ to be the first main group element to achieve so. Based on the computational analysis results, the reaction mechanism bears resemblance with the Baeyer–Villiger (BV) oxidations. Unorthodoxly for BV reactions, Criegee-like intermediate has been identified as the key intermediate for the insertion. Finally, the activation energy was greatly subsided by the steric strain in the Criegee-like intermediate without influencing the ultimate process outcome.

Lastly, we have demonstrated a successful stoichiometric oxygen transfer between $\mathbf{7}^{2+}$ and PMe_3/PCy_3. Investigations of this mechanism and further reactivity of $\mathbf{7}^{2+}$ and $\mathbf{8}^{2+}$ are ongoing and will be reported in due course.

Chapter IV:

Synthesis and reactivity of a carbone-stabilized parent-metaphosphonate

4.1 Introduction

Despite the similar properties that members of the same periodic group can share, this is not always the case. An example includes chemical properties of nitrogen and phosphorus, neighbouring elements within the same periodic group. Contrarily to the stability and abundance of N_2 gas, P_2 is elusive and mostly shortly witnessed at high temperatures.[187] While nitrogen-oxides are stable, isolable, easily accessible and often with significant environmental impacts,[188] phosphorus-oxide analogues are highly reactive and observed in either gas phase or at extremely high temperatures.[189] The first PO-trapping was achieved in a reaction between $[\{Cp^4Ni\}_2\{(CO)_4W\}P_2]$ and bis(trimethylsilyl)- peroxide in 1991 (Scheme 35a);[190] whereas the first P_2O-containing metal cluster was reported several years later (Scheme 35b).[191] However, the field of phosphorus-oxides has remained explored vaguely to this day, twenty years later.

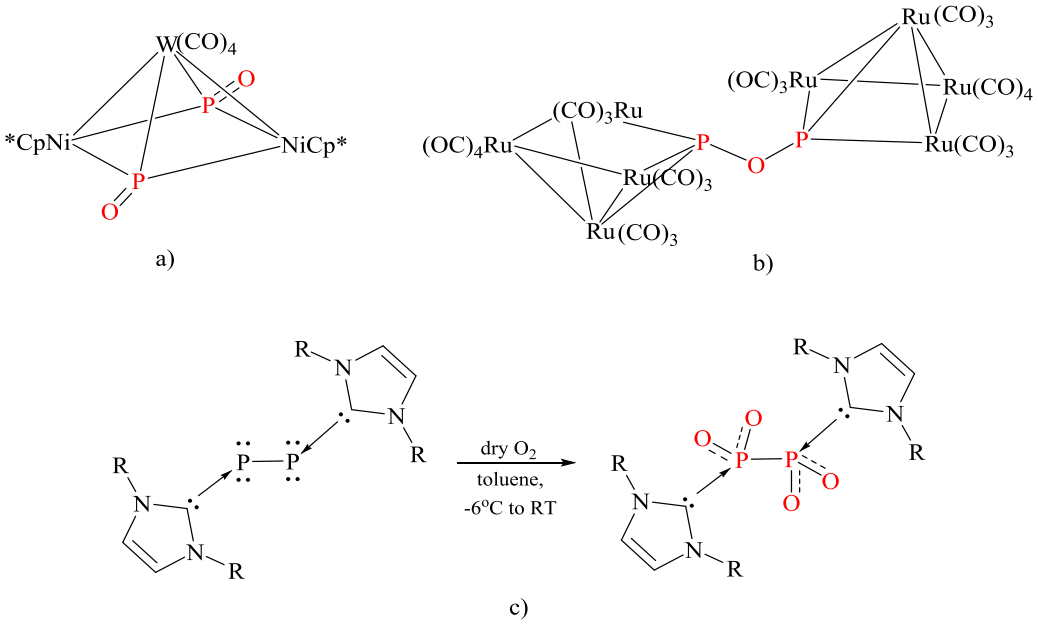

Scheme 35. Examples of different species containing the PO-moiety.

Very recently, Robinson *et al.* have successfully trapped a diphosphorus tetroxide using remarkable stabilizing abilities of an NHC ligand (Scheme 35c).[192] A

unique, Lewis acidic NHC→$(O)_2$P-P$(O)_2$←NHC compound was obtained *via* the molecular splitting of the triplet O_2 from the similar carbene-stabilized P_2 precursor NHC→P-P←NHC. While the synthesis of the diphosphorus tetroxide compound required extremely air- and moisture-free conditions, recrystallization of the final product NHC→$(O)_2$P-P$(O)_2$←NHC could also be achieved in the air, in which case the compound interestingly co-crystalizes with two molecules of water.

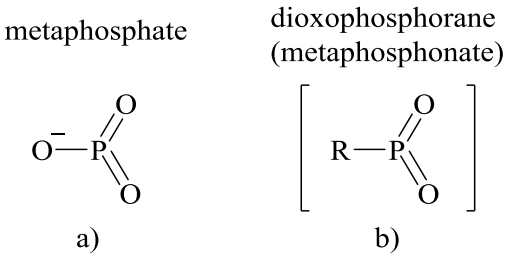

Figure 29. General examples of a metaphosphate (a) and a dioxophosphorane (metaphosphonate) (b).

Dioxophosphoranes (metaphosphonates) (Figure 30b) are precursors and potential sources of the yet another elusive oxide, PO_2. Dioxophosphoranes have been long known as transient species, reaction intermediates (Ph-PO_2) and leaving groups that provide crucial explanations for various reaction mechanisms, especially for phosphorylation reactions. However, the actual search for these organic derivatives of metaphosphoric acid set off in 1955,[193] when the anion of metaphosphoric acid was proposed to be involved in ATP hydrolysis (Scheme 36). Since then, scientists have been attempting to generate and characterise metaphosphoric acid and its derivatives. Despite efforts, 60 years later, when many low-coordinate P-complexes were successfully stabilized, these species remain elusive. Difficulties regarding experimental work and isolation of dioxophosphoranes arise from the strongly electrophilic character located at their positively(+) polarized P(V) atom. However, the same electrophilic property also accounts for their strongly phosphorylating abilities in reactions with many organic substrates. Extensive research that was conducted on

these species suggests that thy are highly reactive with low selectivity with respect to attacking various substrate sites or nucleophiles present in the solution.[194]

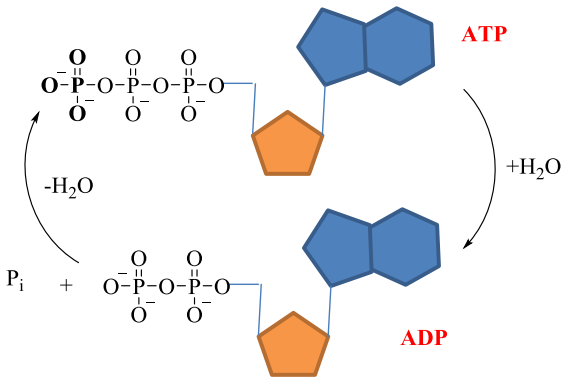

Scheme 36. A schematic representation of the ATP hydrolysis.

To this day, merely one example of a dioxophosphorane ($Cl\text{-}PO_2$) has been directly detected in a solid argon matrix as a result of a photochemical reaction between O_3 and POCl.[195] The short-lived compound was studied *via* IR spectroscopy, which displayed a P-O stretching bond at 1443 cm^{-1} and indicted an OPO bond angle of ~135°, and a particularly strong P-Cl single bond. Ab intio SCF calculations performed by the group confirmed these results and suggested a 4e-3C π-system for the OPO moiety.

Among the numerous approaches to generate metaphosphonates, the most historical ones include flash vacuum pyrolysis (F.V.P.) and high temperatures of about 400-800°C. Some examples include thermal fragmentation of 1,3,2-dioxaphospholanes or phosphonites, which allowed methyl metaphosphate to be observed in the gas phase for the first time. Similarly, the existence of other metaphosphonates was deducted *via* the same method, either by also being observed in gas phase, or deducted from resulting self-condensation products of respective metaphosphonates. For instance, F.V.P. of phenyl-1,3,2-dioxaphospholane leads to the loss of ethylene and a formation of trimeric metaphosphonate, which is presumed to

result from a monomeric Ph-PO_2 intermediate. The same result was obtained *via* a similar F.V.P. of a phosphonite, with a loss of butadiene.[196] The paper also reports the formation of a 5-hydroxydibenzophosphole-5-oxide, resulting from the intramolecular trapping of a monomeric metaphosphonate by an adjacent phenyl ring in the F.V.P. of a cyclic phosphonite. Similarly, F.V.P. of 2-(2,4,6-tri-t-butylphenyl)-1,3,2-dioxaphospholane leads to a dioxaphosphorane insertion into a neighbouring C-H bond of the methyl group to yield 5,7-di-t-butyl-3,3-dimethyl-2,3-dihydro-1-hydroxy-1λ^5-benzophosphol-1-one.[197] Other examples of cyclic phosphonates obtained *via* intramolecular phosphorus insertion into a C-H bond from an F.V.P. reaction are shown in Figure 31 below.

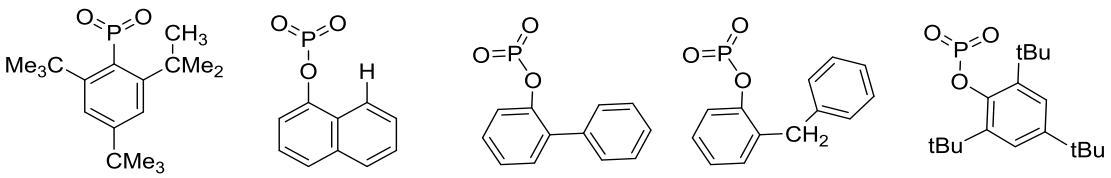

Figure 30. Examples of cyclic phosphonates resulting from an intramolecular phosphorus insertion into a C-H bond

While flash vacuum pyrolysis provided valuable insights into the chemistry of metaphosphonates and paved access to the first metaphosphonate species, this method is not practically feasible due to requirements of high temperatures and low yields of resulting compounds.

More practical techniques to generate metaphosphonates include (thermal) fragmentations in solvents, in the presence of trapping agents, such as amines or alcohols. The first of its kind was fragmentation of monoallkyl β-haloalkylphosphonate dianions, now known as the Conant-Swan reaction. Fragmentation was achieved through the first-order reaction at 70°C in acetonitrile as

an inert solvent. Generated metaphosphonate ($MeO\text{-}PO_2$) was subsequently trapped by a tertiary amine in an electrophilic substitution reaction. While Conant-Swan reaction was historically significant, fragmentation of alkyl-oximinobenzylphosphonates was more feasible, which yielded various metaphosphonates; $MeO\text{-}PO_2$, $EtO\text{-}PO_2$, $^tBuO\text{-}PO_2$ to name a few. Initially, anhydrous HCl in an alcohol solvent was used to instigate the phosphonate fragmentation. Resulting metaphosphonate would then react with the present alcohol, yielding a dialkyl phosphate. The method was later modified to use an inert solvent (toluene) instead, with a minor presence of a trapping alcohol, which allows the generated metaphosphonate to act as a phosphorylating agent towards the alcohol. Latter method allowed even for a successful phosphorylation of ^tBuOH, conventionally challenging to phosphorylate.

Another example includes photolytic or thermal fragmentation of derivatives of 2,3-oxaphosphabicyclo [2.2.2] octene ring system, studied by Quin and coworkers since 1980's.[166c, 166e, 183a, 183c, 198] As in many other instances, highly electrophilic character at phosphorus causes metaphosphonates to undergo self-reaction instantly upon being generated in the solution, resulting in linear or cyclic polymers.

As formerly mentioned in the F.V.P. pyrolysis, metaphopshonates tend to insert into the neighbouring groups. Similar behavior was observed in various attempts to kinetically stabilize metaphosphonates *via* steric protection. On the other hand, aprotic amines and ethers have successfully been employed in trapping the generated metaphosphonate in solutions, yielding Lewis salts. Although this strategy allowed the salts to be characterised only by ^{31}P spectroscopy, they can be used as sources of PO_2. Some examples are shown in Figure 32.

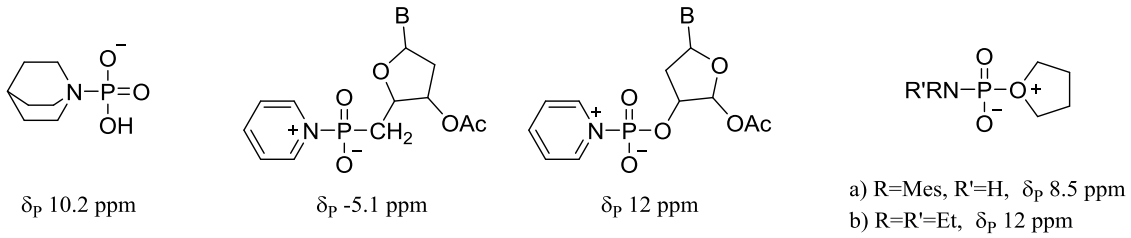

Figure 31. Metaphosphonate trapping by an amine or ether in form of Lewis salts

Complexation with metals represents a conventional route to stabilization of low-coordinate phosphorus compounds; however, this method only recently proved fruitful for the metaphosphonate-stabilization. In 2003, Menye-Biyogo *et al.* reported the first isolation and full characterisation of Ru-stabilized metaphosphonate (**12**) including the crystal structure of the compound.[199] The strategy included reducing the electrophilicity of the PO_2 unit by binding it to an electron-rich moiety, which is a terminal Ru-phosphinidine complex in this case. Interestingly, the resulting [(η^6-*p*-cymene)(PR_3)Ru(η^2-OPOMes*)] (R=Ph or Cy) complex (Scheme 37, **12**) showed only moderate air-sensitivity. Such mild air-sensitivity was surprising, considering the extremely reactive and air-sensitive nature of the free PO_2 unit. In addition, the absence of the reactivity towards most commonly employed dioxophosphorane-trapping agents (MeOH or aniline) implied that the electrophilicity of the PO_2 unit was entirely quenched.

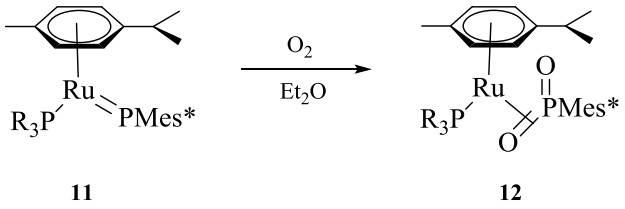

Scheme 37. Synthesis of a Ruthenium complex - stabilized dioxophosphorane moiety [(η^6-p-cymene)(PR_3)Ru(η^2-OPOMes)], **12**, where R=Ph or Cy*

Another group recently reported the synthesis and reactivity of the Mo-stabilized metaphosphonate [$MoCp(CO)_2\{\kappa^2$-OP(O)R$\}]^-$ (R=2,4,6-$C_6H_2{}^tBu_3$) (**14**$^-$) as a orange DHU-H^+ (DBU = 1,8-diazabicyclo[5.4.0]undec-7-ene) salt.[200] This anionic

complex was obtained: 1) as a hydrolysis product of the complex of the phosphinous acid cis-[MoBrCp(CO)$_2${P(OH)(CH$_2$CMe$_2$C$_6$H$_2$^{t}Bu$_2$)}] under basic conditions; and also 2) directly from its phosphinidene oxide complex precursor [MoCp(CO)$_2${P(O)R}]$^-$ (R=2,4,6-C$_6$H$_2$^{t}Bu$_3$) (**13**$^-$) *via* Me$_2$CO$_2$ oxidation (Scheme 38). In contrast to the electrophilic nature of the PO$_2$ moiety, its acid-base chemistry was expected to be reversed due to the overall negative charge of the Mo-complex. Electron density at the bond critical points was calculated to amount to 0.488 eÅ^{-3} (Mo-P bond), 1.40-1.43 eÅ^{-3} (terminal P=O bond) and 1.240 eÅ^{-3} (P-O bond of the Mo-bound oxygen). In addition, high and similar (-0.671 vs -0.615) negative atomic charges for both oxygens pointed out the possible electrophile attachment indifference. While a highly air-sensitive Mo-dioxophosphorane complex [MoCp(CO)$_2${ κ^2-OP(O)R}]$^-$ (R=2,4,6-C$_6$H$_2$^{t}Bu$_3$) couldn't be obtained as pure material, it was possible for it to be used in reactions immediately upon its generation in the solution. With respect to the methylation reaction, the complex showed no reactivity towards MeI, while Me$^+$ cation of a stronger methylating agent (Me$_3$O)BF$_4$ selectively added to the terminal oxygen to yield [MoCp{O,P-OP(OMe)R}(CO)$_2$] due to the electrostatic circumstances and site accessibility for the electrophile attack.

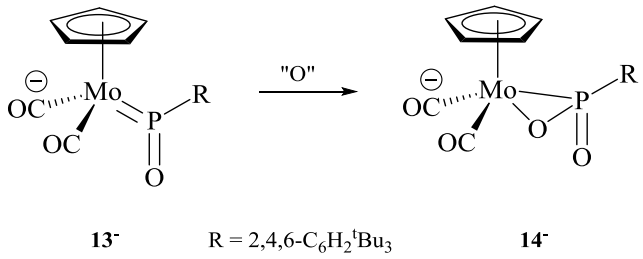

13$^-$ R = 2,4,6-C$_6$H$_2$^{t}Bu$_3$ **14**$^-$

Scheme 38. Synthesis of a Mo-stabilized metaphosphonate [MoCp(CO)$_2${ κ^2-OP(O)R}]$^-$ (R=2,4,6-C$_6$H$_2$^{t}Bu$_3$), ***14***$^-$

Recently, our group has stabilized several highly-reactive species using carbodiphosphorane as a stabilizing ligand, due to its exceptional electron-donor abilities. This project aimed to use the same approach to stabilize dioxophosphorane.

The initial strategy was 1) to reproduce the previously reported synthesis of the $[\{(Ph_3P)_2C\}PCl_2]^+$ cation as a chlorine salt; followed by 2) the counter-ion replacement by a non-coordinating $BAr^F{}_4^-$ or $BAr^{Cl}{}_4^-$ in order to increase stability of the resulting phosphenuim ion; and 3) an oxidation by a base to achieve substituent replacement from chlorine to oxygen atoms, yielding a carbone-stabilized metaphosphonate [L-PO_2] system.

4.2 Results and Discussion

4.2.1 Synthetic methods

Carbone-stabilized metaphosphonate was generated *via* multi-step, *in-situ* reaction procedure presented in Scheme 39. The starting material for the reaction, $[\{(Ph_3P)_2C\}PCl_2][Cl]$, was synthesized according to the earlier mentioned procedure.[141] Similarly, anion exchange was achieved with $NaBAr^X{}_4$ (X= F, Cl). Counterion choice of $BAr^X{}_4^-$ was made due to its non-coordinating nature and bulkiness, improved cation's stability and the ease of handling it in the following steps. Subsequently, oxidation efforts to access **17** were leveraged on potassium hydroxide's basic properties.

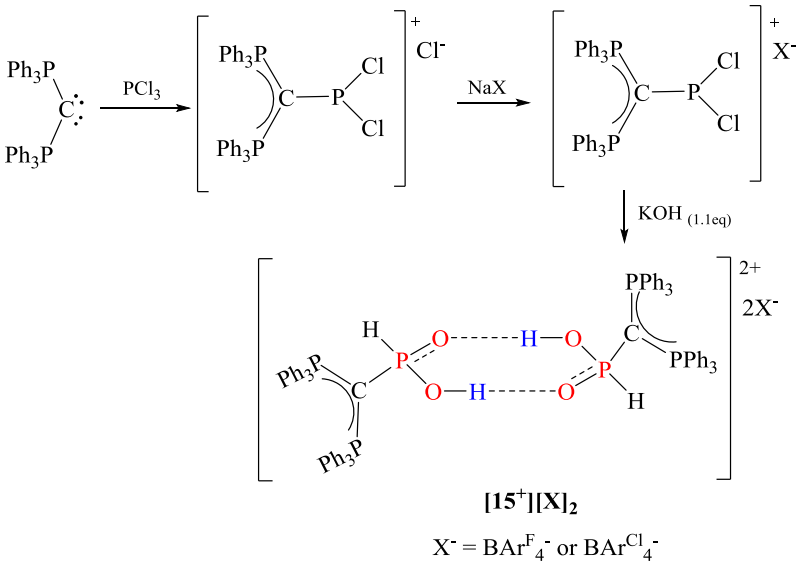

*Scheme 39. The reaction steps for the synthesis of **15**$^+$.*

Treatment of a yellow-orange dichloromethane solution of $[\{(Ph_3P)_2C\}PCl_2][BAr^{F/Cl}{}_4^-]$ with 1.1 equivalent of KOH instantly resulted in the colour change to colourless. ^{31}P NMR indicated a significant upfield shift for the central phosphorus atom, from ~173 ppm to ~36 ppm. Preservation of the L-P bond was indicated by the subsisting $P_{central}$ triplet. In addition, a significant P-H coupling was observed ($^1J_{P\text{-}H}$=636 Hz), implying the presence of a direct P-H bond. Layering the solution with an equivalent amount of hexane resulted in the crystal formation.

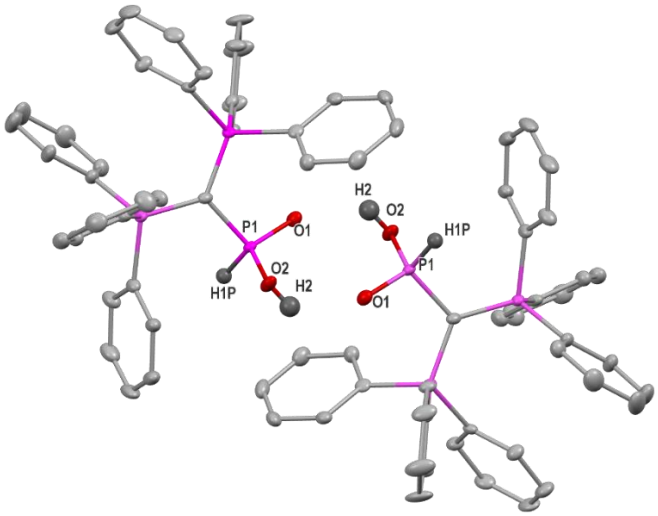

Figure 32. Crystal structure of $\{[(PPh_3)_2CP(O)(OH)(H)][BArF_4]\}_2$ (Thermal ellipsoids are shown at 50% probability). Hydrogen atoms within the phenyl rings and $BAr^F{}_4^-$ counterions have been omitted for clarity. Selected bonds (Å) and angles (°): P1-O1, 1.507(2); P1-O2, 1.534(2); O1-P1-O2, 114.70(12).

Characterisation *via* single crystal X-ray diffraction revealed a dimeric structure **15**$^+$ presented in Figure 34, where two units are interconnected *via* hydrogen bonds. The details of this crystal structure are elaborated in more detail in Section 1.2.1.2.

Subsequent removal of intermolecular hydrogens was attempted by increasing the base amounts. Whereas addition of KOH in 2-3 equivalents allowed us to achieve this goal, the resulting monomeric compound now contained a potassium cation μ-bonded to both oxygens **16**$^+$. This issue was overcome *via* base increment up to 3 equivalents, which finally yielded the targeted parent-metaphosphonate compound **17**

(Figure 33). Upon solvent removal, an impure and oily residue remained, due to the presence of the various potassium- and -borate salts. Attempts to purify the mixture *via* different crystallization and purification techniques failed, resulting in the hydrolysis and the formation of the above-mentioned dimer **15**$^{+}$. Finally, replacement of the KOH base to tetramethylammonium hydroxide proved to be the key to our access to the carbone-stabilized parent-metaphosphonate.

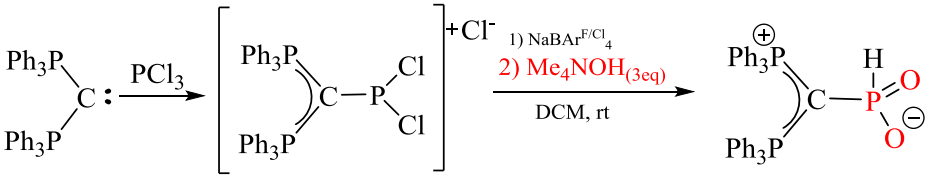

*Scheme 40. The reaction pathway for the synthesis of **17***

The gradual addition of a DCM solution of [{$(Ph_3P)_2C$}PCl_2][$BAr^{F/Cl}_4$] into three equivalents of anhydrous Me_4NOH resulted in the appearance of peaks at δ_P 21.3 (doublet, $P_{carbone}$) and δ_P 13.7 (triplet, $P_{central}$, $^1J_{P\text{-}H}$ = 586 Hz), consistent with our previous results. In comparison to the previously reported PO_2-containing species, ^{31}P NMR resonances in **12** and **14**$^{+}$ for the $P_{central}$ fall in the range between 38.5 ppm and 40.8 ppm, and ^{31}P NMR shift of a gaseous metaphosphoric acid is calculated at δ_P 53 ppm.[199, 201] The significant upfield shift for our product (compared to these compounds), indicates higher nucleophilicity of the $P_{central}$ in **17**, most likely due to the carbone ligand's donor properties and the absence of back-donation to the metal, which is the case in previously reported metal-complexes. It is notable that the position of the phosphorus shift in ^{31}P NMR was highly dependent on the solvent choice. A $P_{central}$-H bond was evidenced also from the ^1H NMR spectroscopic data: a doublet peak at δ_H 6.79 ppm, with a coupling value of 533Hz, coherent with the $^1J_{P\text{-}H}$ of 527 Hz for the $P_{central}$ triplet in ^{31}P NMR. The decrease of about 100 Hz in the $^1J_{P\text{-}H}$ coupling constant value for **17** as compared to the dimer **15**$^{+}$ ($^1J_{P\text{-}H}$ = 636 Hz) suggests

the higher electron-density around $P_{central}$ in **17.** This is also suggested from the ^{31}P NMR, since the signal for the $P_{central}$ in **17** is shifted about 20 ppm upfield from the same signal in the dimeric species $\mathbf{15}^{+}$. The slightly higher electron-density around the $P_{central}$ in **17** can be assigned to the oxygen electrons, which are likely to be shifted closer to the central phosphorus upon the breakage of the O-H bond in $\mathbf{15}^{+}$caused by the removal of the oxygen-bounded hydrogen atom. Stronger P-H bond in **17** is also supported by the IR stretching band at 2304.54 cm^{-1}, versus 2445 cm^{-1} in $\mathbf{15}^{+}$. In general, the IR stretching frequencies of all the bonds around the $P_{central}$ in the compound **17** (see Section 2.2.1.1.) are lower than of the compound $\mathbf{15}^{+}$, suggesting a stronger interaction in case of **17**. The stronger bond interaction is further supported by the melting points of the two compounds, since **17** requires about 25ºC higher temperature to melt (194.9 ºC for **17**; 169.7 ºC for $\mathbf{15}^{+}$).

Similarl y to $\mathbf{15}^{+}$ and $\mathbf{16}^{+}$, the purification of the parent-metaphosphonate moiety remained a challenge. Initial crystallization attempts directly from the solution mixture resulted in a separation of yellow oil, which contained various ammonium-borate salts, several hydrolysis products, and salts of the protonated ligand.

Due to its 5-coordinated phosphorus center, **17** was suspected to be air- and moisture- stable. Indeed, the oily mixture containing **17** endured an overnight bench test towards air- and moisture- stability without any signs of decomposition, allowing for the column chromatography as a mean of purification.

*4.2.1.1 Challenges in column chromatography purification of compound **17***

In order to elute reaction side-products obtained in the synthesis of **17**, eluents of different polarities were used. In general, we observed that using EtOAc resulted in large fraction amounts of protonated carbone and meagre yields (<10%) of the final **17**.

This led us to a suspicion that **17** binds to the silica gel mostly *via* oxygen atoms, leaving carbone ligands on the external face of the material, which easily gets cleaved and protonated by the passing EtOAc. Indeed, elution time drastically improved when DCM or chloroform was used as an eluent instead. Between the two, chloroform allowed better separation for this system, although its use should generally be avoided due to its toxicity and possible health risks.[202]

Interestingly, even solvents of higher polarity (ACN or pyridine) than EtOAc, $CHCl_3$ and CH_2Cl_2 could not elute **17**. Possible reasons might be: the high polarity of **17**, tendency to form hydrogen bonds, and/or strong Si-O bonds formed with the silica inside the column. Nonetheless, Quin *et al.* previously explored trapping properties of silica gel for metaphosphate species generated *via* thermal fragmentation.[198b] In an "*in situ*" reaction between ethyl-metaphosphate and an anhydrous silica gel, they managed to phosphorylate hydroxyl groups on the silica surface and to form monophosphates, which further undergo reactions to form pyrophosphate groups (Scheme 40a). Analogous behaviour was observed for phenyl-dioxophosphonate, with Si-OH groups of various zeolites and even alumina.[201c] A general reaction Scheme (41b) between a dioxophosphorane species and a Si-OH material surface groups is shown below.

In a review, Quin noted: "It is an *essential* feature of the use of dioxophosphoranes of all types for surface phosphorylation that the *OH group is created on phosp*horus".[201c] Having this in mind, it is not surprising that **17** remains as the last column fraction, which can be eluted out of the column only *via* an alcohol. Two possible reasons for it may be: 1) "like dissolves like"; 2) alcohol provides stabilization to **17** *via* H-bonding, allowing the alcohol to be favoured over the silica.

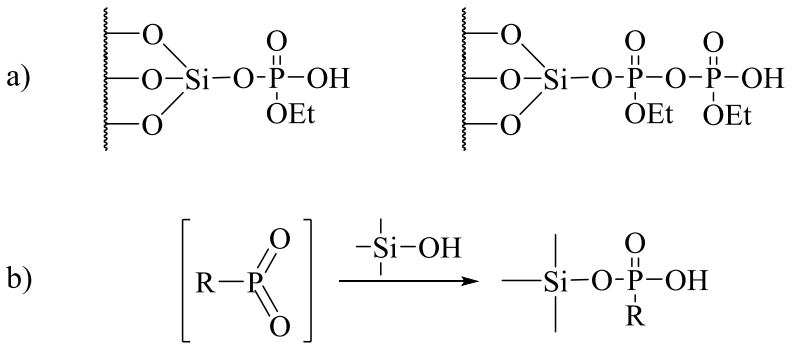

Scheme 41. Metaphosphonate groups binding to silica on the material surface (a); a general reaction between metaphosphonates and Si-OH groups (b).

Furthermore, the reaction yields can be improved to equal up to 79% when the column is packed with alumina instead of silica, and when Et_3N (TEA) is added as a stabilizer. On another hand, the addition of TEA to last eluent (MeOH) might interfere with subsequent reactions, as it can be challenging to separate it from the compound due to the formation of the TEA-H^+. Considering water as one of the side products in the synthesis of **17,** along with the air/moisture stability of **17**, the use of anhydrous Me_4NOH is not required. In fact, wet Me_4NOH or even $Me_3NO{\bullet}2H_2O$ can be used as a base source as well.

Another synthetic pathway consists of using 1.5 equivalents of base to generate a monocationic precursor $[L(H)P(O)(OH)]^+$, followed by the previously described column purification. Elution of the last fraction with MeOH results in the immediate formation of **17**. Alternatively, crystals of $[L(H)P(O)(OH)]^+$ can be reacted with methanol to give **17**, but with overall lower reaction yields.

A solid-state synthesis *via* mechanical milling over 30 min was also attempted. The reaction resulted in the product formation of about 50% yield. The other dominant reaction product displayed a doublet in ^{31}P NMR and a coupling constant of 639 Hz. While mechanical milling can be a convenient synthetic method, it was not preffered

due to the lower yield and a higher impurity content. Finally, recrystallization of the obtained colourless oil with MeOH/Et_2O yields in the colourless crystals of **17**.

Drying **17** proved to be quite challenging as well. Water removal in the presence of 3Å or 4Å drying sieves proved to be unsuccessful. Similar behaviour was observed with $MgSO_4$ as a drying agent. Heating grinded crystals to 110°C under reduced pressure would result in decomposition, while lower temperature hating was ineffective. Water removal was best achieved by drying **17** over B_2O_3 at 50°C overnight. Anhydrus **17** displayed ^{31}P NMR shifts at 6.5 ppm (br, $P_{central}$), very similar to the δ_P 5.8 ppm for $(NHC)_2P_2O_4$.[192] Coupling constant value of the anhydrous **17** was notably (~60 Hz) lower than for the previously obtained **17**•$2H_2O$ ($^1J_{P\text{-}H}$ = 554 Hz). The difference in the coupling constant can be assigned to the existing intermolecular hydrogen bonds between terminal oxygens and lattice water in **17**•$2H_2O$. This interaction weakens the P=O bonds and thus, strengthens the P-H bond, resulting in the higher value of the coupling constant for **17**•$2H_2O$.

Furthermore, the IR stretching frequencies at 2305 (w) cm^{-1}, and 1265 (s) cm^{-1} were assigned to P-H and P=O bonds, respectively. The P=O band is highly compatible with the value obtained for the $(NHC)_2P_2O_4$ of 1279 cm^{-1} for the antisymmetric mode, and it falls in between frequencies for the previously observed RPO_2 moieties (at 1448 cm^{-1}), and the metal-ligated P=O bands in Ruthenium-dioxophosphonate complex **12** (1168 cm^{-1} and 1153cm^{-1}).[192], [195]

*4.2.1.2 X-ray structure analysis of **17***

Single crystal X-ray diffraction analysis revealed a monomeric $\{(Ph_3P)_2C\}PH(O)_2$ unit, which co-crystallized with two molecules of water (Figure 34). As mentioned at the beginning of this chapter, thus far no other parent-

metaphosphonate has been structurally characterized, and only one structural example of a Ruthenium-complex containing a PO_2 unit (**12**) exists to this date. Coordination of water molecules to the terminally bounded oxygens is an evidence of the compound's stabilization by the hydrogen bonds. The geometry around the central four-coordinate phosphorus is pyramidal, with a sum of angles of 336.9°, which is slightly lesser that the sum of angles of ~342° in the dimer $\mathbf{15}^{+}$, but close to the 334.6° angle in $(NHC)_2P_2O_4$. While the PO_2 unit does not retain its planarity, the planarity remains about the C(1) atom, as indicated by the C(1) sum of angles of 359.6°. The same preservation of planarity was observed in its dimeric analogue $\mathbf{15}^{+}$ (C(1) sum of angles of 359.9°). P(1)-C(1) bond value of 1.812(5) Å is significantly longer than P(1)-C(1) bonds in the formerly mentioned compounds $\mathbf{3}^{2+}$ and $\mathbf{7}^{2+}$ (~1.74-1.75 Å), indicating a weaker electron-donation from the ligand to the central phosphorus atom. Predictably, the P1-C1 bond in the $(NHC)_2P_2O_4$ ligand is even longer (1.895(3) Å), consistant with the weaker donor-abilities of the NHC ligand, relative to the CDP ligand.

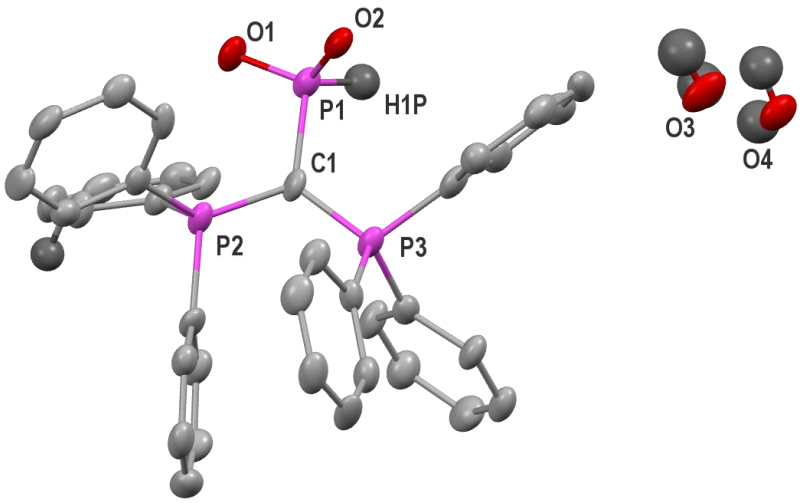

Figure 33. Molecular structure for ***17·2H$_2$O*** *(thermal ellipsoids are shown at 50% probability level). All atoms have been drawn to 50% probability. Hydrogen atoms, except H(1) have been omitted for clarity. Selected bonds (Å) and angles (°): C1-P1, 1.812(5); P1-O1, 1.505(4); P1-O2, 1.500(4); O2-P1-C1, 112.6(6, O1-P1-C1, 106.1(2).*

Having in mind that the analogous P1-C1 bond in the dimeric **15**$^+$ equals to 1.757(3) Å, it is valid to assign the bond elongation to the stronger interaction between the P1 and directly bounded oxygen atoms O1 and O2, resulting from the absence of the direct O-H bond (observed in **15**$^+$). Stronger P-O interaction in **17** can also be inferred from the P1-O2 bond length comparison of the two complexes. While the length of P(1)-O(1) bonds is about the same (1.505(4) Å in **17**, and 1.507(3) Å in **15**$^+$), the difference is obvious in the lengths of the P1-O2 bonds of 1.500(4) Å in **17**, and 1.534(2) Å in **15**$^+$. P1-O2 clearly undergoes shortening in **17** due to the lack of interaction with the directly bounded hydrogen atom. In both complexes (**17** and **15**$^+$), the P-O bond leangths are similar to those found in phosphinidene complexes, and slightly longer than the ones reported by us for a 5-coordinate phosphorus system containing a carbone→P bond. Comparable P=O value of 1.509 Å was calculated for by Alonso *et al.* for **14**$^+$,[200a] and reported by Menye-Biyogo *et al.* found in the compound **12** (1.491(5) Å).[199] On the other hand, slightly shorter P=O values of 1.466(3) Å and 1.470(3) Å were reported for $(NHC)_2P_2O_4$, consistant with the weaker ligand to central-phosphorus interaction as compared to our compounds.

The O(1)-P(1)-O(2) angle of 114.7(1)° in **15**$^+$ undergoes widening to amount to 118.2(2)° in **17** probably due to the oxygen lone pair repulsion upon the proton removal at the O(2). These velues are comparable to the ones found in compounds **12** and **14**$^+$ (120.1(2)° and 120.1(1)°, respectively), and slightly more acute than 125.4(2)° found in $(NHC)_2P_2O_4$. In addition, the electron repulsion between the C(1) and O(2) lone pairs might be responsible for the O(2)-P(1)-C(1) angle of 112.6(2)° being slightly wider than the O(1)-P(1)-C(1) angle of 106.1(2)° in **17**. The same trend and similar angle values are observed in the dimer **15**$^+$ (O(2)-P(1)-C(1) angle of 111.7(2)° ; O(1)-P(1)-C(1) angle of 108.1(2)°) In comparison, both O-P-C_{NHC} angles in

$(NHC)_2P_2O_4$ are about the same (105.7°), owing to the absence of the second lone pair on carbone in the NHC ligand.[192]

In addition, the P-H bond of 1.357Å (**17**) is shorter than the average of 1.470 Å. The strength of this bond is quite apparent even from the earlier discussed IR spectroscopy results (see page 89), as this bond was characterised by a low stretching intensity of the P-H bond.

4.2.2 Reactivity studies

4.2.2.1 Proton/hydride abstraction

Reactivity of P-H bonds in phosphines, primary organophosphines and secondary organophosphines allowed them to be widely used as synthetic intermediates and reagents. Conversion of P-H bonds into P-E bonds (where E = metal, non-metal) is at the core of the chemistry of these species. Conversion often takes place *via* the P-H bond addition to a C-E multiple bond, or *via* the metathetic hydrogen substitution. Some of these processes yield ligands that are indispensable in academic and industrial chemistry (ex. tertiary phosphines).[203]

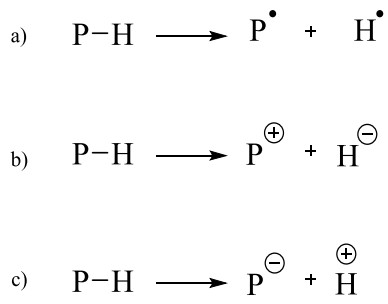

Scheme 42. General P-H cleavage modes: a) homolytic, and heterolytic, where the P-H bond is a hydride donor (b) or a proton donor (c).

General ways of a P-H bond breakage are shown in Scheme 28. Besides the homolytic cleavage (Scheme 42a), phosphorus compounds containing a P-H bond can

serve as both, acids and hydride, donors due to the negligible difference in electronegativities ($\Delta\chi$ = 0.14) of the two atoms, which impedes pronounced polarity.

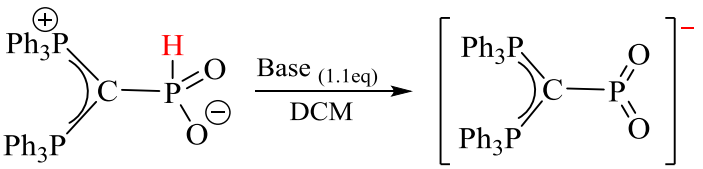

*Scheme 43. The predicted reaction product for the deprotonation of **17***

Proton abstraction studies were unsuccessfully attempted by heating using various bases: $NaNH_2$, KHMDS, KO^{t}Bu, ^{n}BuLi, and ^{t}BuLi (Scheme 43). Among them, $NaNH_2$ caused no reactivity. When added to **17** in an equivalent amount, KHMDS reacts to give $[(Ph_3P)CH(PPh_2(O))]^+$ and carbone, while higher base equivalents favour the formation of solely carbone. Carbone is also a major reaction product when KO^{t}Bu and ^{n}BuLi are used.

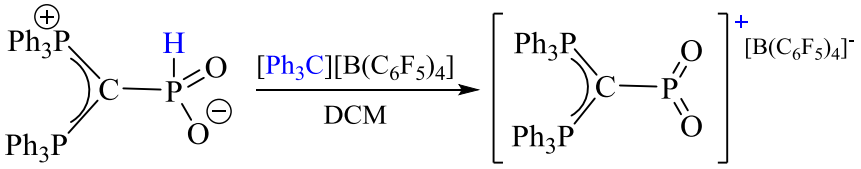

*Scheme 44. The predicated reaction product for the hydride abstraction from **17***

Alternatively, we explored the accessibility to a $[L\text{-}PO_2]^+$ cationic species *via* acidic hydride-removal reaction (Scheme 44), which was supported by the P(1)-C(1) bond value of 1.812(5) Å, indicative of a weak Lewis acidic character on the central phosphorus. Contrarily to our expectations, employment of a trityl tetrakis(pentafluorophenyl)borate resulted in the appearance of a doublet at δ_P 20.5 ppm and a triplet at δ_P 18.2 ppm ($^1J_{P\text{-}H}$ = 488 Hz), which were assigned to a (trityloxy)oxophosphonium salt (Scheme 45). Numerous attempts to crystallize the compound failed, probably due to high air- and moisture- sensitivity. However, we managed to observe it *via* HRMS at 867.2641 m/z. Analogous results were obtained

with trityl-triflate, resulting in the appearance of a doublet and a triplet at δ_P 22 ppm and δ_P 19 ppm, respectively.

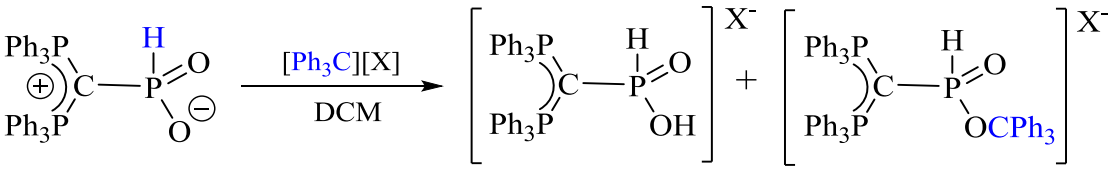

X = $B(C_6F_5)_4^-$, OTf^-

*Scheme 45. The reaction between **17** and trityl-borate*

Another approach for the hydride abstraction included hydrogen substitution, in which we used oxalyl chloride as a halogen source. Unfortunately, the reaction yielded formerly mentioned $[(Ph_3P)_2CPCl_2][Cl]$ (precursor for the synthesis of **17**) instead of the desired product. It can be suggested that the high affinity of **17** for chloride ions prevented the activation of the P-H bond, and instead, caused reactivity at the $P_{central}$.

Inability to remove the hydrogen atom could be assigned to a particularly strong P-H bond of 1.357Å. Literature reports of an intermolecular hydride exchange in a reaction of 2-H-diazaphospholane with P-chloro-diazaphospholene and trichlorogermanate (or trichlorostannate) offer comparable results.[204] For the performed reaction, a computed P-H bond value for 2-H-diazaphospholane equaled to 1.480 Å, and 1.771 Å for a resulting dimer PHC-H-PHC. However, the same reaction did not proceed when a dimer without a P-H-P bond was computed, where a single P-H bond of 1.462 Å was preserved. Having in mind that our bond length of 1.357Å is significantly shorter, difficulties in activating it are not surprising.

4.2.2.2 Methylation

Preference of CPh_3^+ for oxygen corresponds to higher acidity of the terminal oxygen with respect to hydrogen in P-H. This was confirmed in a reaction with

methyl-triflate, which produced a clear doublet of quartets ($^{1}J_{P\text{-}H}$ = 586Hz, $^{3}J_{POCH}$=13Hz) at δ_P 30.5 ppm immediately upon the addition, indicative of the $(Ph_3P)_2CP(O)(OMe)H$ product (Scheme 46).

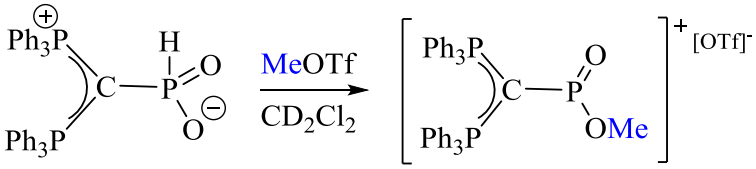

*Scheme 46. The product of a reaction between **17** and MeOTf.*

Coupling constants of the obtained product are in the range of previously reported values in (Me)(H)P(O)(OR), presented in Table 8.[205] $P_{central}$ ^{31}P NMR shifts obtained for **17** fall within the range reported for (Me)(H)P(O)(OR'). A slight downfield shift can be observed in cases where R=H ($H_2P(O)(OR')$), possibly due to the stronger donor-ability of methyl and carbone substituents in comparison to the hydrogen atom.

Table 8. Literature values of ^{31}P NMR shifts and coupling constants for compounds of formula (R)(H)P(O)(OR')

(R)(H)P(O)(OR')				
R	R'	δ_P [ppm]	$^{1}J_{P\text{-}H}$ [Hz]	$^{3}J_{POCH}$ [Hz]
Me	Me	32.8	545	-
	Et	31.3	555	-
H	Me	19.2	569	13
	Et	15.8	570	10
	^{i}Pr	11.8	570	10
	^{t}Bu	8	560	-
	$^{t}C_6H_{11}$	6.3	552	-
	Ph-CH_2	15.1	575	11

Considering that the reported Mo-complex of PO_2 proved to be inactive in the methylation reaction, the successful methylation of **17** by MeOTf emphasized the preserved reactivity of the PO_2 unit within the specie (**17**).

4.2.2.3 Dioxophosphorane-trapping

As previously mentioned, most commonly employed agents for PO_2 trapping are aniline and alcohols (Scheme 47), mainly methanol.

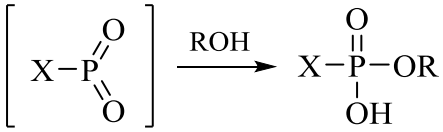

Scheme 47. A general reaction of the dioxophosphorane-intermediate trapping with an alcohol

4.2.2.3.1 Amines

Contrarily to the quenched electrophilicity and absence of reactivity of PO_2 towards methanol and aniline in Ru-complex, **17** reacts with both trapping agents. The reaction between **17** and aniline in large excess causes an immediate solution colour change to brown, and a new peak formation at about δ_P -6 ppm, which decomposes into multiple products about 2 hrs later, prior to the reaction completion. Reactions with other primary amines, namely $MeNH_2$, $^tBuNH_2$, $CyNH_2$, started producing a minor protonated carbone peak after heating the reaction to 80°C for three days. Similarly, **17** did not show any reactivity towards the secondary amine ($^iPr_2NH$) even upon heating.

4.2.2.3.2 Alcohols

Dioxophosphorane trapping was achieved with various alcohols (Table 9) to form compounds of formula $[(Ph_3P)_2CH][HP(O)_2(OR)]$ (Scheme 48).

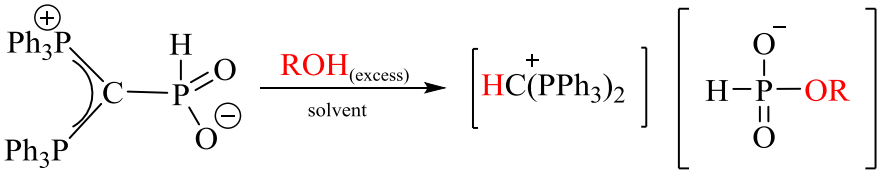

*Scheme 48. A general dioxophosphorane-trapping reaction between **17** and an alcohol*

When the last column fraction of pure **17** in methanol is left on the bench for 48h, a spontaneous and clean conversion into $[(Ph_3P)_2CH][HP(O)_2(OCH_3)]$ occurs. ^{31}P NMR spectra displayed a monoprotonated carbone singlet at δ_P 20.4 ppm, and a doublet of quartets at δ_P 6.3 ppm ($^1J_{P\text{-}H}$ = 557 Hz, $^3J_{POCH}$ = 11 Hz). When the reaction is repeated in wet acetonitrile and heated to 70°C, complete conversion occurs in only 4.5h, producing peaks at δ_P 21.1 (s) δ_P 5.7 ppm (d, $^1J_{P\text{-}H}$ = 615 Hz). The same time is required for this reaction with dry **17**, with peaks occurring at δ_P 21.0 (s) δ_P 6.1 ppm (d, $^1J_{P\text{-}H}$ = 609 Hz). Slight variations in the $P_{central}$ peak positions are assigned to solvent effects and stabilization *via* H-bonding by methanol molecules. This is clearly observed in ^1H spectra as well. In general, MeOH solvent trace peaks occur at δ_H 3.28 ppm (singlet) and δ_H 2.16 ppm (singlet). However, due to the coordination of methanol to the starting material, MeOH peaks now appear at δ_H 3.24 ppm (s) and δ_H 2.59 ppm, which exhibits significant broadening. Upon heating, the peak at δ_H 2.59 ppm disappears, and new peaks form at 5.83 (s) ppm, 2.35 (s) ppm as a P-O-Me bond is being formed. Crystals suitable for single crystal X-Ray diffraction were also successfully grown from DCM/Hexane. Although the quality and the data of the crystals was poor, the existence of the $P(O)_2(OCH_3)$ fragment was confirmed (Figure 36), although insetead of the directly bounded proton, a KCl salt was bounded to the central phosphorus atom, probably due to the impure starting material and the presence of the $BAr^{Cl}{}_4^-$ salts in it.

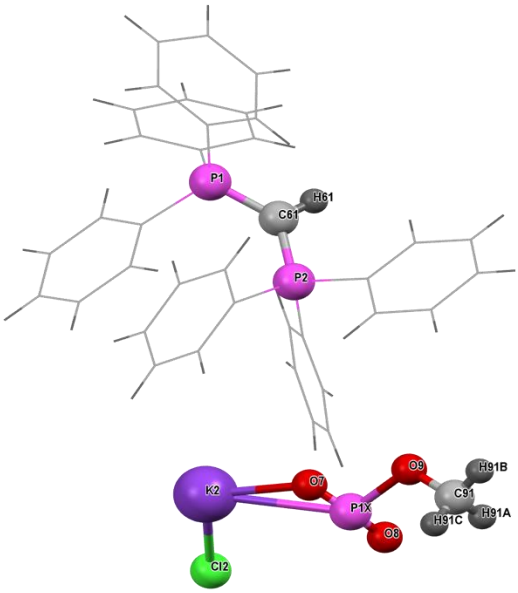

Figure 34. The crystal structure of [HC(PPh$_3$)$_2$][P(μ-KCl)O$_2$(OMe)]

Analogous results were obtained with CD_3OD in acetonitrile (Scheme 49). $P_{carbone}$ peak at δ_P 20.07 and $P_{central}$ at δ_P 5.43 ppm were consistent with the values in $[(Ph_3P)_2CH][HP(O)_2(OCH_3)]$. Furthermore, $P_{central}$ of P-O-CD_3 coupled with the directly bounded proton, which was displayed by a doublet; compared to doublet of quartets for the P-O-CH_3 unit. $^1J_{P-H}$ value of 603 Hz was also consistent with the earlier results. $^2D\{^1H\}$ NMR was also performed. Upon the completion of the reaction, a doublet at 3.34 ppm (-OD, J = 11 Hz) and a broad signal at 2.42 ppm (-CD_3) were observed, again, indicating coordination of the -CD_3 group. ^{31}P NMR spectra confirmed formation of $[(Ph_3P)_2CH][HP(O)_2(OCD_3)]$. The yielded compound was subsequently reacted with MeOTf to yield $HP(O)(OCH_3)(OCD_3)$ (Scheme 49), which displays a doublet in 31P NMR at 11.1 ppm, with a coupling constant of 691Hz, consistent with the values reported in the literature for $HP(O)(OCH_3)_2$. The product was also identified in HRMS at m/z 114.04.

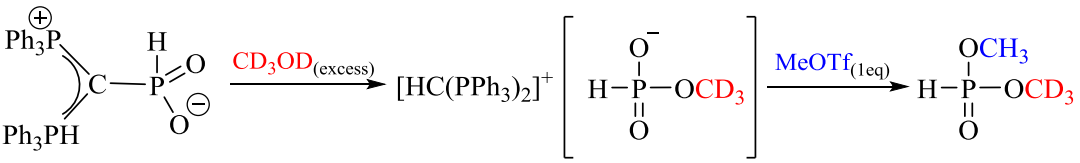

*Scheme 49. The reaction of **17** with deuterated methanol, followed by the methylation with MeOTf.*

Interestingly, the reaction with MeOH completes in 5 h when either methanol or acetonitrile of HPLC grade are used as solvents. In comparison, the same reaction lasts for 3 days when performed in the neat MeOH, and for 6-7 days when ACN or CD_3CN are used. Although **17** reacts with water (discussed below), the presence of water in 1-2% slows down the reaction, which is probably due to the competition for the formation of O-H bonds with MeOH and/or water molecules. It is evident from ^{1}H NMR that both water (δ_H 2.25 ppm) and methanol (δ_H 2.59 ppm) coordinate to the starting material. Both peaks disappear as the reaction proceeds. However, only the $[(Ph_3P)_2CH][HP(O)_2(OCH_3)]$ product formation can be observed in ^{31}P NMR. In addition, the presence of water molecules in the starting material (**17**•$2H_2O$) was not the crucial factor for the faster reaction rates, since the same time was required even with the dry starting material (under above-mentioned conditions); leading us to believe that the water content in the solvents was not increasing reaction rates. This was confirmed in numerous repeated experiments that we conducted using MeOH/ACN of different grades and purification levels, available in the Appendix. The experiments implied that the reaction time was also indifferent to the presence of oxygen and/or salt stabilizers, found on the bottle labels of various suppliers. While $BAr^{Cl/F}{}_4$ salts have been reported to act as catalysts,[206] their presence in our sample would not shorten the reaction time either. To eliminate the possibility of TEA impurities that might have remained from the column to act as a catalyst, we prepared a batch of **17** without using TEA in any stage of the synthesis or preparation (“clean”) and performed reactions displayed in entries 9, 12 and 13 of Table 11 in Appendix.

Parallel reactions were repeated for the presence of TEA in the system (Appendix, Table 1; entries 14-16). Reaction was completed in 5h in cases when methanol or acetonitrile was of HPLC grade, regardless of the presence of TEA (Appendix, Table 1; entries 9, and 13-15), eliminating the possibility that TEA acts as a sole reaction catalyst. However, the presence of ETA affected the outcome of the reaction when both methanol and acetonitrile were dry, distilled, and degassed "D" (Appendix, Table 1; entries 12 and 16). We believed that it was the result of the $TEAH^+$ ion formation, which coordinates to the terminal oxygens of **17** *via* H-bonds, and facilitates the reaction. However, when the reaction was repeated by spiking $TEAH^+$ into a system that contained "clean" **17**, only about 16% of the starting material was converted into the product within 5h, excluding this scenario as a possibility. Unfortunately, we were not able to identify with certainty the exact factor that significantly increases reaction rates. While TEA can aid the process, it does not necessarily change the outcome of all reactions, but we can say with certainty that HPLC grade of alcohol or solvent is required for the faster reaction rates.

17 also reacts with water upon heating to temperatures about 80°C or higher, to give a relatively clean product $[(Ph_3P)_2CH][HP(O)_2(OH)]$, identified by a singlet at 20.8 ppm and a broad peak at 3.6 ppm in $^{31}P\{^1H\}$ NMR, which shows coupling with a proton of the P-H bond ($^1J_{P\text{-}H}$ = 608 Hz). Broadening of the peak is due to hydrogen bonds, which can also be observed in ^1H NMR. When water is added to the starting material, its coordination can be observed in the appearance of a broad peak at δ_H 2.25 ppm. As the reaction progresses, this peak converts into an even broader peak at δ_H 4.8 ppm, which further converts into a new singlet peak at δ_H 5.98 ppm, similar to the δ_H 5.84 ppm in $[(Ph_3P)_2CH][HP(O)_2(OCH_3)]$. This is also followed by a more upfield shift in ^{31}P NMR to δ_P –0.52 ppm (doublet), with a relatively preserved coupling

constant ($^1J_{P-H}$) of 601 Hz, suggesting an intramolecular rearrangement or a formation of a new product. Contrarily to the reaction with MeOH, where the transformation is slowed down in the presence of water, traces of methanol seem to speed up the reactivity of **17** towards the water. While the second conversion is only about 50% completed in 7 days, complete conversion occurs in only 6 days when 1%vv MeOH (with respect to H_2O) is added to the initial reaction mixture, clearly speeding up the process, without any signs of the $[(Ph_3P)_2CH][HP(O)_2(OCH_3)]$ side-product formation.

Furthermore, **17** exhibited analogous behaviour towards different saturated and unsaturated alcohols (Table 9), confirming that **17** can be used as a source of compounds of formula $[(Ph_3P)_2CH][HP(O)_2(OR)]$, precursors for dialkyl-phosponate esters.

As it can be observed from Table 9, reactions with MeOH and EtOH were the fastest. With respect to saturated alcohols, reaction times of the primary and less hindered alcohols were between 3.5-7 hours, whereas bulkier alcohols, such as ^{i}PrOH, ^{t}BuOH, $(CF_3)_3COH$ took significantly more time. This is in accordance with previously reported kinetic studies for dioxophosphorane trapping with alcohols by Jankowski *et al.*,[183d, 207] which revealed faster reaction between metaphosphonates/metathiophosphonates and methanol, over isopropanol and *tert*-butanol. According to the authors, primary alcohols have more negative enthalpies and entropies of activation, which allows them to be more engaged in reactions and or more assistance. In addition, that reaction with MeOH proceeds *via* the first-rate reaction at 30°C which is independent of the MeOH/BuOH concentration above 0.25M, whereas it is inversely proportional to the concentrations of ^{i}PrOH ot ^{t}BuOH. Suggested reasons for it include different reaction mechanism-pathways, *via*

Elimination-Addition mechanism (primary ROH) or *via* Addition-Elimination mechanism (tertiary alcohols).

Table 9. All reactions were performed at 80°C

R	t [h]	d_P [ppm]	Multiplicity	Coupling constant
Me	5	5.69	dq	$^1J_{P-H}$ = 557 Hz; $^3J_{P-O-C-H}$ = 11 Hz
CD_3	5	5.43	d	$^1J_{P-H}$ = 603 Hz
Et	3.5	3.12	dt	$^1J_{P-H}$ = 601 Hz
^{i}Pr	25	-0.18	dd	$^1J_{P-H}$ = 585 Hz; $^3J_{P-O-C-H}$ = 9 Hz
^{t}Bu	>48	-4.56	d	$^1J_{P-H}$ = 586 Hz
Ph	15	-0.71	d	$^1J_{P-H}$ = 625 Hz
$PhCH_2CH_2$	7	3.24	dt	$^1J_{P-H}$ = 600 Hz; $^3J_{P-O-C-H}$ = 9 Hz
$CH_3CHPhCH_2$	6	3.13	dt	$^1J_{P-H}$ = 596 Hz; $^3J_{P-O-C-H}$ = 7 Hz
$(CF_3)_3C$	22	-0.26	d	$^1J_{P-H}$ = 625 Hz
$CH_2=CHCH_2CH_2^*$	90	3.23	dt	$^1J_{P-H}$ = 602 Hz; $^3J_{P-O-C-H}$ = 10 Hz
$CH_2=CH(CH_2)_2CH_2^*$	>90	3.04	dt	$^1J_{P-H}$ = 597 Hz; $^3J_{P-O-C-H}$ = 7 Hz
$HC\equiv CCH_2CH_2^*$	>90	3.39	dt	$^1J_{P-H}$ = 605 Hz; $^3J_{P-O-C-H}$ = 8 Hz
$HC\equiv C(CH_2)_2CH_2^*$	>90	3.31	dt	$^1J_{P-H}$ = 601 Hz; $^3J_{P-O-C-H}$ = 6 Hz

With respect to unsaturated alcohols, the values presented in Table 8 refer to reactions in acetonitrile. When the solvent is changed to 1,2-dichlorotoluene and the working temperature raised to 130°C, starting material is completely depleted within 5 hours. However, the new products show different ^{31}P NMR peaks and possible ring-formation products.

4.2.2.3.2.1 DFT calculations

Three possible pathways calculated for the reaction between **17** and methanol are depicted in Scheme 50.

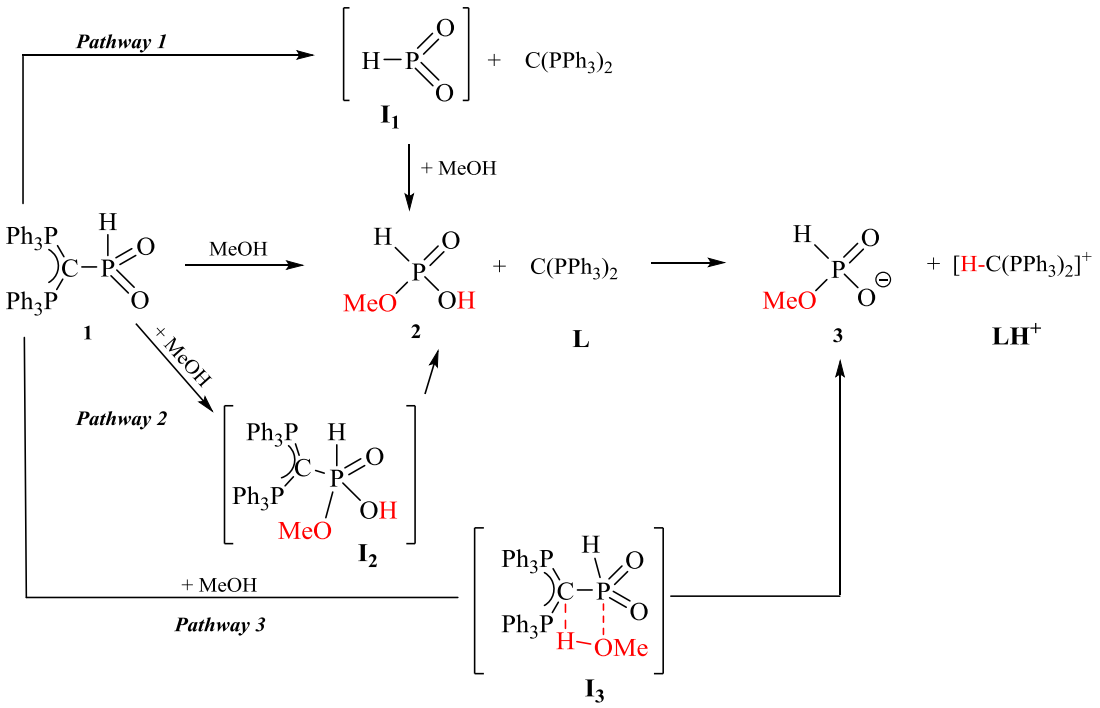

*Scheme 50. Three possible mechanisms for the reaction between the parent-metaphosphonate **17** and methanol; "I" stands for "intermediate" and "L" stands for "ligand".*

Regarding *pathway 1*, calculated bond dissociation enthalpies for the C-P bond, at reaction temperatures of 25°C and 130°C, were 56.0 and 55.9 kcal/mol, respectively. The results showed the significant stability of the reactant **17** (**1**), compared to the intermediate state $\mathbf{I_1}$ + $\mathbf{(PPh_3)_2C}$. Stretching of the P-C bond resulted in the energy increase until the bond breakage. This situation corresponds to the absence of the transition state, meaning that this scenario mechanism is not applicable to the examined reaction.

Concerning the *pathway 2* mechanism, it proceeds *via* three steps, as shown below, in Scheme 51.

Step 1:	**1** + MeOH ⟶ [TS_1] ⟶ $\mathbf{I_2}$	Ea_1 = 12.4 kcal/mol
Step 2:	$\mathbf{I_2}$ ⟶ [TS_2] ⟶ **2 + L**	Ea_2 = 1.7 kcal/mol
Step 3:	**2 + L** ⟶ $\mathbf{3^-{---}H^+L}$	Barrier-less reaction

*Scheme 51. Calculated reaction steps and activation energies for the pathway 2 mechanism in the reaction between **17** and MeOH*

Calculated activation energy, for the conversion of the reactant **1** into the intermediate $\mathbf{I_2}$, amounts to 12.4 kcal/mol (*step 1*). This intermediate ($\mathbf{I_2}$) subsequently undergoes a P-C bond breakage to give an optimized state **2**, which is only 1.7 kcal/mol higher in energy than the intermediate $\mathbf{I_2}$ (*step 2*). Unfortunately, calculations displayed a flat potential energy surface for this stage, making it difficult to confirm the transition state *via* IRC. Based on the normal mode visualisation, P-C bond breakage is obvious. Energy values for a fixed P-C bond scenario are displayed below, in Table 10.

Table 10. Energy values for a scenario when the P-C bond is fixed

	r(P-C) / A	E_{el} / Hartree
I_2	1.96	-2718.91148656
	2.10	-2718.91034267
	2.20	-2718.90900595
	2.30	-2718.90790390
	2.40	-2718.90733790
TS_2	2.44	-2718.90728533
	2.50	-2718.90737322
	2.60	-2718.90780924
	2.70	-2718.90840409
	2.80	-2718.91092221
	2.90	-2718.91059689

Energy slowly rises until the transition state, after which it decreases to 2.80 Å, and then rises again. Such data implies that the P-C bond is relatively loose, allowing **2** to position itself relative to the **L**. Due to the partial positive charge of the proton in the hydroxyl group (-OH), the most stable structure is likely to be the one in which the proton in **2** points towards carbon (in **L**). However, such orientation immediately leads to the proton transfer (from **2** to **L**), resulting in the formation of the final product $\mathbf{3}^-$---$\mathbf{H}^+\mathbf{L}$ (*step 3*), in which $\mathbf{3}^-$ and $\mathbf{H}^+\mathbf{L}$ moieties are connected *via* hydrogen bond. The original bond lengths for the O-H and C-H bonds are 1.0 Å and 1.7 Å, respectively. However, when the C(**L**)-O(**2**) bond length is fixed to 2.7 Å, the proton gets transferred from **2** to **L,** during partial optimization, which implies a barrier-less

transformation into the final products (**3**$^{-}$---**H**$^{+}$**L**). Also, calculated energies (Table 11) show higher stability for the transition state (**TS$_2$**), than the reaction products (**2 + L**). Generally, this cannot be true, as transition states must energetically lye the highest.

*Table 11. Activation and free Gibbs energies of **17** + MeOH reaction reactants, intermediates, transition states and products.*

	E_{el+ZPE} - $E_{el+ZPE(1+MeOH)}$ [kcal/mol]	Ea [kcal/mol]	G - $G_{(1+MeOH)}$ [kcal/mol]
1+MeOH	0.0	Ea_1 = 12.4	0.0
TS_1	12.4		24.4
I_2	7.3	Ea_2 = 1.7	19.4
TS_2	9.0		20.3
2 + L	12.1	Barrierless	8.5
3---LH^+	-31.7		-21.5

However, the calculated energy for **2 + L** refers to molecules at a distance, which does not occur in our case, which explains the discrepancies in the results for calculated energies. Similarly, the in final reaction product **3**$^{-}$---**H**$^{+}$**L**, moieties stay in proximity, reflected by the ΔE_{el+ZPE}, which is calculated at -31.7 kcal/mol. On the contrary, the calculated energy for the distant products **3**$^{-}$ + **H**$^{+}$**L** amounts to 56.6 kcal/mol.

Lastly, *pathway 3* corresponds to a σ-bond metathesis reaction mechanism, through the intermediate state **I$_3$**. However, all the attempts to optimize this reaction mechanism failed, probably due to the very high energy barrier. Thus, this reaction is very unlikely to proceed *via* the *pathway 3*.

The computed structural parameters obtained for compound **17** (e.g. $d_{C\text{-}P}$ = 1.869 Å, $d_{P\text{-}H}$ = 1.423 Å, $d_{P\text{-}O1}$ = 1.515 Å, $d_{P\text{-}O2}$ = 1.516 Å) are also comparable to the experimental values. Calculated atomic charges reveal a highly positive charge accumulation of +3.300 at the central phosphorus, which confirms its highly electrophilic nature, as expected for a dioxophosphorane compound. In addition, -

0.548 negative charge at the hydrogen atom (P-H), provides the reasoning behind previous difficulties to deprotonate the compound. Oxygen atoms bear negative charges of -1.507 and -1.494, respectively; while the central carbon atom in the ligand bears a negative charge of -2.302, clearly indicative of the localization of its remaining lone pair.

4.2.2.3.3 Dehydrogenative coupling

In recent years, Li-Biao Han and co-workers have developed new approaches towards organophosphorus compounds *via* transition-metal catalyzed dehydrogenative coupling of H-phosphonates with terminal alkynes, alcohols and thiols.[208] In general, reaction rates and yields of the products were highly dependent on the choice of the catalyst and solvents. With respect to aerobic oxidative coupling of terminal alkynes, Cu-halides and Cu-acetates proved to be the best. While this reaction could not be catalyzed by $Pd(OAc)_2$, Pd-based catalysts were crucial for dehydrogenative coupling of secondary phosphines with terminal alkynes. Previously reported studies agreed that yields highly depended on solvent choices, with DMSO and THF being highly suitable due to their ability to stabilize the reaction intermediate *via* ligation.

Since our system also contained a P(O)-H unit, we wondered whether it could serve for dehydrogenative coupling, similarly to dialkyl- and diaryl-phosphine oxides. Phenylacetylene and its halogenated derivative 4-bromo-phenylacetylene served as a source of terminal alkynes in the reactions.

Contrarily to the findings by Li-Biao Han et al., our system did not respond to a copper-halides as catalysts, regardless of the presence of base and heating. In addition, DMSO, and THF were not suitable solvents. While no reaction was observed in DMSO, reactions let to very complex mixtures in THF. When $Pd(OAc)_2$ (10 %mol)

was added to **17** in the presence of $AgBF_4$ in acetonitrile, we have immediately observed a $P_{central}$ downfield shift in ^{31}P NMR by ~10ppm, which possibly indicates coordination of the catalyst. P-H coupling of 558 Hz was preserved. Addition of an alkyne did not result in significant changes, apart from the broadening of the triplet for P_{cental}. We believed that coordination of the catalysts or the alkyne would weaken the P-H bond so that it could be activated in the presence of a potent base. However, the addition of ^{t}BuLi in the presence of 18-crown-6 at this stage only reversed the reaction to the starting material before the catalyst coordination, which was yet another confirmation of the exceptionally strong P-H bond.

4.3 Conclusion

In conclusion, we report the synthesis and the full characterisation of the first example of a carbone-stabilized parent-metaphosphonate system $[(Ph_3P)_2CP(O)_2H]$ (**17**), which co-crystalizes with two water molecules **17·2H$_2$O**. Unlike the two previously reported examples of stabilized dioxophosphoranes which lose their reactive nature upon complexation with transition-metals, the P centre in **17** still preserves its electrophilic character. This was confirmed in reactions with various alcohols, typically used as dioxophosphorane-trapping agents. Computational results revealed a stepwise reaction mechanism as the most viable, through an intermediate $[\{(Ph_3P)_2C\}P(O)(OCH_3)(OH)H]$, where the final reaction products $[(Ph_3P)_2CH]^+$ and $[P(O)_2(OR)H]^-$ preserve proximity, which accounts for the ΔE_{el+ZPE} energy of 56.6 kcal/mol. The interesting chemistry of **17** explored in this chapter also includes deprotonation and hydrogen-abstraction reactions, methylations, tritylations, and transition-metal catalyzed dehydrogenative coupling reactions.

Having in mind limited examples of accessible metaphosphonate species, **17** provides a valuable insight into their chemistry, and possible an easier access to the highly elusive PO_2 species.

CHAPTER V:

Experimental and Methods

5.1 General Methods

All reaction manipulations were performed using standard Schlenk line or glovebox techniques under an inert atmosphere of dry argon. All glassware and J. Young NMR tubes were oven-dried at 120°C overnight, then flame-dried and cooled under vacuum prior to use. All solvents were distilled under the atmosphere of dry N_2. Toluene, benzene, n-hexane, and n-pentane, were distilled over sodium; acetonitrile and 1,2-difluorobenzene were distilled over CaH_2; while tetrahydrofuran and diethyl-ether were distilled over sodium/benzophenone. Dichloromethane (DCM) was purchased anhydrous and stored over molecular sieves. Deuterated solvents (C_6D_6, CD_2Cl_2, $CDCl_3$, CD_3CN, CD_3OD, D_2O) were dried according to standard procedures. All solvents were subsequently degassed and stored over 4Å molecular sieves prior to use. CD_2Cl_2 was additionally dried by placing it three times over molecular sieves. Benzene and n-hexane were additionally stored in a storage flask over a sodium or a potassium mirror prior to use.

Commercially available chemicals (triphenylphosphine, trimethylphosphine, tricyclohexylphosphine, potassium *tert*-butoxide, sodium amide, potassium bis(trimethylsilyl)amide, *n*-butyllithium, *t*-butyllithium, sodium trifluoromethanesulfonate, silver trifluoromethanesulfonate, methyl trifluoromethanesulfonate sodium perchlorate, silver perchlorate, sodium tetrafluoroborate, silver tetrafluoroborate, potassium tetrafluoroborate, sodium hexafluorophosphate, silver hexafluorophosphate, potassium hexafluorophosphate, sodium hexafluoroantimonate, silver hexafluoroantimonate, potassium hexafluoroantimonate, gallium trichloride, xenon difluoride, oxalyl chloride, 18-crown-6, 12-crown-4, copper(I) iodide, palladium(II) acetate, 2-phenyl ethanol, 2-phenyl-1-propanol, nonafluoro-*tert*-butyl alcohol, 1-buten-4-ol, 1-butyn-4-ol, 4-

penten-1-ol, 4-pentyn-1-ol, phenylacetylene and bromophenylacetylene) were used without further purification. Phosphorus trichloride, diisopropylamine, dibromomethane, and aniline were distilled prior to use. Pyridine *N*-oxide, trimethylamine *N*-oxide, tetramethylammonium hydroxide and triethylphosphine oxide were sublimed and dried under vacuum before use. **1a**,[209] **1b**,[210] [**2a**]Cl,[142] [**3a**][X]$_2$ (X = $AlCl_4$, $Bar^F{}_4$) (Ar^F = 3,5-$(CF_3)_2$-C_6H_3)),[142] Na[$BAr^{Cl}{}_4$] (Ar^{Cl} = 3,5-Cl_2-C_6H_3), Na[$BAr^F{}_4$], K[$BAr^{Cl}{}_4$], and K[$BAr^F{}_4$] have been prepared according to the reported procedures.[211] Finally, all manipulations with silver salts were performed in the absence of light.

The NMR spectra were obtained on a Bruker Advance III 400 (BBFO 400) spectrometer (^{1}H NMR at 400 MHz; ^{13}C at 100 MHz; ^{31}P NMR at 161 MHz; ^{19}F NMR at 376 MHz; ^{11}B at 128 MHz). ^{31}P, ^{19}F, ^{11}B, and ^{27}Al chemical shifts were referenced to 85% H_3PO_4, $CFCl_3$, $Et_2O{\cdot}BF_3$, and $AlCl_3/D_2O$, respectively; ^{1}H and ^{13}C shifts were referenced to tetramethylsilane(TMS). Mass spectra were collected on the Waters Q-TOF Premier MS and Agilent Technologies 6230TOF LC/MS mass spectrometers using the electrospray ionization (ESI) mode.

Preparation of the Monocationic Precursors [2]Cl

The compound was prepared with slight modifications of the previously reported procedure[192]. One equivalent of a warm (50°C) carbone (**1**) solution in benzene was added to 3 equiv of R"PCl_2 (R = Me, ^{i}Pr, Cy), with vigorous stirring. The formation of a colourless precipitate was immediately observed. The best yields were achieved with 17h of stirring. The solution was filtered, and the resulting solid was dried overnight under reduced pressure.

[$Cy_2NPCl(C(PPh_3)_2)$][Cl] ([2d][Cl]):

1.00 g (1.86 mmol) of **1a** and 1.58 g (5.58 mmol) of Cy_2NPCl_2. Yield: 1.23 g (81%). ^{1}H NMR (400 MHz, CD_2Cl_2, 20 °C): δ_H 0.7–1.4 (20H, C*H*$_2$-Cy), 2.84 (br, 2H, C*H*-Cy), 7.2–7.5 (br, 30H, Ph). ^{13}C{^{1}H} NMR (400 MHz, CD_2Cl_2, 20 °C): δ_C 19.9 (dt, $^1J_{P(carbone)C}$ = 78 Hz, $^1J_{P(carbone)C}$ = 104 Hz, *C*$(PPh_3)_2$); 25.1 (s, δ-*C*H_2-Cy), 25.8 (s, γ-*C*H_2-Cy), 33.0 (br, β-*C*H_2-Cy), 59.1 (br, CH-Cy), 125.7(apparent triplet AA′X, $^1J_{PC}$ + $^3J_{PC}$ = 92 Hz, *ipso*-C, Ph of C$(PPh_3)_2$), 129.3 (virtual triplet, *o*-*C*, Ph of C$(PPh_3)_2$), 134.6 (br, *m*-C, Ph of C$(PPh_3)_2$) ppm. ^{31}P{^{1}H} NMR (161 MHz, CD_2Cl_2, 20 °C): δ_P 26.1 (second-order doublet, $P_{carbone}$), 140.5 (second-order triplet, $P_{central}$) ppm. MS (ES+): *m*/*z* 720 (M^+). HRMS (ES+): calcd for $C_{49}H_{52}NPCl$, *m*/*z* 720.3526; found, 720.3536.

[^{i}Pr$_2$NPClC(Ph$_2$P(CH$_2$)$_3$PPh$_2$)][Cl], [2e][Cl]:

1.0 g (2.36 mmol) of **1b** and 1.43 g (7.08 mmol) of $^iPr_2NPCl_2$. Yield: 0.81 g (55%). ^{1}H NMR (400 MHz, CD_2Cl_2, 20 °C): 0.56 (br, 12H, C*H*$_3$), 2.07 (m, 2H, CH_2), 3.30 (br, 4H, CH_2), 3.73 (br, 2H, CH), 7.2–7.8 (20H, Ph) ppm. ^{13}C{^{1}H} NMR (400 MHz, CD_2Cl_2, 20 °C): δ_C 14.8 (m, P*C*P, cyclic carbone), 15.3 (s, *C*$H_2(CH_2)_2$, cyclic carbone), 22.3 (br, CH(*C*$H_3)_2$), 26.2 (second-order triplet, CH_2(*C*$H_2)_2$, cyclic carbone), 48.2 (br, *C*H$(CH_3)_2$), 128.3–134.3 (m, C_1–C_4, Ph of cyclic carbone) ppm. ^{31}P{^{1}H} NMR (161 MHz, CD_2Cl_2, 20 °C): δ_P 16.3 (second-order doublet, $P_{carbone}$), 138.0 (second-order triplet, $P_{central}$) ppm. MS (ES+): *m*/*z* 590 (M^+). HRMS (ES+): calcd for $C_{34}H_{40}NP_3Cl$, *m*/*z* 590.2062; found, 590.2054.

Synthesis of the Dications [3b][X]$_2$ and [3c][X]$_2$ (X = AlCl$_4$, BAr$^f_4$)

To a DCM (30 mL) solution containing a monocationic precursor ([**2b**]Cl or [**2c**]Cl) was added 2.1 equiv of either $AlCl_3$ or Na[BAr$^f_4$]. The reaction mixture was stirred for 6 h followed by filtration (when Na[BAr$^f_4$] was used), and solvent removal under

reduced pressure yielded a yellow solid. It is worth noting that, regardless of the nature of the counterion, the multinuclear NMR data for the dicationic moieties (**3b**$^{2+}$ and **3c**$^{2+}$) were essentially identical; thus, the data for ion pairs are reported separately.

[$Cy_2NP(C(PPh_3)_2)$]$^{2+}$, [3d][X]$_2$

1.0 g (1.22 mmol) of [**2c**][Cl] and 2.1 equiv of $AlCl_3$ or Na[BAr^f_4]. Yield: 0.81 g (61%) as the $AlCl_4^-$salt and 1.78 g (59%) as the $[BAr^f_4]^-$ salt. ^{1}H NMR (400 MHz, CD_2Cl_2, 20 °C): δ_H 0.47–1.72 (br m, 2H, CH_2-Cy), 3.36 (br, 1H, CH-Cy), 3.53 (br, 1H, CH-Cy), 7.3–7.9 (30H, Ph) ppm. $^{13}C\{^1H\}$ NMR (400 MHz, CD_2Cl_2, 20 °C): δ_C 23.7 (s, δ-*C*H_2-Cy), 24.4 (s, δ-*C*H_2-Cy), 25.0 (s, γ-*C*H_2-Cy), 26.2 (s, γ-*C*H_2-Cy), 30.9 (br, β-*C*H_2-Cy), 39.6 (d, $^3J_{PC}$ = 18 Hz, br, β-*C*H_2-Cy), 64.1 (d, $^2J_{PC}$ = 22 Hz, CH-Cy), 66.0 (m, $C_{carbone}$), 119.4 (apparent triplet AA′X, $^1J_{PC} + {}^3J_{PC}$ = 94 MHz, *ipso*-C, Ph of $C(PPh_3)_2$), 130.9 (*p*-C, Ph of $C(PPh_3)_2$), 133.8 (t, $^3J_{PC}$ = 5.8 Hz, *o*-C, Ph of $C(PPh_3)_2$), 137.7 (*m*-C, Ph of $C(PPh_3)_2$) ppm. $^{31}P\{^1H\}$ NMR (161 MHz, CD_2Cl_2, 20 °C): δ_P 26.0 (second-order doublet, $P_{carbone}$), 360.4 (second-order triplet, $P_{central}$) ppm.

[^{i}$Pr_2NPC(Ph_2P(CH_2)_3PPh_2)$]^2, [3e][X]$_2$

1.0 g (1.60 mmol) of [**2c**][Cl] and 2.1 equiv of $AlCl_3$ or Na[BAr^f_4]. Yield: 0.84 g (59%) as the $AlCl_4^-$salt and 2.19 g (60%) as the $[BAr^f_4]^-$ salt. ^{1}H NMR (400 MHz, CD_2Cl_2, 20 °C): δ_H 0.49 (d, 3H, $^3J_{HH}$ = 6.4 Hz, CH_3), 1.18 (d, 3H $^3J_{HH}$ = 6.8 Hz, CH_3), 2.35 (m, 2H, CH_2), 2.85 (m, 4H, CH_2), 3.73 (m, 1H, CH), 3.92 (m, 1H, CH) 7.3–7.9 (20H, Ph) ppm. $^{13}C\{^1H\}$ NMR (100 MHz, CD_2Cl_2, 20 °C): δ_C 14.9 (s, *C*$H_2(CH_2)_2$, cyclic carbone), 20.8 (br, $CH(CH_3)_2$), 23.9 (second-order triplet, $CH_2(CH_2)_2$, cyclic carbone), 27.9 (d, $^3J_{PC}$ = 15 Hz, $CH(CH_3)_2$), 54.6 (d, $^2J_{PC}$ = 24 Hz, *C*$H(CH_3)_2$), 62.8 (d, $^2J_{PC}$ = 15 Hz, *C*$H(CH_3)_2$), 66.7 (m, $C_{carbone}$),131.5–132.6 (m, C_1–C_4, Ph of cyclic

carbone) ppm. $^{31}P\{^{1}H\}$ NMR (161 MHz, CD_2Cl_2, 20 °C): δ_P 19.1 (second-order doublet, $P_{carbone}$), 351.5 (second-order triplet, $P_{central}$) ppm.

Counterions

$AlCl_4^-$: ^{27}Al NMR (104 MHz, CD_2Cl_2, 20 °C) δ_{Al} 106 ppm. $[BAr^f_4]^-$: ^{1}H NMR (400 MHz, CD_2Cl_2, 20 °C) δ_H 7.3–7.9 (24H, Ph) ppm; $^{13}C\{^{1}H\}$ NMR (100 MHz, CD_2Cl_2, 20 °C) δ_C 117.5 (*p*-C), 124.6 (q, $^{1}J_{CF}$ = 272 Hz, CF_3), 128.9 (q, $^{2}J_{CF}$ = 35 Hz, *m*-C), 137.1 (*o*-C), 161.8 (q, $^{1}J_{CB}$ = 50 Hz, *ipso*-C) ppm; $^{11}B\{^{1}H\}$ NMR (161 MHz, CD_2Cl_2, 20 °C) δ_B −7.6; $^{19}F\{^{1}H\}$ NMR (376 MHz, CD_2Cl_2, 20 °C) δ_F −62.8 ppm.

Reactivity of [2c]Cl toward Different Sources of Anions (MOTf (Tf = O_2SCF_3), $MOCl_4$, MBF_4, MPF_6, $MSbF_6$, $GaCl_3$, $Na[BAr_4]$; M = Na, K, Ag; Ar = Ph, 3,5-Cl_2-C_6H_3 (Ar^{Cl}))

In a typical reaction 0.01 g (0.0135 mmol) of [**2c**]Cl was dissolved in a J. Young NMR tube using about 1 mL of DCM followed by the addition of 2.1 equiv of an anion source. The reaction mixture was left to react for about 6 h by continuous rotation of the NMR tube, and the reaction progress was followed by ^{31}P NMR spectroscopy. Apart from $Na[BAr^{Cl}_4]$, the use of all other Na anion sources did not result in the P–Cl bond cleavage, as the presence of the starting $\mathbf{2c}^+$ monocation was always evident (the use of $NaSbF_6$ resulted in less than 10% conversion to the target dication). On the other hand, the use of Ag salts resulted in cleavage of the P–Cl bond and formation of multiple unidentified products, except for $Ag[SbF_6]$. Then, this reaction was repeated on a preparatory scale using only $Ag[SbF_6]$, $Na[BAr^{Cl}_4]$ and $GaCl_3$ according to the synthetic procedure for the target dications outlined in this work (see above). As the multinuclear NMR spectra for $\mathbf{3c}^{2+}$ were virtually identical regardless of the nature of the counterion, we only report the NMR data regarding the anions.

$[^{i}Pr_2NP(C(PPh_3)_2)]^{2+}$, $[3c][X]_2$

2.1 eq of $Ag[SbF_6]$, $Na[BAr^{Cl}{}_4]$ or $GaCl_3$ was added to a 25 ml DCM solution containing 1.0 g (1.35 mmol) of [**2c**$^+$][Cl], resulting in a solution colour change to yellow, followed by a white precipitate (AgCl) formation. The yellow solution containing the product was filtrated. **$[3c][BAr^{Cl}{}_4]_2$** or **$[3c][GaCl_4]_2$** were isolated *via* solvent removal under reduced pressure. In case of **$[3c][SbF_6]_2$**, the product was isolated *via* dropwise precipitation using dry hexane, and a subsequent filtration. The resulting compound was dried for 5 hours under argon gas. Crystals were also grown from a DCM/hexane mixture. Yield 0.79 g (51%) as the $[SbF_6]^-$ salt (white solid) and 1.42 g (58%) as the $[BAr^{Cl}{}_4]^-$ salt (yellow solid).

$[BAr^{Cl}{}_4]^-$:

^{1}H NMR (400 MHz, CD_2Cl_2, 20 °C) δ_H 7.0–7.5 (Ph, 24H) ppm; $^{13}C\{^1H\}$ NMR (100 MHz, CD_2Cl_2, 20 °C) 123.1 (*p*-C), 133.5 (*o*-C), 133.7 (*m*-C) 164.7 (q, $^1J_{CB}$ = 50 Hz, *ipso*-C) ppm; $^{11}B\{^1H\}$ NMR (161 MHz, CD_2Cl_2, 20 °C) δ_B −6.9 ppm.

Synthesis of $[^{i}Pr_2NPH(OR)(C(PPh_3)_2)][SbF_6]_2$, R = H, Me:

1 eq of ROH (R=H, Me) solution in DCM was added to 1 ml of DCM solution containing 0.010 g (0.00878 mmol) of [**3c**$^{2+}$][SbF_6]$_2$, resulting in an immediate yellow solution discolouring. Removal of volatiles in vacuo yielded a colourless product.

$[^{i}Pr_2NPH(OH)(C(PPh_3)_2)][SbF_6]_2$, $[6a][SbF_6]_2$

^{31}P NMR (CD_2Cl_2, 161 MHz, 25˚C): δ 22.7 (br, $P_{(carbone)}$), δ 31.0 (doublet of br, $^1J_{P(cenetral)H}$ = 493 Hz)

$[^{i}Pr_2NPH(OCH_3)(C(PPh_3)_2)][SbF_6]_2$, $[6b][SbF_6]_2$

^{1}H NMR (400 MHz, CD_2Cl_2, 25˚C): δ 0.68 (d, $^{3}J_{HH}$ = 6.8Hz 6H, $CH(CH_3)_2$), 0.92 (d, $^{3}J_{HH}$ = 6.8 Hz 6H, $CH(CH_3)_2$), 3.39 (br, 3H, OCH_3), 3.7 (sept, $^{3}J_{HH}$ = 7.4 Hz, 2H, $CH(CH_3)_2$), 7.5-7.7 (Ph, 54H), 7.5 (br, $P_{(central)}$-H)

^{31}P NMR (CD_2Cl_2, 161 MHz, 25˚C): δ 23.3 (br, $P_{(carbone)}$), δ 42.3 (doublet of multiplets, $^{1}J_{P(cenetral)H}$ = 1583 Hz)

Synthesis of $[(^{i}Pr_2NP(O)(C(PPh_3)_2(OPy)][SbF_6]_2$, [7][SbF_6]$_2$:

To a 15 ml DCM solution of 120 mg (0.1053 mmol) of $[(C(PPh_3)_2)P(N^{i}Pr_2)][SbF_6]_2$, two equivalents (18 mg, 0.1893 mmol) of Py-O were added. An immediate solution colour change from yellow to colourless was observed. The reaction kinetics was tracked *via* ^{31}P and ^{1}H NMR by taking aliquots of the reaction mixture over time. Crystals suitable for single crystal X-ray diffraction were grown by layering the reaction content with dry hexane in a 1:1 ratio to yield 56mg (43%) of the $[(^{i}Pr_2NP(O)(C(PPh_3)_2(OPy))[SbF_6]_2$ crystals.

^{1}H NMR (400 MHz, CD_2Cl_2, 25˚C) δ 0.52 (d, $^{3}J_{HH}$ = 6.52 Hz, 3H, $CH(CH_3)_2$), 0.78 (d, $^{3}J_{HH}$ = 6.52 Hz, 3H, $CH(CH_3)_2$), 3.59 (m, 1H, $CH(CH_3)_2$), 7.5-7.8 (Ph, 30H), 8.03 (t, J = 7.38 Hz, 2H, meta C-H pyridine), 8.28 (d, J= 6.52 Hz, 2H, ortho C-H pyridine), 8.44 (t, J = 7.78 Hz, 1H, para C-H pyridine). ^{13}C{^{1}H} NMR (100.5 MHz, CD_2Cl_2, 25˚C): δ 22.1 (br, $CH(CH_3)_2$), $C_{(carbone)}$ not observed, 48.2 (d, $^{2}J_{PC}$ = 4.62 Hz, $CH(CH_3)_2$), 123.5 (*ipso*-C, Ph of $C(PPh_3)$), 124.4 (br, *ipso*-C, Ph), 129.6 (virtual triplet, *o*-C, Ph of $C(PPh_3)$), 134.2 (br, *p*-C, Ph of $C(PPh_3)$), 134.7 (virtual triplet, *m*-C, Ph of $C(PPh_3)$), 141.2 (br, Py), 148.2 (br, Py); ^{31}P{1H} NMR (CD_2Cl_2, 161 MHz, 25˚C): δ 23.7 (second order doublet, $P_{(carbone)}$), δ 42.0 (second order triplet, $P_{(central)}$

FTIR (KBr pellets): 2965 (m), 2372 (m), 1474 (m), 1437 (s), 1232 (m), 1097 (s), 748 (s) cm-1 (s = strong; m = medium; w = weak)

m.p. 132°C (onset of decomposition)

Preparation of [(^{i}Pr$_2$NP(O)(OC(PPh$_3$)$_2$(Py)][SbF$_6$]$_2$, [8][SbF$_6$]$_2$:

8^{2+} was prepared from **7**$^{2+}$, by letting the reaction stir at the room temperature for a week, or by heating it for 5 hours at 50˚C. Crystals suitable for single crystal X-ray diffraction were grown by layering the reaction content with dry hexane in a 1:1 ratio, yielding 50 mg (38%) of crystals.

^{1}H NMR (400 MHz, CD_2Cl_2, 25˚C) δ 0.54 (d, $^{3}J_{HH}$ = 6.63 Hz, 3H, CH(CH_3)$_2$), 0.71 (d, $^{3}J_{HH}$ = 6.63 Hz, 3H, CH(CH_3)$_2$), 3.51 (m, 1H, CH(CH$_3$)$_2$), 7.5-7.8 (Ph, 30H), 8.00 (t, J = 6.40 Hz, 2H, meta C-H pyridine), 8.44 (t, J = 7.68 Hz, 1H, ortho C-H pyridine), 8.67 (t, J = 6.40 Hz, 2H, para C-H pyridine). ^{13}C{^{1}H} NMR (100.5 MHz, CD_2Cl_2, 25˚C): δ 22.5 (br, CH(CH$_3$)$_2$), C$_{(carbone)}$ not observed, 48.2 (d, $^{2}J_{PC}$ = 2.98 Hz, CH(CH$_3$)$_2$), 122.7 (apparent triplet AA'X, $^{1}J_{PC}$ + $^{2}J_{PC}$ = 92.2 Hz, *ipso*-C, Ph of C(PPh$_3$)), 129.4 (virtual triplet, *o*-C, Ph of C(PPh$_3$)), 134.3 (br, *p*-C, Ph of C(PPh$_3$)), 134.5 (virtual triplet, *m*-C, Ph of C(PPh$_3$)), 143.1 (d, J = 2.2hz, Py), 148.0 (d, J = 1.2 Hz, Py); ^{31}P{1H} NMR (CD_2Cl_2, 161 MHz, 25˚C): δ 22.3 (br, P$_{(carbone)}$), δ 5.76 (br, P$_{(central)}$).

FTIR (KBr pellets): 2963 (m), 1460 (m), 1366 (m), 1265 (s), 955 (s), 741 (s), 714 (s) cm-1 (s = strong; m = medium; w = weak)

m.p. 117°C (onset of decomposition)

Synthesis of {[(Ph$_3$P)$_2$CP(O)(OH)(H)][BAr$^{F}_4$]}$_2$, [15][BAr$^{F}_4$]:

[(Ph$_3$P)$_2$CPCl$_2$][BAr$^{F}_4$] was prepared according to the previously reported procedure[141] and used *in situ* for the preparation of **17**. A dichlomethane (50 mL) solution of [(Ph$_3$P)$_2$CPCl$_2$][BAr$^{F}_4$] **(**1.93 mmol) was filtered into the reaction schlenk containing

1.5 eq. of anhydrous Me_4NOH (0.26 g, 2.90 mmol). Wet Me_4NOH or $Me_3NO•2H_2O$ can also be used as a base. Reaction mixture was stirred for 5 h. Resulting solution was then filtered from the white precipitate and layered with hexane to yield crystals of the product. Yield: 68 %.

^1H NMR (400 MHz, CD_3CN, 25°C): δ 6.31 ppm (dt, 1H, $^1J_{P-H}$ = 616.12 Hz, $^4J_{H-P-O-H}$ = 5.52 Hz); 7.24 – 7.72 ppm (m, Ph). ^{13}C NMR (100 MHz, CD_3CN, 25°C): δ 67.74 ppm (t, $^1J_{C(carbone)-P(carbone)}$ = 350.99 Hz), 117.45 ppm (s, p-C, BAr^F_4), 124.57 ppm (q, $-CF_3$, $^1J_{C-F}$ = 270.65 Hz), 128.87 ppm (q, m-C, BAr^F_4, $^2J_{C-C-F}$ = 34.07 Hz), 130.24 ppm (s, o-C, Ph); 133.58 ppm (t, m-C, Ph), 134.78 (s, o-C, BAr^F_4) 135.28 ppm (t, p-C, Ph), 161.74 ppm (q, J_{C-F} = 49.31 Hz ipso-C, BAr^F_4); ^{31}P {^1H} NMR (161 MHz, CD_2Cl_2, 25°C): δ 30.3 ppm (t, $^2J_{P(carbone)P(central)}$ = 26.13 Hz); 21.53 ppm (d, P(carbone) $^2J_{P(central)P(carbone)}$ = 26.13 Hz). ^{31}P NMR (161 MHz, CD_2Cl_2, 25°C): δ 30.3 ppm (dt, H(metaphosphonate), $^1J_{P-H}$ = 609.7 Hz, $^2J_{P(central)P(carbone)}$ = 26.13Hz); 21.26 ppm (br, P(carbone)). ^{11}B{^1H} NMR (161 MHz, CD_2Cl_2, 25 °C) δ_B −7.58 ppm. ^{19}F{^1H} NMR (376 MHz, CD_2Cl_2, 25 °C) δ_F −62.8 ppm. IR Spectroscopy: 3383.14 cm^{-1} (br, O-H stretch), 3070.68 cm^{-1} (m, C-H stretch in phenyl) 2445.04 cm^{-1} (w, P-H stretch) 1438.90 cm^{-1} (m, P-Ph stretch) 1278.81 cm^{-1} (s, P=O stretch). Anal. Calcd for $C_{106}H_{76}BO_4F_{24}P_6$: C, 49.87; H, 3.38; N, 0.00%. Found $C_{106}H_{76}BO_4F_{24}P_6•8CH_2Cl_2$: C, 49.01; H, 3.11; N, 0.63.. Melting Point: 169.7°C.

Synthesis of $(Ph_3P)_2CP(O)_2H$, 17:

$[(Ph_3P)_2CPCl_2][BAr^F_4]$ was prepared according to the previously reported procedure and used *in situ* for the preparation of **17**. A dichlomethane (50 mL) solution of $[(Ph_3P)_2CPCl_2][BAr^F_4]$ **(**1.93 mmol) was filtered into the reaction schlenk containing 3 eq. of anhydrous Me_4NOH (0.52 g, 5.79 mmol). Wet Me_4NOH or $Me_3NO•2H_2O$ can

also be used as a base. The resulting mixture was stirred overnight, gradually changing colour from pale-brown to colourless. Colourless solution was then filtered from the white precipitate and concentrated *via* rotovap to about 2-3 mL of volume, resulting in yellow oil. The mixture was purified *via* Column Chromatography using a Hexane/$CHCl_3$ mixture and 1% Et_3N as a stabilizer. Minor polar impurities were removed with a 100% ACN flush. The product remained as a final fraction, which was eluted with 100% MeOH, then recrystallized from MeOH/Et_2O. $(Ph_3P)_2CP(O)_2H•2H_2O$ was obtained as air- and moisture-stable, colourless powder. Yield: 90%.

^1H NMR (400 MHz, CD_3CN, 25°C): δ 6.79 ppm (d, 1H, $^1J_{P-H}$ = 532.6 Hz); 7.19 ppm (m, 30H, Ph). ^{13}C NMR (100 MHz, CD_3CN, 25°C): δ 15.07 ppm (dt, $^1J_{P(central)C}$ = 88.2 Hz and $^1J_{P(carbone)C}$ = 76.7 Hz); 128.94 ppm (apparent triplet, ipso-C); 129.26 ppm (t, p-C),132.86 ppm (s, o-C); 135.34 ppm (t, m-C); ^{31}P {^1H} NMR (161 MHz, CD_3OD, 25°C): δ 6.3 ppm (t, $^2J_{P(carbone)P(central)}$ = 12.62 Hz); 21.25 ppm (d, P(carbone) $^2J_{P(central)P(carbone)}$ = 12.26 Hz). ^{31}P NMR (161 MHz, CD_3OD, 25°C): δ 6.3 ppm (dt, H(metaphosphonate), $^1J_{P-H}$ = 526.6 Hz, $^2J_{P(central)P(carbone)}$ = 12.47 Hz); 21.26 ppm (br, P(carbone)). IR Spectroscopy: 3053.32 cm^{-1} 2985.81 cm^{-1} (m, C-H stretch in phenyl) 2304.94 cm^{-1} (w, P-H stretch) 1421.54 cm^{-1} (m, P-Ph stretch) 1265.30 cm^{-1} (s, P=O stretch). Anal. Calcd for $C_{37}H_{35}O_4P_3$: C, 69.81; H, 5.54; N, 0.00%. Found: C, 69.81; H, 5.99; N, 1.07. ES-MS Calcd. for $C_{37}H_{35}O_4P_3$: m/z 867.2687. Found: 867.2641. Melting Point: 194.9°C.

Reactivity Studies of 17

Proton/Hydride Abstraction Reaction Attempts

KHMDS, KOtBu, $NaNH_2$, ^nBuLi, ^tBuLi

Proton abstraction reaction attempts have been performed *in situ*, in the J. Young NMR tubes. To a DCM solution containing 5 mg (0.00833 mmol) of **17**, 2.5 eq. of a crown ether (18-crown-6 for K^+ ions, or 12-crown-4 for Li^+ ions) was added, followed by an addition of 2.5 eq. of corresponding base (KHMDS, KO^tBu, ^nBuLi, or ^tBuLi). In case of ^nBuLi and ^tBuLi, the solution was cooled to -78^{o}C prior to the addition of the base. The reaction content inside the NMR tube was manually stirred. In case of KHMDS and KO^tBu, the tube was subject to 50°C overnight heating due to the lack of initial reaction activity. The reactions were followed *via* ^{31}P NMR.

$[Ph_3C][B(C_6F_5)_4]$:

$[Ph_3C][B(C_6F_5)_4]$ was prepared and used "*in situ*". Ph_3CCl (11 mg, 0.0333 mmol) and $LiB(C_6F_5)_4$ (28 mg, 0.0333 mmol) were mixed in equivalent amounts, using DCM as a solvent (1 mL). Upon stirring for 4h at room temperature, the yellow solution containing $[Ph_3C][B(C_6F_5)_4]$ filtered into 1mL DCM solution of $(PPh_3)_2CP(O)_2H$ (20 mg, 0.0333 mmol). An instant disappearance of yellow solution colour was immediately observed. All attempts to grow crystals suitable for a single-crystal X-ray Diffraction analysis were unsuccessful.

$^{31}P\{^1H\}$ NMR (161 MHz, CH_2Cl_2, 25°C): δ_P 18.19 ppm (t, $P_{central}$, $^2J_{P(central)P(carbone)}$ = 16.57 Hz), 20.57 ppm (d, $P_{carbone}$, $^2J_{P(central)P(carbone)}$ = 16.43 Hz); ^{31}P NMR (161 MHz, CH_2Cl_2, 25°C): δ 18.19 ppm (dt, $P_{central}$, $^1J_{P(central)-H}$ = 487.5 Hz, $^2J_{P(central)P(carbone)}$ = 16.57 Hz); 20.57 ppm (d, $P_{carbone}$, $^2J_{P(central)P(carbone)}$ = 16.43 Hz). ES-MS Calcd. for $C_{37}H_{35}O_4P_3$: m/z 867.2687. Found: 867.2641. We were not able to perform any other compound characterisations, as the compound was extremely air- and moisture-sensitive, and would also decompose very rapidly, within minutes.

Oxalyl chloride

To a 1 mL DCM solution of **17** (15 mg, 0.025 mmol), 1.2 eq. of oxalyl chloride (2.6 μL, 0.03 mmol) was added, resulting in an immediate cloudy white precipitate formation. Afer stirring the mixture overnight at room temperature overnight, solution was separated *via* filtration, and layered with hexane in 1:1 ratio. Crystals of previously reported $[(Ph_3P)_2CPCl_2][Cl]$[31] were obtained.

Reaction of 17 with trityl-triflate $[Ph_3C][OTf]$:

$[Ph_3C][OTf]$ was prepared and used "*in situ*". Ph_3CCl (128 mg, 0.03663 mmol) was dissolved in DCM, and subsequently added to AgOTf (12 mg, 0.03663 mmol), which resulted in a bright yellow suspension. The mixture was stirred about 2 hours at room temperature. Subsequently, the yellow solution containing approximately 2.2 eq (0.03663 mmol) of $[Ph_3C][OTf]$ was filtered into a flask containing $(PPh_3)_2CP(O)_2H$ (10 mg, 0.01665 mmol). Immediate reaction was apparent from the discolouration of the yellow solution colour. $^{31}P\{^1H\}$ NMR (161 MHz, CH_2Cl_2, 25°C): δ_P 19.11 ppm (t, $P_{central}$, $^2J_{P(central)P(carbone)}$ = 21.14 Hz), 21.32 ppm (d, $P_{carbone}$, $^2J_{P(central)P(carbone)}$ = 21.24 Hz); ^{31}P NMR (161 MHz, CH_2Cl_2, 25°C): δ 19.11 ppm (dt, $P_{central}$, $^1J_{P(central)-H}$ = 610.1 Hz, $^2J_{P(central)P(carbone)}$ = 16.57 Hz); 21.32 ppm (d, $P_{carbone}$, $^2J_{P(central)P(carbone)}$ = 21.24 Hz).

Reaction of 17 with MeOTf

3.65 μL of MeOTf (0.0333 mmol) was spiked into a 1 mL CD_2Cl_2 solution of $(Ph_3P)_2CP(O)_2H$ (20 mg, 0.0333 mmol) in a vial. The colourless mixture was immediately transferred to a J. Young NMR tube, and the reaction progress was tracked *via* ^{31}P NMR. The reaction mixture was subsequently layered with hexane, yielding crystals of protonated ligand or the starting material. All attempts to yield the targeted crystals were unsuccessful.

^{1}H NMR (400 MHz, CD_3CN, 25°C): δ 3.12 ppm (d, 3H, CH_3, $^{3}J_{P\text{-}O\text{-}C\text{-}H}$ = 13.2 Hz), 7.44-7.66 (30H, Ph); $^{31}P\{^{1}H\}$ NMR (161 MHz, CH_2Cl_2, 25°C): δ_P 21.91 ppm (d, $P_{carbone}$, $^{2}J_{P(central)P(carbone)}$ = 21.33 Hz), 30.74 ppm (t, $P_{central}$, $^{2}J_{P(central)P(carbone)}$ = 20.85 Hz); ^{31}P NMR (161 MHz, CH_2Cl_2, 25°C): δ_P 21.91 ppm (d, $P_{carbone}$, $^{2}J_{P(central)P(carbone)}$ = 21.3 Hz), 30.74 ppm (dq, $P_{central}$, $^{1}J_{P(central)\text{-}H}$ = 585.7 Hz, $^{3}J_{P(central)\text{-}H}$ = 13.5 Hz).

Reactivity towards MeOH, $[HL][P(O)_2(OCH_3)(H)]$

20 mg (0.0333 mmol) of $(Ph_3P)_2CP(O)_2H$ was dissolved in 0.75 mL CD_3CN. To that, excess MeOH (0.25 mL, 5.96 mmol) was added, and the reaction was heated at 70°C for 5 h. The reaction can also proceed and be completed spontaneously, in the large excess of alcohol at room temperature, in the absence of CD_3CN, overnight.

^{1}H NMR (400 MHz, CD_3CN, 25°C): δ 2.35 ppm (t, 1H, H-$C_{(carbone)}$, $^{2}J_{P\text{-}C\text{-}H}$ = 6.36 Hz), 3.32 ppm (d, 3H, CH_3, $^{3}J_{P\text{-}O\text{-}C\text{-}H}$ = 11.4 Hz), 6.58 ppm (d, 1H, $^{1}J_{H\text{-}P(central)}$ = 561 Hz), 7.42-7.64 ppm (m, 30H, Ph); $^{13}C\{^{1}H\}$ NMR (100 MHz, CD_3CN, 25°C): δ 50.1 ppm (d, CH_3, $^{2}J_{C\text{-}P(central)}$ = 4.58 Hz), 127.7 ppm (apparent triplet, AA'X, $^{1}J_{P\text{-}C}$ + $^{4}J_{P\text{-}C}$ = 103.4 Hz, ipso-C, Ph of $HC(PPh_3)_2$); 130.2 ppm (t, p-C, Ph of $HC(PPh_3)_2$), 133.9 – 133.96 ppm (m, o-C and m-C, Ph of $HC(PPh_3)_2$); $^{31}P\{^{1}H\}$ NMR (161 MHz, CD_3CN, 25°C): δ 20.87 ppm (s, $P_{(protonated\text{-}carbone)}$), 3.61 ppm (s, $P_{central}$); ^{31}P NMR (161 MHz, CD_3CN, 25°C): δ 20.86 ppm (s, $P_{(protonated\text{-}carbone)}$), δ 3.61 ppm (dq, $P_{central}$, $^{1}J_{P\text{-}H}$ = 557.9 Hz, $^{3}J_{P(central)\text{-}H}$ = 11.58 Hz).

Reactivity towards CD_3OD Synthesis of $[DL][P(O)_2(OCD_3)(H)]$:

The procedure was analogous to the above described for MeOH.

$^{2}H\{^{1}H\}$ NMR (61.4 MHz, CH_3CN, 25°C): δ 2.41 (br, 1D, D-$C_{(carbone)}$), 3.33 (d, 3D, $^{3}J_{D\text{-}C\text{-}O\text{-}P}$ = 1.75 Hz); $^{31}P\{^{1}H\}$ NMR (161 MHz, CH_3CN, 25°C): δ 21.08 ppm (s, $P_{(D\text{-}}$

$_{carbone)}$), 6.60 ppm (s, $P_{central}$); ^{31}P NMR (161 MHz, CH_3CN, 25°C): δ 20.08 ppm (s, $P_{(D-carbone)}$), δ 6.60 ppm (d, $P_{central}$, $^{1}J_{P-H}$ = 602.3 Hz).

Reaction between **[DL][P(O)$_2$(OCD$_3$)(H)] and MeOTf:**

1 eq (4 μL, 0.0333 mmol) of MeOTf was added "*in situ*" into the acetonitrile solution of **[DL][P(O)$_2$(OCD$_3$)(H)]**, derived from the above described procedure. $^{2}H\{^{1}H\}$ NMR (61.4 MHz, CH_3CN, 25°C): δ 2.29 (br, 1D, D-$C_{(carbone)}$), 3.66 (d, 3D, $^{3}J_{D-C-O-P}$ = 1.82 Hz); $^{31}P\{^{1}H\}$ NMR (161 MHz, CH_3CN, 25°C): δ 11.1 ppm (s, $P_{central}$); ^{31}P NMR (161 MHz, CH_3CN, 25°C): δ 11.1 ppm (dq, $P_{central}$, $^{1}J_{P-H}$ = 691 Hz, $^{3}J_{P-O-C-H}$ = 8.9 Hz). ES-MS Calcd. for $C_{37}H_{35}O_4P_3$: m/z 114.0399. Found: 114.0398.

Reaction of (Ph$_3$P)$_2$CP(O)$_2$H with H$_2$O

The procedure was analogous to the above described for MeOH.

^{1}H NMR (400 MHz, CD_3CN, 25°C): δ 2.25 ppm (br, 1H, OH,), 7.00 ppm (d, 1H, $^{1}J_{H-P(central)}$ = 502 Hz), 7.34-7.60 ppm (m, 30H, Ph); $^{31}P\{^{1}H\}$ NMR (161 MHz, CD_3CN, 25°C): δ 20.83 ppm (s, $P_{(protonated-carbone)}$), 3.62 ppm (br, $P_{central}$); ^{31}P NMR (161 MHz, CD_3CN, 25°C): δ 20.83 ppm (s, $P_{(protonated-carbone)}$), δ 3.62 ppm (d, $P_{central}$, $^{1}J_{P-H}$ = 608 Hz).

With prolonged heating at 70°C, peaks change to following:

^{1}H NMR (400 MHz, CD_3CN, 25°C): δ 5.98 ppm (s, 1H, OH,), 7.00 ppm (d, 1H, $^{1}J_{H-P(central)}$ = 502 Hz), 7.34-7.60 ppm (m, 30H, Ph); $^{31}P\{^{1}H\}$ NMR (161 MHz, CD_3CN, 25°C): δ 20.83 ppm (s, $P_{(protonated-carbone)}$), 0.19 ppm (s, $P_{central}$); ^{31}P NMR (161 MHz, CD_3CN, 25°C): δ 20.83 ppm (s, $P_{(protonated-carbone)}$), δ 0.19 ppm (d, $P_{central}$, $^{1}J_{P-H}$ = 601 Hz).

Reactivity of 17 towards other alcohols

All reactions have been carried out "*in situ*" in the J. Young NMR tubes. A general procedure consisted of dissolving 10 mg (0.0167 mmol) of **17** in 1 ml of ACN, to which 200 eq (3.34 mmol) of the respective alcohol was added. The reaction mixture was subsequently subjected to heating at 80°C. Reaction progress was monitored over time *via* $^{31}P\{^{1}H\}$ and ^{31}P NMR. All reactions have been successfully performed 100% alcohol as well. Upon reaction completion, the solutions were layered with Et_2O (1:1), subjected to slow evaporation, or evaporation under conditions of low temperature and pressure, in attempts to grow crystals. Unfortunately, targeted crystals were not obtained.

EtOH, [HC(PPh$_3$)$_2$][P(O)$_2$(OCH$_2$CH$_3$)(H)]:

^{31}P $\{^{1}H\}$ NMR (161 MHz, CH_3CN, 25°C): δ 3.12 ppm (s, $P_{central}$), 20.87 (s, PPh_3); ^{31}P NMR (161 MHz, CH_3CN, 25°C): δ 3.12 ppm (dt, $P_{central}$, $^{1}J_{P\text{-}H}$ = 601 Hz), 20.87 (s, PPh_3).

^{i}PrOH, [HC(PPh$_3$)$_2$][P(O)$_2$(OCH(CH$_3$)$_2$(H))]:

^{31}P $\{^{1}H\}$ NMR (161 MHz, CH_3CN, 25°C): δ -0.18 ppm (s, $P_{central}$), 20.83 (s, PPh_3); ^{31}P NMR (161 MHz, CH_3CN, 25°C): δ -0.18 ppm (dd, $P_{central}$, $^{1}J_{P\text{-}H}$ = 585 Hz, $^{3}J_{P\text{-}O\text{-}C\text{-}H}$ = 9.3 Hz), 20.83 (s, PPh_3).

^{t}BuOH, [HC(PPh$_3$)$_2$][P(O)$_2$(OC(CH$_3$)$_3$(H))]:

^{31}P $\{^{1}H\}$ NMR (161 MHz, CH_3CN, 25°C): δ -4.56 ppm (s, $P_{central}$), 20.83 (s, PPh_3); ^{31}P NMR (161 MHz, CH_3CN, 25°C): δ -0.18 ppm (d, $P_{central}$, $^{1}J_{P\text{-}H}$ = 586 Hz), 20.83 (s, PPh_3).

PhOH, [HC(PPh$_3$)$_2$][P(O)$_2$(OC$_6$H$_5$)(H)]:

^{1}H NMR (400 MHz, CD_3CN, 25°C): δ 6.86–7.43 ppm (35H, Ph); $^{13}C\{^{1}H\}$ NMR (100 MHz, CD_3CN, 25°C): δ 115.3 ppm (o-C, Ph), 119.8 (p-C, Ph), 129.9 (m-C, Ph), 156.9 (ipso-C, Ph); $^{31}P\ \{^{1}H\}$ NMR (161 MHz, CD_3CN, 25°C): δ -0.71 ppm (s, $P_{central}$), 20.84 (s, PPh_3); ^{31}P NMR (161 MHz, CD_3CN, 25°C): δ -0.18 ppm (d, $P_{central}$, $^{1}J_{P\text{-}H}$ = 625 Hz), 20.84 (s, PPh_3).

$PhCH_2CH_2OH$, $[HC(PPh_3)_2][P(O)_2(OCH_2CH_2C_6H_5)(H)]$:

$^{31}P\ \{^{1}H\}$ NMR (161 MHz, CH_3CN, 25°C): δ 3.24 ppm (s, $P_{central}$), 20.65 (s, PPh_3); ^{31}P NMR (161 MHz, CH_3CN, 25°C): δ 3.24 ppm (dt, $P_{central}$, $^{1}J_{P\text{-}H}$ = 600 Hz, $^{3}J_{P\text{-}O\text{-}C\text{-}H}$ = 8.5 Hz), 20.65 (s, PPh_3).

$PhCH(CH_3)CH_2OH$, $[HC(PPh_3)_2][P(O)_2(OCH_2CH(CH_3)C_6H_5)(H)]$

$^{31}P\ \{^{1}H\}$ NMR (161 MHz, CH_3CN, 25°C): δ 3.13 ppm (s, $P_{central}$), 20.63 (s, PPh_3); ^{31}P NMR (161 MHz, CH_3CN, 25°C): δ 3.13 ppm (dt, $P_{central}$, $^{1}J_{P\text{-}H}$ = 596 Hz, $^{3}J_{P\text{-}O\text{-}C\text{-}H}$ = 7.1 Hz), 20.63 (s, PPh_3).

$C(CF_3)_3OH$, $[HC(PPh_3)_2][P(O)_2(OC(CF_3)_3)(H)]$

$^{31}P\ \{^{1}H\}$ NMR (161 MHz, CH_3CN, 25°C): δ -0.26 ppm (s, $P_{central}$), 20.80 (s, PPh_3); ^{31}P NMR (161 MHz, CH_3CN, 25°C): δ -0.26 ppm (d, $P_{central}$, $^{1}J_{P\text{-}H}$ = 525.0 Hz), 20.80 (s, PPh_3).

$CH_2=CHCH_2CH_2OH$, $[HC(PPh_3)_2][P(O)_2(OCH_2CH_2CHCH_2)(H)]$

$^{31}P\ \{^{1}H\}$ NMR (161 MHz, CH_3CN, 25°C): δ 3.23 ppm (s, $P_{central}$), 20.61 (s, PPh_3); ^{31}P NMR (161 MHz, CH_3CN, 25°C): δ 3.23 ppm (dt, $P_{central}$, $^{1}J_{P\text{-}H}$ = 602 Hz, $^{3}J_{P\text{-}O\text{-}C\text{-}H}$ = 10.4 Hz), 20.61 (s, PPh_3).

$CH_2=CH(CH_2)_2CH_2OH$, $[HC(PPh_3)_2][P(O)_2(OCH_2(CH_2)_2CHCH_2)(H)]$

^{31}P {^{1}H} NMR (161 MHz, CH_3CN, 25°C): δ 3.04 ppm (s, $P_{central}$), 20.57 (s, PPh_3); ^{31}P NMR (161 MHz, CH_3CN, 25°C): δ 3.04 ppm (dt, $P_{central}$, $^{1}J_{P-H}$ = 597 Hz, $^{3}J_{P-O-C-H}$ = 6.5 Hz), 20.57 (s, PPh_3).

HC≡CCH$_2$CH$_2$OH, [HC(PPh$_3$)$_2$][P(O)$_2$(OCH$_2$CH$_2$CCH)(H)]

^{1}H NMR (400 MHz, CD_3CN, 25°C): δ 1.28 ppm (s, 1H, CH), 2.36 (s, 2H, CH_2), 3.24 (s, 2H, CH_2), 3.59 (1H, CH), 7.45-7.59 (30H, Ph); ^{13}C{^{1}H} NMR (100 MHz, CD_3CN, 25°C): δ 22.3 ppm (s, CH_2), 55.1 (d, $C_{carbone}$, $^{1}J_{C-P}$ = 3.85 Hz), 60.1 (s, CH), 69.7(s, CH_2), 82.3 (s, CH_2), 126.5 (apparent triplet, AA'X, $^{1}J_{P-C}$ + $^{4}J_{P-C}$ = 95.1 Hz, ipso-C, Ph),

129.3 (m, o-C, Ph), 133.0 (m, m-C, Ph), 133.1 (s, p-C, Ph); ^{31}P {^{1}H} NMR (161 MHz, CH_3CN, 25°C): δ 3.39 ppm (s, $P_{central}$), 20.8 ppm (s, PPh_3); ^{31}P NMR (161 MHz, CH_3CN, 25°C): δ 3.39 ppm (dt, $P_{central}$, $^{1}J_{P-H}$ = 605 Hz, $^{3}J_{P-O-C-H}$ = 7.7 Hz), 20.81 (s, PPh_3).

HC≡C(CH$_2$)$_2$CH$_2$OH, [HC(PPh$_3$)$_2$][P(O)$_2$(OCH$_2$(CH$_2$)$_2$CCH)(H)]

^{31}P {^{1}H} NMR (161 MHz, CH_3CN, 25°C): δ 3.31 ppm (s, $P_{central}$), 20.58 (s, PPh_3); ^{31}P NMR (161 MHz, CH_3CN, 25°C): δ 3.31 ppm (dt, $P_{central}$, $^{1}J_{P-H}$ = 601 Hz, $^{3}J_{P-O-C-H}$ = 6.1 Hz), 20.58 (s, PPh_3).

Dehydrogenative coupling reactions with of (Ph$_3$P)$_2$CP(O)$_2$H

Following reactions have been carried out *in situ* in the J. Young NMR tubes.

Catalysis with CuI:

In a vial containing 1 mL of solvent (DMSO or ACN) , 20 mg (0.0333 mmol) of **17**, 10% mol CuI, and 10% mol TEA, 2.5 eq. of phenylacetylene (5.4 μL, 0.0833 mmol)

was added. Reaction content was then heated to 50°C, which resulted in a colour change. The same reaction was repeated without the presence of the base.

Catalysis with Palladium:

In a vial containing 1 mL of THF solution, 15 mg (0.025 mmol) of ***17,*** and 2 eq. $AgBF_4$ (10 mg, 0.05 mmol), 10% mol $Pd(OAc)_2$ (10 uL, 0.0025 mmol) was added, followed by the addition of 1 eq. of phenylacetylene (3 uL, 0.025 mmol) or bromophenylacetylene (5 mg, 0.025 mmol). The reaction was heated overnight at 70°C.

5.2 Crystallographic Methods

Single crystals were mounted on quartz fibres, and the X-ray intensity data were collected at 103(2) K (150.0(1) K for [**3c**][BAr^f_4]$_2$) on a Bruker X8 APEX (Bruker Kappa APEX II for [**3c**][BAr^f_4]$_2$) system, using Mo Kα radiation, with the SMART suite of programs.[212] Data were processed and corrected for Lorentz and polarization effects with SAINT[213] (DENZO and COLLECT for [**3c**][BAr^f_4]$_2$) and for absorption effects with SADABS[214] (DENZO/SCALEPACK[215] for [**3c**][BAr^f_4]$_2$). Structural solution and refinement were carried out with the SHELXTL suite of programs.[216]The structure was solved by direct methods and refined for all data by full-matrix least-squares methods on F^2. All non-hydrogen atoms were subjected to anisotropic refinement. The hydrogen atoms were generated geometrically and allowed to ride on their respective parent atoms; they were assigned appropriate isotopic thermal parameters.

Crystallographic data for [3c][SbF_6]$_2$:

Table 12. Crystal data and structure refinement forc [(Ph_3P)$_2$CP(N^iPr_2)][SbF_6]$_2$, ***[3c][SbF_6]$_2$***

Identification code	dv191	
Chemical formula	$C_{44}H_{46}Cl_2F_{12}NP_3Sb_2$	
Formula weight	1224.13	
Temperature	103(2) K	
Wavelength	0.71073 Å	
Crystal size	0.240 x 0.300 x 0.360 mm	
Crystal habit	colourless block	
Crystal system	monoclinic	
Unit cell dimensions	a = 11.180(8) Å	α = 90.00°
	b = 19.337(12) Å	β = 92.114(3)°
	c = 24.324(16) Å	γ = 90.00°
Volume	5254.7(6) Å^3	
Z	4	
Density (calculated)	1.547 g/cm^3	
Absorption coefficient	1.294 mm^{-1}	
F(000)	2424	
Theta range for data collection	1.68 to 28.34°	
Index ranges	-14<=h<=14, -25<=k<=25, -32<=l<=32	
Reflections collected	62748	
Independent reflections	13065 [R(int) = 0.1270]	
Coverage of independent reflections	99.6%	
Max. and min. transmission	0.7460 and 0.6530	
Refinement method	Full-matrix least-squares on F^2	
Refinement program	SHELXL-2013 (Sheldrick, 2013)	
Function minimized	Σ w(F$_o^2$ - F$_c^2$)^2	
19036 / 4 / 707	13065 / 316 / 673	
Goodness-of-fit on F^2	1.052	
Final R indices	6446 data; I>2σ(I)	R1 = 0.0964, wR2 = 0.2769
	all data	R1 = 0.1945, wR2 = 0.3420
Weighting scheme	w=1/[σ2(Fo2)+(0.1665P)2+39.3582P] where P=(F$_o^2$+2F$_c^2$)/3	
Largest diff. peak and hole	3.589 and -2.343 eÅ^{-3}	
R.M.S. deviation from mean	0.240 eÅ^{-3}	

Crystallographic data for **[7][SbF$_6$]$_2$:**

Table 13.Crystal data and structure refinement for [(Ph$_3$P)$_2$CP(N^{i}Pr$_2$)(O)(C$_5$H$_5$NO)][SbF$_6$]$_2$, ***[7][SbF$_6$]$_2$***

Identification code	dv210	
Chemical formula	$C_{100}H_{107}Cl_8F_{24}N_4O_4P_6Sb_4$	
Formula weight	2841.31	
Temperature	103(2) K	
Wavelength	0.71073 Å	
Crystal size	0.160 x 0.260 x 0.300 mm	
Crystal habit	colourless block	
Crystal system	monoclinic	
Unit cell dimensions	a = 11.7233(4) Å	α = 90°
	b = 27.6193(11) Å	β = 90.9776(14)°
	c = 17.4494(7) Å	γ = 90°
Volume	5649.1(4) Å^3	
Z	2	
Density (calculated)	1.670 g/cm^3	
Absorption coefficient	1.311 mm^{-1}	
F(000)	2826	
Theta range for data collection	1.48 to 26.00°	
Index ranges	-15<=h<=13, -35<=k<=36, -23<=l<=21	
Reflections collected	68295	
Independent reflections	22190 [R(int) = 0.0458]	
Coverage of independent reflections	100.0%	
Max. and min. transmission	0.8180 and 0.6940	
Refinement method	Full-matrix least-squares on F^2	
Refinement program	SHELXL-2013 (Sheldrick, 2013)	
Function minimized	Σ w(F$_o^2$ - F$_c^2$)^2	
19036 / 4 / 707	22190 / 717 / 1428	
Goodness-of-fit on F^2	1.063	
Final R indices	18696 data; I>2σ(I)	R1 = 0.0773, wR2 = 0.1970
	all data	R1 = 0.0957, wR2 = 0.2204
Weighting scheme	w=1/[σ^2(F$_o^2$)+(0.1189P)^2+36.9311P] where P=(F$_o^2$+2F$_c^2$)/3	
Largest diff. peak and hole	3.135 and -2.037 eÅ^{-3}	
R.M.S. deviation from mean	0.201 eÅ^{-3}	

Crystallographic data for **[8][SbF$_6$]$_2$**:

Table 14. Crystal data and structure refinement for [(Ph$_3$P)$_2$COP(N^{i}Pr$_2$)(O)(C$_5$H$_5$N)][SbF$_6$]$_2$, ***[8][SbF$_6$]$_2$***

Identification code	dv228	
Chemical formula	$C_{50}H_{53}Cl_4F_{12}N_2O_2P_3Sb_2$	
Formula weight	1420.15	
Temperature	103(2) K	
Wavelength	0.71073 Å	
Crystal size	0.200 x 0.220 x 0.340 mm	
Crystal habit	colourless block	
Crystal system	triclinic	
Unit cell dimensions	a = 11.1214(4) Å	α = 92.4868(13)°
	b = 12.5295(4) Å	β = 101.5914(13)°
	c = 20.9643(6) Å	γ = 97.2151(14)°
Volume	2831.96(16) Å^3	
Z	2	
Density (calculated)	1.665 g/cm^3	
Absorption coefficient	1.307 mm^{-1}	
F(000)	1412	
Theta range for data collection	1.64 to 31.65°	
Index ranges	-16<=h<=16, -18<=k<=18, -30<=l<=30	
Reflections collected	60187	
Independent reflections	19036 [R(int) = 0.0455]	
Coverage of independent reflections	99.60%	
Max. and min. transmission	0.7800 and 0.6650	
Refinement method	Full-matrix least-squares on F^2	
Refinement program	SHELXL-2013 (Sheldrick, 2013)	
Function minimized	$\Sigma w(F_o^2 - F_c^2)^2$	
19036 / 4 / 707	19036 / 4 / 707	
Goodness-of-fit on F^2	1.061	
Final R indices	14725 data; I>2σ(I)	R1 = 0.0467, wR2 = 0.1113
	all data	R1 = 0.0671, wR2 = 0.1300
Weighting scheme	$w=1/[\sigma^2(F_o^2)+(0.0589P)^2+3.7706P]$ where $P=(F_o^2+2F_c^2)/3$	
Largest diff. peak and hole	2.085 and -1.390 eÅ^{-3}	
R.M.S. deviation from mean	0.175 eÅ^{-3}	

Crystallographic data for $\{[(PPh_3)_2CP(O)(OH)(H)][BArF_4]\}_2$, **[15][BAr$^F_4$]**:

*Table 15. Crystal data and structure refinement for $\{[(PPh_3)_2CP(O)(OH)(H)][BArF_4]\}_2$, **[15][BAr$^F_4$]**.*

Identification code	dv63	
Chemical formula	$C_{144}H_{93}B_2F_{49}O_4P_6$	
Formula weight	3025.62 g/mol	
Temperature	103(2) K	
Wavelength	0.71073 Å	
Crystal size	0.080 x 0.200 x 0.280 mm	
Crystal system	triclinic	
Unit cell dimensions	a = 10.147(4) Å	α = 83.60(6)°
	b = 17.859(15) Å	β = 76.57(4)°
	c = 19.289(16) Å	γ = 80.46(4)°
Volume	3343.(3) Å^3	
Z	1	
Density (calculated)	1.510 g/cm^3	
Absorption coefficient	0.206 mm^{-1}	
F(000)	1530	
Theta range for data collection	1.66 to 30.86°	
Index ranges	-14<=h<=14, -25<=k<=25, -27<=l<=27	
Reflections collected	65408	
Independent reflections	20457 [R(int) = 0.0752]	
Coverage of independent reflections	97.60%	
Max. and min. transmission	0.9840 and 0.9450	
Refinement method	Full-matrix least-squares on F^2	
Refinement program	SHELXL-2014/7 (Sheldrick, 2014)	
Function minimized	$\Sigma\, w(F_o^2 - F_c^2)^2$	
Data / restraints / parameters	20457 / 166 / 987	
Goodness-of-fit on F^2	1.041	
Final R indices	12255 data; I>2σ(I)	R1 = 0.0765, wR2 = 0.1837
	all data	R1 = 0.1357, wR2 = 0.2163
Weighting scheme	$w=1/[\sigma^2(F_o^2)+(0.1013P)^2+1.6328P]$ where $P=(F_o^2+2F_c^2)/3$	
Largest diff. peak and hole	0.822 and -0.986 eÅ^{-3}	
R.M.S. deviation from mean	0.117 eÅ^{-3}	

Crystallographic data for **17**:

*Table 16. Crystal data and structure refinement for $(Ph_3P)_2CP(O)_2H{\cdot}2H_2O$, **$17{\cdot}2H_2O$**.*

Identification code	dv365s	
Chemical formula	$C_{37}H_{35}O_4P_3$	
Formula weight	636.56 g/mol	
Temperature	103(2) K	
Wavelength	0.71073 Å	
Crystal size	0.060 x 0.400 x 0.420 mm	
Crystal habit	colourless plate	
Crystal system	monoclinic	
Space group	P 1 21/c 1	
Unit cell dimensions	a = 9.860(7) Å	α = 90°
	b = 18.996(13) Å	β = 94.139(15)°
	c = 17.206(12) Å	γ = 90°
Volume	3214.(4) Å3	
Z	4	
Density (calculated)	1.315 g/cm3	
Absorption coefficient	0.225 mm-1	
F(000)	1336	
Theta range for data collection	1.60 to 25.93°	
Reflections collected	6174	
Coverage of independent reflections	98.40%	
Absorption correction	Multi-Scan	
Max. and min. transmission	0.9870 and 0.9110	
Structure solution technique	direct methods	
Structure solution program	XS, VERSION 2013/1	
Refinement method	Full-matrix least-squares on F2	
Refinement program	SHELXL-2014/7 (Sheldrick, 2014)	
Function minimized	Σ w(Fo2 - Fc2)2	
Data / restraints / parameters	6174 / 7 / 412	
Goodness-of-fit on F2	1.019	
Final R indices	3206 data; I>2σ(I)	R1 = 0.0922, wR2 = 0.1877
	all data	R1 = 0.1829, wR2 = 0.2271
Weighting scheme	w=1/[σ2(Fo2)+(0.0973P)2] where P=(Fo2+2Fc2)/3	
Largest diff. peak and hole	0.627 and -0.386 eÅ-3	
R.M.S. deviation from mean	0.089 eÅ-3	

References

[1] R. Criegee, *Justus Liebigs Annalen der Chemie* **1948**, *560*, 127-135.
[2] R. M. Bullock, *Catalysis without Precious Metals*, **2010**.
[3] B. List, *Chemical Reviews* **2007**, *107*, 5413-5415.
[4] aA. Corma, H. García, *Chemical Reviews* **2003**, *103*, 4307-4366; bT. Werner, *Advanced Synthesis and Catalysis* **2009**, *351*, 1469-1481; cR. Qiu, Y. Chen, S.-F. Yin, X. Xu, C.-T. Au, *RSC Advances* **2012**, *2*, 10774-10793; dT. Heckel, R. Wilhelm, in *Comprehensive Enantioselective Organocatalysis: Catalysts, Reactions, and Applications, Vol. 2-3*, **2013**, pp. 431-462; eO. Sereda, S. Tabassum, R. Wilhelm, in *Asymmetric Organocatalysis* (Ed.: B. List), Springer Berlin Heidelberg, Berlin, Heidelberg, **2009**, pp. 86-117.
[5] aT. Ooi, *ACS Catalysis* **2015**, *5*, 8980-8988; bB. List, R. A. Lerner, C. F. Barbas Iii, *Journal of the American Chemical Society* **2000**, *122*, 2395-2396; cK. A. Ahrendt, C. J. Borths, D. W. C. MacMillan, *Journal of the American Chemical Society* **2000**, *122*, 4243-4244.
[6] I. Seayad, B. List, *Organic and Biomolecular Chemistry* **2005**, *3*, 719-724.
[7] M. Benkhaled, S. Morin, C. Pichon, C. Thomazeau, C. Verdon, D. Uzio, *Applied Catalysis A: General* **2006**, *312*, 1-11.
[8] Y. Yang, F. Diederich, J. S. Valentine, *Journal of the American Chemical Society* **1991**, *113*, 7195-7205.
[9] G. K. S. Prakash, T. Mathew, G. A. Olah, *Accounts of Chemical Research* **2012**, *45*, 565-577.
[10] S. Robinson, J. McMaster, W. Lewis, A. J. Blake, S. T. Liddle, *Chemical Communications* **2012**, *48*, 5769-5771.
[11] O. Sereda, S. Tabassum, R. Wilhelm, in *Topics in Current Chemistry, Vol. 291*, **2010**, pp. 349-393.
[12] G. N. Lewis, *Valence and the Structure of Atoms and Molecules*, Chemical Catalogue Co., New York, **1923**.
[13] W. Petz, *Coordination Chemistry Reviews* **2015**, *291*, 1-27.
[14] K. Fukui, T. Yonezawa, C. Nagata, H. Shingu, *The Journal of Chemical Physics* **1954**, *22*, 1433-1442.
[15] aH. I. Schlesinger, H. C. Brown, B. Abraham, A. C. Bond, N. Davidson, A. E. Finholt, J. R. Gilbreath, H. Hoekstra, L. Horvitz, E. K. Hyde, J. J. Katz, J. Knight, R. A. Lad, D. L. Mayfield, L. Rapp, D. M. Ritter, A. M. Schwartz, I. Sheft, L. D. Tuck, A. O. Walker, *Journal of the American Chemical Society* **1953**, *75*, 186-190; bS. W. Chaikin, W. G. Brown, *Journal of the American Chemical Society* **1949**, *71*, 122-125.
[16] aN. Miyaura, A. Suzuki, *Chemical Reviews* **1995**, *95*, 2457-2483; bA. Suzuki, *Journal of Organometallic Chemistry* **1999**, *576*, 147-168; cA. Suzuki, *Angew. Chem. Int. Ed.* **2011**, *50*, 6722-6737.
[17] aH. C. Brown, *Hydroboration* **1962**; bD. Männig, H. Nöth, *Angewandte Chemie International Edition in English* **1985**, *24*, 878-879.
[18] aZ. Guo, I. Shin, J. Yoon, *Chemical Communications* **2012**, *48*, 5956-5967; bC. R. Wade, A. E. J. Broomsgrove, S. Aldridge, F. P. Gabbaï, *Chemical Reviews* **2010**, *110*, 3958-3984; cE. Galbraith, T. D. James, *Chemical Society Reviews* **2010**, *39*, 3831-3842.
[19] aG. Kaur, N. Lin, H. Fang, B. Wang, *Topics in Fluorescence Spectroscopy* **2006**, *11*, 377-397; bS. Jin, Y. Cheng, S. Reid, M. Li, B. Wang, *Medicinal Research Reviews* **2010**, *30*, 171-257; cB. Pappin, M. J. Kiefel, T. A. Houston, *Carbohydrates-Comprehensive Studies on Glycobiology and Glycotechnology*

2012, 37-54; dB. Rout, L. Unger, G. Armony, M. A. Iron, D. Margulies, *Angewandte Chemie - International Edition* **2012**, *51*, 12477-12481.

[20] aK. Severin, *Dalton Transactions* **2009**, 5254-5264; bB. Icli, E. Sheepwash, T. Riis-Johannessen, K. Schenk, Y. Filinchuk, R. Scopelliti, K. Severin, *Chemical Science* **2011**, *2*, 1719-1721; cE. Sheepwash, N. Luisier, M. R. Krause, S. Noé, S. Kubik, K. Severin, *Chemical Communications* **2012**, *48*, 7808-7810; dE. Sheepwash, K. Zhou, R. Scopelliti, K. Severin, *European Journal of Inorganic Chemistry* **2013**, 2558-2563.

[21] aW. Yang, X. Gao, B. Wang, *Medicinal Research Reviews* **2003**, *23*, 346-368; bS. J. Baker, J. W. Tomsho, S. J. Benkovic, *Chemical Society Reviews* **2011**, *40*, 4279-4285; cV. M. Dembitsky, A. A. A. Al Quntar, M. Srebnik, *Chemical Reviews* **2011**, *111*, 209-237.

[22] aH. Yamamoto, *Lewis Acids in Organic Synthesis* **2000**; bH. Yamamoto, *Lewis Acid Reagents* **1999**.

[23] aX. Yang, C. L. Stern, T. J. Marks, *Journal of the American Chemical Society* **1994**, *116*, 10015-10031; bX. Yang, C. L. Stern, T. J. Marks, *Journal of the American Chemical Society* **1991**, *113*, 3623-3625; cE. Y.-X. Chen, T. J. Marks, *Chemical Reviews* **2000**, *100*, 1391-1434; dG. C. Welch, R. R. San Juan, J. D. Masuda, D. W. Stephan, *Science* **2006**, *314*, 1124-1126; eP. A. Chase, G. C. Welch, T. Jurca, D. W. Stephan, *Angewandte Chemie - International Edition* **2007**, *46*, 8050-8053; fD. W. Stephan, *Accounts of Chemical Research* **2015**, *48*, 306-316; gD. W. Stephan, *Journal of the American Chemical Society* **2015**, *137*, 10018-10032; hD. W. Stephan, G. Erker, *Angewandte Chemie - International Edition* **2010**, *49*, 46-76; iD. W. Stephan, G. Erker, *Angewandte Chemie - International Edition* **2015**, *54*, 6400-6441; jC. B. Caputo, D. W. Stephan, *Organometallics* **2012**, *31*, 27-30; kP. A. Chase, T. Jurca, D. W. Stephan, *Chemical Communications* **2008**, 1701-1703.

[24] aD. W. Stephan, *Dalton Transactions* **2009**, 3129-3136; bG. C. Welch, L. Cabrera, P. A. Chase, E. Hollink, J. D. Masuda, P. Wei, D. W. Stephan, *Dalton Transactions* **2007**, 3407-3414.

[25] aA. E. Ashley, T. J. Herrington, G. G. Wildgoose, H. Zaher, A. L. Thompson, N. H. Rees, T. Krämer, D. Öhare, *Journal of the American Chemical Society* **2011**, *133*, 14727-14740; bS. C. Binding, H. Zaher, F. Mark Chadwick, D. O'Hare, *Dalton Transactions* **2012**, *41*, 9061-9066; cM. A. Dureen, D. W. Stephan, *Journal of the American Chemical Society* **2009**, *131*, 8396-8397; dÁ. Gyömöre, M. Bakos, T. Földes, I. Pápai, A. Domján, T. Soós, *ACS Catalysis* **2015**, *5*, 5366-5372; eT. J. Herrington, A. J. W. Thom, A. J. P. White, A. E. Ashley, *Dalton Transactions* **2012**, *41*, 9019-9022; fG. Ménard, T. M. Gilbert, J. A. Hatnean, A. Kraft, I. Krossing, D. W. Stephan, *Organometallics* **2013**, *32*, 4416-4422; gD. O'Hare, A. Ashley, **2012**; hD. J. Scott, M. J. Fuchter, A. E. Ashley, *Angewandte Chemie - International Edition* **2014**, *53*, 10218-10222.

[26] aS. A. Cummings, M. Iimura, C. J. Harlan, R. J. Kwaan, I. Vu Trieu, J. R. Norton, B. M. Bridgewater, F. Jäkle, A. Sundararaman, M. Tilset, *Organometallics* **2006**, *25*, 1565-1568; bJ. M. Farrell, J. A. Hatnean, D. W. Stephan, *Journal of the American Chemical Society* **2012**, *134*, 15728-15731.

[27] I. B. Sivaev, V. I. Bregadze, *Coordination Chemistry Reviews* **2014**, *270-271*, 75-88.

[28] P. Eisenberger, C. M. Crudden, *Dalton Transactions* **2017**, *46*, 4874-4887.

[29] in *Chemistry of the Elements (Second Edition)*, Butterworth-Heinemann, Oxford, **1997**, pp. 216-267.

[30] T. Arai, H. Sasai, K.-i. Aoe, K. Okamura, T. Date, M. Shibasaki, *Angewandte Chemie* **1996**, *108*, 103-105.
[31] Z. Liu, R. Ganguly, D. Vidovic, *Dalton Transactions* **2017**, *46*, 753-759.
[32] Z. Liu, J. H. Q. Lee, R. Ganguly, D. Vidović, *Chemistry – A European Journal* **2015**, *21*, 11344-11348.
[33] S. Dagorne, S. Bellemin-Laponnaz, in *The Group 13 Metals Aluminium, Gallium, Indium and Thallium: Chemical Patterns and Peculiarities*, John Wiley & Sons, Ltd, **2011**, pp. 654-700.
[34] R. Amemiya, M. Yamaguchi, *European Journal of Organic Chemistry* **2005**, *2005*, 5145-5150.
[35] J. Chen, D. Wu, F. He, M. Liu, H. Wu, J. Ding, W. Su, *Tetrahedron Letters* **2008**, *49*, 3814-3818.
[36] J. A. B. Abdalla, I. M. Riddlestone, R. Tirfoin, S. Aldridge, *Angewandte Chemie International Edition* **2015**, *54*, 5098-5102.
[37] A. D. Dilman, S. L. Ioffe, *Chemical Reviews* **2003**, *103*, 733-772.
[38] aK. Mikami, Y. Mikami, Y. Matsumoto, J. Nishikido, F. Yamamoto, H. Nakajima, *Tetrahedron Lett.* **2001**, *42*, 3047; bK. Mikami, Y. Mikami, H. Matsuzawa, Y. Matsumoto, J. Nishikido, F. Yamamoto, H. Nakajima, *Tetrahedron* **2002**, *58*, 4015; cB. Mathieu, L. Ghosez, *Tetrahedron Letters* **1997**, *38*, 5497-5500.
[39] K. C. Kim, C. A. Reed, D. W. Elliott, L. J. Mueller, F. Tham, L. Lin, J. B. Lambert, *Science* **2002**, *297*, 825-827.
[40] aS. Inoue, M. Ichinohe, T. Yamaguchi, A. Sekiguchi, *Organometallics* **2008**, *27*, 6056-6058; bS. Inoue, J. D. Epping, E. Irran, M. Driess, *Journal of the American Chemical Society* **2011**, *133*, 8514-8517; cS. Inoue, M. Ichinohe, A. Sekiguchi, *Journal of the American Chemical Society* **2008**, *130*, 6078-6079; dH. F. T. Klare, M. Oestreich, *Dalton Transactions* **2010**, *39*, 9176-9184.
[41] aC. Douvris, O. V. Ozerov, *Science* **2008**, *321*, 1188; bR. Panisch, M. Bolte, T. Müller, *Journal of the American Chemical Society* **2006**, *128*, 9676-9682; cV. J. Scott, R. Çelenligil-Çetin, O. V. Ozerov, *Journal of the American Chemical Society* **2005**, *127*, 2852-2853.
[42] aK. Hara, R. Akiyama, M. Sawamura, *Organic Letters* **2005**, *7*, 5621-5623; bH. F. T. Klare, K. Bergander, M. Oestreich, *Angewandte Chemie International Edition* **2009**, *48*, 9077-9079.
[43] aN. Lühmann, R. Panisch, T. Müller, *Applied Organometallic Chemistry* **2010**, *24*, 533-537; bO. Allemann, S. Duttwyler, P. Romanato, K. K. Baldridge, J. S. Siegel, *Science* **2011**, *332*, 574.
[44] J. Bah, J. Franzén, *Chemistry – A European Journal* **2014**, *20*, 1066-1072.
[45] aS. Kobayashi, S. Matsui, T. Mukaiyama, *Chemistry Letters* **1988**, *17*, 1491-1494; bS. Kobayashi, M. Murakami, T. Mukaiyama, *Chem. Lett.* **1985**; cS. Lin, G. V. Bondar, C. J. Levy, S. Collins, *Journal of Organic Chemistry* **1998**, *63*, 1885-1892; dT. Mukaiyama, S. Kobayashi, M. Murakami, *Chem. Lett.* **1984**, 1759-1762; eT. Mukaiyama, S. Kobayashi, M. Murakami, *Chem. Lett.* **1985**; fT. Mukaiyama, S. Kobayashi, S. Shoda, *Chem. Lett.* **1984**, 1529-1530; gT. Mukaiyama, S. Matsui, K. Kashiwagi, *Chem. Lett.* **1989**, 993-996; hT. Mukaiyama, K. Narasaka, *Org. Synth.* **1987**, *65*, 6; iM. Ohshima, M. Murakami, T. Mukaiyama, *Chem. Lett.* **1985**.
[46] aJ. Bah, V. R. Naidu, J. Teske, J. Franzén, *Advanced Synthesis & Catalysis* **2015**, *357*, 148-158; bR. K. Schmidt, K. Müther, C. Mück-Lichtenfeld, S.

Grimme, M. Oestreich, *Journal of the American Chemical Society* **2012**, *134*, 4421-4428.
[47] D. Vidovic, M. Findlater, A. H. Cowley, *Journal of the American Chemical Society* **2007**, *129*, 8436-8437.
[48] H. Braunschweig, M. Kaupp, C. Lambert, D. Nowak, K. Radacki, S. Schinzel, K. Uttinger, *Inorganic Chemistry* **2008**, *47*, 7456-7458.
[49] R. Dinda, O. Ciobanu, H. Wadepohl, O. Hübner, R. Acharyya, H.-J. Himmel, *Angewandte Chemie International Edition* **2007**, *46*, 9110-9113.
[50] P. A. Rupar, V. N. Staroverov, P. J. Ragogna, K. M. Baines, *Journal of the American Chemical Society* **2007**, *129*, 15138-15139.
[51] P. A. Rupar, V. N. Staroverov, K. M. Baines, *Science* **2008**, *322*, 1360.
[52] aP. A. Rupar, R. Bandyopadhyay, B. F. T. Cooper, M. R. Stinchcombe, P. J. Ragogna, C. L. B. Macdonald, K. M. Baines, *Angewandte Chemie International Edition* **2009**, *48*, 5155-5158; bF. Cheng, A. L. Hector, W. Levason, G. Reid, M. Webster, W. Zhang, *Angewandte Chemie International Edition* **2009**, *48*, 5152-5154; cR. Bandyopadhyay, B. F. T. Cooper, A. J. Rossini, R. W. Schurko, C. L. B. Macdonald, *Journal of Organometallic Chemistry* **2010**, *695*, 1012-1018.
[53] K. Hensen, T. Stumpf, M. Bolte, C. Näther, H. Fleischer, *Journal of the American Chemical Society* **1998**, *120*, 10402-10408.
[54] aJ. Petuškova, M. Patil, S. Holle, C. W. Lehmann, W. Thiel, M. Alcarazo, *Journal of the American Chemical Society* **2011**, *133*, 20758-20760; bJ. J. Weigand, K.-O. Feldmann, F. D. Henne, *Journal of the American Chemical Society* **2010**, *132*, 16321-16323; cM. Azouri, J. Andrieu, M. Picquet, H. Cattey, *Inorganic Chemistry* **2008**, *48*, 1236-1242; dK. B. Dillon, A. E. Goeta, J. A. K. Howard, P. K. Monks, H. J. Shepherd, A. L. Thompson, *Dalton Transactions* **2008**, 1144-1149.
[55] A. Schmidpeter, S. Lochschmidt, K. Karaghiosoff, W. S. Sheldrick, *J. Chem. Soc., Chem. Commun.* **1985**, 1447-1448.
[56] J. D. Burton, R. M. K. Deng, K. B. Dillon, P. K. Monks, R. J. Olivey, *Heteroatom Chemistry* **2005**, *16*, 447-452.
[57] K. B. Dillon, R. J. Olivey, *Heteroatom Chemistry* **2004**, *15*, 150-154.
[58] J. J. Weigand, N. Burford, A. Decken, A. Schulz, *European Journal of Inorganic Chemistry* **2007**, *2007*, 4868-4872.
[59] A. P. M. Robertson, N. Burford, R. McDonald, M. J. Ferguson, *Angewandte Chemie International Edition* **2014**, *53*, 3480-3483.
[60] J. M. Bayne, D. W. Stephan, *Chemical Society Reviews* **2016**, *45*, 765-774.
[61] G. Wittig, U. Schöllkopf, *Chemische Berichte* **1954**, *87*, 1318-1330.
[62] K. C. Kumara Swamy, N. Satish Kumar, *Accounts of Chemical Research* **2006**, *39*, 324-333.
[63] E. L. Muetterties, W. Mahler, R. Schmutzler, *Inorganic Chemistry* **1963**, *2*, 613-618.
[64] aC. Y. Wong, D. K. Kennepohl, R. G. Cavell, *Chemical Reviews* **1996**, *96*, 1917-1951; bM. Well, P. G. Jones, R. Schmutzler, *Journal of Fluorine Chemistry* **1991**, *53*, 261-275.
[65] K. I. The, L. Vande Griend, W. A. Whitla, R. G. Cavell, *Journal of the American Chemical Society* **1977**, *99*, 7379-7380.
[66] N. Kurono, M. Yamaguchi, K. Suzuki, T. Ohkuma, *Journal of Organic Chemistry* **2005**, *70*, 6530-6532.

[67] aR. Córdoba, J. Plumet, *Tetrahedron Letters* **2003**, *44*, 6157-6159; bX. Wang, S. K. Tian, *Tetrahedron Letters* **2007**, *48*, 6010-6013.
[68] M. Selva, A. Perosa, P. Tundo, D. Brunelli, *Journal of Organic Chemistry* **2006**, *71*, 5770-5773.
[69] Y. S. Hon, C. F. Lee, *Tetrahedron* **2001**, *57*, 6181-6188.
[70] Y. S. Hon, C. F. Lee, *Tetrahedron Letters* **1999**, *40*, 2389-2392.
[71] M. Terada, M. Kouchi, *Tetrahedron* **2006**, *62*, 401-409.
[72] aC. B. Caputo, L. J. Hounjet, R. Dobrovetsky, D. W. Stephan, *Science* **2013**, *341*, 1374-1377; bC. B. Caputo, D. Winkelhaus, R. Dobrovetsky, L. J. Hounjet, D. W. Stephan, *Dalton Transactions* **2015**, *44*, 12256-12264.
[73] M. Pérez, L. J. Hounjet, C. B. Caputo, R. Dobrovetsky, D. W. Stephan, *Journal of the American Chemical Society* **2013**, *135*, 18308-18310.
[74] M. Pérez, Z. W. Qu, C. B. Caputo, V. Podgorny, L. J. Hounjet, A. Hansen, R. Dobrovetsky, S. Grimme, D. W. Stephan, *Chemistry - A European Journal* **2015**, *21*, 6491-6500.
[75] M. Pérez, C. B. Caputo, R. Dobrovetsky, D. W. Stephan, *Proceedings of the National Academy of Sciences of the United States of America* **2014**, *111*, 10917-10921.
[76] H. Hoffmann, H. J. Diehr, *Angewandte Chemie International Edition in English* **1964**, *3*, 737-746.
[77] aN. Burford, P. J. Ragogna, *Journal of the Chemical Society, Dalton Transactions* **2002**, 4307-4315; bD. Gudat, *Accounts of Chemical Research* **2010**, *43*, 1307-1316; cO. Guerret, G. Bertrand, *Accounts of Chemical Research* **1997**, *30*, 486-493.
[78] B. D. Ellis, P. J. Ragogna, C. L. B. Macdonald, *Inorganic Chemistry* **2004**, *43*, 7857-7867.
[79] A. H. Cowley, R. A. Kemp, *Chem. Rev.* **1985**, *85*, 367-382.
[80] A. Schmidpeter, *Multiple Bonds and Low Coordination Chemistry, Phophorus Chemistry*, Georg Thieme Verlag, Stuttgart, **1990**.
[81] M. R. M. M. Sanchez, L. Lamandé, R. Wolf, in *Phosphorus Chemistry* (Ed.: O. S. M. Regitz), Georg Thieme Verlag, Stuttgart, **1990**, p. 129ff.
[82] A. Schmidpeter, M. Thiele, *Angewandte Chemie International Edition in English* **1991**, *30*, 308-310.
[83] A. H. Cowley, R. A. Kemp, *Chemical Reviews* **1985**, *85*, 367-382.
[84] E. Jungermann, J. J. McBride, R. Clutter, A. G. O. Mais, *The Journal of Organic Chemistry* **1962**, *27*, 606-610.
[85] I. Granoth, J. C. Martin, *Journal of the American Chemical Society* **1979**, *101*, 4618-4622.
[86] S. Fleming, M. K. Lupton, K. Jekot, *Inorganic Chemistry* **1972**, *11*, 2534-2540.
[87] C. W. Schultz, R. W. Parry, *Inorganic Chemistry* **1976**, *15*, 3046-3050.
[88] N. Burford, P. J. Ragogna, K. N. Robertson, T. S. Cameron, N. J. Hardman, P. P. Power, *Journal of the American Chemical Society* **2002**, *124*, 382-383.
[89] N. Burford, J. A. C. Clyburne, P. Losier, T. M. Parks, T. S. Cameron, J. F. Richardson, *Phosphorus, Sulfur Silicon Relat. Elem.* **1994**, *93-94*, 301-304.
[90] W. W. Schoeller, U. Tubbesing, *Journal of Molecular Structure: THEOCHEM* **1995**, *343*, 49-55.
[91] aL. D. Hutchins, R. T. Paine, C. F. Campana, *Journal of the American Chemical Society* **1980**, *102*, 4521-4523; bL. D. Hutchins, E. N. Duesler, R. T. Paine, *Organometallics* **1982**, *1*, 1254-1256.

[92] aT. G. Traylor, J. C. Ware, *Journal of the American Chemical Society* **1967**, *89*, 2304-2316; bJ. D. Fitzpatrick, L. Watts, R. Pettit, *Tetrahedron Letters* **1966**, *7*, 1299-1303; cR. E. Davis, H. D. Simpson, N. Grice, R. Pettit, *Journal of the American Chemical Society* **1971**, *93*, 6688-6690.
[93] A. H. Cowley, S. K. Mehrotra, *Journal of the American Chemical Society* **1983**, *105*, 2074-2075.
[94] E. R. Alton, R. G. Montemayor, R. W. Parry, *Inorganic Chemistry* **1974**, *13*, 2267-2270.
[95] aD. Gudat, *Coordination Chemistry Reviews* **1997**, *163*, 71-106; bL. Rosenberg, *Coordination Chemistry Reviews* **2012**, *256*, 606-626.
[96] aB. Breit, *Chemical Communications* **1996**, 2071-2072; bB. Breit, *Journal of Molecular Catalysis A: Chemical* **1999**, *143*, 143-154; cK. Sakakibara, M. Yamashita, K. Nozaki, *Tetrahedron Letters* **2005**, *46*, 959-962.
[97] N. Kuhn, J. Fahl, D. Bläser, R. Boese, *Zeitschrift für anorganische und allgemeine Chemie* **1999**, *625*, 729-734.
[98] D. Gudat, M. Nieger, E. Niecke, *Journal of the Chemical Society, Dalton Transactions* **1989**, 693-700.
[99] aR. G. Pearson, *Journal of the American Chemical Society* **1985**, *107*, 6801-6806; bR. G. Pearson, *Journal of Chemical Education* **1987**, *64*, 561.
[100] N. Burford, P. Losier, C. Macdonald, V. Kyrimis, P. K. Bakshi, T. S. Cameron, *Inorganic Chemistry* **1994**, *33*, 1434-1439.
[101] R. W. Reed, Z. Xie, C. A. Reed, *Organometallics* **1995**, *14*, 5002-5004.
[102] E. Niecke, M. Nieger, F. Reichert, *Angewandte Chemie International Edition in English* **1988**, *27*, 1715-1716.
[103] aA. J. Arduengo, III, J. C. Calabrese, A. H. Cowley, H. V. R. Dias, J. R. Goerlich, W. J. Marshall, B. Riegel, *Inorg. Chem.* **1997**, *36*, 2151-2158; bA. J. Arduengo, III, H. V. R. Dias, J. C. Calabrese, *Chem. Lett.* **1997**, 143-144; cN. Kuhn, J. Fahl, D. Blaser, R. Boese, *Z. Anorg. Allg. Chem.* **1999**, *625*, 729-734; dN. J. Hardman, M. B. Abrams, M. A. Pribisko, T. M. Gilbert, R. L. Martin, G. J. Kubas, R. T. Baker, *Angew. Chem., Int. Ed.* **2004**, *43*, 1955-1958; eN. Burford, T. S. Cameron, D. J. LeBlanc, A. D. Phillips, T. E. Concolino, K.-C. Lam, A. L. Rheingold, *J. Am. Chem. Soc.* **2000**, *122*, 5413-5414.
[104] aM. B. Abrams, B. L. Scott, R. T. Baker, *Organometallics* **2000**, *19*, 4944-4956; bN. Burford, T. S. Cameron, J. A. C. Clyburne, K. Eichele, K. N. Robertson, S. Sereda, R. E. Wasylishen, W. A. Whitla, *Inorg. Chem.* **1996**, *35*, 5460-5467; cN. Burford, D. J. LeBlanc, *Inorg. Chem.* **1999**, *38*, 2248-2249; dN. Burford, T. S. Cameron, D. J. LeBlanc, P. Losier, S. Sereda, G. Wu, *Organometallics* **1997**, *16*, 4712-4717.
[105] N. Burford, J. A. C. Clyburne, P. K. Bakshi, T. S. Cameron, *Organometallics* **1995**, *14*, 1578-1585.
[106] aC. W. Schultz, R. W. Parry, *Inorg. Chem.* **1976**, *15*, 3046-3050; bN. Burford, P. Losier, A. D. Phillips, P. J. Ragogna, T. S. Cameron, *Inorg. Chem.* **2003**, *42*, 1087-1091; cN. Burford, A. D. Phillips, H. A. Spinney, K. N. Robertson, T. S. Cameron, R. McDonald, *Inorg. Chem.* **2003**, *42*, 4949-4954.
[107] W. S. Sheldrick, A. Schmidpeter, F. Zwaschka, K. B. Dillon, A. W. G. Platt, T. C. Waddington, *J. Chem. Soc., Dalton Trans.* **1981**, 413-418.
[108] T. Kaukorat, I. Neda, R. Schmutzler, *Coord. Chem. Rev.* **1994**, *137*, 53-107.
[109] N. Burford, P. J. Ragogna, K. N. Robertson, T. S. Cameron, N. J. Hardman, P. P. Power, *J. Am. Chem. Soc.* **2002**, *124*, 382-383.

[110] M. Q. Y. Tay, Y. P. Lu, R. Ganguly, D. Vidovic, *A Carbone-Stabilized Two-Coordinate Phosphorus(III)-Centered Dication*.
[111] aH. Schmidbaur, *Angewandte Chemie International Edition* **2007**, *46*, 2984-2985; bG. Frenking, B. Neumüller, W. Petz, R. Tonner, F. Öxler, *Angewandte Chemie International Edition* **2007**, *46*, 2986-2987.
[112] G. Frenking, R. Tonner, in *Pure and Applied Chemistry, Vol. 81*, **2009**, p. 597.
[113] F. Ramirez, N. B. Desai, B. Hansen, N. McKelvie, *Journal of the American Chemical Society* **1961**, *83*, 3539-3540.
[114] aR. Tonner, G. Frenking, *Chemical Communications* **2008**, 1584-1586; bR. Tonner, G. Frenking, *Chemistry – A European Journal* **2008**, *14*, 3260-3272; cR. Tonner, G. Frenking, *Chemistry – A European Journal* **2008**, *14*, 3273-3289; dR. Tonner, G. Frenking, *Angewandte Chemie International Edition* **2007**, *46*, 8695-8698; eR. Tonner, G. Heydenrych, G. Frenking, *ChemPhysChem* **2008**, *9*, 1474-1481; fR. Tonner, F. Öxler, B. Neumüller, W. Petz, G. Frenking, *Angewandte Chemie International Edition* **2006**, *45*, 8038-8042; gW. Petz, C. Kutschera, M. Heitbaum, G. Frenking, R. Tonner, B. Neumüller, *Inorganic Chemistry* **2005**, *44*, 1263-1274.
[115] M. A. Celik, R. Sure, S. Klein, R. Kinjo, G. Bertrand, G. Frenking, *Chemistry - A European Journal* **2012**, *18*, 5676-5692.
[116] A. Igau, H. Grutzmacher, A. Baceiredo, G. Bertrand, *Journal of the American Chemical Society* **1988**, *110*, 6463-6466.
[117] A. J. Arduengo, R. L. Harlow, M. Kline, *Journal of the American Chemical Society* **1991**, *113*, 361-363.
[118] A. D. McNaught, A. Wilkinson, *I{UPAC}. Compendium of Chemical Terminology, 2nd ed. (the "Gold Book")*, WileyBlackwell; 2nd Revised edition edition.
[119] E. P. L. Hunter, S. G. Lias, *Journal of Physical and Chemical Reference Data* **1998**, *27*, 413-656.
[120] aA. M. Magill, B. F. Yates, *Australian Journal of Chemistry* **2004**, *57*, 1205-1210; bA. M. Magill, K. J. Cavell, B. F. Yates, *Journal of the American Chemical Society* **2004**, *126*, 8717-8724; cD. A. Dixon, Arduengo, A. J., *journal of Physical Chemistry* **1991**, *95*, 4180; dH. Chen, Justes, D. R., Cooks, R. G. , *Organic Letters* **2005**, *7*, 3949; eR. W. Alder, Blake, M. E., Oliva, J. M. , *journal of Physical Chemistry* **1999**, *103*, 11200.
[121] W. Petz, F. Öxler, B. Neumüller, R. Tonner, G. Frenking, *European Journal of Inorganic Chemistry* **2009**, *2009*, 4507-4517.
[122] B. Inés, M. Patil, J. Carreras, R. Goddard, W. Thiel, M. Alcarazo, *Angewandte Chemie - International Edition* **2011**, *50*, 8400-8403.
[123] aD. Himmel, I. Krossing, A. Schnepf, *Angewandte Chemie International Edition* **2014**, *53*, 370-374; bG. Frenking, *Angewandte Chemie International Edition* **2014**, *53*, 6040-6046.
[124] H. G. Viehe, Z. Janousek, R. G. Und, D. Lach, *Angewandte Chemie* **1973**, *85*, 581-582.
[125] A. El-Hellani, J. Monot, S. Tang, R. Guillot, C. Bour, V. Gandon, *Inorganic Chemistry* **2013**, *52*, 11493-11502.
[126] A. Fürstner, M. Alcarazo, R. Goddard, C. W. Lehmann, *Angew. Chem., Int. Ed.* **2008**, *47*, 3210.
[127] W. Petz, G. Frenking, in *Transition Metal Complexes of Neutral eta1-Carbon Ligands* (Eds.: R. Chauvin, Y. Canac), Springer Berlin Heidelberg, Berlin, Heidelberg, **2010**, pp. 49-92.

[128] C. A. Dyker, V. Lavallo, B. Donnadieu, G. Bertrand, *Angew. Chem., Int. Ed.* **2008**, *47*, 3206.
[129] N. Dordevic, R. Ganguly, M. Petkovic, D. Vidovic, *Chemical Communications* **2016**, *52*, 9789-9792.
[130] H. Schmidbaur, T. Costa, *Chem. Ber.* **1981**, *114*, 3063.
[131] aW. Petz, C. Kutschera, S. Tsan, F. Weller, B. Neumueller, *Z. Anorg. Allg. Chem.* **2003**, *629*, 1235; bJ. S. Driscoll, D. W. Grisley, J. V. Pustinger, J. E. Harris, C. N. Matthews, *The Journal of Organic Chemistry* **1964**, *29*, 2427-2431.
[132] I. Kuzu, N.-J. H. Kneusels, M. Bauer, B. Neumüller, R. Tonner, *Zeitschrift für anorganische und allgemeine Chemie* **2014**, *640*, 417-422.
[133] S. Khan, G. Gopakumar, W. Thiel, M. Alcarazo, *Angewandte Chemie International Edition* **2013**, *52*, 5644-5647.
[134] H. Schmidbaur, E. Weiss, B. Zimmer-Gasser, *Angewandte Chemie International Edition in English* **1979**, *18*, 782-784.
[135] aD. J. Burton, Z.-Y. Yang, W. Qiu, *Chemical Reviews* **1996**, *96*, 1641-1716; bD. G. Cox, D. J. Burton, *The Journal of Organic Chemistry* **1988**, *53*, 366-374; cW. Petz, I. Kuzu, G. Frenking, D. M. Andrada, B. Neumüller, M. Fritz, J. E. Münzer, *Chemistry – A European Journal* **2016**, *22*, 8536-8546; dD. J. Burton, *Journal of Fluorine Chemistry* **1983**, *23*, 339-357; eR. Appel, H. Veltmann, *Tetrahedron Letters* **1977**, *18*, 399-400; fW. Petz, B. Neumüller, *Zeitschrift für anorganische und allgemeine Chemie* **2013**, *639*, 2331-2336.
[136] M. S. Hussain, H. Schmidbaur, in *Zeitschrift für Naturforschung B, Vol. 31*, **1976**, p. 721.
[137] aH. Schmidbaur, W. Tronich, *Chemische Berichte* **1968**, *101*, 3545-3555; bW. Uedelhoven, K. Eberl, W. Sieber, F. Roland Kreissl, *Journal of Organometallic Chemistry* **1982**, *236*, 301-307; cJ. Bestmann Hans, H. Oechsner, in *Zeitschrift für Naturforschung B, Vol. 38*, **1983**, p. 861; dM. Alcarazo, C. Gomez, S. Holle, R. Goddard, *Angewandte Chemie International Edition* **2010**, *49*, 5788-5791.
[138] C. Bianchini, A. Meli, A. Orlandini, L. Sacconi, *Angewandte Chemie International Edition in English* **1980**, *19*, 1021-1022.
[139] M. Q. Y. Tay, Y. Lu, R. Ganguly, D. Vidovic, *Chem. - Eur. J.* **2014**, *20*, 6628-6631.
[140] aW. E. Piers, *Organometallics* **2011**, *30*, 13-16; bN. S. Lewis, D. G. Nocera, *Proceedings of the National Academy of Sciences* **2006**, *103*, 15729-15735; cO. V. Ozerov, *Chemical Society Reviews* **2009**, *38*, 83-88; dE. Poverenov, I. Efremenko, A. I. Frenkel, Y. Ben-David, L. J. W. Shimon, G. Leitus, L. Konstantinovski, J. M. L. Martin, D. Milstein, *Nature* **2008**, *455*, 1093-1096; eD. G. H. Hetterscheid, J. I. van der Vlugt, B. de Bruin, J. N. H. Reek, *Angewandte Chemie International Edition* **2009**, *48*, 8178-8181.
[141] C. Gurnani, N. Orević, S. Muthaiah, D. Dimić, R. Ganguly, M. Petković, D. Vidović, *Chemical Communications* **2015**, *51*, 10762-10764.
[142] M. Q. Y. Tay, Y. Lu, R. Ganguly, D. Vidovič, *Angewandte Chemie - International Edition* **2013**, *52*, 3132-3135.
[143] T. E. Mallouk, G. L. Rosenthal, G. Mueller, R. Brusasco, N. Bartlett, *Inorganic Chemistry* **1984**, *23*, 3167-3173.
[144] aK. O. Christe, D. A. Dixon, D. McLemore, W. W. Wilson, J. A. Sheehy, J. A. Boatz, *Journal of Fluorine Chemistry* **2000**, *101*, 151-153; bL. O. Müller, D.

Himmel, J. Stauffer, G. Steinfeld, J. Slattery, G. Santiso-Quiñones, V. Brecht, I. Krossing, *Angewandte Chemie International Edition* **2008**, *47*, 7659-7663.
[145] H. Bohrer, N. Trapp, D. Himmel, M. Schleep, I. Krossing, *Dalton Transactions* **2015**, *44*, 7489-7499.
[146] aS. Tang, J. Monot, A. El-Hellani, B. Michelet, R. Guillot, C. Bour, V. Gandon, *Chem.—Eur. J.* **2012**, *18*, 10239; bA. El-Hellani, J. Monot, R. Guillot, C. Bour, V. Gandon, *Inorganic Chemistry* **2013**, *52*, 506-514.
[147] M. S. D. o. t. N. I. o. S. a. T. N. M. M. L. (MML), Aug 17th, 2007 ed., National Institute of Standards and Technology, **2007**.
[148] F. Mathey, *Angewandte Chemie International Edition* **2003**, *42*, 1578-1604.
[149] S. Alvarez, *Dalton Transactions* **2013**, *42*, 8617-8636.
[150] D. Gudat, *Cationic low coordinated phosphorus compounds as ligands: recent developments*.
[151] S. Muthaiah, D. C. H. Do, R. Ganguly, D. Vidović, *Organometallics* **2013**, *32*, 6718-6724.
[152] aA. Schnurr, M. Bolte, H.-W. Lerner, M. Wagner, *European Journal of Inorganic Chemistry* **2012**, *2012*, 112-120; bM. A. Beckett, G. C. Strickland, J. R. Holland, K. Sukumar Varma, *Polymer* **1996**, *37*, 4629-4631; cP. Laszlo, M. Teston-Henry, *Journal of Physical Organic Chemistry* **1991**, *4*, 605-610.
[153] G. J. P. Britovsek, J. Ugolotti, A. J. P. White, *Organometallics* **2005**, *24*, 1685-1691.
[154] aJ. T. F. Fenwick, J. W. Wilson, *Inorganic Chemistry* **1975**, *14*, 1602-1604; bL. Luo, T. Marks, *Topics in Catalysis* **1999**, *7*, 97-106.
[155] G. A. Olah, S. Kobayashi, M. Tashiro, *Journal of the American Chemical Society* **1972**, *94*, 7448-7461.
[156] aC. S. Branch, S. G. Bott, A. R. Barron, *Journal of Organometallic Chemistry* **2003**, *666*, 23-34; bD. Fărcaşiu, M. Stan, *Journal of the Chemical Society. Perkin Transactions 2* **1998**, 1219-1222; cR. J. Gillespie, J. S. Hartman, *Canadian Journal of Chemistry* **1968**, *46*, 2147-2157; dD. P. N. Satchell, R. S. Satchell, *Chemical Reviews* **1969**, *69*, 251-278; eM. F. Lappert, *Journal of the Chemical Society (Resumed)* **1962**, 542-548.
[157] aU. Mayer, V. Gutmann, W. Gerger, *Monatshefte für Chemie* **1975**, *106*, 1235-1257; bV. Gutmann, *Coordination Chemistry Reviews* **1976**, *18*, 225-255.
[158] R. F. Childs, D. L. Mulholland, A. Nixon, *Canadian Journal of Chemistry* **1982**, *60*, 801-808.
[159] aI. B. Sivaev, V. I. Bregadze, *Coordination Chemistry Reviews* **2014**, *270–271*, 75-88; bJ. Mohr, M. Durmaz, E. Irran, M. Oestreich, *Organometallics* **2014**, *33*, 1108-1111; cC. F. Jiang, O. Blacque, T. Fox, H. Berke, *Dalton Transactions* **2011**, *40*, 1091-1097.
[160] M. H. Holthausen, M. Mehta, D. W. Stephan, *Angewandte Chemie International Edition* **2014**, *53*, 6538-6541.
[161] J. M. Slattery, S. Hussein, *Dalton Transactions* **2012**, *41*, 1808-1815.
[162] M. H. Holthausen, M. Mehta, D. W. Stephan, *Angewandte Chemie - International Edition* **2014**, *53*, 6538-6541.
[163] aM. Gouygou, P. Kalck, M. Urrutigoity, *Comprehensive Inorganic Chemistry II* **2013**, 223-247; bD. Ager, in *Comprehensive Organic Synthesis: Second Edition, Vol. 8*, **2014**, pp. 605-631; cP. J. Chirik, *Accounts of Chemical Research* **2015**, *48*, 1687-1695; dT. Zell, D. Milstein, *Accounts of Chemical Research* **2015**, *48*, 1979-1994; eA. E. Shilov, G. B. Shul'pin, *Chemical Reviews* **1997**, *97*, 2879-2932; fP. P. Y. Chen, R. B. G. Yang, J. C. M. Lee, S. I.

Chan, *Proceedings of the National Academy of Sciences of the United States of America* **2007**, *104*, 14570-14575; gT. Newhouse, P. S. Baran, *Angewandte Chemie - International Edition* **2011**, *50*, 3362-3374.

[164] aH. C. Brown, G. Zweifel, *Journal of the American Chemical Society* **1959**, *81*, 247-248; bH. C. Brown, S. K. Gupta, *Journal of the American Chemical Society* **1972**, *94*, 4370-4371.

[165] aK. Tamao, N. Ishida, M. Humada, *Journal of Organic Chemistry* **1983**, *48*, 2120-2122; bK. Tamao, N. Ishida, T. Tanaka, M. Kumada, *Organometallics* **1983**, *2*, 1694-1696; cI. Fleming, R. Henning, H. Plaut, *Chem. Commun.* **1984**, 29; dI. Fleming, P. E. J. Sanderson, *Tetrahedron Letters* **1987**, *28*, 4229-4232.

[166] aY. Kashman, O. Awerbouch, *Tetrahedron* **1975**, *31*, 45-51; bL. D. Quin, J. C. Kisalus, K. A. Mesch, *Journal of Organic Chemistry* **1983**, *48*, 4466-4472; cL. D. Quin, B. G. Marsi, *Journal of the American Chemical Society* **1985**, *107*, 3389-3390; dL. D. Quin, J. Szewczyk, K. M. Szewczyk, A. T. McPhail, *Journal of Organic Chemistry* **1986**, *51*, 3341-3347; eL. D. Quin, X. P. Wu, *Heteroatom Chemistry* **1991**, *2*, 359-367; fS. Jankowski, G. Keglevich, T. Nonas, H. Forintos, M. Główka, J. Rudziński, *Tetrahedron* **2004**, *60*, 2789-2797; gS. Jankowski, K. Huben, *Current Organic Chemistry* **2006**, *10*, 79-92; hH. Wang, C. Li, D. Geng, H. Chen, Z. Duan, F. Mathey, *Chemistry - A European Journal* **2010**, *16*, 10659-10661.

[167] aK. M. Carsch, T. R. Cundari, *Computational and Theoretical Chemistry* **2012**, *980*, 133-137; bT. M. Figg, T. R. Cundari, *Organometallics* **2012**, *31*, 4998-5004; cT. M. Figg, T. R. Cundari, *Dalton Transactions* **2013**, *42*, 4114-4121; dT. M. Figg, T. R. Cundari, T. B. Gunnoe, *Organometallics* **2011**, *30*, 3779-3785; eT. M. Figg, G. Schoendorff, B. Chilukuri, T. R. Cundari, *Organometallics* **2013**, *32*, 4993-4996; fE. C. Garrett, T. M. Figg, T. R. Cundari, *Inorganic Chemistry* **2014**, *53*, 7789-7798; gD. R. Pahls, J. T. Groves, T. B. Gunnoe, T. R. Cundari, *Organometallics* **2014**, *33*, 1936-1944; hB. M. Prince, T. B. Gunnoe, T. R. Cundari, *Dalton Transactions* **2014**, *43*, 7608-7614.

[168] aO. Mallow, J. Bolsinger, P. Finke, M. Hesse, Y.-S. Chen, A. Duthie, S. Grabowsky, P. Luger, S. Mebs, J. Beckmann, *Journal of the American Chemical Society* **2014**, *136*, 10870-10873; bM. J. Pouy, E. M. Milczek, T. M. Figg, B. M. Otten, B. M. Prince, T. B. Gunnoe, T. R. Cundari, J. T. Groves, *Journal of the American Chemical Society* **2012**, *134*, 12920-12923; cJ. L. Smeltz, P. D. Boyle, E. A. Ison, *Journal of the American Chemical Society* **2011**, *133*, 13288-13291.

[169] aY. H. Chiu, N. J. Lipscomb, *Am. Chem. Soc.* **1963**, *91*, 4150; bM. W. Wieczorek, G. D. Bujacz, R. Bodalski, L. D. Quin, *Journal of Chemical Crystallography* **1994**, *24*, 431-435.

[170] V. Mouriès, F. Mercier, L. Ricard, F. Mathey, *European Journal of Organic Chemistry* **1998**, 2683-2687.

[171] aM. Q. Y. Tay, Y. Lu, R. Ganguly, G. Frison, L. Ricard, D. Vidović, D. Carmichael, *Phosphorus, Sulfur, and Silicon and the Related Elements* **2015**, *190*, 785-788; bM. Q. Y. Tay, Y. Lu, R. Ganguly, D. Vidovič, *Chemistry - A European Journal* **2014**, *20*, 6628-6631.

[172] W. E. Acree, G. Pilcher, M. da Silva, *The dissociation enthalpies of terminal (N-O) bonds in organic compounds*.

[173] I. Despotović, R. Vianello, *Chemical Communications (Cambridge, England)* **2014**, *50*, 10941-10944.

[174] aM. Renz, B. Meunier, *European Journal of Organic Chemistry* **1999**, *1999*, 737-750; bG. J. ten Brink, I. W. C. E. Arends, R. A. Sheldon, *Chemical Reviews* **2004**, *104*, 4105-4124; cC. Bolm, C. Palazzi, O. Beckmann, *Transition Metals for Organic Synthesis* **2004**, *2*, 267-274; dM. Uyanik, K. Ishihara, *ACS Catalysis* **2013**, *3*, 513-520.
[175] aC. A. Taatjes, G. Meloni, T. M. Selby, A. J. Trevitt, D. L. Osborn, C. J. Percival, D. E. Shallcross, *Journal of the American Chemical Society* **2008**, *130*, 11883-11885; bM. Nakajima, Y. Endo, *Journal of Chemical Physics* **2013**, *139*.
[176] P. A. Krasutsky, I. V. Kolomitsyn, P. Kiprof, R. M. Carlson, A. A. Fokin, *The Journal of Organic Chemistry* **2000**, *65*, 3926-3933.
[177] A. D. Hendsbee, N. A. Giffin, Y. Zhang, C. C. Pye, J. D. Masuda, *Angewandte Chemie International Edition* **2012**, *51*, 10836-10840.
[178] T. C. C. D. C. (CCDC).
[179] aV. P. Andreev, V. A. Tafeenko, S. N. Ivashevskaya, *Russ J Gen Chem* **2014**, *84*, 255-258; bC. B. Caputo, S. J. Geier, D. Winkelhaus, N. W. Mitzel, V. N. Vukotic, S. J. Loeb, D. W. Stephan, *Dalton Transactions* **2012**, *41*, 2131-2139.
[180] aK. George, A. L. Hector, W. Levason, G. Reid, G. Sanderson, M. Webster, W. Zhang, *Dalton Transactions* **2011**, *40*, 1584-1593; bB. M. Kraft, W. W. Brennessel, *Organometallics* **2013**, *33*, 158-171.
[181] A. D. Hendsbee, N. A. Giffin, Y. Zhang, C. C. Pye, J. D. Masuda, *Angewandte Chemie* **2012**, *124*, 10994-10998.
[182] W. v. E. Doering, E. Dorfman, *Journal of the American Chemical Society* **1953**, *75*, 5595-5598.
[183] aL. D. Quin, C. Bourdieu, G. S. Quin, *Phosphorus, Sulfur, and Silicon and the Related Elements* **1991**, *63*, 349-362; bS. Jankowski, L. D. Quin, *J. Am. Chem. Soc.* **1991**, *113*; cL. D. Quin, X. P. Wu, G. S. Quin, S. Jankowski, *Phosphorus, Sulfur, and Silicon and the Related Elements* **1993**, *76*, 91-94; dT. Nonas, S. Jankowski, *The Journal of Organic Chemistry* **2005**, *70*, 562-566.
[184] M. Nakajima, Y. Endo, *The Journal of Chemical Physics* **2013**, *139*, 101103.
[185] L. Canovese, F. Visentin, G. Chessa, P. Uguagliati, G. Bandoli, *Organometallics* **2000**, *19*, 1461-1463.
[186] A. P. M. Robertson, S. S. Chitnis, H. A. Jenkins, R. McDonald, M. J. Ferguson, N. Burford, *Chemistry – A European Journal* **2015**, *21*, 7902-7913.
[187] F. A. Cotton, *Advanced inorganic chemistry*, New York : Wiley, c1999.
6th ed. / F. Albert Cotton ... [et al.]. **1999**.
[188] R. B. Schlesinger, in *Environmental Toxicants*, John Wiley & Sons, Inc., **2008**, pp. 823-868.
[189] Z. Mielke, M. McCluskey, L. Andrews, *Chemical Physics Letters* **1990**, *165*, 146-154.
[190] O. J. Scherer, J. Braun, P. Walther, C. Heckmann, G. Wolmershäuser, *Angewandte Chemie International Edition in English* **1991**, *30*, 852-854.
[191] W. Wang, G. D. Enright, A. J. Carty, *Journal of the American Chemical Society* **1997**, *119*, 12370-12371.
[192] Y. Wang, Y. Xie, P. Wei, H. F. Schaefer, P. v. R. Schleyer, G. H. Robinson, *Journal of the American Chemical Society* **2013**, *135*, 19139-19142.
[193] aW. W. Butcher, F. H. Westheimer, *Journal of the American Chemical Society* **1955**, *77*, 2420-2424; bP. W. C. Barnard, C. A. Bunton, D. R. Llewellyn, K. G. Oldham, B. L. Silver, C. A. Vernon, *Chem. Ind. (London)* **1955**.

[194] A. C. Satterthwait, F. H. Westheimer, *Journal of the American Chemical Society* **1980**, *102*, 4464-4472.
[195] R. Ahlrichs, C. Ehrhardt, M. Lakenbrink, S. Schunck, H. Schnockel, *Journal of the American Chemical Society* **1986**, *108*, 3596-3602.
[196] S. Bracher, J. I. G. Cadogan, I. Gosney, S. Yaslak, *Journal of the Chemical Society, Chemical Communications* **1983**, 857-858.
[197] J. I. G. Cadogan, A. H. Cowley, I. Gosney, M. Pakulski, S. Yaslak, *Journal of the Chemical Society, Chemical Communications* **1983**, 1408-1409.
[198] aL. D. Quin, C. Bourdieu, G. S. Quin, *Tetrahedron Letters* **1990**, *31*, 6473-6476; bL. D. Quin, A. N. Hughes, X. Wu, L. C. Dickinson, *Journal of the Chemical Society, Chemical Communications* **1988**, 555-556; cL. D. Quin, B. Pete, J. Szewczyk, A. N. Hughes, *Tetrahedron Letters* **1988**, *29*, 2627-2630; dL. D. Quin, N. D. Sadanani, X. P. Wu, *Journal of the American Chemical Society* **1989**, *111*, 6852-6853; eL. D. Quin, X. P. Wu, E. Breuer, M. Mahajna, *Tetrahedron Letters* **1990**, *31*, 6281-6282; fL. D. Quin, X. P. Wu, I. Lukes, R. O. Day, *Tetrahedron Letters* **1992**, *33*, 3975-3978; gL. D. Quin, X. P. Wu, N. D. Sadanani, I. Lukeš, A. S. Ionkin, R. O. Day, *Journal of Organic Chemistry* **1994**, *59*, 120-129.
[199] R. Menye-Biyogo, F. Delpech, A. Castel, H. Gornitzka, P. Rivière, *Angewandte Chemie International Edition* **2003**, *42*, 5610-5612.
[200] aM. Alonso, M. A. Alvarez, M. E. Garcia, D. Garcia-Vivo, M. A. Ruiz, *Dalton Transactions* **2014**, *43*, 16074-16083; bM. Alonso, M. A. Alvarez, M. E. García, M. A. Ruiz, H. Hamidov, J. C. Jeffery, *Journal of the American Chemical Society* **2005**, *127*, 15012-15013.
[201] aM. Alonso, M. A. Alvarez, M. E. García, D. García-Vivó, M. A. Ruiz, *Dalton Transactions* **2014**, *43*, 16074-16083; bA. Mardyukov, D. Niedek, P. R. Schreiner, *Journal of the American Chemical Society* **2017**, *139*, 5019-5022; cL. D. Quin, *Coordination Chemistry Reviews* **1994**, *137*, 525-559.
[202] A. f. T. S. a. D. R. (ATSDR), Department of Health and Human Services, Public Health Service
, Atlanta, GA, **1997**.
[203] L. D. Quin, *A guide to organophosphorus chemistry*, New York : Wiley, c2000., **2000**.
[204] S. Burck, D. Gudat, M. Nieger, W.-W. Du Mont, *Journal of the American Chemical Society* **2006**, *128*, 3946-3955.
[205] aI. H. Lukes, Petr, C07D 257/02, A61P 39/04 ed. (Ed.: W. I. P. Organization), Therapharm Gmbh, Switz., **2003**; bM. J. Gallagher, H. Honegger, *Journal of the Chemical Society, Chemical Communications* **1978**, 54-55.
[206] D. C. H. Do, S. Muthaiah, R. Ganguly, D. Vidović, *Organometallics* **2014**, *33*, 4165-4168.
[207] aA. Cieplucha, S. Jankowski, *Phosphorus, Sulfur, and Silicon and the Related Elements* **2009**, *184*, 1448-1453; bS. Jankowski, J. Kovács, K. Huben, M. Błaszczyk, M. Główka, G. Keglevich, *Heteroatom Chemistry* **2006**, *17*, 369-375.
[208] aJ. Yang, T. Chen, Y. Zhou, S.-F. Yin, L.-B. Han, *Organometallics* **2015**, *34*, 5095-5098; bY. Zhu, T. Chen, S. Li, S. Shimada, L.-B. Han, *Journal of the American Chemical Society* **2016**, *138*, 5825-5828; cJ.-S. Zhang, J.-Q. Zhang, T. Chen, L.-B. Han, *Organic & Biomolecular Chemistry* **2017**; dT. Chen, J.-S. Zhang, L.-B. Han, *Dalton Transactions* **2016**, *45*, 1843-1849; eC. Li, T. Chen, L.-B. Han, *Dalton Transactions* **2016**, *45*, 14893-14897.

[209] F. Ramirez, N. B. Desai, B. Hansen, N. McKelvie, *Journal of the American Chemical Society* **1961**, *83*, 3539-3540.
[210] U. Schubert, C. Kappenstein, B. Milewski-Mahrla, H. Schmidbaur, *Chemische Berichte* **1981**, *114*, 3070-3078.
[211] A. B. Chaplin, A. S. Weller, *European Journal of Inorganic Chemistry* **2010**, 5124-5128.
[212] *SMART Version 5.628* **2001**.
[213] *SAINT+ Version 6.22a* **2001**.
[214] Z. Otwinowski, W. Minor, in *Methods in Enzymology, Vol. 276*, **1997**, pp. 307-326.
[215] G. M. Sheldrick, *SADABS* **1996**.
[216] G. M. Sheldrick, *SHELXTL, Version 6.10* **2000**.
[217] M. J. Frisch, *Gaussian 09, Revision C.01* **2009**.
[218] A. D. Becke, *The Journal of Chemical Physics* **1993**, *98*, 5648-5652.
[219] aE. D. Glendening, J. K. Badenhoop, F. Weinhold, *Journal of Computational Chemistry* **1998**, *19*, 628-646; bE. D. Glendening, F. Weinhold, *Journal of Computational Chemistry* **1998**, *19*, 593-609; cE. D. Glendening, F. Weinhold, *Journal of Computational Chemistry* **1998**, *19*, 610-627.

Appendix

*Table 17. **17** and MeOH reaction conditions*

Nr.	**17**	MeOH	ACN	t_R = 5h
1	D	D	W_{HPLC}, sieves, not distilled, not degassed	>
2		D + $H_2O_{(additional)}$	W_{HPLC}, sieves, not distilled, not degassed	>
3		D	CD_3CN, degassed, dried	>
4		D + $H_2O_{(additional)}$	CD_3CN, degassed, dried	>
5		W_{HPLC}, degassed	CD_3CN, degassed, dried	>
6		W_{HPLC}, degassed	-	>
7		W_{HPCL}	W_{HPLC}	=
8	W	W_{HPCL}	W_{HPLC}	=
9		D	W_{HPLC}	=
10		D	$W_{(30\ ppm\ H2O)}$	=
11		D	$W_{(99.999\%\ ACN)}$	=
12		D	D	>
13		W_{HPCL}	D	=
14	W + TEA	D	W_{HPCL}	=
15		W_{HPCL}	D	=
16		D	D	=
17	W + $TEAH^+$	D	D	>
18	W + Me_4NBAr^{Cl}	D	W_{HPCL}	Did not start
19		W	D	Did not start
20		D	D	>

NMR spectra

[(^{i}Pr$_2$NP(O)(C(PPh$_3$)$_2$(OPy))[SbF$_6$]$_2$, [7][SbF$_6$]$_2$

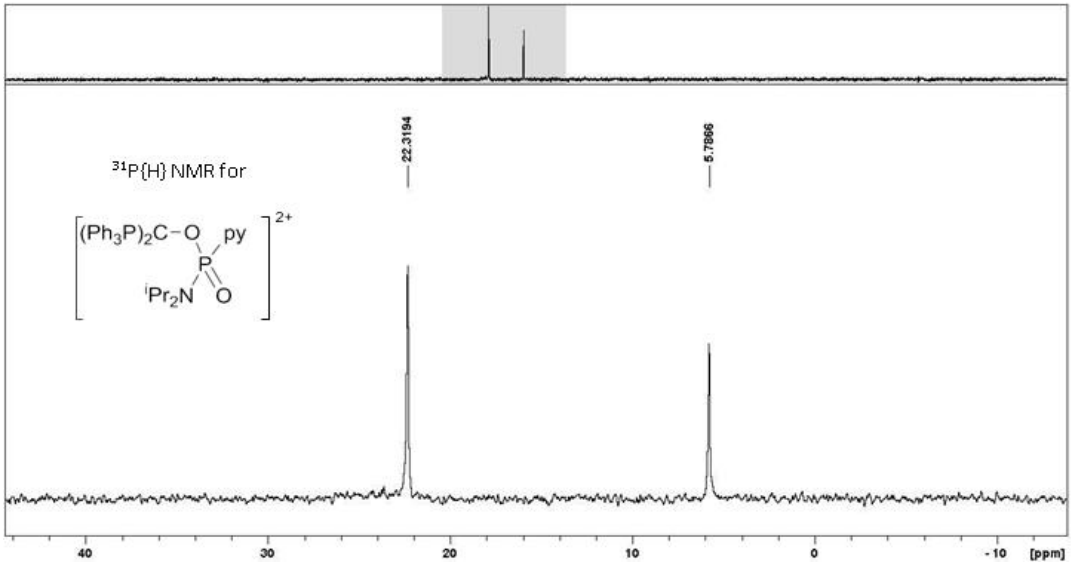

*Figure 35. 31P{H} NMR spectra of **[7][SbF$_6$]$_2$***

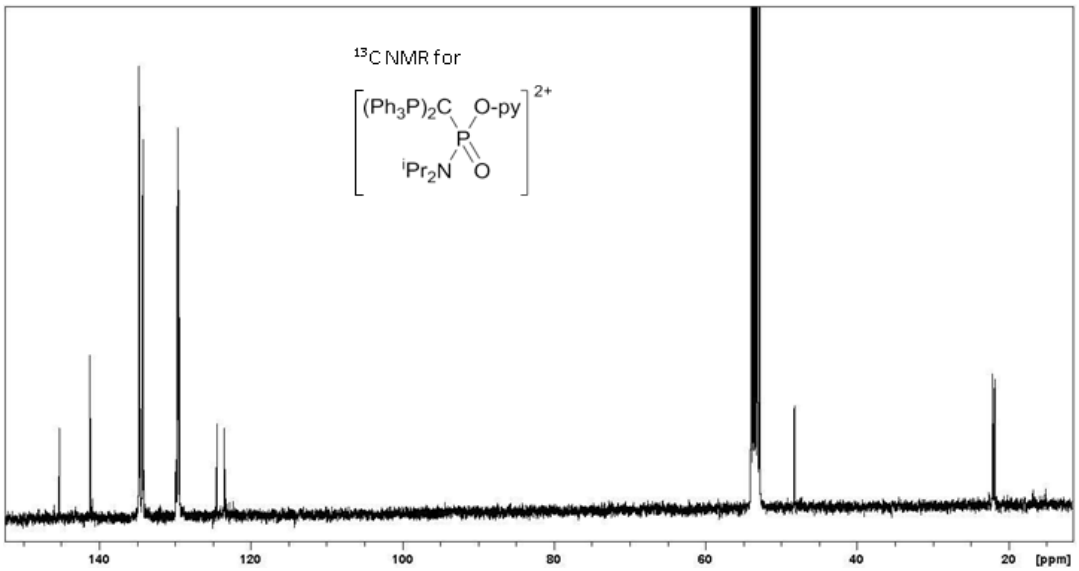

*Figure 36. 13C NMR spectra of **[7][SbF$_6$]$_2$***

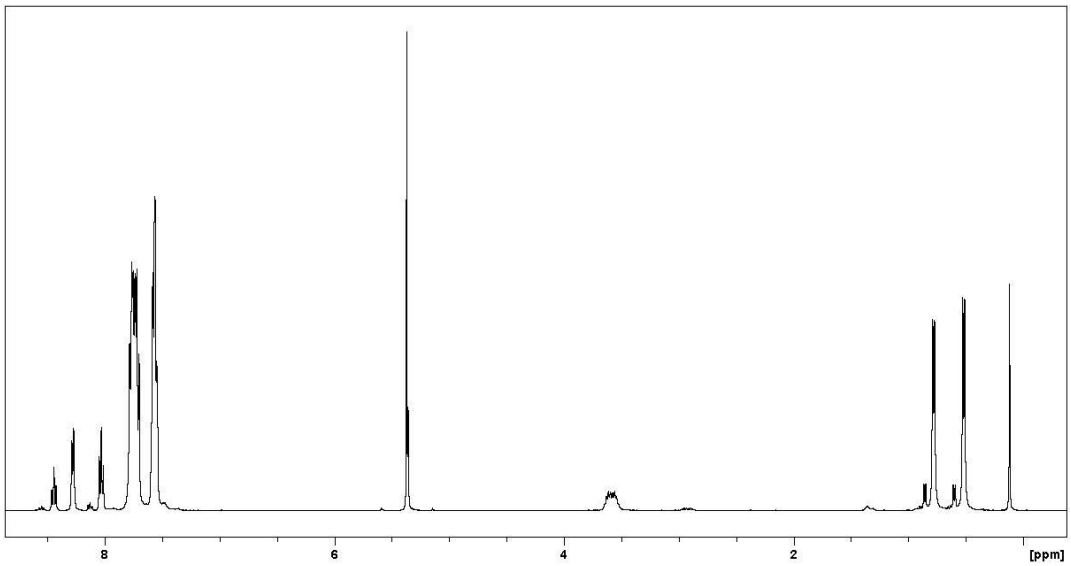

Figure 37. 1H NMR spectra of ***[7][SbF$_6$]$_2$***

[(^{i}Pr$_2$NP(O)(OC(PPh$_3$)$_2$(Py))[SbF$_6$]$_2$, [8][SbF$_6$]$_2$:

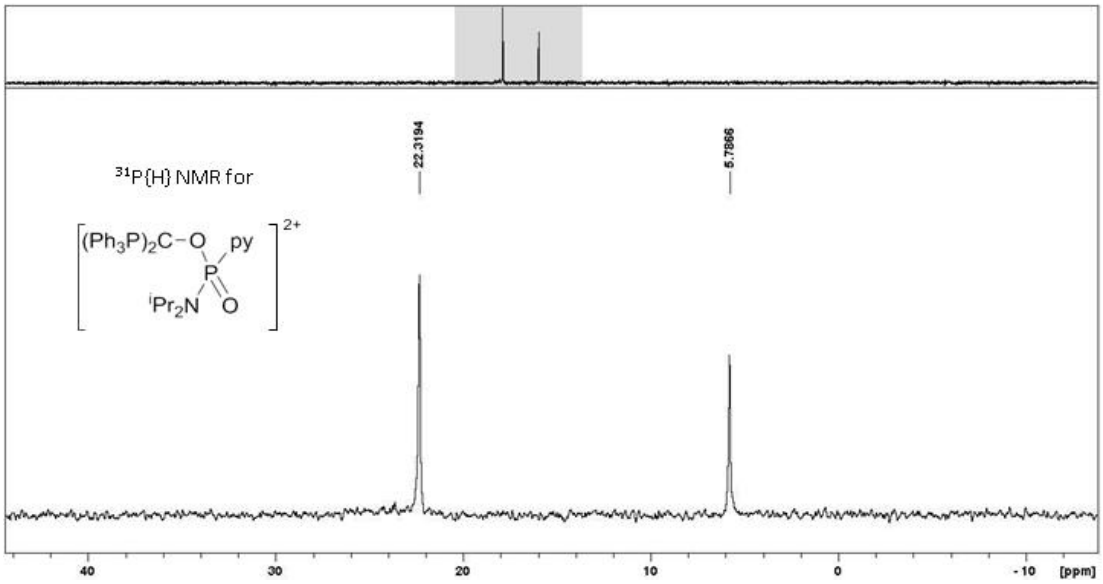

Figure 38. 31P{1H} NMR spectra of ***[8][SbF$_6$]$_2$:***

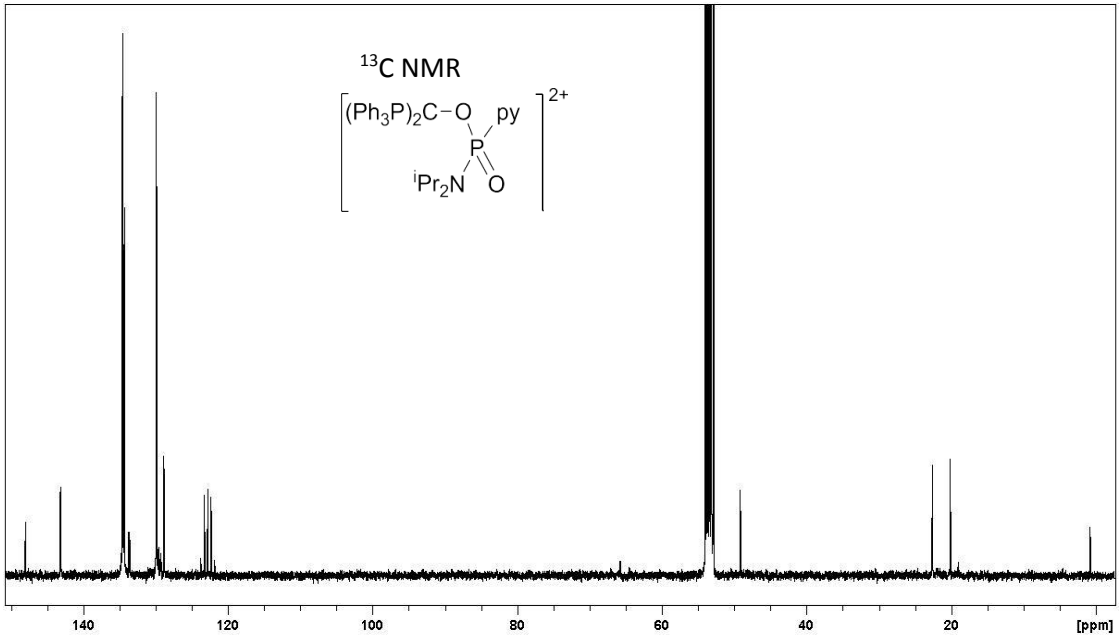

*Figure 39. 13C NMR spectra of **[8][SbF$_6$]$_2$:***

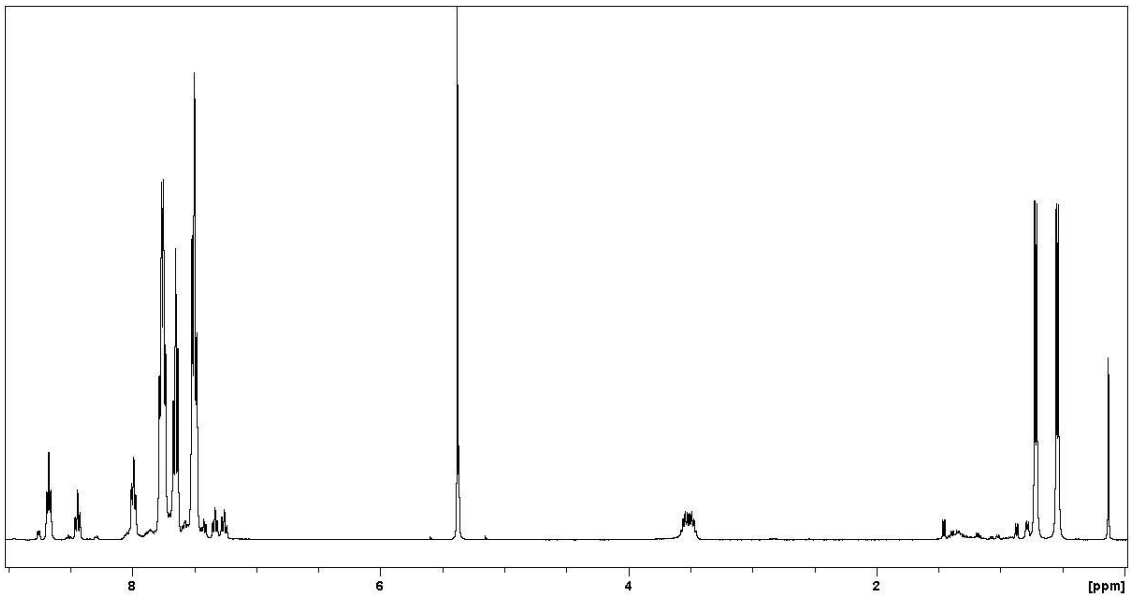

*Figure 40. 1H NMR spectra of **[8][SbF$_6$]$_2$:***

{[$(Ph_3P)_2CP(O)(OH)(H)$][BAr^F_4]}$_2$, [15][BAr^F_4]:

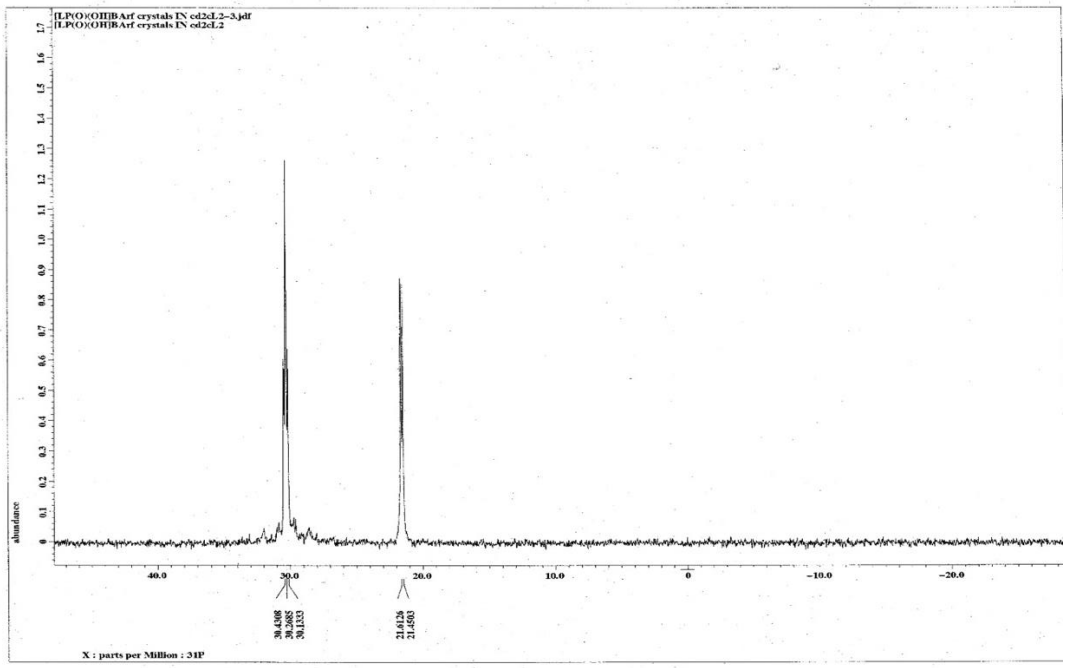

Figure 41. 31P{1H} spectra of [15][BAr^F_4]$_2$

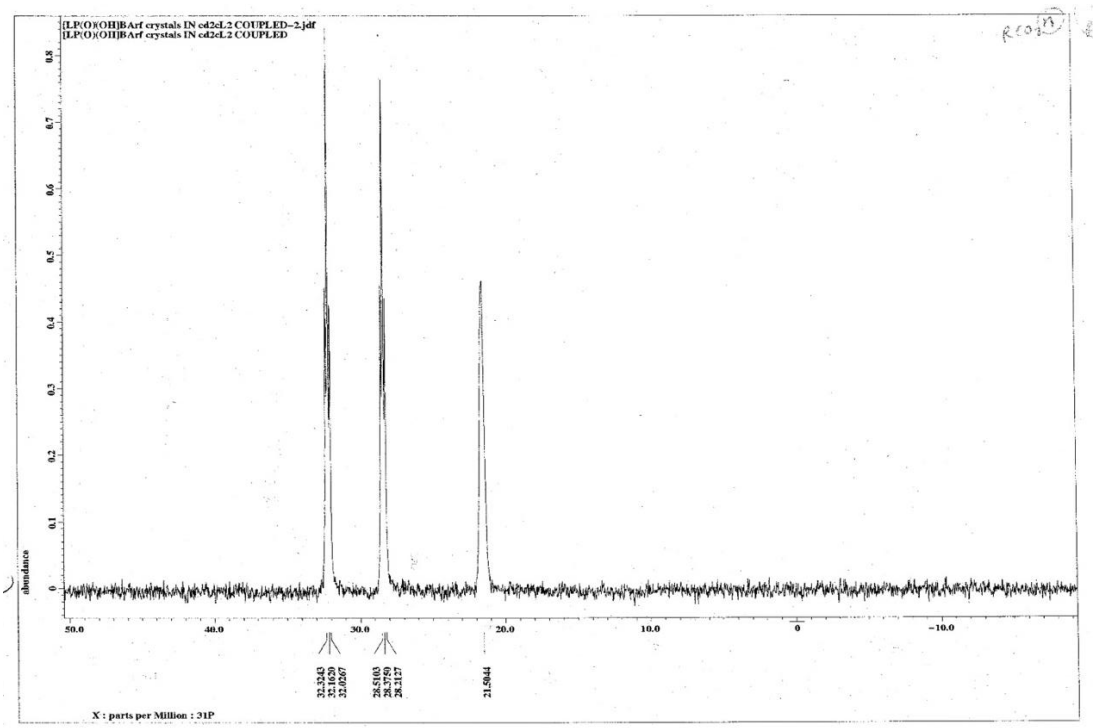

*Figure 42. 31P NMR spectra of **[15]**[BAr^F_4]$_2$*

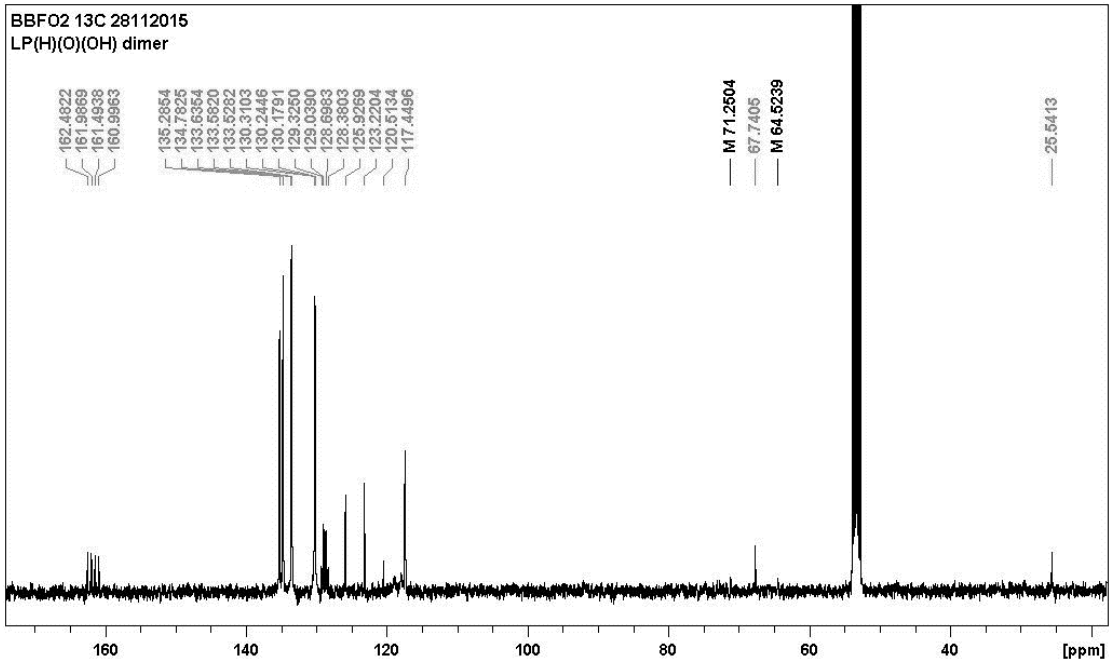

Figure 43. 13C NMR spectra of [15][BAr$^{F}_{4}$]$_2$

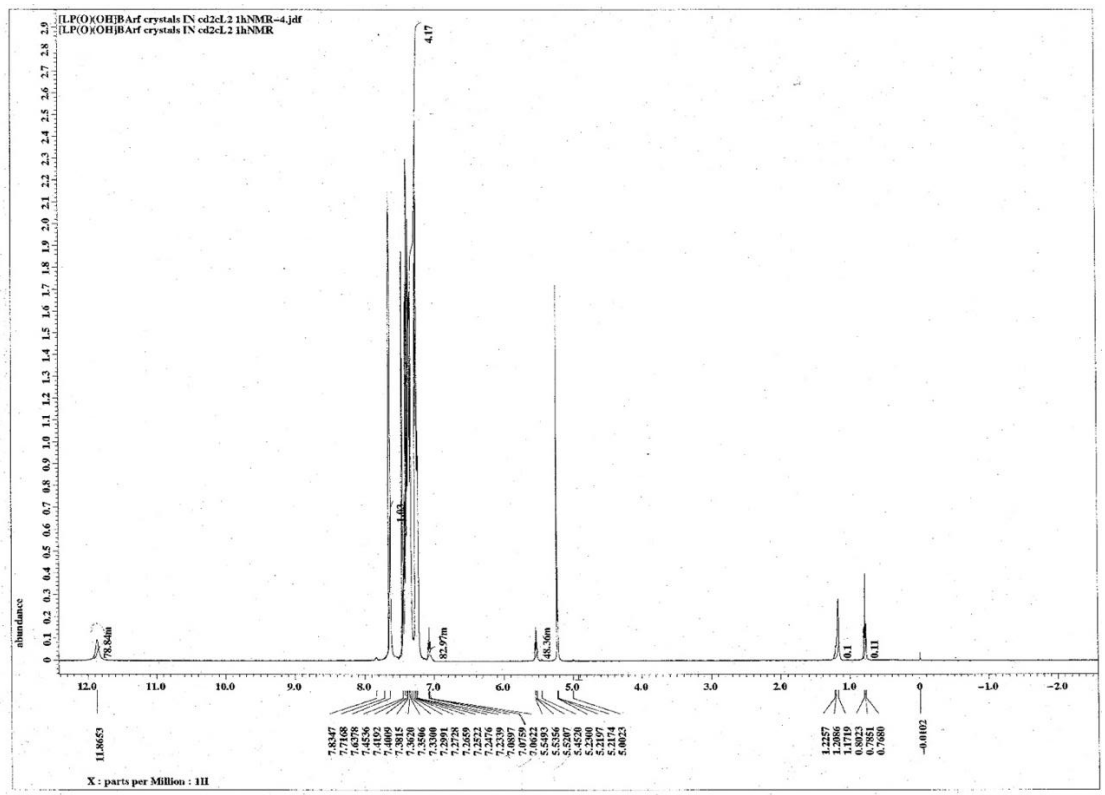

Figure 44. 1H NMR spectra of [15][BAr$^{F}_{4}$]$_2$

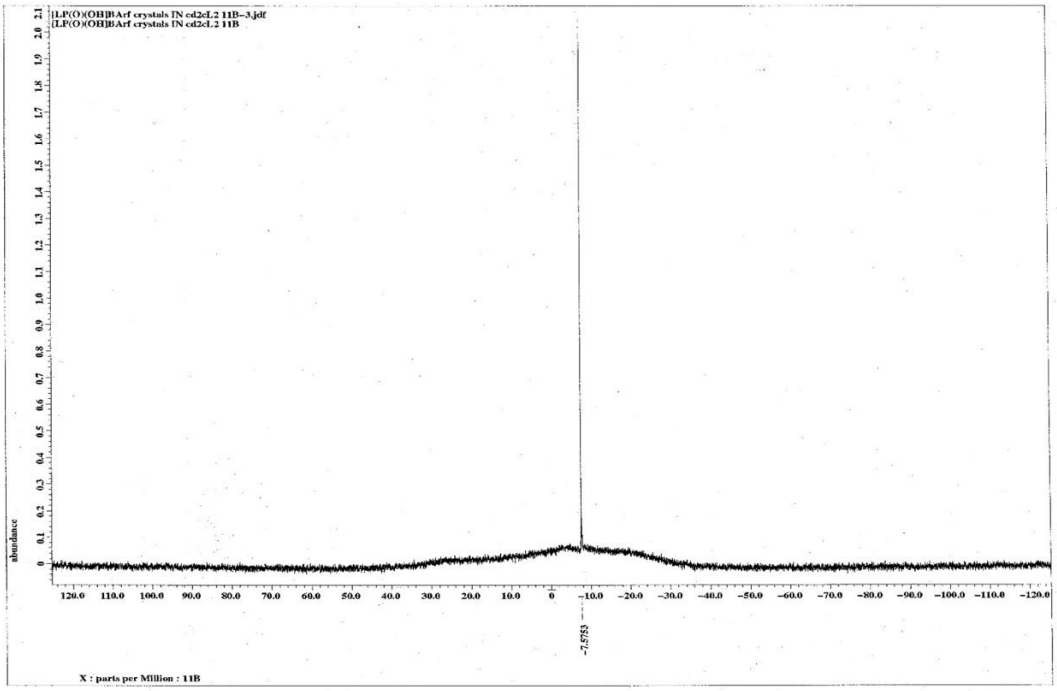

Figure 45. 13B NMR spectra of [15][BAr$^{F}_{4}$]$_2$

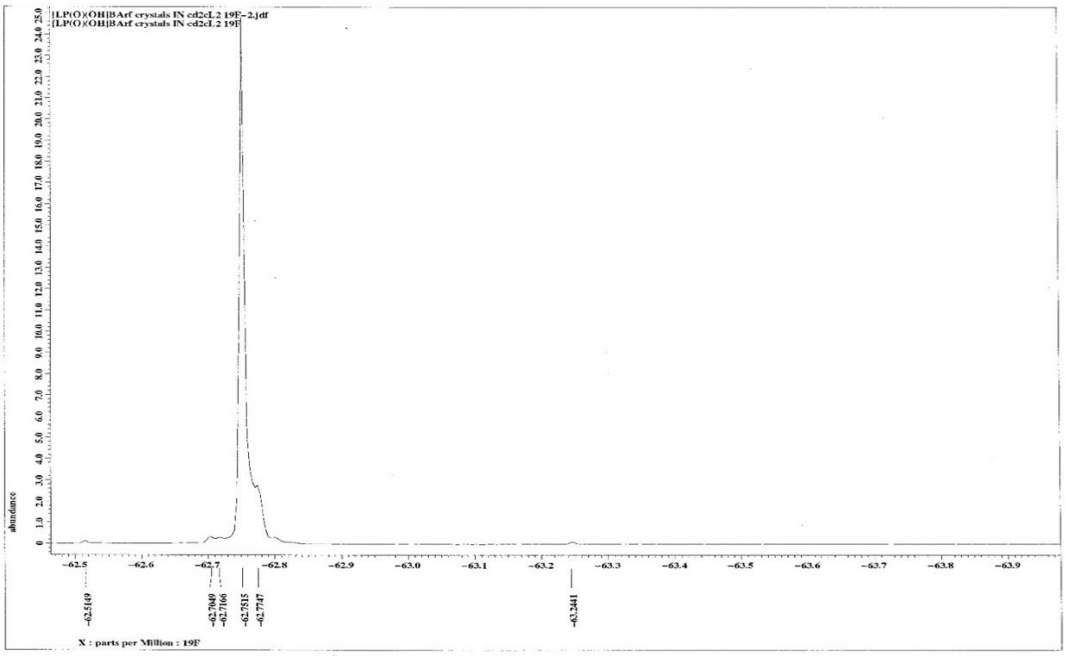

Figure 46. 19F NMR spectra of [15][BAr$^{F}_{4}$]$_2$

$(Ph_3P)_2CP(O)_2H$, 17:

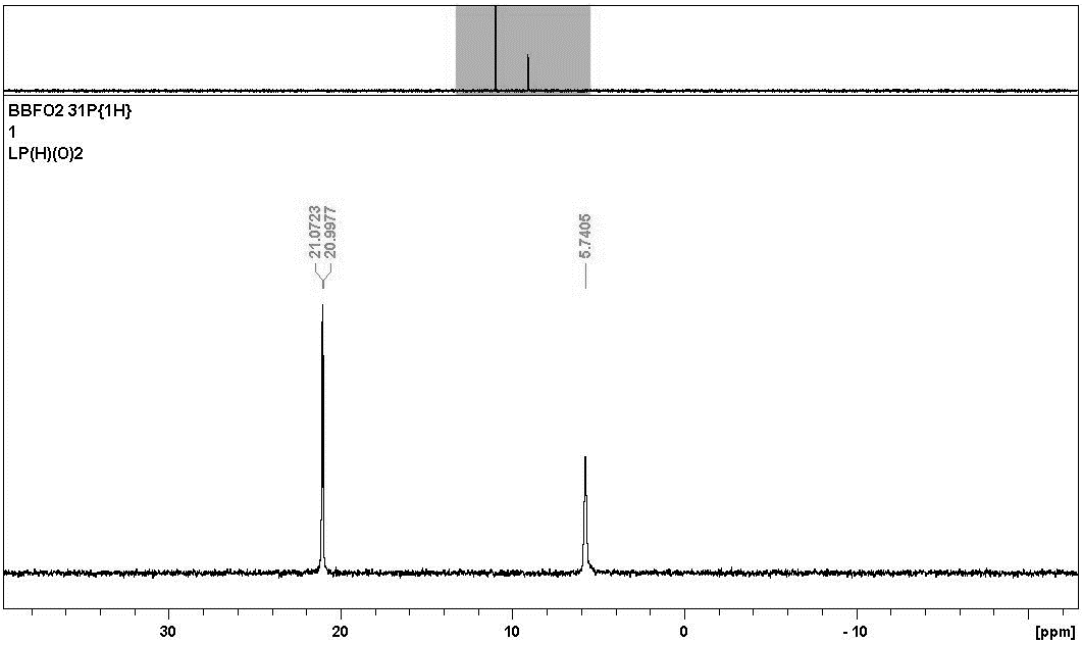

*Figure 47. 31P{1H} NMR spectra of **17***

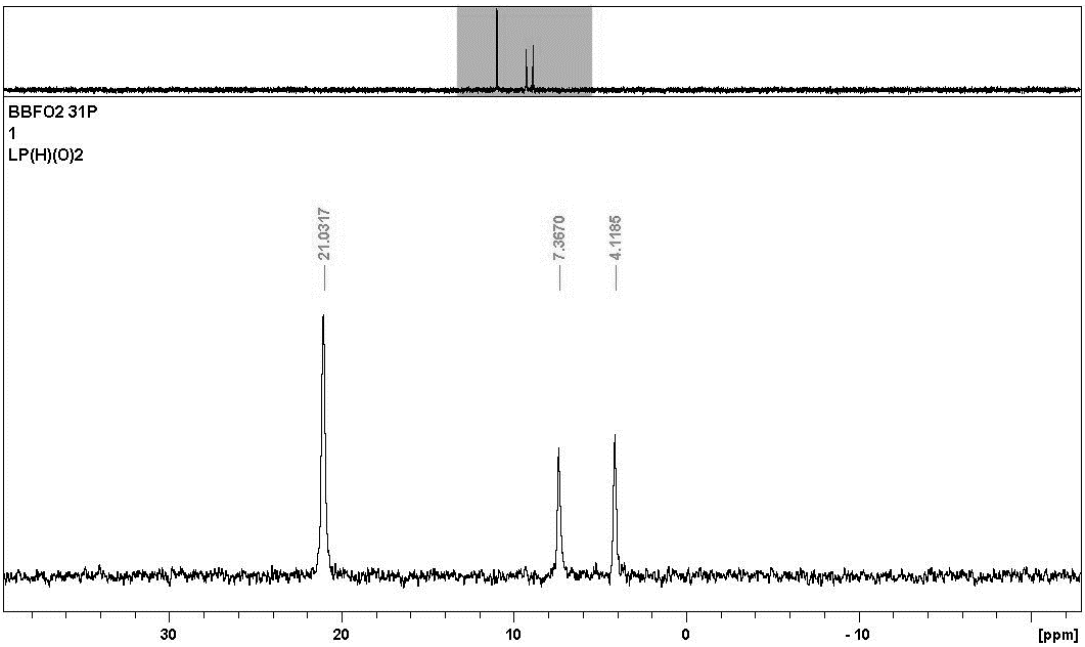

*Figure 48. 31P NMR spectra of **17***

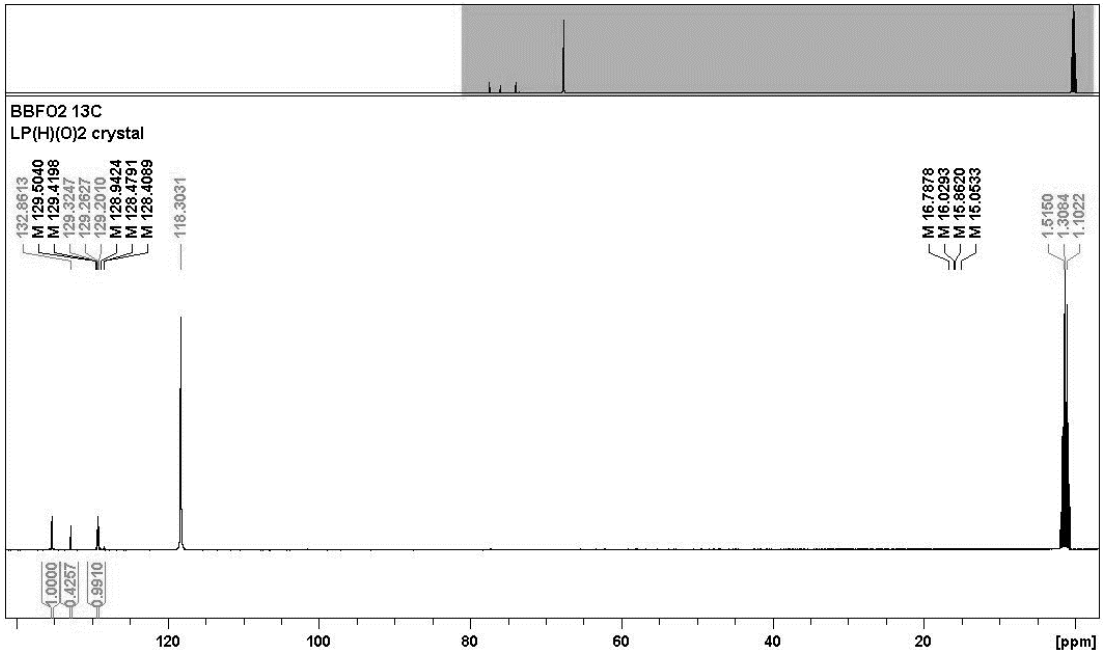

*Figure 49. 13C NMR spectra of **17***

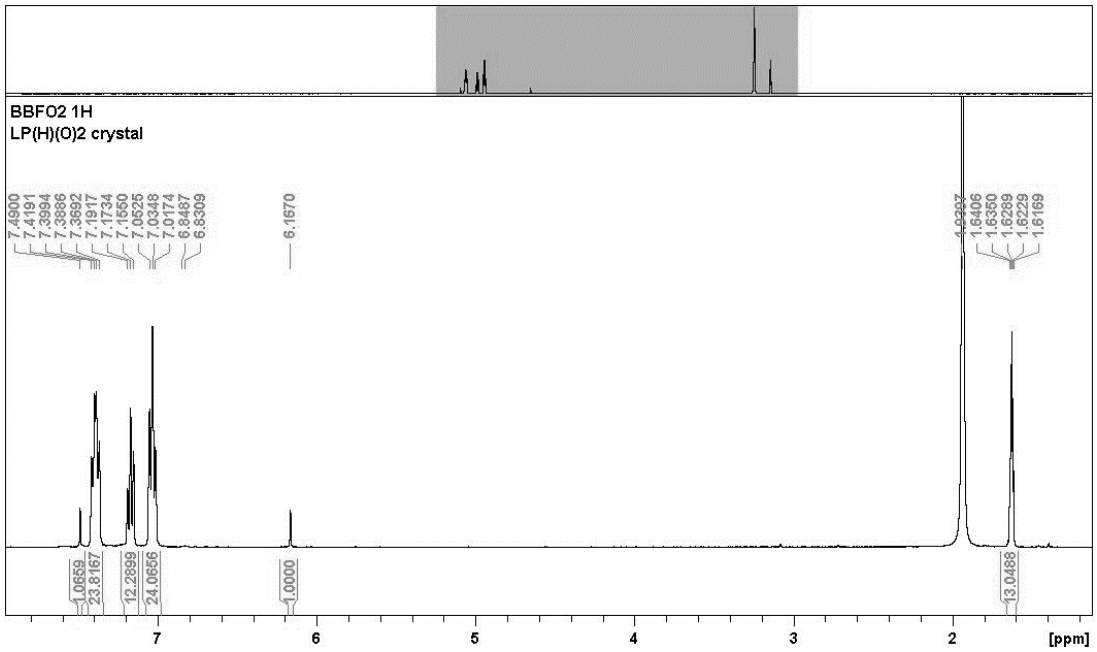

*Figure 50. 1H NMR spectra of **17***

Reaction of 17 with MeOTf:

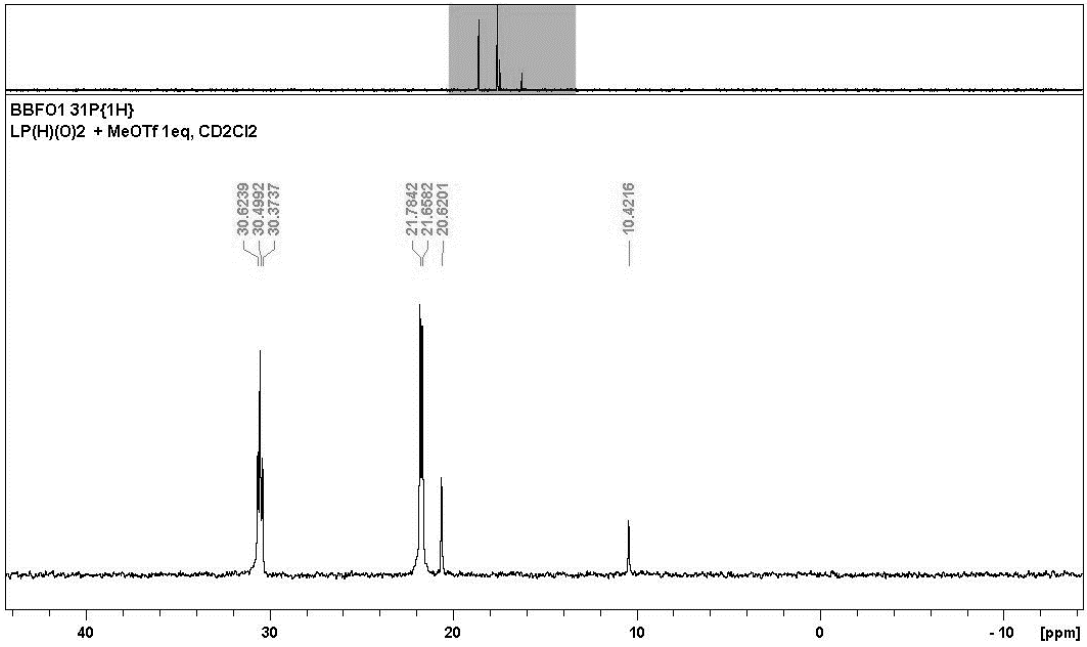

*Figure 51. 31P{1H} NMR spectra of the reaction between **17** and MeOTf*

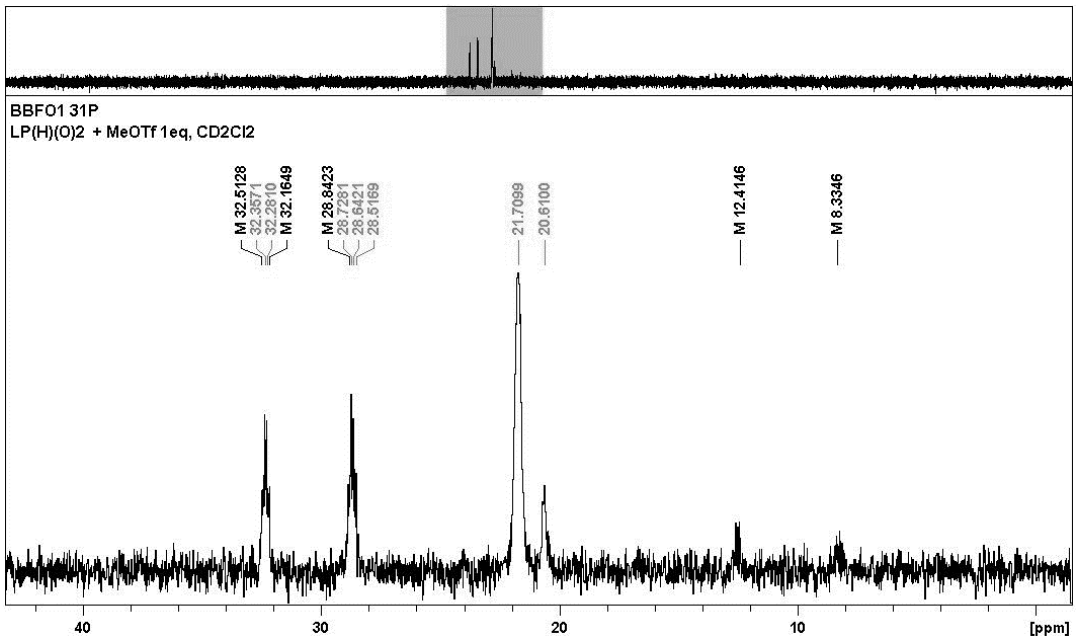

*Figure 52. 31P NMR spectra of the reaction between **17** and MeOTf*

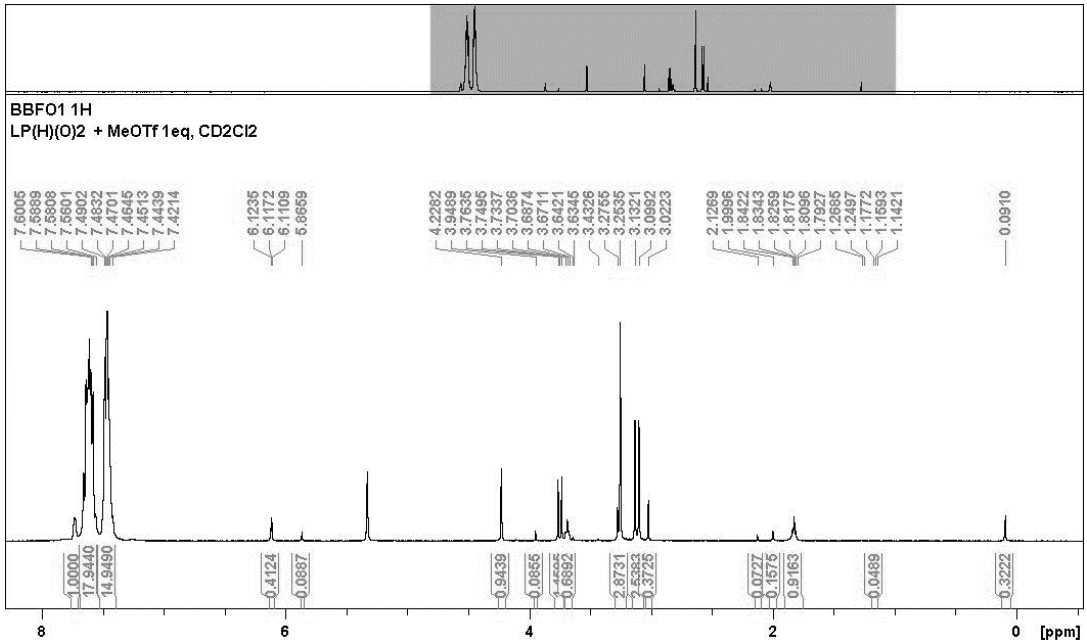

*Figure 53. 1H NMR spectra of the reaction between **17** and MeOTf*

Reactivity towards MeOH, $[HC(PPh_3)_2][P(O)_2(OCH_3)(H)]$

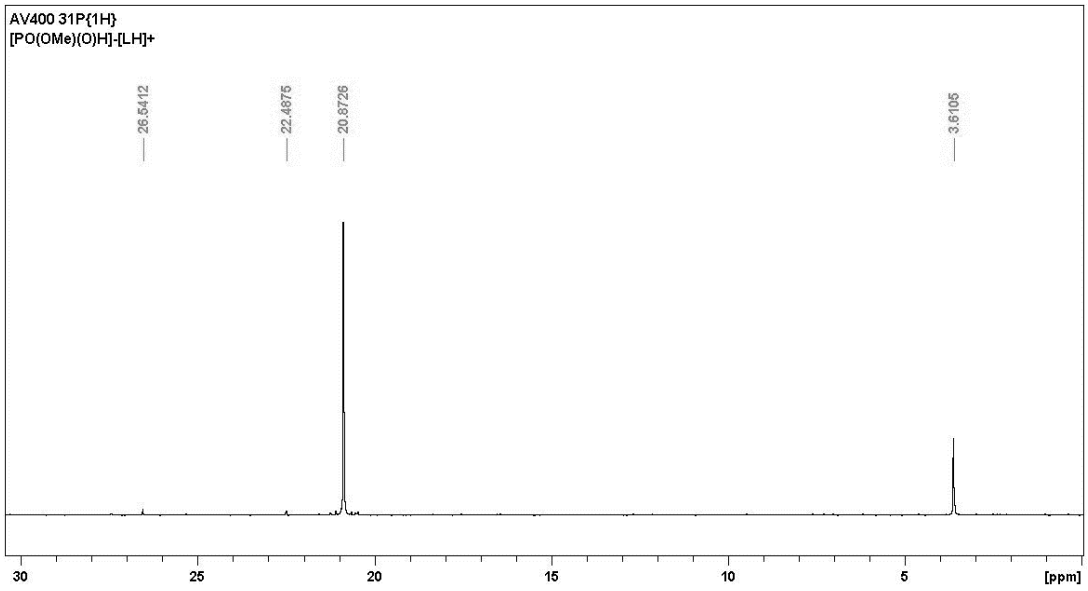

*Figure 54. 31P{1H} NMR spectra of **$[HC(PPh_3)_2][P(O)_2(OCH_3)(H)]$***

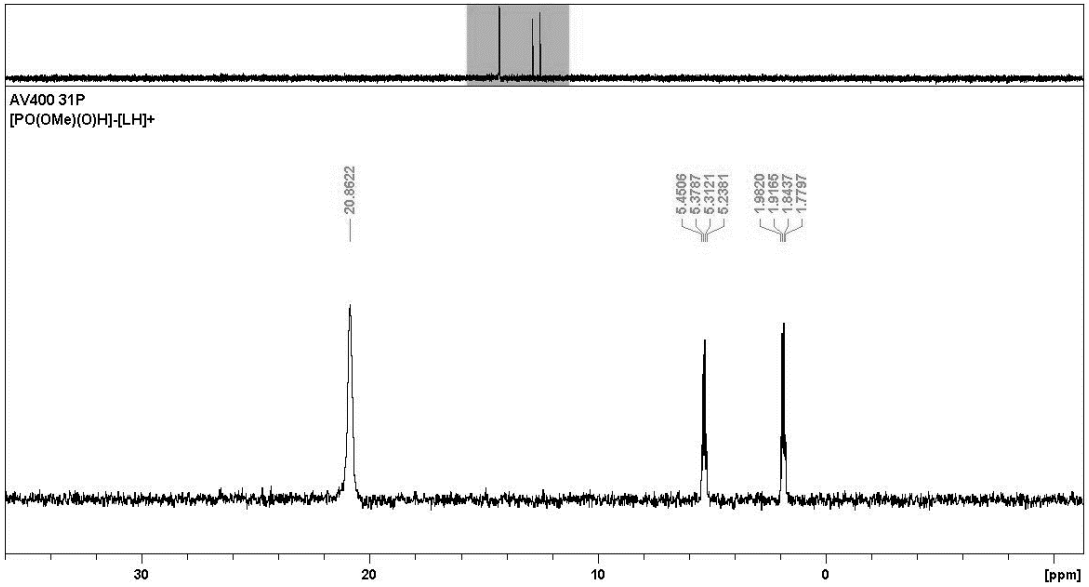

Figure 55. 31P NMR spectra of $[HC(PPh_3)_2][P(O)_2(OCH_3)(H)]$

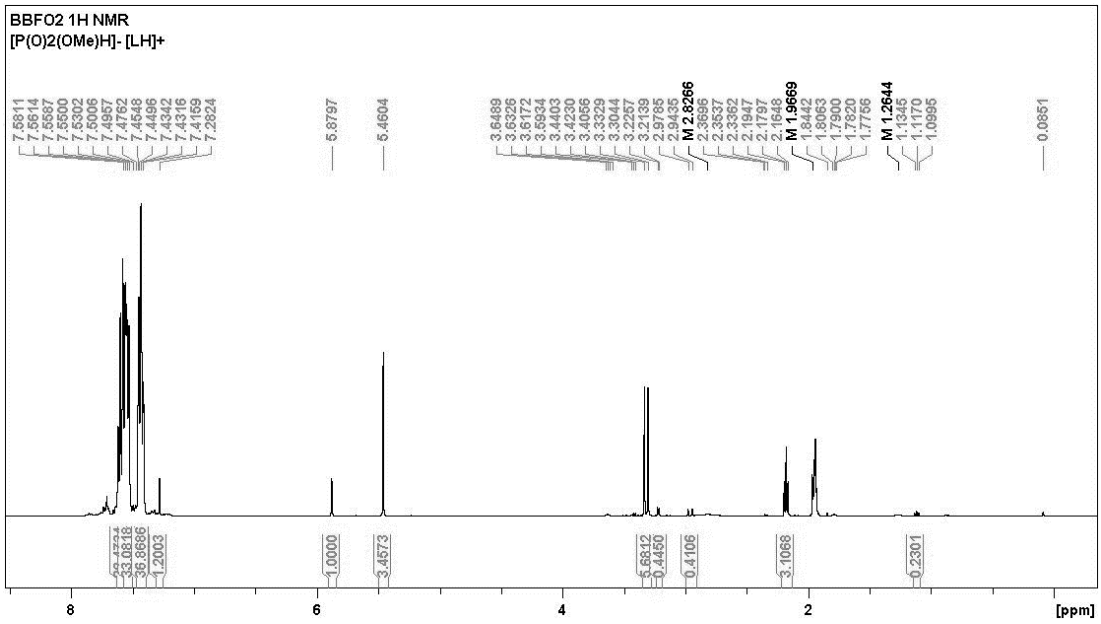

Figure 56. 1H NMR spectra of $[HC(PPh_3)_2][P(O)_2(OCH_3)(H)]$

Reactivity towards CD_3OD; synthesis of $[DC(PPh_3)_2][P(O)_2(OCD_3)(H)]$:

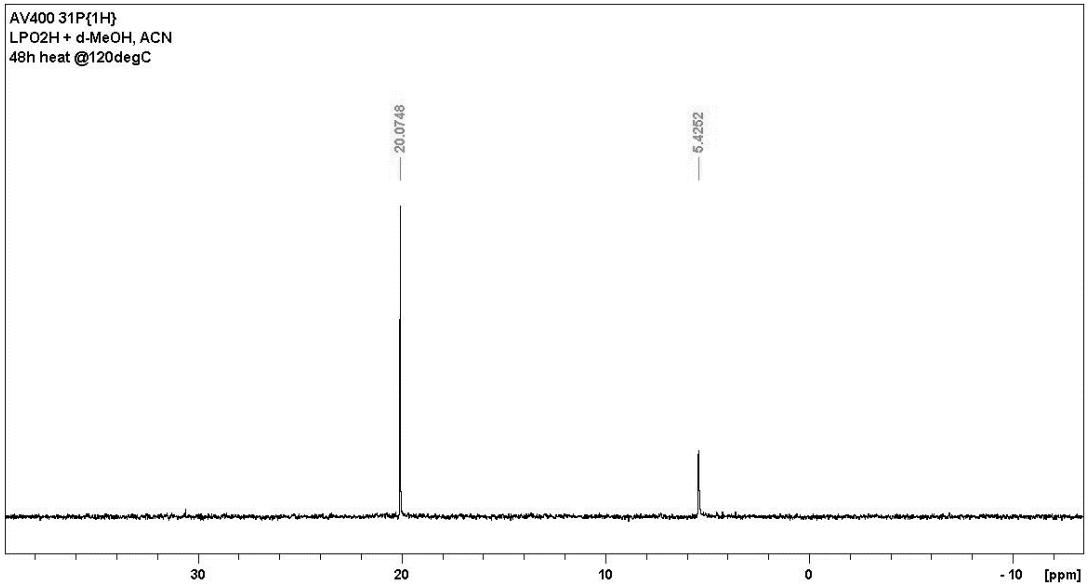

Figure 57. 31P{1H} NMR spectra of $[DC(PPh_3)_2][P(O)_2(OCD_3)(H)]$

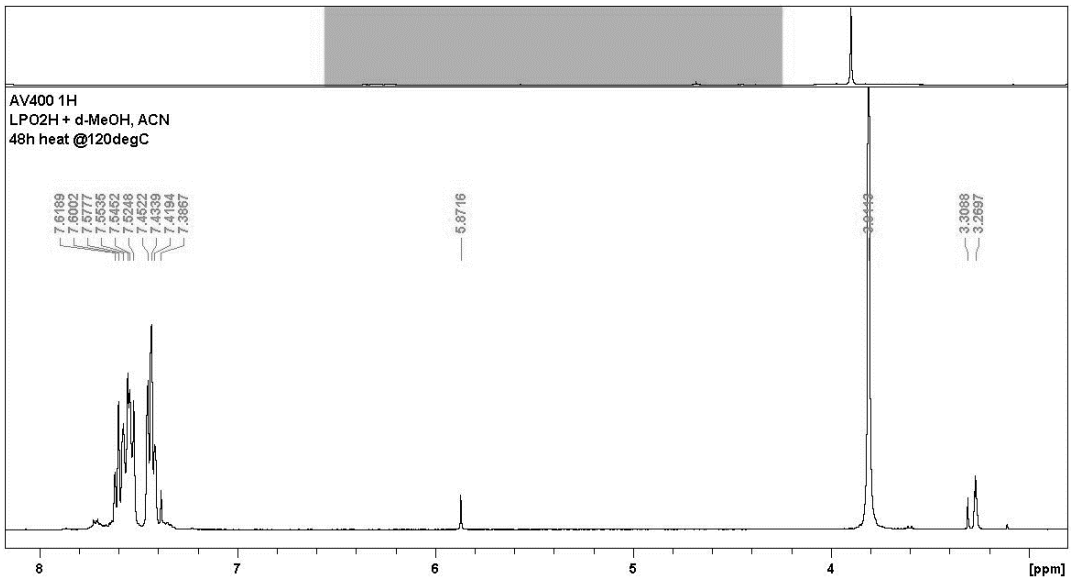

Figure 58. 1H NMR spectra of $[DC(PPh_3)_2][P(O)_2(OCD_3)(H)]$

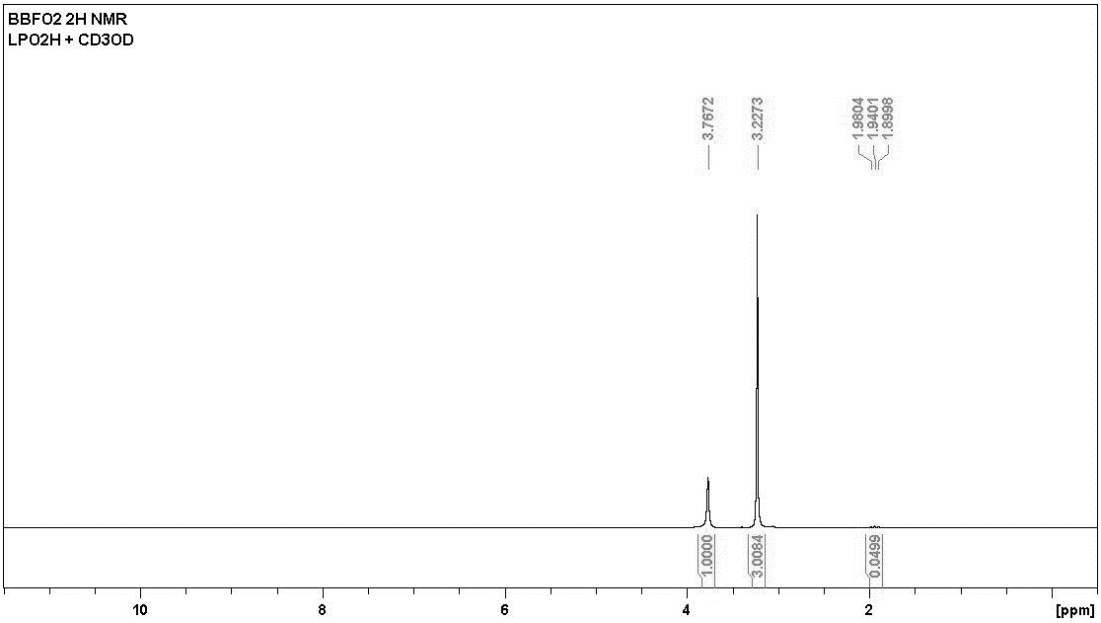

Figure 59. 2H NMR spectra of [DC(PPh3)2][P(O)2(OCD3)(H)]

Reaction between **[DC(PPh$_3$)$_2$][P(O)$_2$(OCD$_3$)(H)] and MeOTf:**

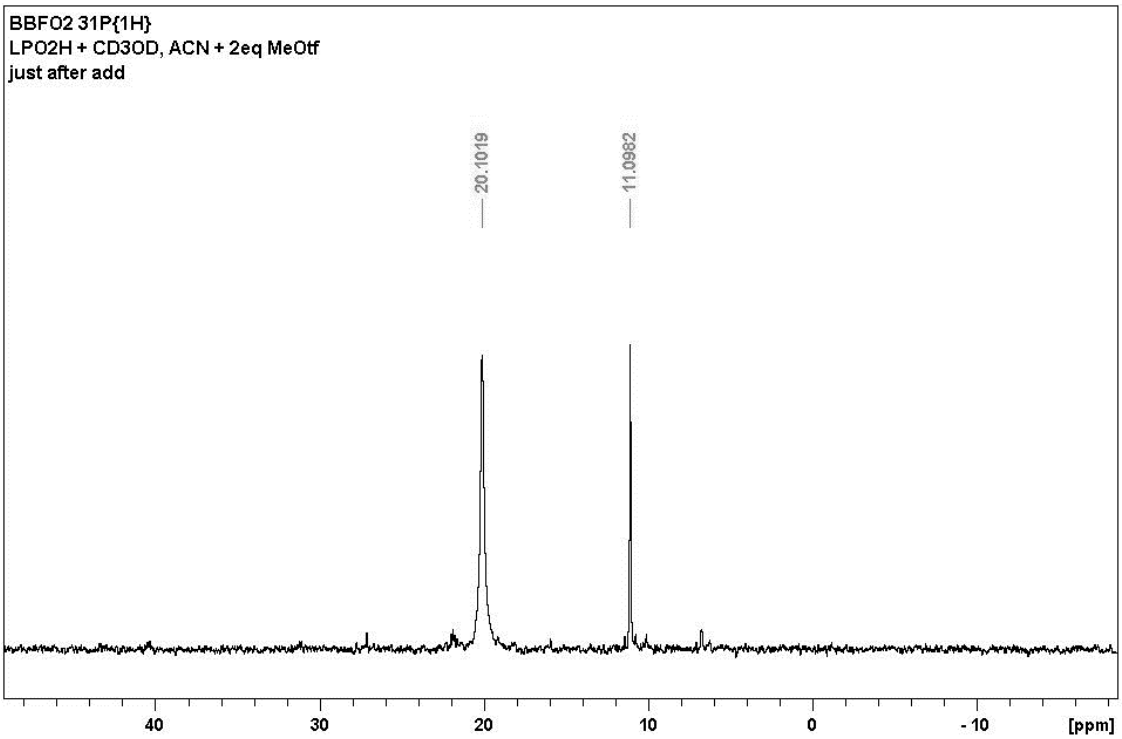

*Figure 60. 31P{1H} NMR spectra of the reaction between **[DC(PPh$_3$)$_2$][P(O)$_2$(OCD$_3$)(H)] and MeOTf:***

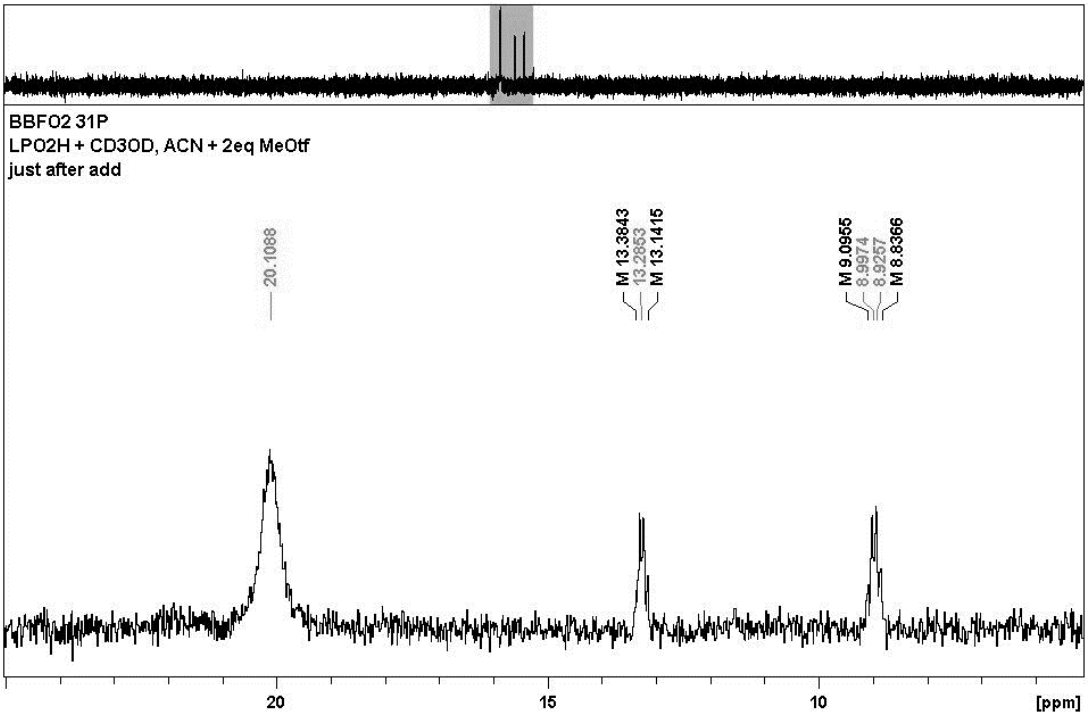

Figure 61. 31P NMR spectra of the reaction between ***$[DC(PPh_3)_2][P(O)_2(OCD_3)(H)]$ and MeOTf***

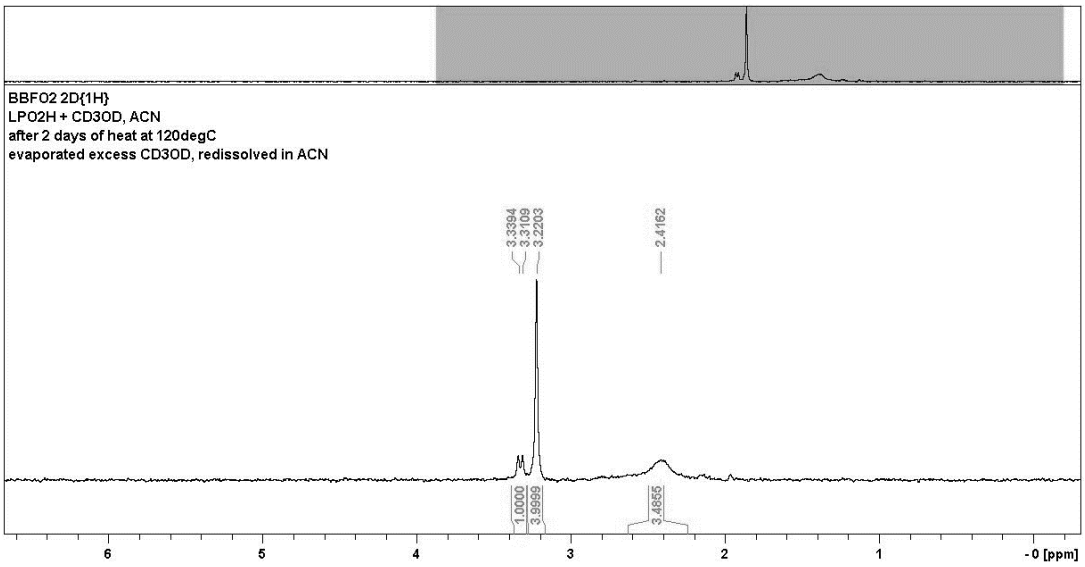

Figure 62. 2D{1H} NMR spectra of the reaction between ***$[DC(PPh_3)_2][P(O)_2(OCD_3)(H)]$ and MeOTf***

PhOH, [HC(PPh$_3$)$_2$][P(O)$_2$(OC$_6$H$_5$)(H)]:

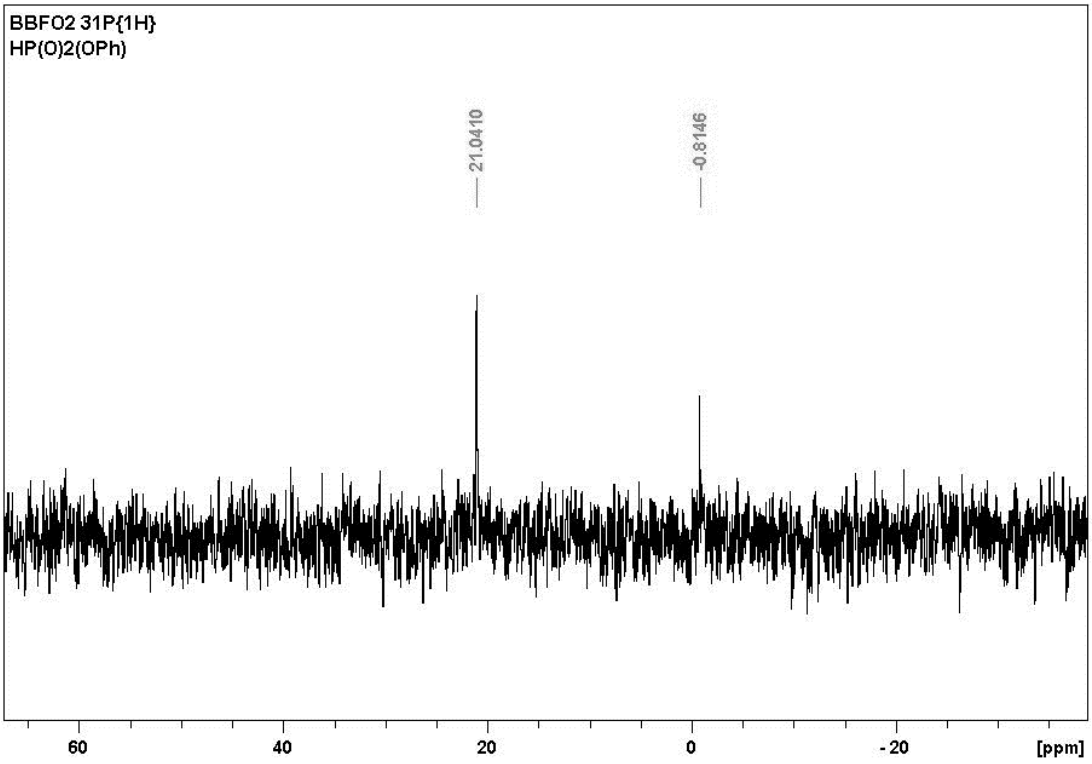

Figure 63. 31P{1H} NMR spectra of [HC(PPh$_3$)$_2$][P(O)$_2$(OC$_6$H$_5$)(H)]

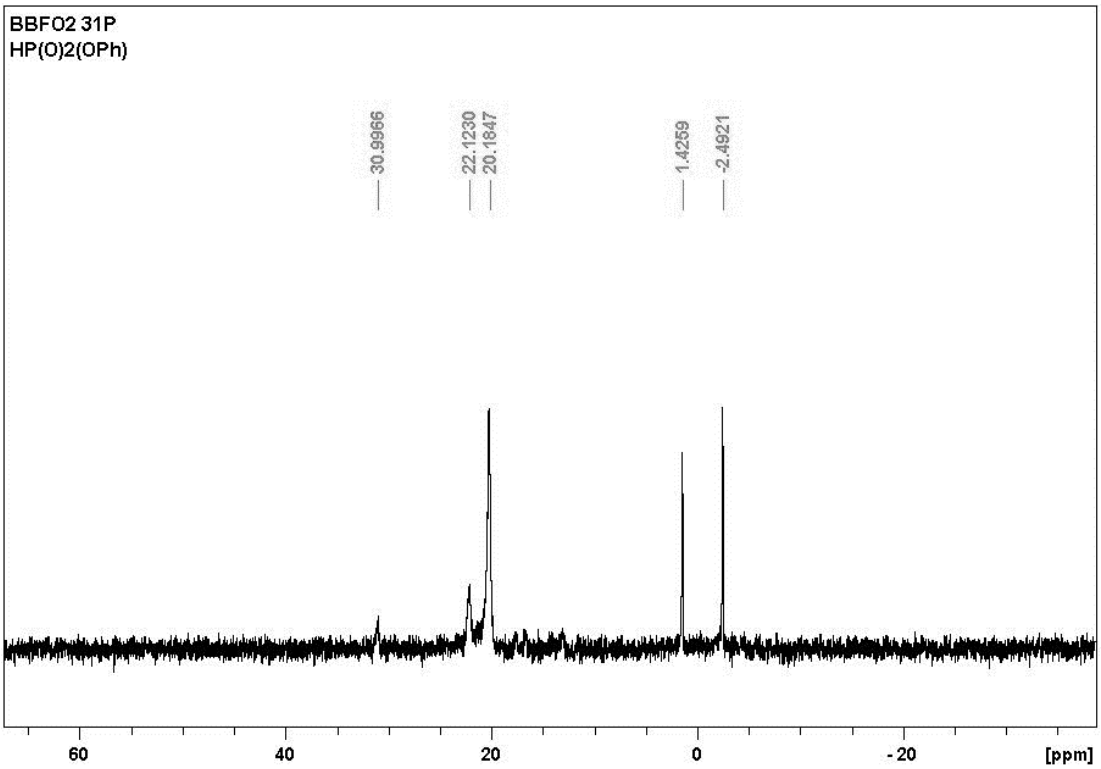

Figure 64. 31P{1H} NMR spectra of [HC(PPh$_3$)$_2$][P(O)$_2$(OC$_6$H$_5$)(H)]

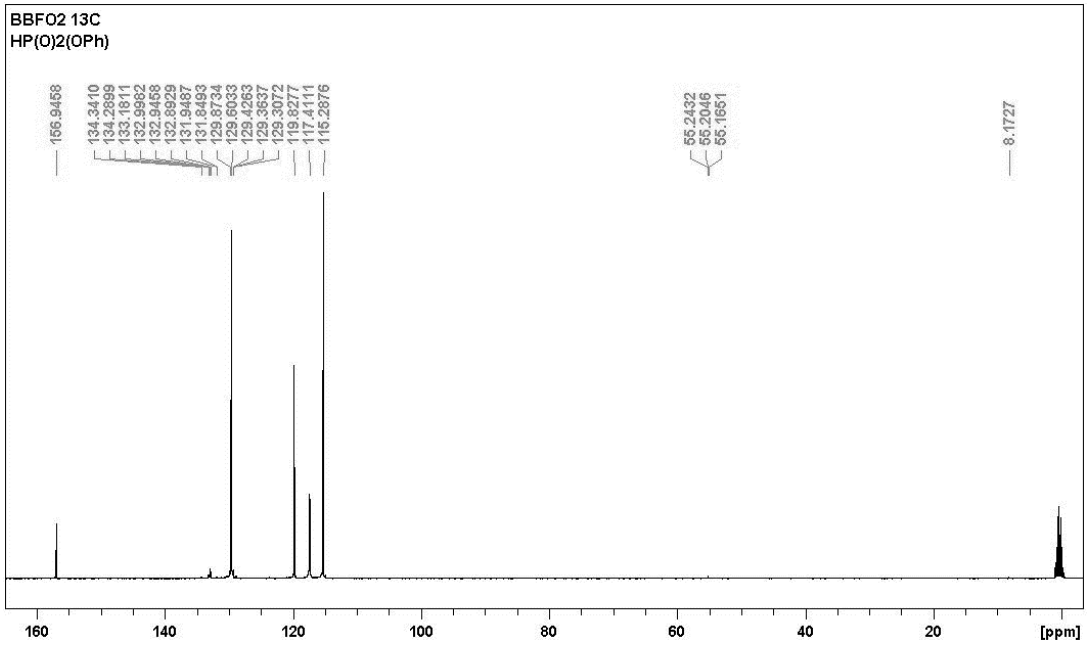

Figure 65. 13C NMR spectra of [HC(PPh3)2][P(O)2(OC6H5)(H)]

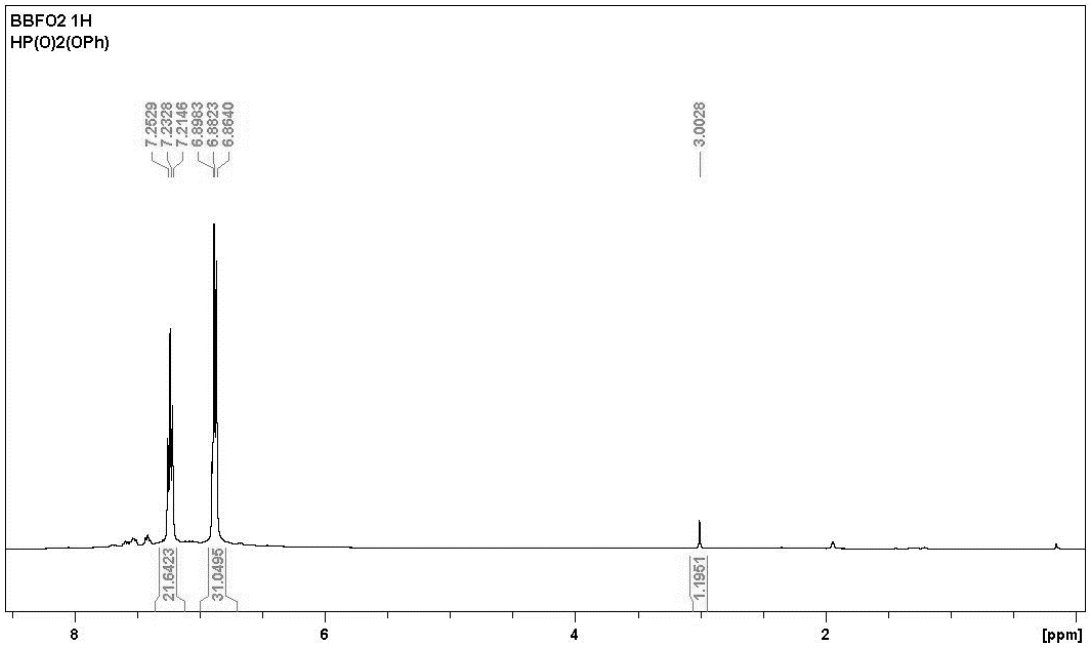

Figure 66. 31P{1H} NMR spectra of [HC(PPh3)2][P(O)2(OC6H5)(H)]

HC≡C(CH$_2$)$_2$CH$_2$OH, [HC(PPh$_3$)$_2$][P(O)$_2$(OCH$_2$(CH$_2$)$_2$CCH)(H)]

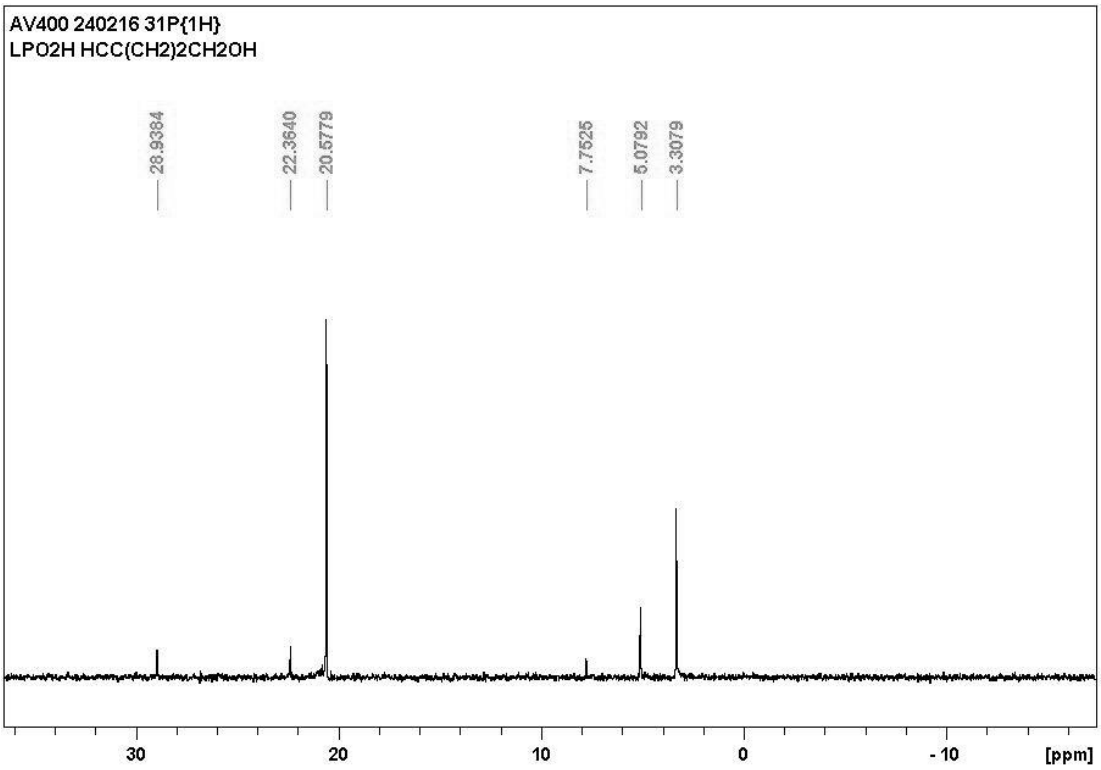

Figure 67. 31P{1H} NMR spectra of [HC(PPh$_3$)$_2$][P(O)$_2$(OCH$_2$(CH$_2$)$_2$CCH)(H)]

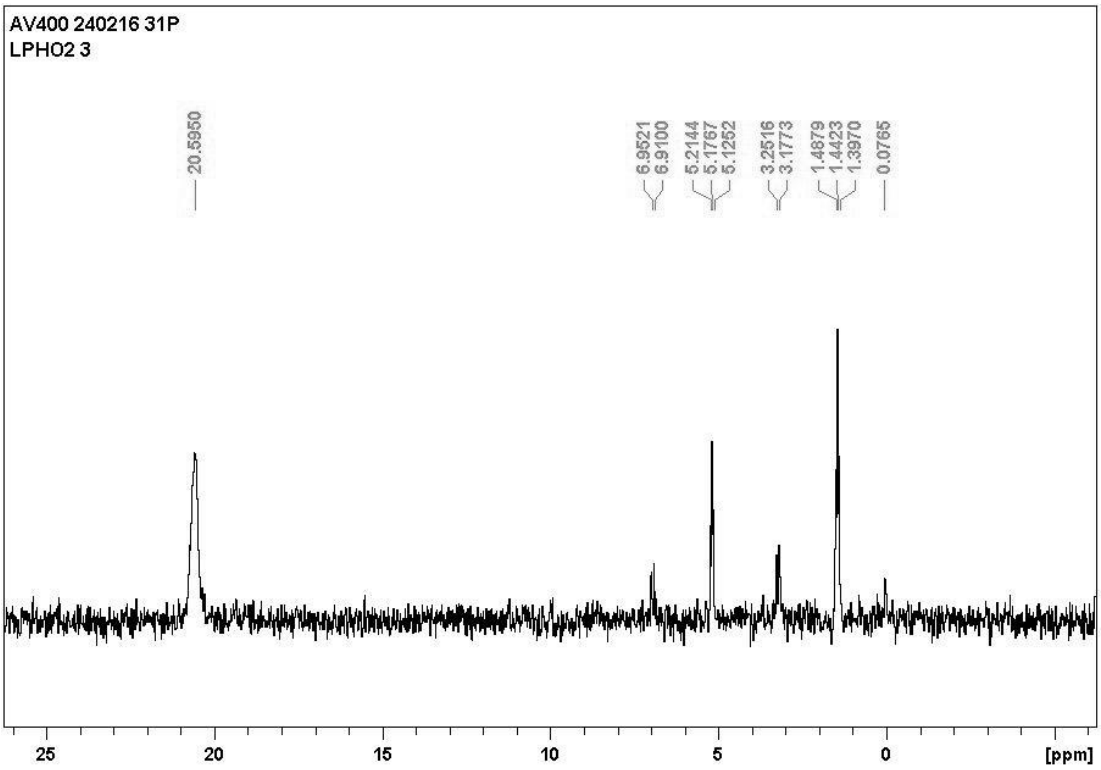

Figure 68. 31P NMR spectra of [HC(PPh$_3$)$_2$][P(O)$_2$(OCH$_2$(CH$_2$)$_2$CCH)(H)]

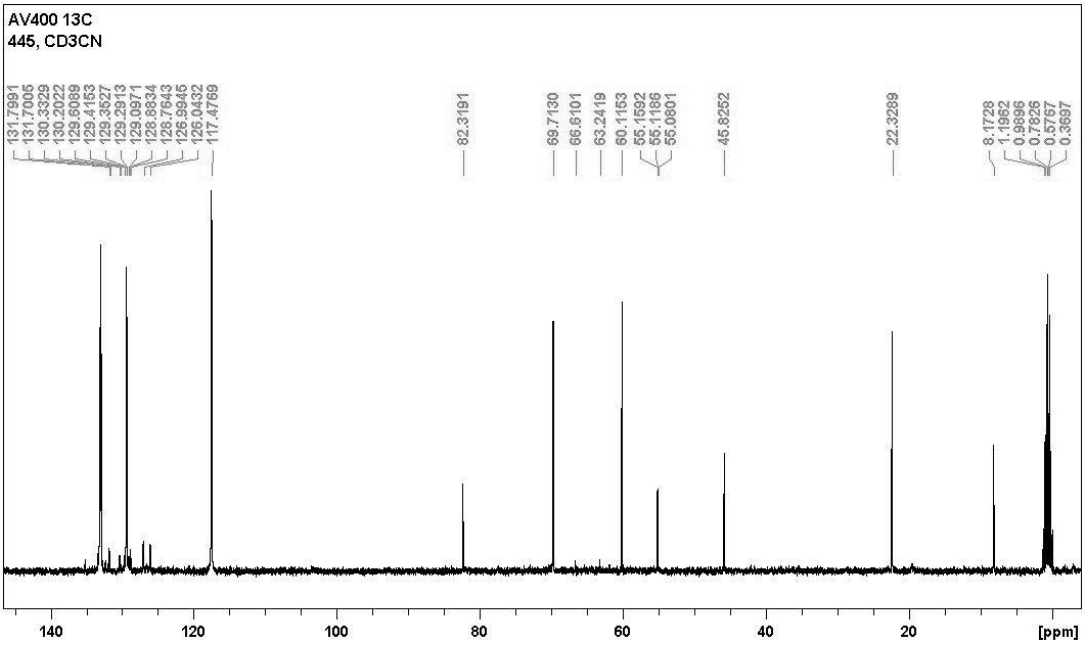

Figure 69. 1H NMR spectra of [HC(PPh$_3$)$_2$][P(O)$_2$(OCH$_2$(CH$_2$)$_2$CCH)(H)]

Computational Methods

All calculations for the **chapter II** were carried out with the Gaussian09 package,[217] and all structures were optimized at the DFT level by means of the B3PW91 functional in conjunction with the 6-31G(d) basis set.[218] Geometry optimizations were performed without constraints, except for **3g$_p$**$^{2+}$, **3g$_C$**$^{2+}$, and **3g$_N$**$^{2+}$, for which the P–C–P–N and C–P–N–H dihedral angles were fixed at 0 and 0° (**3g$_p$**$^{2+}$), ±90 and 0° (**3g$_C$**$^{2+}$), and 0 and ±90° (**3g$_N$**$^{2+}$). Final energy calculations at the B3PW91 level associated with the 6-311+G(d,p) basis set have been achieved on the B3PW91/6-31G(d) geometries. To get accurate geometries, the SCF convergence criterion was systematically tightened to 10^{-8} au, and the force minimizations were carried out until the rms force became smaller than (at least) 1×10^{-5} au. Electronic structures obtained at the B3PW91/6-311+G(d,p)//B3PW91/6-31G(d) level were explored by means of natural bond order (NBO) analysis[219] using the NBO6 program. NBO analysis gives the atomic charges through natural population analysis (NPA). The π-electron population is obtained from the occupancy of the $p_\pi$natural atomic orbitals. It was also used to interpret the wave function of the systems in terms of natural localized bond orbitals, to study bond polarization and to evaluate the relative contribution of the C═P–N and C–P═N resonance structures by means of natural resonance theory (NRT).[219] Second-order perturbation theory was used to estimate the second-order interaction energy (*E*(2)) associated with two-electron donor–acceptor orbital interactions.

Cartesian coordinates and energies of the optimized geometries at the DFT level

3c^{2+}

E(B3PW91/6-311+G(d,p)//B3PW91/6-31G(d)) = -2743.046842 u.a.

P	0.000000	0.000000	0.000000	H	5.997336	0.167250	0.342072
N	0.000000	0.000000	1.647285	C	4.332580	-0.870037	-1.663855
C	1.526148	0.000000	-0.846027	C	5.009533	0.110581	-2.408268
C	-1.411452	-0.097089	2.211070	C	5.928062	-0.268512	-3.382512
C	1.070186	0.142242	2.670353	C	6.186334	-1.619539	-3.615031
P	3.212610	-0.383641	-0.314005	C	5.520800	-2.595395	-2.874246
P	1.174862	0.194420	-2.628110	C	4.597023	-2.227788	-1.900233
H	-1.265522	-0.025491	3.290443	H	4.841319	1.165292	-2.220200
C	-2.290948	1.077524	1.785335	H	6.456259	0.494465	-3.946956
H	-1.806387	2.035953	1.995707	H	6.917620	-1.910735	-4.363819
H	-2.544564	1.037412	0.720862	H	5.730542	-3.647420	-3.042790
H	-3.229284	1.044883	2.348469	H	4.102531	-2.998004	-1.318454
C	-2.046077	-1.452837	1.911577	C	1.955797	1.655692	-3.364688
H	-1.396387	-2.276379	2.223058	C	2.643461	2.601649	-2.597856
H	-2.991036	-1.542759	2.457032	C	3.132032	3.763336	-3.194346
H	-2.269270	-1.563656	0.844254	C	2.930346	3.989169	-4.554169
H	2.010547	0.178403	2.118675	C	2.222142	3.060417	-5.318931
C	0.920383	1.459412	3.437609	C	1.723923	1.903073	-4.729737
H	0.843791	2.318387	2.764581	H	2.789639	2.446701	-1.534707
H	1.800093	1.601143	4.073425	H	3.662521	4.494823	-2.591659
H	0.044771	1.460430	4.094086	H	3.309689	4.895594	-5.017038
C	1.124886	-1.059021	3.613754	H	2.044536	3.243918	-6.374476
H	1.227959	-1.997459	3.064345	H	1.141153	1.208918	-5.329302
H	0.240583	-1.123437	4.255051	C	1.632983	-1.314889	-3.524288
H	1.991402	-0.950665	4.273237	C	2.465691	-1.288282	-4.649404
C	3.156679	-1.801510	0.823568	C	2.723726	-2.466048	-5.348140
C	2.274735	-2.863214	0.572658	C	2.159960	-3.670380	-4.932129
C	2.340276	-4.021973	1.343901	C	1.342265	-3.705215	-3.801578
C	3.278960	-4.127411	2.370400	C	1.081436	-2.534545	-3.096360
C	4.148887	-3.069007	2.630553	H	2.924594	-0.361336	-4.975064
C	4.093673	-1.908797	1.861462	H	3.367007	-2.438702	-6.222660
H	1.550860	-2.796043	-0.233081	H	2.356923	-4.583284	-5.486828
H	1.659182	-4.843533	1.141078	H	0.901677	-4.642749	-3.474776
H	3.330614	-5.032768	2.968237	H	0.433106	-2.570404	-2.224056
H	4.875685	-3.144912	3.433995	C	-0.601779	0.503099	-2.895034
H	4.775124	-1.092709	2.079921	C	-1.463524	-0.474009	-3.408886
C	4.013075	1.035190	0.493356	C	-2.803793	-0.164678	-3.635522
C	3.276334	2.148036	0.920628	C	-3.288830	1.110430	-3.354305
C	3.916898	3.210818	1.553601	C	-2.429092	2.091544	-2.855906
C	5.294067	3.168571	1.768492	C	-1.089462	1.796231	-2.633137
C	6.035052	2.067327	1.338956	H	-1.099702	-1.464970	-3.656441

C	5.403851	1.005325	0.696698	H	-3.465249	-0.922517	-4.044916
H	2.205281	2.193671	0.744430	H	-4.332927	1.346883	-3.538191
H	3.340749	4.073550	1.875153	H	-2.799632	3.092798	-2.656466
H	5.792029	3.997814	2.262596	H	-0.423647	2.575356	-2.271623
H	7.109457	2.037532	1.494575				

3g^{2+}

E(B3PW91/6-311+G(d,p)//B3PW91/6-31G(d)) = -1120.952071 u.a.

C	1.596045	0.031412	-0.494315	H	4.188412	0.182337	0.023433
P	2.974025	-0.221863	0.599597	H	2.816931	0.547821	1.761203
P	-0.059323	0.391401	-0.086378	H	3.160266	-1.550316	1.021417
N	-0.239356	0.347346	1.532026	H	2.838186	0.820514	-2.724689
P	1.845566	-0.057369	-2.258883	H	2.191999	-1.333084	-2.733733
H	-1.165840	0.593542	1.886670	H	0.643103	0.298935	-2.886424
H	0.397268	0.079325	2.278608				

3g$_P$$^{2+}$

E(B3PW91/6-311+G(d,p)//B3PW91/6-31G(d)) = -1120.949064 u.a.

C	1.567586	0.000000	-0.513228	H	4.181577	0.000000	-0.111718
P	2.964249	0.000000	0.583841	H	2.994000	1.122669	1.428584
P	-0.120273	0.000000	-0.083001	H	2.994000	-1.122669	1.428584
N	-0.258062	0.000000	1.540845	H	3.193481	0.000000	-2.570380
P	1.821660	0.000000	-2.285646	H	1.285080	-1.125856	-2.930596
H	-1.210902	0.000000	1.910780	H	1.285080	1.125856	-2.930596
H	0.439804	0.000000	2.281067				

3g$_N$$^{2+}$

E(B3PW91/6-311+G(d,p)//B3PW91/6-31G(d)) = -1120.923631 u.a.

C	0.297532	0.005423	0.000000	H	0.792158	2.604679	0.000000
P	-0.287089	1.708956	0.000000	H	-1.053139	2.007891	-1.134457
P	-0.830245	-1.301408	0.000000	H	-1.053140	2.007896	1.134455
N	-2.326352	-0.543241	0.000000	H	2.733686	0.025215	1.130100
P	2.042240	-0.439080	0.000000	H	2.109508	-1.840129	-0.000003
H	-2.818536	-0.293825	0.855822	H	2.733684	0.025220	-1.130099
H	-2.818548	-0.293819	-0.855814				

3g$_C$$^{2+}$

E(B3PW91/6-311+G(d,p)//B3PW91/6-31G(d)) = -1120.923758 u.a.

C	-0.274381	-0.000001	-0.157548	H	-2.436071	-1.466630	-0.380508
P	-1.110630	-1.524716	0.080897	H	-0.472594	-2.535383	-0.654802
P	1.454054	-0.000008	-0.650410	H	-1.198024	-2.028960	1.392729

N 2.301399 -0.000013 0.738370
P -1.110606 1.524728 0.080897
H 3.328107 -0.000017 0.699080
H 1.929385 -0.000012 1.692034
H -2.436041 1.466675 -0.380529
H -1.198009 2.028964 1.392731
H -0.472537 2.535388 -0.654783

$(PH_3)_2C=PH^{2+}$
E(B3PW91/6-311+G(d,p)//B3PW91/6-31G(d)) = -1065.542903 u.a.
C -0.009245 0.116669 -0.000004
P -1.650829 -0.648551 0.000000
P 0.300401 1.800052 0.000001
P 1.469778 -0.934897 0.000000
H -1.863375 -1.456735 1.129787
H -2.620332 0.361923 0.000003
H -1.863384 -1.456735 -1.129785
H 1.536192 -1.765449 1.130777
H 1.536189 -1.765481 -1.130754
H 2.594946 -0.098213 -0.000013
H -1.055022 2.231624 -0.000004

$H_2N=PH^{+}$
E(B3PW91/6-311+G(d,p)//B3PW91/6-31G(d)) = -397.577723 u.a.
P -0.616040 -0.099303 0.000000
N 0.996406 0.017963-0.000002
H 1.573852 -0.825815 0.000005
H 1.537808 0.884762 0.000004
H -0.845907 1.304859 0.000001

$H_2C=P-NH_2$
E(B3PW91/6-311+G(d,p)//B3PW91/6-31G(d)) = -436.565476 u.a.

H 1.718690 -0.130478 -0.591182
C 2.570368 -0.018237 0.077496
H 2.348470 -0.010113 1.141119
P 4.159833 0.169988 -0.366222
N 4.182288 0.196818 -2.060341
H 5.071926 0.066873 -2.519502
H 3.386914 -0.074851 -2.624435

H_3C-PH_2
E(B3PW91/6-311+G(d,p)//B3PW91/6-31G(d)) = -382.435027 u.a.
C -1.192619 -0.000001 0.025045
H -1.588742 -0.882333 -0.487332
H -1.588730 0.882343 -0.487321
H -1.551941 -0.000003 1.057329
P 0.668424 -0.000001 -0.124711
H 0.929374 1.034654 0.818852
H 0.929386 -1.034642 0.818864

$H_2C=PH$
E(B3PW91/6-311+G(d,p)//B3PW91/6-31G(d)) = -381.191777 u.a.
C 1.074635 0.025138 0.000001

H 1.676607 -0.882039 0.000002
H 1.637086 0.956043 -0.000006
P -0.591745 -0.101605 -0.000001
H -0.885320 1.299237 0.000006

H_2N-PH_2
E(B3PW91/6-311+G(d,p)//B3PW91/6-31G(d)) = -398.478438 u.a.
P -0.599772 -0.123638 -0.027690
H -0.948296 1.035859 -0.774549
N 1.110761 0.043599 -0.078781
H 1.544117 0.841249 0.370682
H 1.601621 -0.809957 0.153082
H -0.976198 0.482234 1.217600

HN=PH
E(B3PW91/6-311+G(d,p)//B3PW91/6-31G(d)) = -397.231241 u.a.
P 0.521221 -0.123029 0.000000
H 1.009006 1.228848 0.000003
N -1.038446 0.187652 -0.000001
H -1.558194 -0.696977 0.000005

All computational studies for **Section III** were performed with the Gaussian program package[S6] by employing the B3LYP functional in conjunction with the 6-31G(d) basis set. Absence of imaginary frequencies confirmed that the oxophosphonium dication with the O-py ligand removed (**7a**$^{2+}$), oxophosphonium dication (**7**$^{2+}$) and inserted product **8**$^{2+}$ represent minima on the potential energy surface, while TS with a single imaginary frequency is a first order saddle point. Intrinsic reaction coordinate calculations confirmed that this transition state connects minima that correspond to **7**$^{2+}$ and **8**$^{2+}$ structures.

Coordinates (Å) for the optimized structure for **7**$^{2+}$.

6	-1.262263	-4.047963	-0.4835656	-1.597164	2.060118	1.390031
6	-1.243738	-2.733460	-0.9741116	-1.318418	1.528277	2.661330
6	-1.162145	-2.525519	-2.3611506	-2.102499	1.877275	3.760232
6	-1.149213	-3.607132	-3.2404716	-3.172766	2.761522	3.603921
6	-1.189654	-4.911769	-2.7449786	-3.461024	3.285248	2.342859
6	-1.232394	-5.127288	-1.3672746	-2.682328	2.936762	1.238528
15	-1.444941	-1.312360	0.166759 6	2.092163	0.340849	-2.647171
6	-3.144881	-0.667554	-0.1233866	3.393010	1.142290	-2.795718
6	-3.895530	-0.155755	0.950662 6	1.552328	-0.096615	-4.017005
6	-5.215506	0.249619	0.759897 6	4.351661	-2.171348	-1.215280

6	-5.808087	0.152656	-0.499553	1	2.889772	-1.936460	2.137526
6	-5.075174	-0.360713	-1.570248	1	5.158842	-2.468271	3.135793
6	-3.757252	-0.774654	-1.385015	1	7.035488	-0.837807	2.785469
6	-0.139555	-0.080550	-0.113791	1	6.584979	1.262136	1.482009
15	-0.469372	1.678291	-0.002001	1	4.243995	1.649960	0.596323
6	-1.181706	2.395820	-1.528259	1	-0.501356	0.829518	2.795218
6	-1.533390	1.582564	-2.611436	1	-1.877819	1.457137	4.735984
6	-2.071919	2.140353	-3.772318	1	-3.780424	3.037358	4.460567
6	-2.265423	3.518612	-3.859777	1	-4.297801	3.964782	2.212572
6	-1.909433	4.342164	-2.787462	1	-2.939807	3.336446	0.265538
6	-1.365526	3.789711	-1.630014	1	-1.372716	0.514198	-2.548950
15	1.444845	-0.887930	-0.250917	1	-2.338052	1.498292	-4.606610
7	2.242993	-0.803945	-1.702912	1	-2.685232	3.953543	-4.761780
6	3.173032	-1.913143	-2.157876	1	-2.048962	5.416776	-2.854881
6	2.436709	-3.208495	-2.507879	1	-1.075654	4.446630	-0.815719
8	2.303274	0.192502	0.922508	1	0.904525	2.610581	2.470635
7	3.560195	-0.143988	1.356337	1	2.782136	4.132927	2.868434
6	3.750377	-1.284955	2.059941	1	3.985318	5.176708	0.954050
6	5.008814	-1.550786	2.577661	1	3.265059	4.669637	-1.373678
6	6.049153	-0.641523	2.377709	1	1.368842	3.168038	-1.784150
6	5.805291	0.528292	1.652822	1	-3.462713	-0.083400	1.940678
6	4.539355	0.764355	1.143397	1	-5.781435	0.634315	1.602702
8	1.510949	-2.249791	0.356356	1	-6.839476	0.460811	-0.642834
6	-1.502802	-1.993559	1.867667	1	-5.533814	-0.460520	-2.549245
6	-0.451318	-1.813876	2.775721	1	-3.230991	-1.214076	-2.222189
6	-0.518332	-2.372608	4.052078	1	-1.101016	-1.520763	-2.763765
6	-1.629241	-3.127784	4.431109	1	-1.102173	-3.430436	-4.311079
6	-2.678532	-3.320208	3.530102	1	-1.180478	-5.754701	-3.429295
6	-2.620755	-2.755272	2.256667	1	-1.245464	-6.139002	-0.973548
6	1.015024	2.734425	0.309142	1	-1.290074	-4.238037	0.582019
6	1.425666	3.031050	1.619996	1	0.419275	-1.240672	2.483601
6	2.493327	3.897675	1.848214	1	0.299025	-2.221564	4.751374
6	3.167916	4.484476	0.773709	1	-1.678270	-3.564913	5.423908
6	2.764202	4.201000	-0.531774	1	-3.545668	-3.906976	3.817325
6	1.690768	3.337324	-0.763663	1	-3.448890	-2.909167	1.572281
1	3.747641	1.512957	-1.829810	1	3.149994	-3.922926	-2.933697
1	4.189703	0.543429	-3.248377	1	1.982055	-3.658224	-1.622933
1	3.229081	2.004931	-3.450483	1	5.060981	-2.843666	-1.709016
1	1.328318	0.789827	-4.619435	1	4.887621	-1.246586	-0.975812
1	2.277169	-0.694942	-4.577490	1	4.023529	-2.660379	-0.294962
1	0.635581	-0.682409	-3.914740	1	3.597164	-1.514725	-3.081822
1	1.655862	-3.031002	-3.250429	1	1.337277	0.995063	-2.205096

Coordinates (Å) for the optimized structure for $\mathbf{8}^{2+}$.

6	0.321497	0.024444	0.042744	6	-1.723998	4.273530	-1.940977
8	-1.066966	-0.110931	0.510012	6	-0.808768	3.237095	-1.751232
15	1.293519	-1.439948	0.228638	6	2.059032	1.716609	-1.603291
6	0.741850	-2.760378	-0.912875	6	3.345549	2.270991	-1.541244
6	0.815489	-4.119178	-0.560657	6	4.129389	2.346535	-2.693953
6	0.553650	-5.104400	-1.513189	6	3.639557	1.874925	-3.911919
6	0.226733	-4.747307	-2.823325	6	2.363982	1.307609	-3.977406
6	0.138099	-3.399073	-3.175756	6	1.578266	1.220705	-2.830180
6	0.384725	-2.408218	-2.225216	6	-4.425585	-2.155431	1.947562
6	1.294041	-2.134986	1.927329	1	-2.329740	-1.704616	1.802200
6	2.253466	-3.099895	2.285973	1	-4.518795	-3.111122	-0.551427
6	2.262450	-3.638831	3.572308	1	-2.893904	0.664704	2.155899
6	1.324579	-3.217122	4.517485	1	-4.596239	2.244552	3.075498
6	0.380452	-2.247794	4.175384	1	-6.031415	3.538676	1.470055
6	0.363143	-1.708558	2.887745	1	-5.645242	3.246142	-0.993924
6	3.051018	-1.116779	-0.153026	1	-3.884184	1.618960	-1.750321
6	3.582669	-1.453053	-1.408677	1	-0.362639	-0.944400	2.634085
6	4.940190	-1.265221	-1.664403	1	-0.339607	-1.906459	4.913496
6	5.777822	-0.748638	-0.674283	1	1.337457	-3.635238	5.519486
6	5.256661	-0.419273	0.578890	1	3.009286	-4.380832	3.837953
6	3.901499	-0.606774	0.844599	1	3.006818	-3.419413	1.572297
15	0.944111	1.666097	-0.158085	1	1.076839	-4.415923	0.448621
6	1.799420	2.411973	1.285231	1	0.613886	-6.151386	-1.231732
6	1.869571	1.722863	2.502678	1	0.037878	-5.517440	-3.565311
6	2.465741	2.317293	3.617676	1	-0.128845	-3.116843	-4.189821
6	2.994441	3.604581	3.524597	1	0.298121	-1.363710	-2.500287
6	2.911943	4.307242	2.318453	1	2.948934	-1.870383	-2.182398
6	2.309678	3.722270	1.206520	1	5.344130	-1.535635	-2.635120
15	-2.292520	-0.306731	-0.528413	1	6.836999	-0.615277	-0.873817
7	-3.373938	1.070268	0.175445	1	5.907082	-0.031001	1.356848
6	-3.537606	1.247005	1.509854	1	3.518379	-0.371464	1.830613
6	-4.481817	2.130164	2.003163	1	1.451002	0.725860	2.587740
6	-5.273168	2.852912	1.104749	1	2.513779	1.773832	4.556727
6	-5.067305	2.689671	-0.264522	1	3.461005	4.065641	4.389977
6	-4.104528	1.792471	-0.704694	1	3.309827	5.314958	2.246180
7	-3.086554	-1.686186	-0.143633	1	2.229405	4.292209	0.285567
6	-3.067928	-2.281161	1.239958	1	0.591455	0.771528	-2.887053
6	-2.581951	-3.734693	1.214191	1	1.980968	0.933670	-4.922338
8	-2.121901	0.043297	-1.953266	1	4.249966	1.944302	-4.807390
6	-4.044905	-2.321214	-1.136633	1	5.124798	2.776238	-2.635934
6	-5.157369	-1.377815	-1.605129	1	3.749060	2.628208	-0.601523

6	-3.314591	-2.980544	-2.306453	1	-0.661673	3.294486	1.656117
6	-0.418039	2.866835	-0.454848	1	-2.291023	5.106455	1.309300
6	-0.973310	3.542620	0.646748	1	-2.946164	5.777232	-0.995834
6	-1.890536	4.574629	0.451074	1	-1.994888	4.568190	-2.950531
6	-2.259334	4.949484	-0.843349	1	-0.382384	2.750038	-2.618397
1	-5.898630	-1.952274	-2.169626	1	-2.469938	-4.095687	2.241870
1	-4.772194	-0.604181	-2.276644	1	-1.617034	-3.821734	0.710090
1	-5.675587	-0.907279	-0.762945	1	-3.294752	-4.397417	0.713164
1	-4.038389	-3.529547	-2.918654	1	-4.330290	-2.507802	2.979991
1	-2.561325	-3.688622	-1.952783	1	-5.195694	-2.768793	1.469878
1	-2.826106	-2.235857	-2.939631	1	-4.787821	-1.123058	1.975036

Coordinates (Å) for the transition state for the $\mathbf{7^{2+}} \rightarrow \mathbf{8^{2+}}$ reaction.

6	1.043337	3.568886	-1.704240	6	-4.649306	-1.041824	-1.699240
6	1.649978	2.304648	-1.580325	6	-2.709172	-2.214247	-2.827272
6	2.431352	1.818440	-2.644085	6	-3.548120	2.111955	-2.927569
6	2.604148	2.579451	-3.799176	1	-3.158843	2.725446	0.786534
6	2.010428	3.837376	-3.907642	1	-5.255602	3.646707	1.848479
6	1.233390	4.327948	-2.856791	1	-6.815500	2.047806	2.994513
15	1.453701	1.365951	-0.010946	1	-6.236363	-0.394269	3.031908
6	3.100239	0.659163	0.413559	1	-4.102470	-1.136415	1.914898
6	3.715274	1.052704	1.616045	1	0.203446	-0.398477	2.815971
6	5.012543	0.637765	1.917080	1	1.379069	-0.595587	4.964317
6	5.717449	-0.176513	1.031632	1	3.395668	-2.039019	5.161711
6	5.106557	-0.597500	-0.150671	1	4.242035	-3.254048	3.165333
6	3.809982	-0.189982	-0.456894	1	3.088332	-3.061023	1.010515
6	0.144930	0.032286	-0.184974	1	0.918147	-0.837422	-2.525518
15	0.516182	-1.708819	0.237558	1	1.937211	-1.914764	-4.497947
6	1.342161	-2.487787	-1.189426	1	2.932897	-4.184833	-4.308183
6	1.358664	-1.824447	-2.427842	1	2.861064	-5.389973	-2.135187
6	1.932136	-2.434980	-3.544866	1	1.816379	-4.349684	-0.170955
6	2.486858	-3.711361	-3.438859	1	-1.325027	-1.934712	2.566956
6	2.450388	-4.388295	-2.216680	1	-3.064701	-3.558726	3.149994
6	1.873372	-3.789057	-1.098042	1	-3.683896	-5.368018	1.557986
15	-1.445817	0.750168	-0.715542	1	-2.517817	-5.532904	-0.632748
7	-2.413672	0.087467	-1.871349	1	-0.769883	-3.920862	-1.230325
6	-2.687548	0.861982	-3.145909	1	3.194056	1.685671	2.322004
6	-1.412380	1.156130	-3.941230	1	5.471716	0.962281	2.845857
8	-1.756733	0.209774	0.775064	1	6.733143	-0.484171	1.261420
7	-3.614064	0.783113	1.326698	1	5.640378	-1.241167	-0.843408
6	-3.878533	2.091988	1.296513	1	3.362444	-0.562890	-1.367459
6	-5.041642	2.583737	1.888697	1	2.930727	0.862408	-2.586064
6	-5.905705	1.689436	2.522700	1	3.217043	2.191587	-4.607038

6	-5.588845	0.329461	2.547885	1	2.155817	4.433290	-4.803663
6	-4.411969	-0.096238	1.933859	1	0.767126	5.305528	-2.931853
8	-1.288522	2.224730	-0.860065	1	0.411703	3.952360	-0.915830
6	1.079706	2.588982	1.291622	1	-0.618451	1.576364	2.159847
6	0.050927	2.423176	2.227419	1	-0.939291	3.243554	3.950115
6	-0.137931	3.376561	3.229303	1	0.537840	5.236436	4.084261
6	0.689870	4.496961	3.303804	1	2.359259	5.540522	2.417464
6	1.713707	4.669025	2.369076	1	2.713941	3.870549	0.649382
6	1.912285	3.722506	1.366032	1	-4.953548	-0.340193	-0.918457
6	-0.921383	-2.789779	0.613240	1	-5.041588	-0.681025	-2.655195
6	-1.585532	-2.702544	1.850982	1	-5.124696	-2.008106	-1.498460
6	-2.576664	-3.623245	2.181738	1	-3.145121	-3.195960	-2.617245
6	-2.920648	-4.643828	1.289497	1	-3.068597	-1.910301	-3.815320
6	-2.266372	-4.737995	0.062743	1	-1.621789	-2.323565	-2.883780
6	-1.269950	-3.819993	-0.276008	1	-0.847341	0.237047	-4.133281
6	1.531478	-1.750906	1.759887	1	-1.680205	1.590150	-4.910320
6	1.072332	-1.042795	2.885456	1	-0.770503	1.873183	-3.422957
6	1.743466	-1.146089	4.102229	1	-3.861087	2.506167	-3.900697
6	2.878057	-1.952686	4.211180	1	-4.452289	1.874219	-2.358443
6	3.350414	-2.638950	3.092273	1	-2.993144	2.890086	-2.400743
6	2.685312	-2.540631	1.869507	1	-3.278896	0.162139	-3.739213
6	-3.124050	-1.220311	-1.732188	1	-2.817516	-1.626486	-0.766834

Coordinates (Å) for the optimized structure for **7a**$^{2+}$.

6	-1.855299	-3.352650	-0.219373	6	-3.290570	-3.688569	-2.139305
6	-1.134616	-2.370542	-0.921840	6	-2.922987	-4.009397	-0.831909
6	-1.513009	-2.051356	-2.238647	15	0.334093	-1.577398	-0.172916
6	-2.587348	-2.703904	-2.838424	6	1.758952	-1.911974	-1.277880
6	1.804101	-1.294509	-2.544726	1	-4.119851	-4.204332	-2.613962
6	2.822647	-1.604497	-3.445110	1	-3.465286	-4.773578	-0.283443
6	3.805613	-2.534697	-3.100175	1	-1.598789	-3.604268	0.801948
6	3.772762	-3.145004	-1.845425	1	0.295620	-0.543409	2.571045
6	2.758047	-2.838353	-0.936702	1	0.620455	-1.613489	4.774369
6	0.175049	0.210303	-0.075608	1	1.085202	-4.049820	4.920987
15	1.468634	1.242650	-0.586733	1	1.195599	-5.416938	2.847738
8	1.256103	2.216320	-1.684272	1	0.858487	-4.370948	0.650180
15	-1.387292	1.126625	0.145082	1	1.050189	-0.574585	-2.844894
6	-2.378610	1.327834	-1.367618	1	2.841898	-1.123419	-4.418128

6	-1.751587	1.463626	-2.619018	1	4.592611	-2.782116	-3.805963
6	-2.515452	1.722756	-3.755860	1	4.537938	-3.863497	-1.567812
6	-3.902638	1.857377	-3.657429	1	2.763534	-3.315362	0.035332
6	-4.528008	1.745155	-2.414379	1	-3.393248	-1.030382	0.033167
6	-3.774145	1.485507	-1.269956	1	-4.847466	-2.045819	1.734178
6	-0.899958	2.788769	0.715410	1	-4.785867	-1.236573	4.084289
6	-1.447617	3.926931	0.102787	1	-3.254149	0.617784	4.713320
6	-1.112006	5.198515	0.568485	1	-1.798357	1.649482	3.028394
6	-0.237449	5.347431	1.645896	1	0.406935	2.075866	2.297285
6	0.309784	4.219386	2.262649	1	0.980854	4.332736	3.108942
6	-0.014517	2.944406	1.800498	1	0.015803	6.339404	2.007257
6	-2.450841	0.355110	1.411334	1	-1.535738	6.073281	0.085309
6	-3.332707	-0.682630	1.057048	1	-2.124980	3.827981	-0.737385
6	-4.163562	-1.252711	2.020437	1	-0.672367	1.410237	-2.702684
6	-4.129778	-0.796207	3.339534	1	-2.024415	1.831891	-4.718137
6	-3.266630	0.241992	3.694844	1	-4.493139	2.061321	-4.545594
6	-2.432623	0.820182	2.738982	1	-5.603972	1.862782	-2.330552
6	0.597302	-2.363625	1.448883	1	-4.275989	1.412192	-0.311676
6	0.514537	-1.603930	2.625503	1	4.236243	-1.136381	0.402385
6	0.690332	-2.210290	3.870101	1	5.358200	0.036542	1.118977
6	0.946354	-3.579341	3.952380	1	4.469045	-1.070575	2.158897
6	1.011333	-4.348781	2.787227	1	3.632895	0.979856	3.483825
6	0.831618	-3.751188	1.541137	1	4.437136	2.091949	2.378429
7	2.926035	1.243002	0.126706	1	2.694984	2.243685	2.664050
6	3.239720	0.527754	1.414822	1	3.494925	3.882845	0.655580
6	3.513629	1.529283	2.544361	1	4.656899	4.146480	-0.651113
6	4.047353	2.095548	-0.472888	1	2.946991	3.897167	-1.037984
6	4.412555	1.647415	-1.889512	1	5.311581	2.186024	-2.205436
6	3.754394	3.595276	-0.367558	1	4.630921	0.575977	-1.925963
6	4.395096	-0.465947	1.249167	1	3.619099	1.878854	-2.604894
1	-0.981618	-1.296495	-2.804206	1	4.893219	1.868605	0.177469
1	-2.868940	-2.448658	-3.855204	1	2.338960	-0.034754	1.664571

Table S1. NBO charges of selected atoms in **7a**$^{2+}$, **7**$^{2+}$, TS and **8**$^{2+}$ obtained at the B3LYP/6-31G(d) level.

	C_1	P_1	O_1	N_1	O_2	N_2
7a^{2+}	-1.521	+2.161	-0.952	-0.791	n/a	n/a
7^{2+}	-1.539	+2.343	-1.086	-0.869	-0.624	+0.024
TS	-1.171	+2.400	-1.081	-0.874	-0.700	-0.285
8^{2+}	-0.798	+2.507	-1.051	-0.883	-0.849	-0.586

Table S2. Lengths (Å) and Wiberg indices (in parentheses) of selected bonds in **7a**$^{2+}$, **7**$^{2+}$, TS and **8**$^{2+}$ obtained at the B3LYP/6-31G(d) level.

	7a^{2+}	**7**$^{2+}$	TS	**8**$^{2+}$
P_1-C_1	1.732 (1.070)	1.784 (0.915)	1.824 (0.712)	2.696 (0.018)
P_1-N_1	1.623 (1.054)	1.659 (0.874)	1.647 (0.879)	1.638 (0.890)
P_1=O_1	1.482 (1.359)	1.493 (1.204)	1.490 (1.191)	1.477 (1.304)
P_1-O_2	n/a	1.811 (0.464)	1.616 (0.709)	1.618 (0.715)
O_2-N_2	n/a	1.372 (1.018)	2.021 (0.344)	2.613 (0.026)
C_1-O_2	n/a	2.668 (0.031)	2.138 (0.479)	1.471 (0.837)
P_1-N_2	n/a	2.759 (0.007)	2.979 (0.011)	1.887 (0.466)

Selected bond orbital makeup according to the NBO analysis: For **7**$^{2+}$

- (1.97568) BD (1) P 22 - N 23 (i.e. P1-N1)
  (26.07%) 0.5106* P 22 s(30.95%)p 2.17(67.25%)d 0.06(1.79%)
  (73.93%) 0.8598* N 23 s(31.97%)p 2.13(68.02%)d 0.00(0.01%)

- (1.98475) BD (1) P 22 - O 33 (i.e. P1-O1)
  (24.36%) 0.4935* P 22 s(32.02%)p 2.08(66.68%)d 0.04(1.29%)
  (75.64%) 0.8697* O 33 s(36.13%)p 1.76(63.43%)d 0.01(0.44%)

- (1.69715) LP (1) C 14 (i.e. C1) s(0.08%)p99.99(99.92%)d 0.02(0.00%)

For TS

- (1.85820) BD (1) C 14 - O 26 (i.e. C1-O2)
  (50.02%) 0.7073* C 14 s(0.38%)p99.99(99.60%)d 0.04(0.02%)
  (49.98%) 0.7070* O 26 s(0.08%)p99.99(99.82%)d 1.16(0.10%)

For **8**$^{2+}$

- (1.97171) BD (1) P 23 - N 31 (i.e. P1-N1)
  (26.19%) 0.5117* P 23 s(33.19%)p 1.95(64.88%)d 0.06(1.93%)
  (73.81%) 0.8591* N 31 s(30.70%)p 2.26(69.28%)d 0.00(0.02%)

- (1.98315) BD (1) P 23 - O 24 (i.e. P1-O1)
  (24.56%) 0.4956* P 23 s(35.13%)p 1.81(63.60%)d 0.04(1.26%)
  (75.44%) 0.8686* O 24 s(34.98%)p 1.84(64.53%)d 0.01(0.48%)

- (1.70665) LP (1) C 14 (i.e. C1) s(2.54%)p38.39(97.44%)d 0.01(0.02%)

All calculations for the **Section IV** were performed with the Gaussian program package [S6] by employing the B3LYP functional in conjunction with the 6-31G(d) basis set. All structures were optimized with default convergence criteria and an ultrafine integration grid. Each reported transition state has a single imaginary frequency, and intrinsic reaction coordinate calculations confirmed that those first order saddle points connect the minima of interest. Reported atomic charges are obtained through QTAIM analysis (Quantum Theory of Atoms in Molecules) [S7] performed with the AIMAll program package [S8].

S1. SMART version 5.628; Bruker AXS Inc.: Madison, WI, **2001**.
S2. SAINT+ version 6.22a; Bruker AXS Inc.: Madison, WI, **2001**.
S3. Sheldrick, G. M. SADABS; **1996**.
S4. SHELXTL version 5.1; Bruker AXS Inc.: Madison, WI, **1997**.
S5. M. J. Frisch et al. Gaussian 09 Revision D.01, Gaussian Inc. Wallingford, CT, **2009**.
S6. Gaussian 09, Revision D.01, M. J. Frisch, G. W. Trucks, H. B. Schlegel, G. E. Scuseria, M. A. Robb, J. R. Cheeseman, G. Scalmani, V. Barone, B. Mennucci, G. A. Petersson, H. Nakatsuji, M. Caricato, X. Li, H. P. Hratchian, A. F. Izmaylov, J. Bloino, G. Zheng, J. L. Sonnenberg, M. Hada, M. Ehara, K. Toyota, R. Fukuda, J. Hasegawa, M. Ishida, T. Nakajima, Y. Honda, O. Kitao, H. Nakai, T. Vreven, J. A. Montgomery, Jr., J. E. Peralta, F. Ogliaro, M. Bearpark, J. J. Heyd, E. Brothers, K. N. Kudin, V. N. Staroverov, T. Keith, R. Kobayashi, J. Normand, K. Raghavachari, A. Rendell, J. C. Burant, S. S. Iyengar, J. Tomasi, M. Cossi, N. Rega, J. M. Millam, M. Klene, J. E. Knox, J. B. Cross, V. Bakken, C. Adamo, J. Jaramillo, R. Gomperts, R. E. Stratmann, O. Yazyev, A. J. Austin, R. Cammi, C. Pomelli, J. W. Ochterski, R. L. Martin, K. Morokuma, V. G. Zakrzewski, G. A. Voth, P. Salvador, J. J. Dannenberg, S. Dapprich, A. D. Daniels, O. Farkas, J. B. Foresman, J. V. Ortiz, J. Cioslowski, and D. J. Fox, Gaussian, Inc., Wallingford CT, 2013.
S7. R. F. W. Bader (1990) Atoms in molecules. A quantum theory. Oxford Univ. Press, Oxford
S8. T. A. Keith, AIMAll (version 15.09.27), (http://aim.tkgristmill.com), T.G.S. Todd A. Keith, Overland Park KS, USA, (aim.tkgristmill.com), Todd A. Keith, TK Gristmill Software, Overland Park KS, USA, (aim.tkgristmill.com), 2